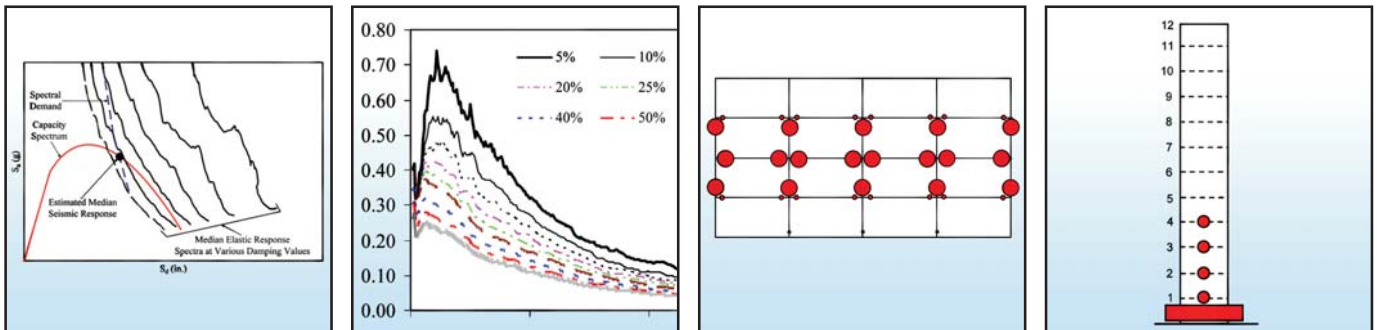


Development and Appraisal of a Numerical Cyclic Loading Protocol for Quantifying Building System Performance

by
**Andre Filiatrault, Assawin Wanitkorkul and
Michael Constantinou**



Technical Report MCEER-08-0013

April 27, 2008

NOTICE

This report was prepared by the University at Buffalo, State University of New York as a result of a contract from the Federal Emergency Management Agency (FEMA) to the Applied Technology Council (ATC). Neither MCEER, associates of MCEER, its sponsors, the University at Buffalo, State University of New York, nor any person acting on their behalf:

- a. makes any warranty, express or implied, with respect to the use of any information, apparatus, method, or process disclosed in this report or that such use may not infringe upon privately owned rights; or
- b. assumes any liabilities of whatsoever kind with respect to the use of, or the damage resulting from the use of, any information, apparatus, method, or process disclosed in this report.

Any opinions, findings, and conclusions or recommendations expressed in this publication are those of the author(s) and do not necessarily reflect the views of MCEER, FEMA, ATC, or other sponsors.

Development and Appraisal of a Numerical Cyclic Loading Protocol for Quantifying Building System Performance

by

Andre Filiatrault,¹ Assawin Wanitkorkul² and Michael Constantinou¹

Publication Date: April 27, 2008

Submittal Date: April 4, 2008

Technical Report MCEER-08-0013

Subcontract to the authors from the Applied Technology Council (ATC)
as part of the ATC-63 Project

- 1 Professor, Department of Civil, Structural and Environmental Engineering, University at Buffalo, State University of New York
- 2 Senior Structural Engineer, Connell Wagner (Thailand); former Post-doctoral Associate, Department of Civil, Structural and Environmental Engineering, University at Buffalo, State University of New York

MCEER

University at Buffalo, State University of New York

Red Jacket Quadrangle, Buffalo, NY 14261

Phone: (716) 645-3391; Fax (716) 645-3399

E-mail: mceer@buffalo.edu; WWW Site: <http://mceer.buffalo.edu>

NTIS DISCLAIMER

- ❖ This document has been reproduced from the best copy furnished by the sponsoring agency.

Preface

The Multidisciplinary Center for Earthquake Engineering Research (MCEER) is a national center of excellence in advanced technology applications that is dedicated to the reduction of earthquake losses nationwide. Headquartered at the University at Buffalo, State University of New York, the Center was originally established by the National Science Foundation in 1986, as the National Center for Earthquake Engineering Research (NCEER).

Comprising a consortium of researchers from numerous disciplines and institutions throughout the United States, the Center's mission is to reduce earthquake losses through research and the application of advanced technologies that improve engineering, pre-earthquake planning and post-earthquake recovery strategies. Toward this end, the Center coordinates a nationwide program of multidisciplinary team research, education and outreach activities.

MCEER's research is conducted under the sponsorship of two major federal agencies: the National Science Foundation (NSF) and the Federal Highway Administration (FHWA), and the State of New York. Significant support is derived from the Federal Emergency Management Agency (FEMA), other state governments, academic institutions, foreign governments and private industry.

Following the award of a contract from the Federal Emergency Management Agency (FEMA) to the Applied Technology Council (ATC) entitled "Seismic and Multi-Hazard Technical Guidance Development and Support," the authors of this report received a sub-contract to participate in the program. The FEMA contract comprised a number of tasks, including one entitled "Quantification of Building System Performance and Response Parameters," which became known as the ATC-63 Project. The purpose of ATC-63 was to establish and document a recommended methodology for reliably quantifying building system performance and response parameters for use in seismic design. As part of this effort, the authors were tasked with developing a numerical cyclic loading protocol. This report describes the results of this effort. The ATC-63 Project Report is available from the ATC website at: <http://www.atcouncil.org>.

The main objective of this study is to develop a numerical cyclic loading protocol, based on available experimental and numerical studies, to quantify building system performance. The first part of the report reviews and compares existing experimental loading protocols that have been developed for the quasi-static cyclic testing of structural components and systems. Numerical studies that have included cyclic pushover analyses of structural components or systems are also reviewed. Based on this review, a numerical cyclic loading protocol is proposed for quantifying building system performance. In the second part of the report, a sensitivity analysis on the influence of the number of repeating cycles of the proposed numerical cyclic loading protocol on the equivalent elastic lateral stiffness and viscous damping properties of a 4-story reinforced concrete building model is investigated. Based on these results, the proposed numerical cyclic loading protocol is used in a simplified capacity spectrum methodology to estimate the seismic response of three different building structure models: two 4-story building models and a 12-story building model.

ABSTRACT

The study described in this report focused on the development of a numerical cyclic loading protocol to be used for quantifying building system performance based on a review of available experimental and numerical studies. The proposed loading protocol first consists of a preliminary monotonic pushover analysis in order to establish the expected failure roof displacement of the building model considered. Once the expected failure roof displacement of the building model considered is established, the general loading sequence of the proposed numerical cyclic loading protocol is established as a fraction of this expected failure roof displacement. A sensitivity analysis on the influence of the number of repeating cycles of the proposed numerical cyclic loading protocol on the equivalent elastic lateral stiffness and viscous damping properties of a 4-story SMF reinforced concrete building model was investigated. The numerical cyclic loading protocol was implemented using a force-based procedure in which the load vector was proportional to the first mode shape of the building under elastic conditions. Higher mode effects were disregarded. It is found that the number of repeating cycles has minor influences on the effective lateral stiffness and energy dissipation characteristics of the building model. Based on these results, the proposed numerical cyclic loading protocol was used in a simplified capacity spectrum methodology to estimate the seismic response of the same building model. It was found that the recommended simplified analysis procedure under-estimated the predictions of nonlinear dynamic analyses by 12% to 39% across intensity levels and protocol versions when compared to the counted median of the response history analysis. (When compared to the surviving median of the response history analysis, the under-prediction across all levels and protocols was lesser). The largest under-prediction occurred in the case of the strongest seismic input. In the case of the least number of cycles (case of one cyclic dwell with a total of seven cycles) the simplified procedure under-predicted the counted median roof displacement response by 12% to 31% across all intensity levels. Inspection of the graphs comparing the spectral capacity and the spectral demand curves for all cases analyzed revealed that for the case of the strongest excitation the two curves were nearly asymptotic, which indicates that collapse is imminent. Therefore, a small increase in the level of excitation would have resulted in prediction of collapse. Conversely, a different extrapolation of results for the spectral capacity curve (one that better represents the available data at large displacements) would have resulted in prediction of collapse at lower excitation level, that is, in better agreement with the results of response history analysis.

ACKNOWLEDGEMENTS

The material described in this report was developed as background material for the ATC-63 Project “Quantification of Building System Performance and Response Parameters,” which was funded by the Department of Homeland Security’s Federal Management Agency (FEMA). The authors kindly acknowledge Dr. Charles Kircher, Chair of the ATC-63 Project Management Committee, and Mr. Christopher Rojahn, ATC-63 Project Executive Director, for their guidance and support during the course of this project.

TABLE OF CONTENTS

SECTION	TITLE	PAGE
1	INTRODUCTION	1
2	REVIEW OF EXPERIMENTAL QUASI-STATIC CYCLIC TEST PROTOCOLS	3
2.1	Cyclic Loading Protocols for Concrete Structures	3
2.2	Cyclic Loading Protocols for Steel Structures	5
2.3	Cyclic Loading Protocols for Wood Structures	7
2.4	Cyclic Loading Protocols for Masonry Structures	15
2.5	ATC-58 Loading Protocol for Fragility Racking Testing of Nonstructural Components	16
2.6	Comparison of Test Protocols	18
3	REVIEW OF NUMERICAL CYCLIC PUSHOVER ANALYSES	25
4	RECOMMENDED NUMERICAL CYCLIC LOADING PROTOCOL FOR QUANTIFYING BUILDING PERFORMANCE	29
4.1	Criteria	29
4.2	Proposed Numerical Cyclic Protocol	30
5	LATERAL LOAD DISTRIBUTION FOR CYCLIC PUSHOVER ANALYSIS	33
6	ANALYSIS OF 4-STORY REINFORCED CONCRETE SPECIAL MOMENT FRAME	35
6.1	Scope	35
6.2	Four-story Special Moment-Resisting Reinforced Concrete Frame Building	35
6.3	Monotonic Pushover Analysis	36
6.4	Cyclic Loading Protocols	36
6.5	Cyclic Pushover Analyses	38
6.6	Sensitivity of Effective Lateral Stiffness	38
6.7	Sensitivity of Spectral Capacity Curves	41
6.8	Sensitivity of Hysteretic Energy	42
6.9	Sensitivity of Equivalent Viscous Damping Ratio	44
6.10	Estimation of Seismic Response	44
6.11	Response Spectra used in Simplified Analysis	45
6.12	Calculation of Response and Comparison to Results of Nonlinear Dynamic Analysis	51
6.13	Damage Predicted by Simplified Analysis and by Nonlinear Dynamic Analysis	53
7	ANALYSIS OF 4-STORY REINFORCED CONCRETE INTERMEDIATE MOMENT FRAME	55

TABLE OF CONTENTS (cont'd)

SECTION	TITLE	PAGE
8	ANALYSIS OF A 12-STORY SPECIAL WALL BUILDING	59
8.1	Calculation of Damage Predicted by Simplified Analysis and by Nonlinear Dynamic Analysis	64
9	SUMMARY OF PROPOSED NUMERICAL CYCLIC LOADING PROTOCOL AND ESTIMATION OF SEISMIC RESPONSE	67
10	CONCLUSIONS	69
11	REFERENCES	71
Appendix A	MEDIAN SPECTRAL ACCELERATION VALUES FOR 60 GROUND MOTIONS USED IN ANALYSES	75
Appendix B	PREDICTIONS OF MEDIAN ROOF DISPLACEMENT OF 4-STORY SMF USING SIMPLIFIED CAPACITY SPECTRUM METHOD	77
Appendix C	PREDICTIONS OF MEDIAN ROOF DISPLACEMENT OF 4-STORY IMF USING SIMPLIFIED CAPACITY SPECTRUM METHOD	91
Appendix D	PREDICTIONS OF MEDIAN ROOF DISPLACEMENT OF 12-STORY SPECIAL WALL BUILDING USING SIMPLIFIED CAPACITY SPECTRUM METHOD	95

LIST OF FIGURES

FIGURE	TITLE	PAGE
2-1	Determination of First Yield Displacement, Δ_y , of New Zealand Protocol	4
2-2	New Zealand Protocol	4
2-3	ATC-24 Loading Protocol	5
2-4	SAC Standard Loading Protocol	6
2-5	FCC Loading Protocol	8
2-6	ASTM E72 Loading Protocol	9
2-7	ASTM E564 Loading Protocols	10
2-8	CEN Loading Protocols	11
2-9	ISO Loading Protocol	12
2-10	Calculation of Δ and Δ_{max} for CUREE-Caltech Protocol	14
2-11	CUREE-Caltech Standard Protocol	14
2-12	SPD Loading Protocol	15
2-13	Conceptual Representation of the ATC-58 Loading Protocol	17
2-14	ATC-58 Loading Protocol $a_1 = 0.048\Delta_m$	18
2-15	Total Number of Cycles for Loading Protocols	19
2-16	Number of Initiation Cycles for Loading Protocols	20
2-17	Number of Primary Cycles for Loading Protocols	21
2-18	Maximum Number of Repeating Cycles for Loading Protocols	22
2-19	Amplitude Increase of Primary Cycles for Loading Protocols	23
3-1	Cyclic Pushover Curve for Woodframe Apartment Building	26
3-2	Normalized Secant Lateral Stiffness versus Normalized Drift Levels for Woodframe Buildings	27
3-3	Equivalent Viscous Damping Ratios of Woodframe Buildings	28
4-1	Calculation of Δ_f for Proposed Numerical Cyclic Loading Protocol	30
4-2	Proposed Numerical Cyclic Loading Protocol	31
4-3	Amplitude Increase of Primary Cycles for Proposed Numerical Cyclic Loading Protocols	32
6-1	Special Moment-Resisting 4-Story Concrete Frame Building Model	35
6-2	Result of Monotonic Pushover Analysis of 4-story SMF	37
6-3	Numerical Cyclic Loading Protocols used for 4-story SMF	37
6-4	Results of Cyclic Pushover Analyses for 4-story SMF	38
6-5	Definition of Effective Lateral Stiffness	39
6-6	Effective Stiffness as Function of Spectral Displacement of 4-story SMF	40
6-7	Spectral Capacity Curves of 4-story SMF	42
6-8	Variations of Hysteretic Energy Dissipated by 4-story SMF with Spectral Displacement	43
6-9	Variations of Equivalent Viscous Damping Ratio with Spectral Displacement for 4-story SMF	45
6-10	Estimation of Seismic Response of Building Model	46

LIST OF FIGURES (cont'd)

FIGURE	TITLE	PAGE
6-11	Median Response Spectra for 0.11g Intensity Motions	47
6-12	Median Response Spectra for 0.32g Intensity Motions	47
6-13	Median Response Spectra for 1.12 g Intensity Motions	48
6-14	Median Response Spectra for 1.92g Intensity Motions	48
6-15	Median, Maximum and Minimum Spectral Values for 0.11g Intensity Motions	49
6-16	Median, Maximum and Minimum Spectral Values for 0.32g Intensity Motions	49
6-17	Median, Maximum and Minimum Spectral Values for 1.12g Intensity Motions	50
6-18	Median, Maximum and Minimum Spectral Values for 1.92g Intensity Motions	50
6-19	Diagrams Showing Collapse Modes of 4-story SMF Observed in Dynamic Analysis	54
6-20	Damage Pattern of 4-story SMF Observed in Simplified Analysis at $S_{a1} = 1.92$ g (near collapse)	54
7-1	Result of Monotonic Pushover Analysis of 4-story IMF	56
7-2	Results of Cyclic Pushover Analyses for 4-story IMF	56
7-3	Effective Stiffness as Function of Spectral Displacement of 4-story IMF	56
7-4	Effective Damping as Function of Spectral Displacement of 4-story IMF	57
7-5	Spectral Capacity Curves of 4-story IMF	57
8-1	Plan View of The 12-story Building with Special Core Walls	59
8-2	12-story with Special Core Wall Building Model	60
8-3	Result of Monotonic Pushover Analysis of 12-story Special Wall Building	61
8-4	Results of Cyclic Pushover Analyses for 12-story Special Wall Building	62
8-5	Effective Stiffness as Function of Spectral Displacement of 12-story Special Wall Building	62
8-6	Effective Damping as Function of Spectral Displacement of 12-story Special Wall Building	62
8-7	Spectral Capacity Curves of 12-story Special Wall Building	63
8-8	Diagrams Showing Collapse Modes of 12-story Special Wall Building Observed in Dynamic Analysis	65
8-9	Damage Pattern of 12-story Special Wall Building Observed in Simplified Analysis at $S_{a1} = 1.92$ g (near collapse)	66

LIST OF TABLES

TABLE	TITLE	PAGE
2-1	Sequence of Loading of New Zealand Protocol	4
2-2	Sequence of Loading of ATC-24 Protocol	6
2-3	Sequence of Loading of SAC Standard Protocol	7
2-4	Sequence of Loading of FCC Protocol	8
2-5	Sequence of Loading of ASTM 72 Protocol	9
2-6	Sequence of Loading of ASTM E564 Protocol	10
2-7	Sequence of Loading of CEN Protocols	12
2-8	Sequence of Loading of ISO Protocol	13
2-9	Sequence of Loading of CUREE-Caltech Protocol	14
4-1	Sequence of Loading of Proposed Numerical Cyclic Loading Protocol	31
6-1	Lumped Tributary Weights and Modal Properties of Analyzed 4-story Special Moment Frame	36
6-2	Best Fit Values of Constants in Equation (10) for 4-story SMF	41
6-3	Best Fit Values of Constants in Equation (14) for 4-story SMF	44
6-4	Estimated Median Roof Displacement of 4-story SMF, $S_{a1} = 0.11$ g	51
6-5	Estimated Median Roof Displacement of 4-story SMF, $S_{a1} = 0.32$ g	51
6-6	Estimated Median Roof Displacement of 4-story SMF, $S_{a1} = 1.12$ g	52
6-7	Estimated Median Roof Displacement of 4-story SMF, $S_{a1} = 1.92$ g	52
7-1	Lumped Tributary Weights and Modal Properties of Analyzed 4-story Intermediate Moment Frame	55
7-2	Estimated Median Roof Displacement of 4-story IMF, $S_{a1} = 0.11$ g	58
7-3	Estimated Median Roof Displacement of 4-story IMF, $S_{a1} = 0.32$ g	58
7-4	Estimated Median Roof Displacement of 4-story IMF, $S_{a1} = 1.12$ g	58
8-1	Lumped Tributary Weights and Modal Properties of Analyzed 12-story Special Wall Building	61
8-2	Estimated Median Roof Displacement of 12-story Special Wall Building, $S_{a1} = 0.11$ g	63
8-3	Estimated Median Roof Displacement of 12-story Special Wall Building, $S_{a1} = 0.32$ g	64
8-4	Estimated Median Roof Displacement of 12-story Special Wall Building, $S_{a1} = 1.12$ g	64
8-5	Estimated Median Roof Displacement of 12-story Special Wall Building, $S_{a1} = 1.92$ g	64
A-1	Median Response Spectra for 0.11g Intensity Motions	75
A-2	Median Response Spectra for 0.32g Intensity Motions	75
A-3	Median Response Spectra for 1.12g Intensity Motions	76
A-4	Median Response Spectra for 1.92g Intensity Motions	76

SECTION 1

INTRODUCTION

The main objective of this report is to develop a numerical cyclic loading protocol to be used for quantifying building system performance based on available experimental and numerical studies. The first part of the report reviews and compares existing experimental loading protocols that have been developed for the quasi-static cyclic testing of structural components and systems. Numerical studies that have included cyclic pushover analyses of structural components or systems are also reviewed. Based on this review, a numerical cyclic loading protocol is proposed for quantifying building system performance.

In the second part of the report, a sensitivity analysis on the influence of the number of repeating cycles of the proposed numerical cyclic loading protocol on the equivalent elastic lateral stiffness and viscous damping properties of a 4-story reinforced concrete building model is investigated. Based on these results, the proposed numerical cyclic loading protocol is used in a simplified capacity spectrum methodology to estimate the seismic response of three different building structure models: two 4-story building models and a 12-story building model.

SECTION 2

REVIEW OF EXPERIMENTAL QUASI-STATIC CYCLIC TEST PROTOCOLS

Several loading protocols have been proposed over the years for the cyclic testing of structural components and systems. Since it would be unrealistic to review all experimental studies that have used cyclic loading in one form or another, this section is limited to formal loading protocols that have been proposed and widely utilized. Because of the nature of various materials and structural systems, the loading protocols reviewed are classified by types of structural materials: concrete structures, steel structures, wood structures, and masonry structures. Finally, the loading protocol developed as part of the ATC-58 project for the fragility racking testing of nonstructural components is reviewed.

2.1 Cyclic Loading Protocols for Concrete Structures

A large number of cyclic testing of reinforced concrete subassemblies have been conducted by several investigators using a variety of loading protocols over the last two decades. However, a formal cyclic loading protocol was developed by researchers in New Zealand for testing reinforced concrete structures. Several subsequent experimental studies made use of this, or variations of the New Zealand Protocol.

The New Zealand Protocol (1991)

The New Zealand loading protocol, developed as part of a United States / New Zealand / Japan / China collaborative research project (Cheung et al., 1991), is based on a yield displacement (Δ_y) obtained by extrapolating the displacement of the test specimen at 75% of the theoretical strength (V_i) measured during the third cycle of the loading sequence, as illustrated in Fig. 2-1. Therefore, the protocol does not require a preliminary monotonic test but a preliminary analysis must be conducted in order to determine the theoretical strength of the test specimen.

The quasi-static loading history of the New Zealand protocol is shown in Fig. 2-2. The first three cycles of the protocol are load controlled. The first two cycles impose a lateral force corresponding to 50% of V_i . The first yield displacement (Δ_y) is determined in the third cycle of loading, as described in the previous paragraph. Subsequent pairs of cycles are displacement controlled with increasing imposed displacement ductility factor $\mu = \Delta/\Delta_y$. Table 2-1 presents the sequence of loading of the New Zealand loading protocol.

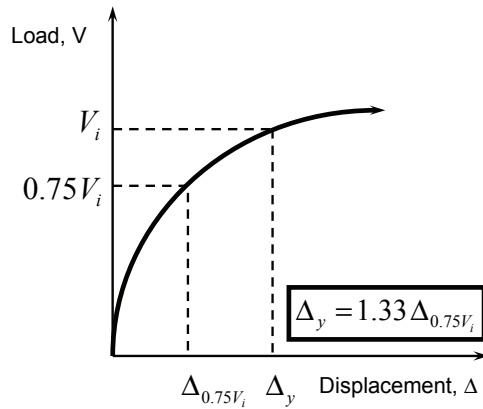


Figure 2-1. Determination of First Yield Displacement, Δ_y , of New Zealand Protocol

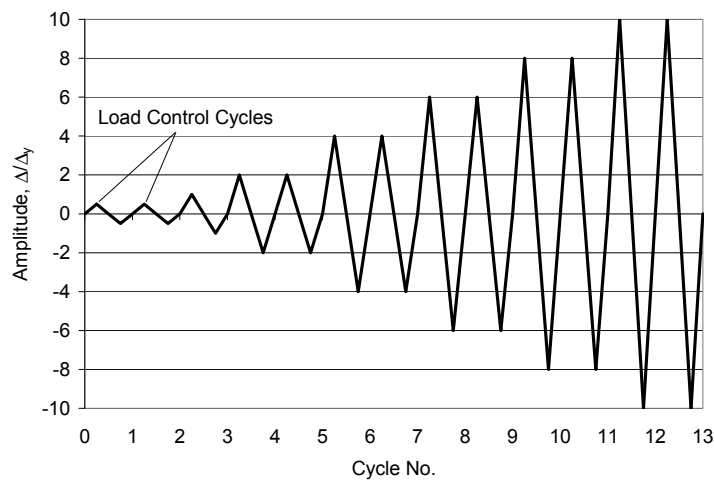


Figure 2-2. New Zealand Protocol

Table 2-1. Sequence of Loading of New Zealand Protocol

Cycle Group	Number of Cycles	Control Variable	Amplitude
1	2	V_i^*	$0.50 V_i$
2	1**	Δ_y	$1 \Delta_y$
3	2		$2 \Delta_y$
4	2		$4 \Delta_y$
5	2		$6 \Delta_y$
6	2		$8 \Delta_y$
7	2		$10 \Delta_y$
8 and greater	2		Increment of $2 \Delta_y$ until failure

*Theoretical strength obtained from preliminary analysis of test specimen.

**First part of cycle used to determine yield displacement, Δ_y .

2.2 Cyclic Loading Protocols for Steel Structures

Two loading protocols have been developed and used extensively for the cyclic testing of structural steel components and systems: the ATC-24 protocol and the SAC protocol. Both protocols were developed by Helmut Krawinkler from Stanford University.

The ATC-24 Protocol (1992)

As part of the ATC-24 project, Krawinkler developed a loading protocol for the cyclic testing of components of steel structures (Applied Technology Council, 1992). Similar to the New Zealand test protocol described above, the ATC-24 protocol is based on a yield deformation (δ_y) obtained by extrapolating the deformation of the test specimen at 75% of its theoretical strength (Q_y) measured either during the third cycle of the loading sequence, as illustrated in Fig. 2-1, or during a preliminary monotonic test. The cyclic loading history of the ATC-24 protocol shown in Fig. 2-3 was developed based on statistical studies on the nonlinear time-history dynamic response of bilinear and stiffness degrading Single-Degree-of-Freedom (SDOF) systems subjected to a set of 15 Western United States earthquake ground motions (Hadidi-Tamjed, 1987, Nassar and Krawinkler, 1991). These studies provided statistical information on seismic demand parameters for inelastic systems having ductility capacities between 2 and 8. The parameters that were analyzed in order to provide support in the development of the ATC-24 protocol were: the number of inelastic excursions, the individual plastic deformation ranges and the cumulative plastic deformation ranges. Table 2-2 presents the sequence of loading of the ATC-24 protocol.

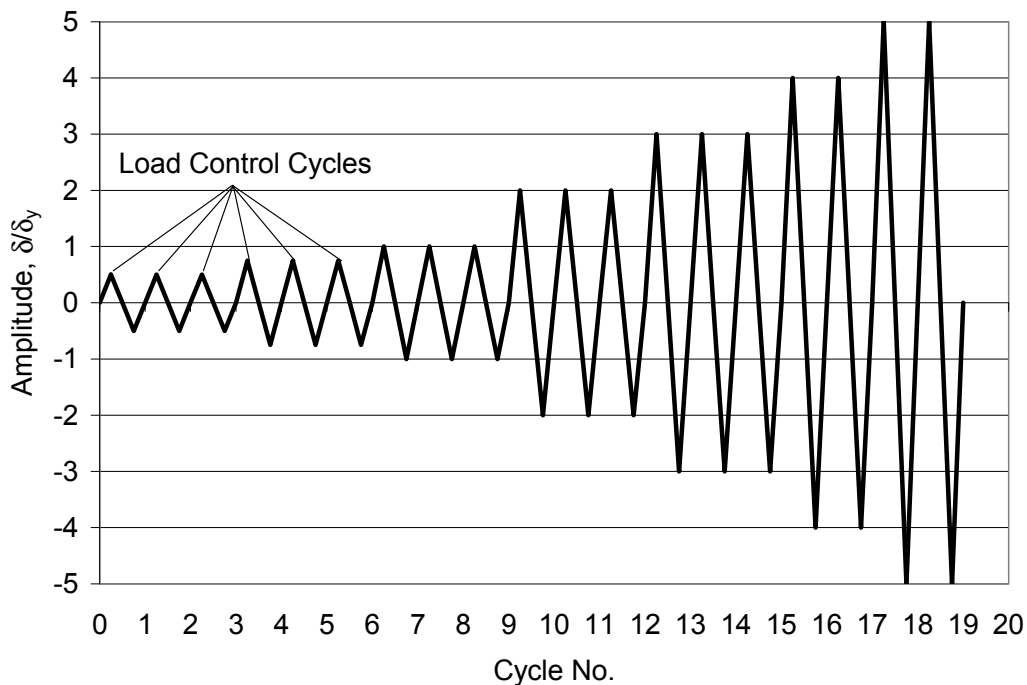


Figure 2-3. ATC-24 Loading Protocol

Table 2-2. Sequence of Loading of ATC-24 Protocol

Cycle Group	Number of Cycles	Control Variable	Amplitude
1	3	Q_y^*	$0.50 Q_y$
2	3**		$0.75 Q_y$
3	3	δ_y	$1 \delta_y$
4	3		$2 \delta_y$
5	3		$3 \delta_y$
6	2		$4 \delta_y$
7	2		$5 \delta_y$
8 and greater	2		Increment of δ_y until failure

*Theoretical yield strength obtained from preliminary analysis of test specimen or monotonic test.

**Cycles used to determine yield deformation, δ_y .

The SAC Protocols (1997)

Krawinkler (SAC, 1997) developed two loading protocols for the cyclic testing of steel moment-resisting connections for the SAC steel research project: a standard loading protocol and a near-fault loading protocol. Near-fault effects are not considered and only the standard loading protocol is reviewed herein, as illustrated in Fig. 2-4. The standard SAC loading protocols are based on the inter-story drift angle, which is defined as the inter-story displacement divided by the story height. The loading history used in the SAC Protocol has been developed based on a series of nonlinear time-history dynamic analyses of hypothetical steel moment-resisting frame structures subjected to a range of seismic input. Table 2-3 presents the sequence of loading of the SAC protocol. A major advantage of the SAC protocol is that no prior testing is required to obtain the governing parameters necessary for characterization of the protocol.

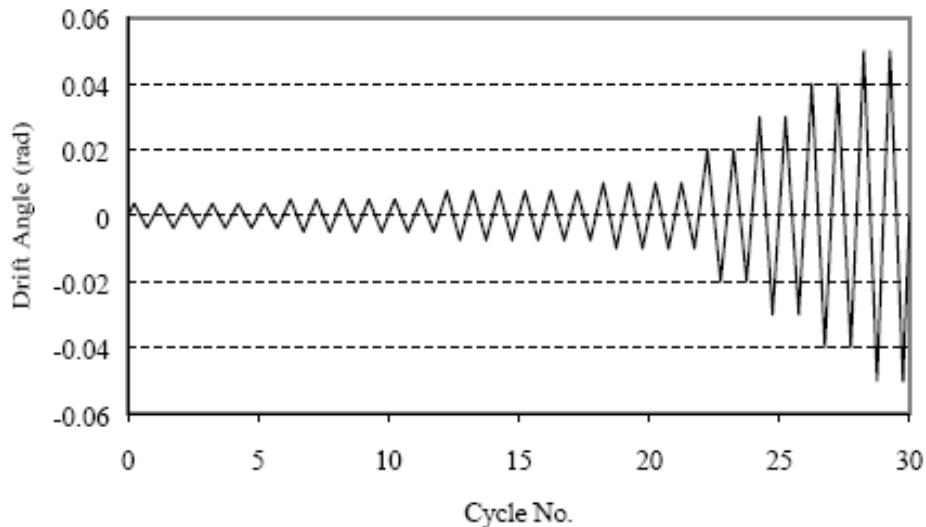


Figure 2-4. SAC Standard Loading Protocol

Table 2-3. Sequence of Loading of SAC Standard Protocol

Cycle Group	Number of Cycles	Drift Angle Amplitude (rad)
1	6	0.00375
2	6	0.005
3	6	0.0075
4	4	0.01
5	2	0.015
6	2	0.02
7	2	0.03
8 and greater	2	Increment of 0.01 until failure

2.3 Cyclic Loading Protocols for Wood Structures

Since the 1994 Northridge earthquake in California in which wood structures suffered significant damage, there has been a renewed interest in the seismic response of wood subassemblies and systems. Because wood structures are particularly difficult to model numerically, there has been a proliferation of full-scale cyclic testing on wood subassemblies, particularly wood shear walls. In parallel, a significant number of cyclic loading protocols have been proposed and used in experimental studies. This section reviews seven cyclic loading protocols that have been proposed and used extensively in the cyclic testing of wood structural subassemblies and systems.

The FCC Protocol (1993)

The FCC protocol, developed by the Forintek Canada Corporation (Karacabeyli, 1998), consists of cycle groups of three equal magnitude cycles, as shown in Fig. 2-5. Cycle group amplitude is determined from the nominal yield slip (Δ_{yield}), defined as half the ultimate load displacement and found from prior monotonic testing. The first cycle group amplitude is equal to 50% of Δ_{yield} followed by 100% of Δ_{yield} and then 50% again for the third cycle group. A similar pattern is repeated in subsequent cycle groups, as shown in Table 2-4, until specimen failure is reached.

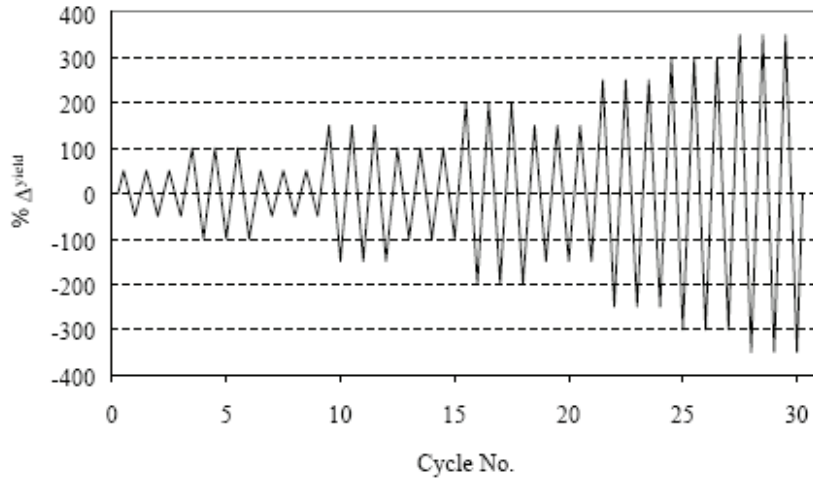


Figure 2-5. FCC Loading Protocol

Table 2-4. Sequence of Loading of FCC Protocol

Cycle Group	Number of Cycles	Amplitude (% of Δ_{yield}^*)
1	3	50 %
2	3	100 %
3	3	50 %
4	3	150 %
5	3	100 %
6	3	200 %
7	3	150 %
8	3	250%
9	3	300 %
10	3	350 %
10 and greater	3	Increment of 50 % until failure

* Δ_{yield} equals to half ultimate load displacement as found from prior monotonic testing

The ASTM E 72 Protocol (1995)

The American Society of Testing and Materials ASTM (1995a) has developed a standard procedure for the evaluation of sheathing panels used in wood frame shear walls. According to this standard, the shear wall panel specimen is loaded at a constant rate to 3.0, 7.0, and 10.5 kN with complete unloading between each load increment, as shown in Fig. 2-6. After the 10.5 kN load is applied, the specimen is unloaded and then reloaded monotonically until failure. Table 2-5 presents the sequence of loading of the ASTM 72 loading protocol. Note that this procedure is not intended to test a shear wall assembly due to the overturning forces being resisted by the steel rod at the end of the wall.

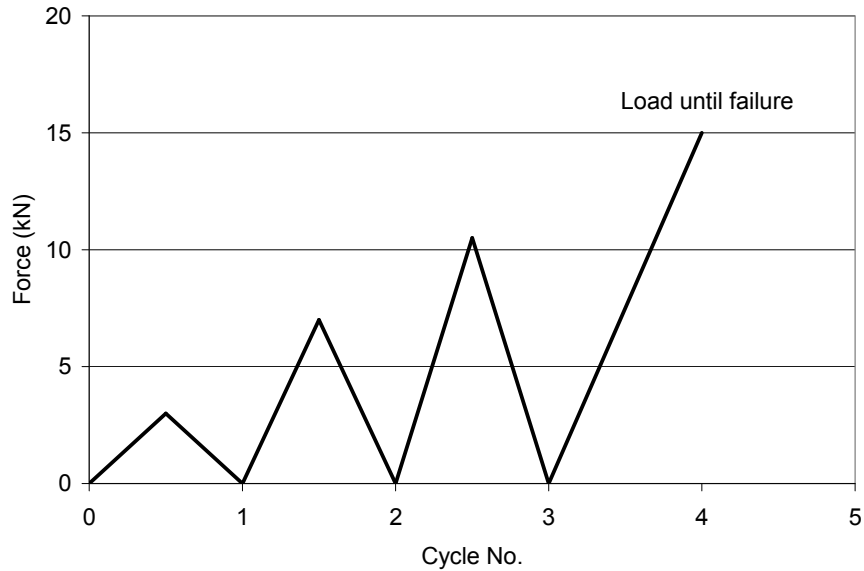


Figure 2-6. ASTM E72 Loading Protocol

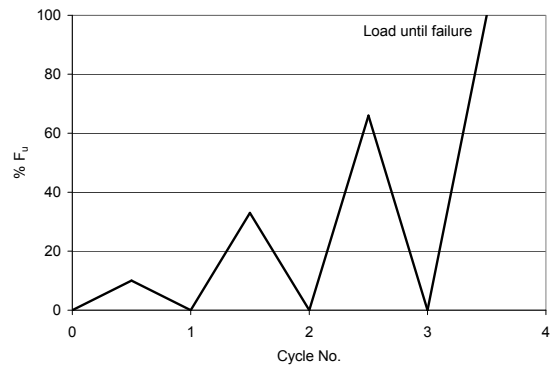
Table 2-5. Sequence of Loading of ASTM 72 Protocol

Cycle Group	Number of Half Cycles	Force Amplitude (kN)
1	1	3.0
2	1	7.0
3	1	10.5
4	---	Load until failure

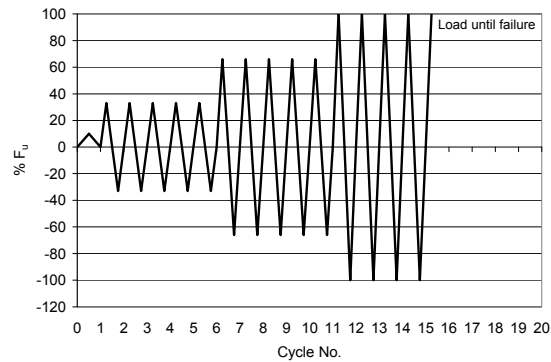
The ASTM E564 Protocols (1995)

A standard for testing an entire woodframe shearwall as opposed to just the sheathing is provided by the ASTM E564 test protocol (ASTM, 1995b). The standard provides two loading sequences: a static load sequence with only positive excursions and an optional cyclic load sequence. In the static test, the specimen is preloaded to 10% of the expected ultimate load (F_u) to “seat” the connections of the specimen and then unloaded. This expected ultimate load would need to be estimated based on a preliminary monotonic test. After seating the connections, three load increments are applied starting with one-third the expected ultimate load followed by increases of one-third the ultimate load until the ultimate load is reached in the third increment. At each increment the specimen is unloaded before application of the next higher load increment, as shown in Fig. 2-7(a). In the optional cyclic load sequence the 10% static preload is applied and removed. A load increment of one-third the expected ultimate load is then applied and removed, followed by an equal magnitude load in the reverse direction. The reversed load is then released to form a complete cycle, as shown in Fig. 2-7(b). Five cycles are completed at each one-third load increment specified in the static test until failure of the specimen. ASTM states that “The duration of load application at each increment shall be sufficient to permit load and deflection readings to be recorded.” This statement implies that the optional cyclic

loading procedure is a quasi-static test. Table 2-6 presents the sequence of loading of the ASTM E564 loading protocol.



a)



b)

Figure 2-7. ASTM E564 Loading Protocols, a) Static Loading Sequence, b) Cyclic Loading Protocol

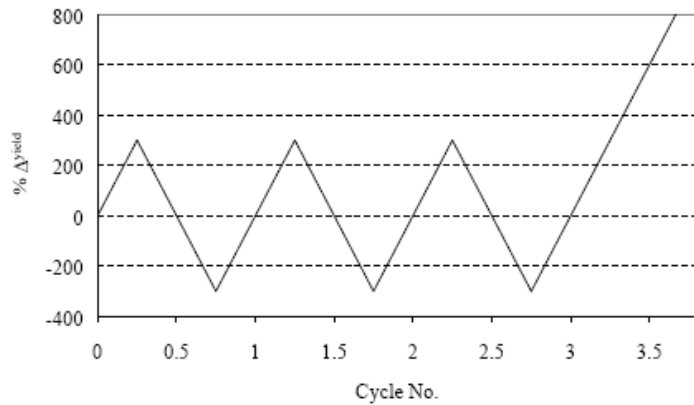
Table 2-6. Sequence of Loading of ASTM E564 Protocol

Static Loading Sequence		
Cycle Group	Number of Half Cycles	Amplitude (% F_u^*)
1	1	10
2	1	33
3	1	66
4	1	100
Cyclic Loading Sequence		
Cycle Group	Number of Cycles	Amplitude (% F_u^*)
1	1	10
2	5	33
3	5	66
4	5	100

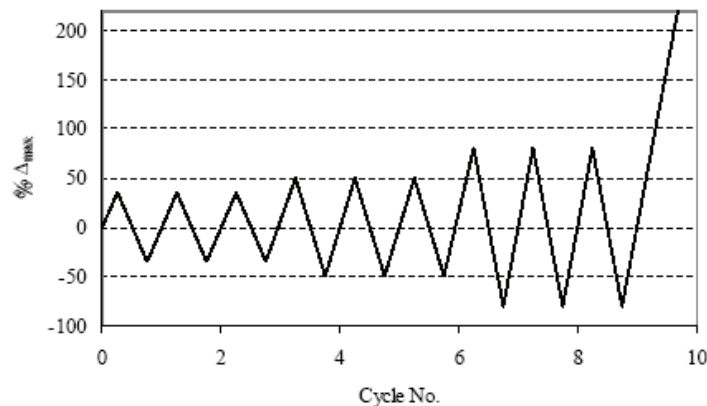
* F_u = Expected ultimate obtained from prior monotonic testing

The CEN Protocols (1995)

The Comité Européen de Normalisation (CEN) developed two protocols for the cyclic testing of wood connections: a short protocol and a long protocol (CEN, 1995). The short protocol consists of three equal amplitude cycles followed by a constant ramp load until failure. The amplitude of the three initial cycles is found by multiplying the yield displacement, or yield slip for wood connections, (Δ_{yield}) by an assumed ductility (D). An initial monotonic test must be performed to determine the yield slip. An example of a typical displacement history for $D = 3$ is given in Fig. 2-8(a). The CEN long protocol consists of three cycle groups with three equal amplitude cycles per group. The third cycle group is followed by a constant ramp load until failure. The amplitude of the first cycle group is equal to 35% of the ultimate load displacement (Δ_{max}) followed by 50% and 80% for the second and third cycle groups respectively, as shown in Fig. 2-8(b). Again, the displacement at maximum load must be found from previous monotonic testing. Also, the CEN provision stipulates that the rate of loading be held constant at a value between 0.02 and 0.2 mm/sec. Table 2-7 presents the sequence of loading of the CEN loading protocol.



(a) CEN Short



(b) CEN Long

Figure 2-8. CEN Loading Protocols, a) Short Protocol, $D = 3$, b) Long Protocol

Table 2-7. Sequence of Loading of CEN Protocols

Short Protocol		
Cycle Group	Number of Cycles	Amplitude (% Δ_{yield}^*)
1	3	100D ^{**}
2	---	Load until failure
Long Protocol		
Cycle Group	Number of Cycles	Amplitude (% Δ_{max}^{***})
1	3	35
2	3	50
3	3	80
4	---	Load until failure

* Δ_{yield} = Yield displacement or slip obtained from prior monotonic testing

** D = Assumed ductility of wood connection

*** Δ_{max} = Ultimate load displacement or slip obtained from prior monotonic testing

The ISO Protocol (1998)

Working Group 7 of the ISO Technical Committee on Timber Structures developed the ISO loading protocol (ISO 2003). Originally developed for wood connection testing, the procedure is also considered appropriate for the testing of woodframe shearwalls. The load history is based on the displacement at ultimate load (Δ_{max}) obtained from the mean values of prior monotonic tests. The amplitude of each cycle is a percentage of Δ_{max} , as shown in Fig. 2-9. Table 2-8 presents the sequence of loading of the ISO loading protocol.

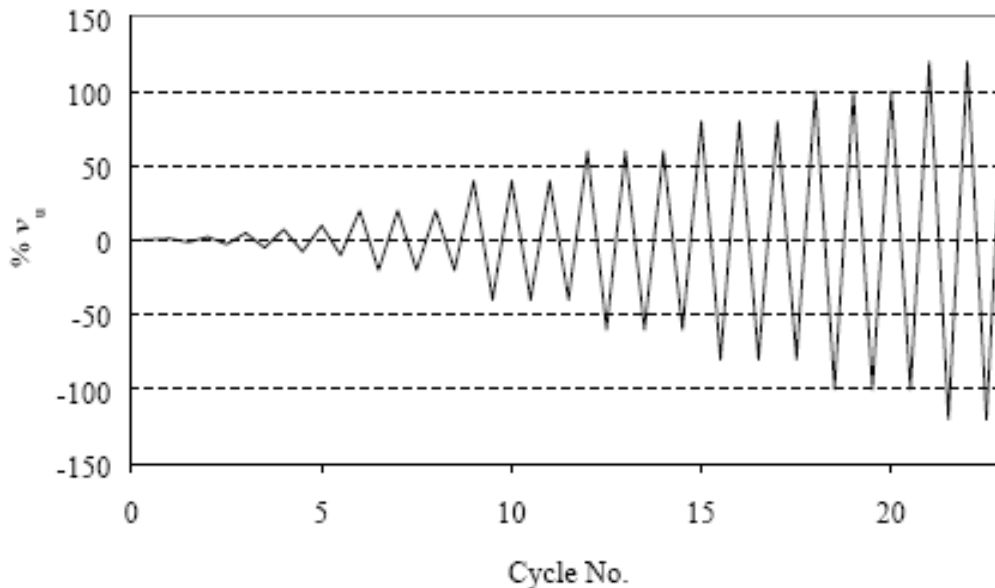


Figure 2-9. ISO Loading Protocol

Table 2-8. Sequence of Loading of ISO Protocol

Cycle Group	Number of Cycles	Amplitude (% Δ_{max}^*)
1	3	2.5
2	3	5.0
3	3	7.5
4	3	10.0
5	3	12.5
6	3	25.0
7	3	50.0
8	3	75.0
9	3	100.0
> 9	3	Increment of 25 % until failure

*** Δ_{max} = Ultimate load displacement obtained from mean value of prior monotonic tests

The CUREE-Caltech Protocol (2000)

As part of the CUREE-Caltech Woodframe Project, Krawinkler et al. (2000) developed new cyclic loading protocols intended for the testing of woodframe components. Based on a statistical analysis of the response peaks obtained from nonlinear dynamic analyses of hysteretic single-degree-of-freedom systems representative of wood structures under both ordinary and near-fault ground motions, two protocols were developed: a standard protocol and a near-fault protocol. Near-fault effects are not considered and only the standard loading protocol is reviewed herein

The standard protocol is based on a reference displacement (Δ) and contains three categories of cycles namely initiation cycles, primary cycles and trailing cycles. The reference displacement (Δ) is calculated as a fraction of the ultimate displacement (Δ_m) obtained from a prior monotonic test. Figure 2-10 provides an illustration of the calculation of Δ and Δ_m . The standard protocol begins with a sequence of six small initiation cycles intended to address cumulative damage from small earthquakes that would have occurred in the life of the specimen prior to a main seismic event. The initiation cycles are then followed by large amplitude cycles consisting of primary and trailing cycles, as shown in Fig. 2-11. The amplitude of each group of trailing cycles is equal to 75% of the amplitude of the corresponding main cycle. Table 2-9 presents the sequence of loading of the CUREE-Caltech loading protocol.

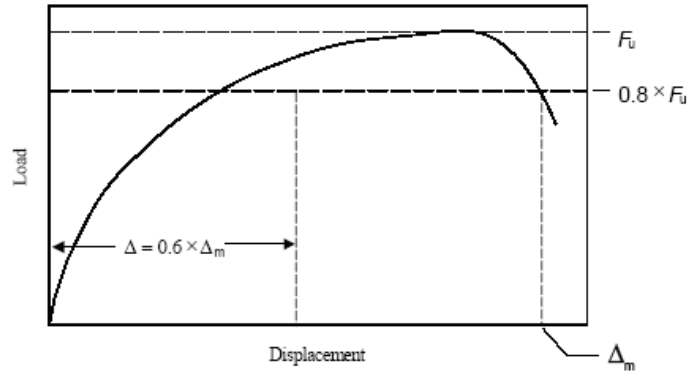


Figure 2.6 Calculation of Δ and Δ_m

Figure 2-10. Calculation of Δ and Δ_{max} for CUREE-Caltech Protocol

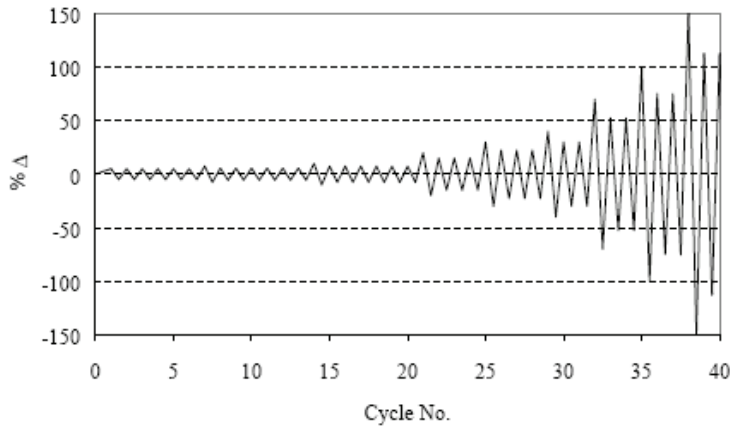


Figure 2-11. CUREE-Caltech Standard Protocol

Table 2-9. Sequence of Loading of CUREE-Caltech Protocol

Cycle Group	Primary Cycles		Trailing Cycles	
	Number	Amplitude (% Δ^*)	Number	Amplitude (% Δ^*)
1	6**	5	0	---
2	1	7.5	6	5.625
3	1	10	6	7.5
4	1	20	3	15.0
5	1	30	3	22.5
6	1	40	2	30
7	1	70	2	52.5
8	1	100	2	75%
9	1	150	2	112.5
> 9	1	Increment of 50% until failure	2	Increment of 37.5% until failure

* Δ = Reference displacement obtained from prior monotonic test (see Fig. 2-10)

** Initiation cycles

2.4 Cyclic Loading Protocols for Masonry Structures

The Sequential Phase Displacement (SPD) Protocol

The Sequential Phased Displacement (SPD) test protocol was developed by the Technical Coordinating Committee on Masonry Research (Porter, 1987). The SPD protocol was then adopted with minor modifications by the Structural Engineers Association of Southern California (SEAOSC) for woodframe shearwall testing. The protocol is based on the so-called First Major Event (FME), which can generally be considered as the displacement at which the structure starts to deform inelastically (anticipated yield displacement). Prior monotonic testing must be performed to determine the FME for the SPD protocol. The displacement history is composed of groups of stabilization and degradation cycles that are repeated at higher amplitudes, as shown in Fig. 2-12.

In order to monitor the elastic performance of the structure, the SPD procedure starts with three phases consisting of ordinary reversed cyclic displacement cycles at displacement levels smaller than the FME displacement. An initial displacement level of 25 percent of FME displacement, followed by 50 percent and 75 percent of FME for phase two and three, respectively. The displacement level of the fourth phase is then increased to 100 percent of the FME for the initial cycle, which is followed by three degradation and three stabilization cycles. The amplitude of each consecutive decay cycle decreases by a quarter of the initial displacement. The displacement then increases to the initial displacement level and is kept constant over sufficient cycles to obtain the stabilized response of the system. Stabilized response is defined as a decrease in load between two successive cycles of not more than 5 percent. The stabilized response is an important characteristic to assess structural performance after high wind events and during repetitive cyclic earthquake loading. Furthermore, the utilization of three cycles at the same displacement level allows the monitoring of the stiffness degradation of the system. All following phases consist of initial, decay, and stabilization cycles.

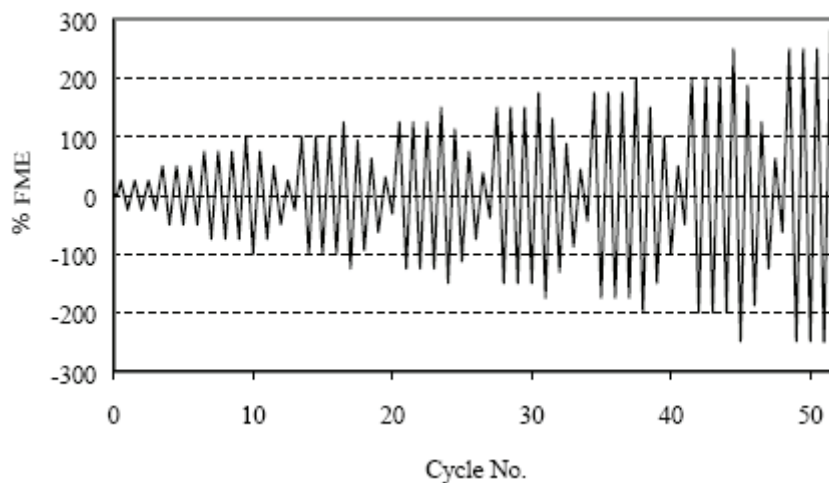


Figure 2-12. SPD Loading Protocol

2.5 ATC-58 Loading Protocol for Fragility Racking Testing of Nonstructural Components

As part of the ATC-58 project, Krawinkler et al. (2005) developed a loading protocol quasi-static cyclic testing of nonstructural components for the purpose of seismic performance assessment. In the context of performance assessment, the scope of this testing protocol is to provide data for the estimation of fragility functions of nonstructural components, which in turn will be used to estimate direct losses (repair or replacement costs, fatalities) or to establish criteria for adherence to specific functional criteria such as the need to declare the component unfit for a specified function.

The development of the ATC-58 protocol was based on statistical analyses of the response of structures to an ensemble of 20 “ordinary” (no near-fault effect) ground motion records. The set of records is the same one used to develop the CUREE-Caltech loading protocol for wood structures, as discussed above. This ensemble of ground motions was used to perform response history analysis of elastic and inelastic (with a target ductility of 3) SDOF systems and MDOF frame structures. Systems with periods of 0.2, 0.3, 0.5, 0.9, and 3.6 sec. were evaluated. For each system the deformation response (displacement for SDOF systems and story drift for MDOF systems) for each ground motion was re-arranged in excursions using the rain flow cycle counting method. The deformation range (peak-to-peak value) of each excursion was centered with respect to the origin (i.e., the deformation amplitude is assumed to be half of the range, which implies that mean effects are ignored) and was normalized to the amplitude of the largest excursion of the response. When ordered in magnitude, this resulted in a string of numbers from 2.0 on downwards, identifying the relative magnitudes of all excursions of the response. For the ensemble of records, statistical measures (median and 84th percentile) of each normalized range (the largest one, the second largest one, the third largest one, etc.) were computed, providing statistical values of the ranges relative to the largest one. These statistical values were then used as the basis to construct the loading history.

The resulting loading history of the ATC-58 protocol consists of cycles of step-wise increasing deformation amplitudes, as conceptually shown in Fig. 2-13. Two cycles per amplitude needs to be applied. The loading history is defined by the following four parameters:

- Δ_o = the targeted smallest deformation amplitude of the loading history (it must be safely smaller than the amplitude at which the lowest damage state is first observed, i.e., at the lowest damage state at least six cycles must have been executed). A recommended value for this amplitude (in terms of story drift index δ/h) is around 0.0015.
- Δ_m = the targeted maximum deformation amplitude of the loading history. It is estimated as the value at which the largest damage level is first observed. This value has to be estimated prior to the test (it can be estimated from a monotonic test). If the last damage state has not yet occurred at the target value, the loading history shall be continued by using further increments of amplitude of

$0.3\Delta_m$. A recommended value for this amplitude (in terms of story drift index δ/h) is 0.03.

- n = the number of steps (or increments) in the loading history. It shall be 10 or larger.
- a_i = the amplitude of the cycles, as they increase in magnitude, i.e., the first amplitude, a_1 , is Δ_0 (or a value close to it), and the last planned amplitude, a_n , is Δ_m (or a value close to it). Whenever possible, the test shall be continued beyond Δ_m even if the last damage state has been attained and shall be terminated only when the capabilities of the test set-up have been reached or the test specimen has degraded so severely that no relevant additional information about performance can be acquired.

The amplitude a_{i+1} of the step $i+1$ (not of each cycle, since each step has two cycles) is given by the following equation:

$$\frac{a_{i+1}}{a_n} = \left(1.4 \frac{a_i}{a_n} \right) \quad (1)$$

where a_i is the amplitude of the preceding step, and a_n is the amplitude of the step close to the target Δ_m .

If the specimen has not reached the final damage state at Δ_m , the amplitude shall be increased further by the constant increment $0.3\Delta_m$. A loading history with $a_n = \Delta_m$ and $a_1 = 0.048\Delta_m$ (i.e., $n = 10$, or $10 \times 2 = 20$ cycles) is shown in Fig. 2-14.

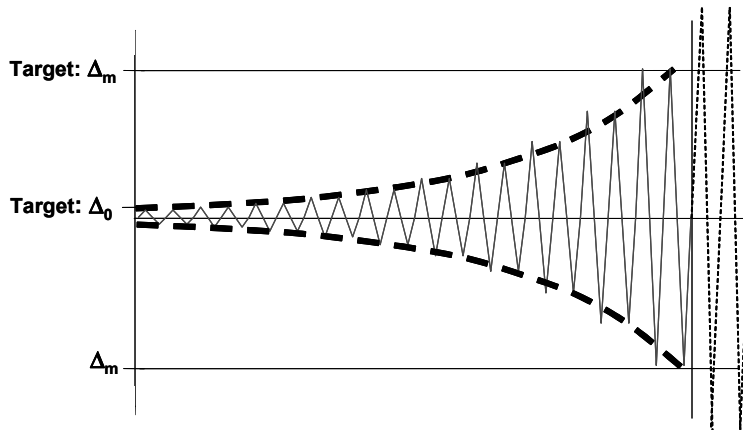


Figure 2-13. Conceptual Representation of the ATC-58 Loading Protocol

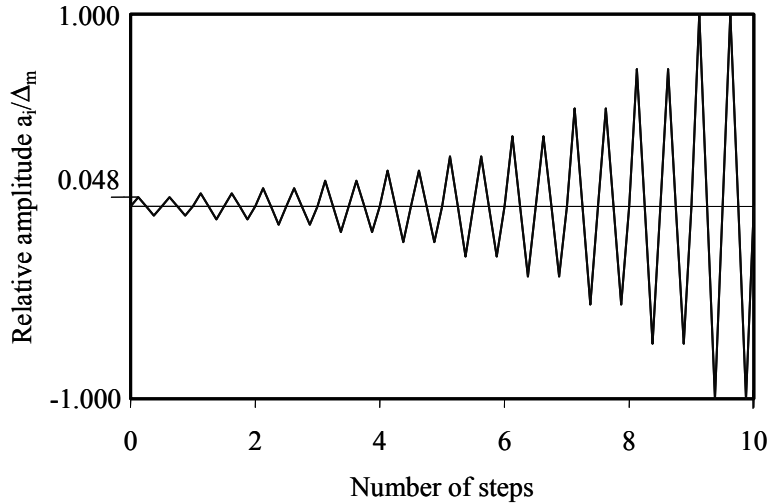


Figure 2-14. ATC-58 Loading Protocol $a_1 = 0.048\Delta_m$

2.6 Comparison of Test Protocols

In this section, the different loading protocols described in the previous sections are compared. The comparison is made in terms of the following parameters:

- Total number of cycles
- Number of initiation cycles
- Number of primary cycles
- Inclusion of trailing cycles
- Inclusion of repeating cycles
- Sequence of amplitudes of primary cycles
- Reference parameter
- Loading symmetry

The section concludes with a review of experimental results obtained with various testing protocols on similar test specimens.

Comparison of Total Number of Cycles

The total number of cycles of a loading protocol must be determined based on a balance between an estimation of the seismic energy transmitted by a seismic event to a test specimen and the time required to complete a test in the laboratory. For the cyclic numerical protocol, the same balance must be considered since the total number of loading cycles will also influence the computer time required to conduct each cyclic pushover analysis.

Figure 2-15 compares the total number of cycles for the 11 loading protocols reviewed. By far, the SPD protocol exhibits the largest total number of cycles. Attributed to this large number of cycles, which is mainly a result of the decay cycles, the energy demand of the SPD protocol is much higher than that of the other protocols and most likely much higher than the true energy demand observed in past earthquakes. It is suspected also that

the high number of cycles leads to failure modes, such as fastener fatigue, that have rarely been observed following earthquakes. Also shown in Fig. 2-15 is the mean total number of cycles across all protocols (23 cycles).

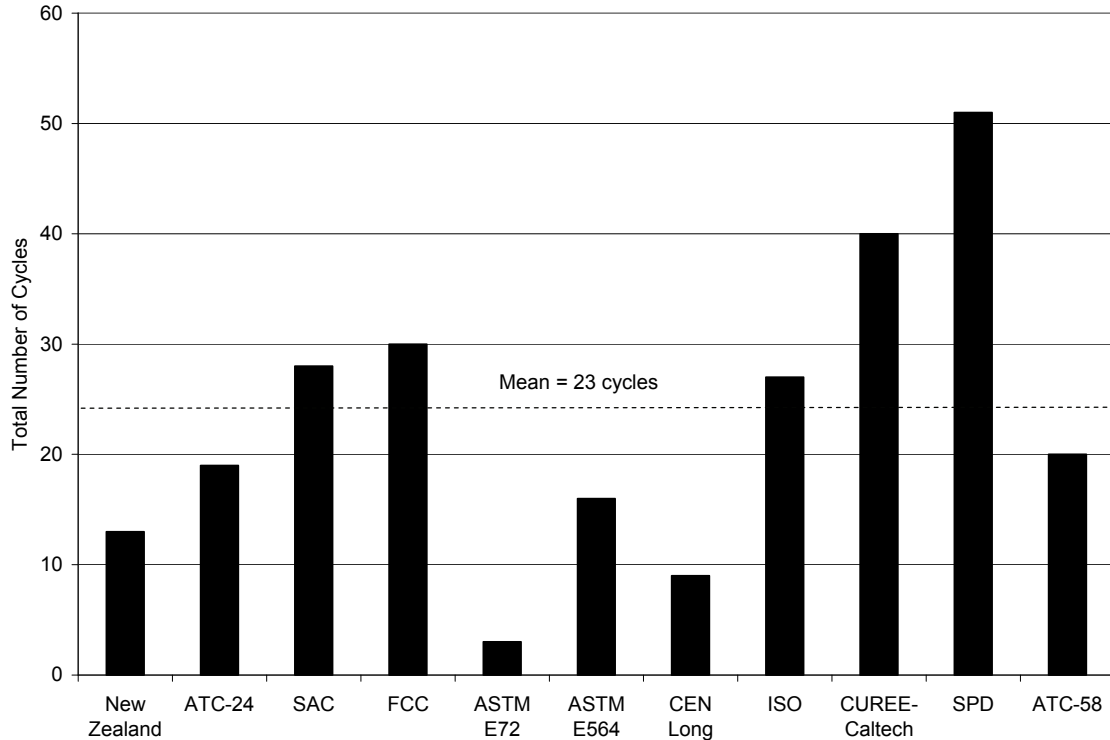


Figure 2-15. Total Number of Cycles for Loading Protocols

Comparison of Number of Initiation Cycles

Most protocols begin with a number of initiation cycles intended to represent the cumulative damage that the specimen would have suffered from small earthquakes that would have occurred in its life span to a main seismic event. For the cyclic numerical protocol, the number of initiation cycles will only influence building models incorporating hysteresis laws that behave nonlinearly over the entire deformation range. For hysteresis laws exhibiting inelastic response only beyond a specified yield deformation, the number of initiation cycles will have no influence since the response of the building model will be in the elastic range with its initial elastic stiffness and no damping capacity.

Figure 2-16 compares the number of initiation cycles for the 11 loading protocols reviewed. Only five protocols incorporate initiation cycles. The other six protocols, although may have some cycles resulting in elastic response of the test specimen, are based on fraction of ultimate displacements or deformation without specifying a yield level. Again, the SPD protocol exhibits the largest number of initiation cycles.

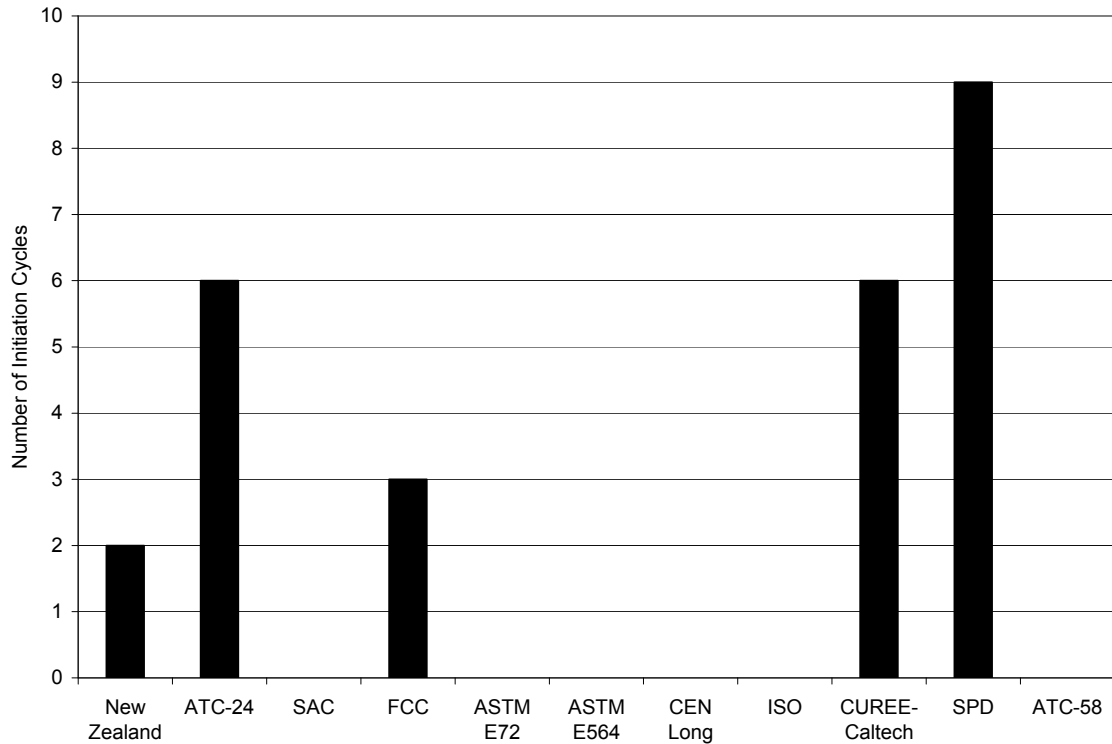


Figure 2-16. Number of Initiation Cycles for Loading Protocols

Comparison of Number of Primary Cycles

Primary cycles are intended to represent the largest response peak of a test specimen during a seismic event. Each primary cycle represents the first cycle pushing the hysteretic envelope of the test specimen to a new value of displacement or force. Primary cycles are obviously important for the cyclic numerical protocol since it is intended to capture the nonlinear response of building models of their entire nonlinear ranges. Figure 2-17 compares the number of primary cycles for the 11 loading protocols reviewed.

Inclusion of Trailing Cycles

The SPD, FCC and CUREE-Caltech protocols are the only three protocols that have “trailing cycles;” i.e. cycles that have amplitudes smaller than previous cycles. These trailing cycles may be more indicative of the behavior of actual seismic events and also allow for observation of the specimen response to these trailing cycles. For the cyclic numerical protocol, trailing cycles may not be relevant since the purpose is to evaluate the equivalent viscous damping of structural systems as a function of full cyclic response of increasing deformation amplitudes.

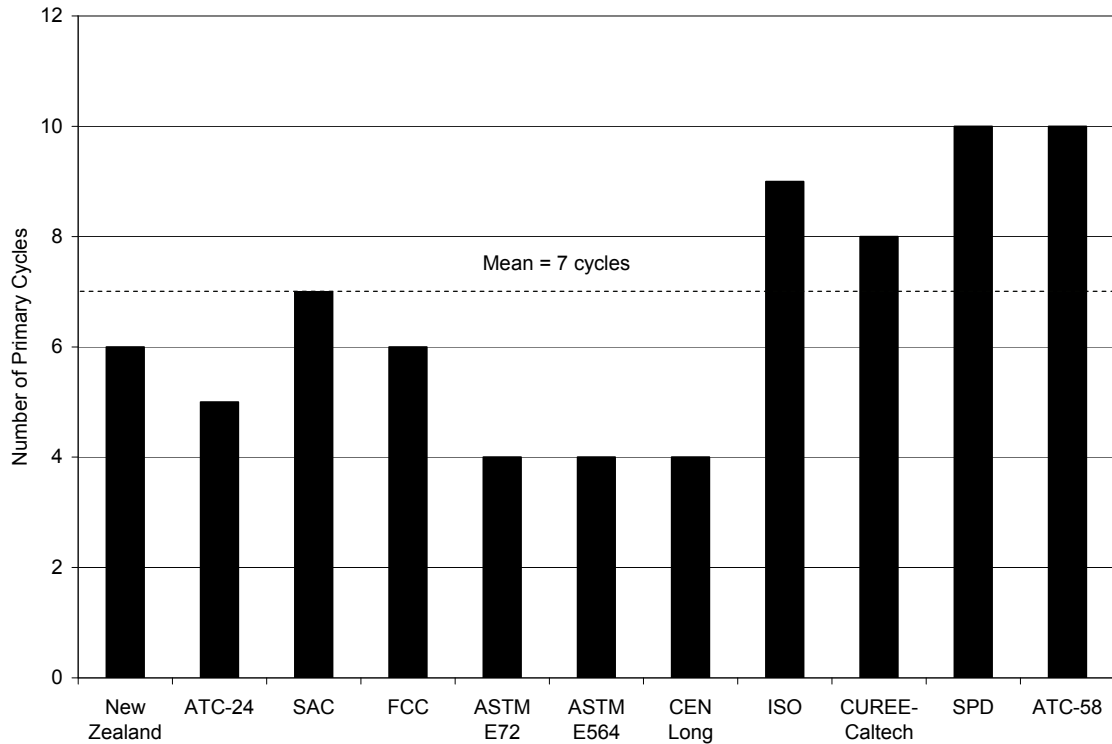


Figure 2-17. Number of Primary Cycles for Loading Protocols

Inclusion of Repeating Cycles

The New Zealand, ATC-24, SAC, FCC, ASTM E564, CEN, ISO, CUREE-Caltech and ATC-58 protocols have “repeating cycles;” i.e. cycles that have amplitudes similar as that of previous cycles. These repeating cycles may be useful to assess the strength and/or stiffness degradation of a test specimen under repeated cycles of constant amplitude. For the cyclic numerical protocol, repeating cycles may be important since the equivalent viscous damping characteristics of structural systems may be reduced with increasing number of cycles at constant amplitude. Figure 2-18 compares the maximum number of repeating cycles contained in each of the eight protocols listed above. Six of these eight protocols include a maximum of either two or three repeating cycles with a mean value of three repeating cycles.

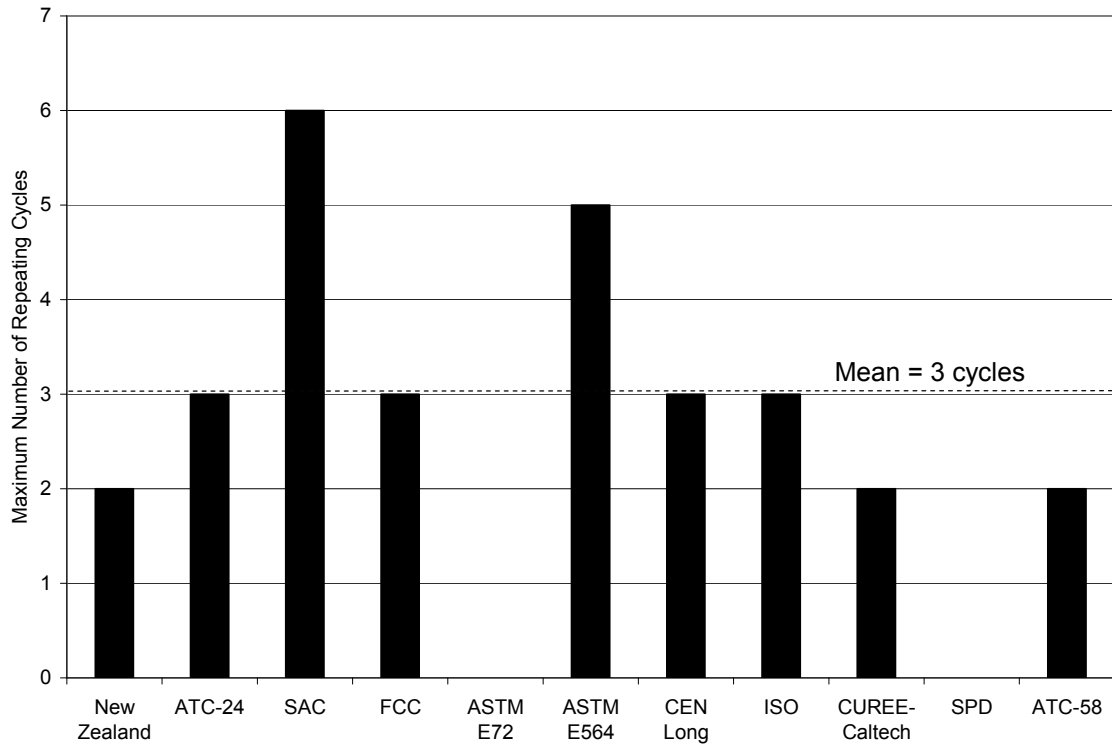


Figure 2-18. Maximum Number of Repeating Cycles for Loading Protocols

Rate of Amplitude Increase of Primary Cycles

The rate of amplitude increase of primary cycles is an important parameter for a loading protocol as this sequence can be related to the rate of input energy fed into a structure during an earthquake. If the rate of amplitude increase is too low, a large number of primary cycles will be required to achieve a target deformation level, which could lead to unrealistic failure mechanisms for seismic events (e.g., nail fatigues in wood shearwalls). Similarly, if the rate of amplitude increase is too high, a very small number of primary cycles will be required to achieve the same target deformation level. The development of a loading protocol for near-field seismic event would typically be characterized by a high rate of amplitude increase of primary cycles.

The rate of amplitude increase of primary cycles in a loading protocol can be characterized by the ratio a_i/a_1 , where a_i is the amplitude of a group of primary cycles i , and a_1 is the amplitude of the first group of primary cycles of loading. Figure 2-19 compares this ratio for the 11 loading protocols reviewed. The slope of each curve shown in Figure 2-19 represents the rate of amplitude increase of primary cycles of each corresponding loading protocol. As expected, the SPD protocol exhibits the lowest rate, while the ASTM E564 protocol exhibits the highest. The rate of amplitude increase of primary cycles increases after the first five primary cycle groups for most loading

protocols. The rate of amplitude increase of primary cycles of the CUREE-Caltech loading protocol matches fairly well the mean rate taken across the 11 loading protocols reviewed.

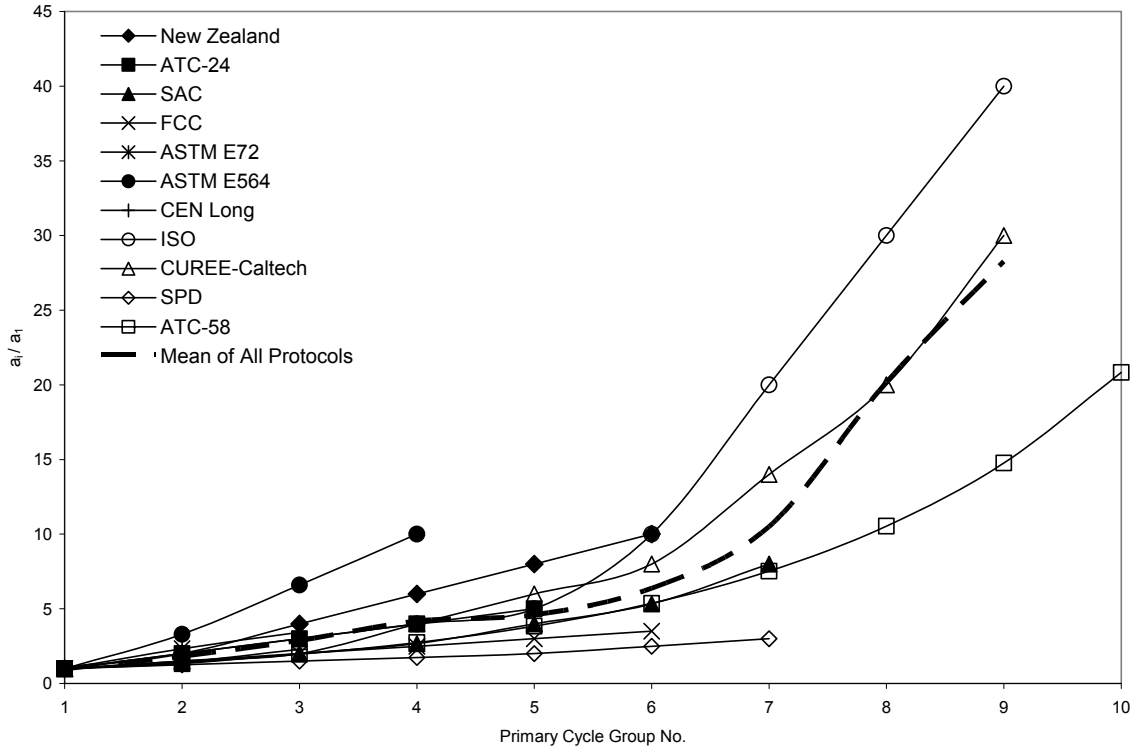


Figure 2-19. Amplitude Increase of Primary Cycles for Loading Protocols

Comparison of Reference Parameters

With the exception of the SAC and the ASTM E-72 protocols, a reference displacement determined from either prior monotonic testing or a prior estimate of the specimen response is required. The lack of a requirement for prior knowledge of the specimen behavior provides not only the advantage of convenience, but helps to provide consistency between different tests. The reference displacements for four of the protocols are based on the yield displacement (New Zealand, ATC-24, FCC and SPD) as opposed to the displacement at ultimate load. For the cyclic numerical protocol, the need of a preliminary monotonic pushover analysis is not a major disadvantage since the computer time required to perform such analysis is usually not excessive.

Loading Symmetry

The ASTM E72 protocol is the only protocol that is nonsymmetrical. Although earthquakes are never perfectly symmetric, they are often very close (except for near-fault earthquakes), hence, most loading protocols have been defined as symmetric. The symmetry also allows for observation of how the specimen responds to negative

excursions of the same amplitude as the positive excursions. For the cyclic numerical protocol, a symmetric loading history is required.

Experimental Comparison of Loading Protocols

Experimental studies involving various loading protocols on similar test specimens could be found only for wood structures. Because of the highly nonlinear and pinched hysteretic behavior of wood subassemblies and systems even at low deformations, the effect of the loading history of a given protocol will influence substantially their cyclic responses.

Yasumura (1999) applied both the CEN and the ISO protocols to bolted wood joints with steel side plates. He observed little variation of results of the two regimes in terms of displacement at capacity and peak load.

As part of the CUREE-Caltech Woodframe Project, Gatto and Uang (2003) tested standard 2.4m x 2.4m woodframe shearwalls using different loading protocols. The CUREE-Caltech protocol was compared with the SPD and ISO protocols. Findings from the research indicated that the loading protocol has a significant influence on shearwall performance. Protocols with a large number of cycles (SPD) tended to produce nail fatigue fractures, which were not nearly as prevalent in protocols with lower numbers of cycles (CUREE-Caltech and ISO). The research clearly showed that the nail fatigue fractures were associated with a large energy demand related to the number of cycles, which resulted in a reduced ultimate strength and deformation capacity. Note that nail fatigue fractures have rarely been observed following earthquakes. The initial stiffness of the specimens was relatively unaffected by the loading protocol used. These findings are in agreement with previous findings obtained by He et al. (1998) in Canada.

SECTION 3

REVIEW OF NUMERICAL CYCLIC PUSHOVER ANALYSES

Only a few numerical investigations that involved cyclic pushover analyses could be found and are reviewed in this section.

Nathan et al. (1995) developed a finite element model to predict the nonlinear behavior of the historic Cesar E Chavez Avenue Bridge in the city of Los Angeles. This bridge structure consists of a combination of reinforced concrete flat slabs, tee beams, box girders and an arch bridge. The finite element model incorporated nonlinear beam elements in conjunction with special purpose concrete and rebar constitutive models. A unique aspect of the pushover analysis technique used was that the bridge was cycled transversely and longitudinally to evaluate the bridge's cyclic behavior and predict damage associated with hysteretic degradation. The numerical results obtained were used to develop retrofit schemes that would prevent a collapse of the structure in a major earthquake yet maintain its original architectural values.

Filiatrault et al. (2003, 2004) performed monotonic and cyclic pushover analyses along the two orthogonal directions of four full-scale woodframe building models. The main objective of these analyses was to estimate the equivalent secant lateral stiffness and viscous damping ratios of woodframe buildings as a function of building drift. From these analyses, simple design equations were obtained for these parameters to be implemented in a direct-displacement based seismic design strategy for woodframe buildings. Because this study is highly relevant to the ATC 63 Project, some details of the analysis procedure and results obtained are discussed below.

From a preliminary monotonic pushover analysis, the roof (building) drift δ_{\max} corresponding to the maximum base shear was identified for each building configuration. A cyclic pushover analysis was then performed using a modified version of the CUREE-Caltech loading protocol. Only two repetitions of each primary cycles contained in the CUREE-Caltech loading protocol were applied since the hysteretic model used for the wall elements of the structure included a strength and stiffness degradation that stabilize after the second cycle at a given deformation amplitude (Filiatrault et al., 2003, 2004). As shown in Fig. 3-1 for one particular primary cycle amplitude, the stiffness degradation and pinching response of the structure are evident. Also, the stiffness and energy dissipation characteristics are much different in the first cycle than in the other cycles.

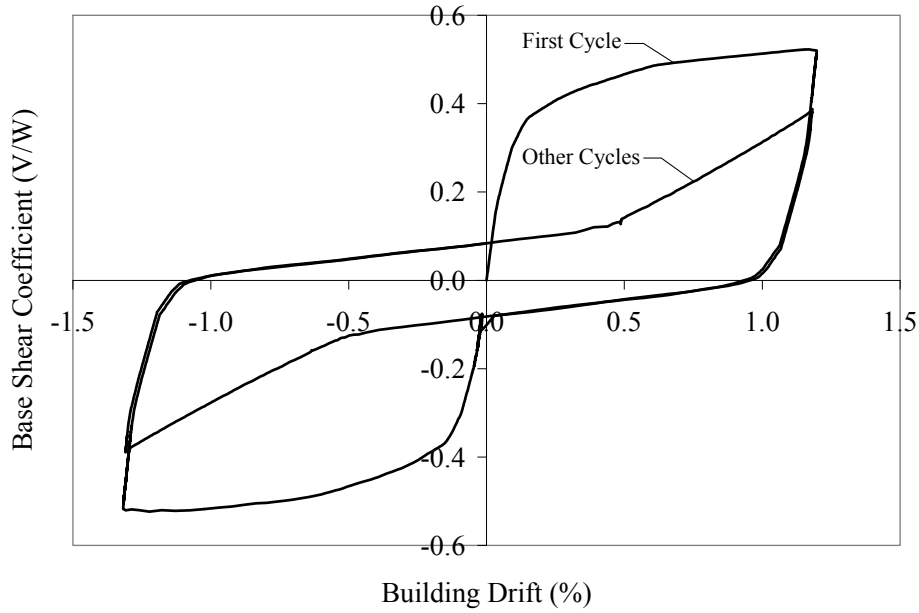


**Figure 3-1. Cyclic Pushover Curve for Woodframe Apartment Building
(from Filiatrault et al., 2004)**

For each building model and drift level, the ratio k_s/k_o , where k_o is the initial lateral stiffness of the building and k_s the corresponding secant lateral stiffness, was computed. The results of this analysis are shown in Fig. 3-2. The variation of secant lateral stiffness with building drift ratio for all of the woodframe buildings analyzed falls within a fairly narrow band. Consequently, this variation is not strongly dependent on the building configuration. Analytically, this variation was represented adequately by two piece-wise linear segments, as follows:

$$\frac{k_s}{k_o} = \begin{cases} -2.4 \frac{\delta}{\delta_{\max}} + 1 & \text{for } \frac{\delta}{\delta_{\max}} \leq 0.33 \\ -0.2 \left(\frac{\delta}{\delta_{\max}} - 0.33 \right) + 0.21 & \text{for } \frac{\delta}{\delta_{\max}} > 0.33 \end{cases} \quad (2)$$

Assuming first mode response, Equation (2) was transformed into a period variation equation:

$$\frac{T_s}{T_o} = \begin{cases} \frac{1}{\sqrt{-2.4 \frac{\delta}{\delta_{\max}} + 1}} & \text{for } \frac{\delta}{\delta_{\max}} \leq 0.33 \\ \frac{1}{\sqrt{-0.2 \left(\frac{\delta}{\delta_{\max}} - 0.33 \right) + 0.21}} & \text{for } \frac{\delta}{\delta_{\max}} > 0.33 \end{cases} \quad (3)$$

where T_s is the secant period corresponding to the target drift level δ , and T_o is the initial (elastic) fundamental period.

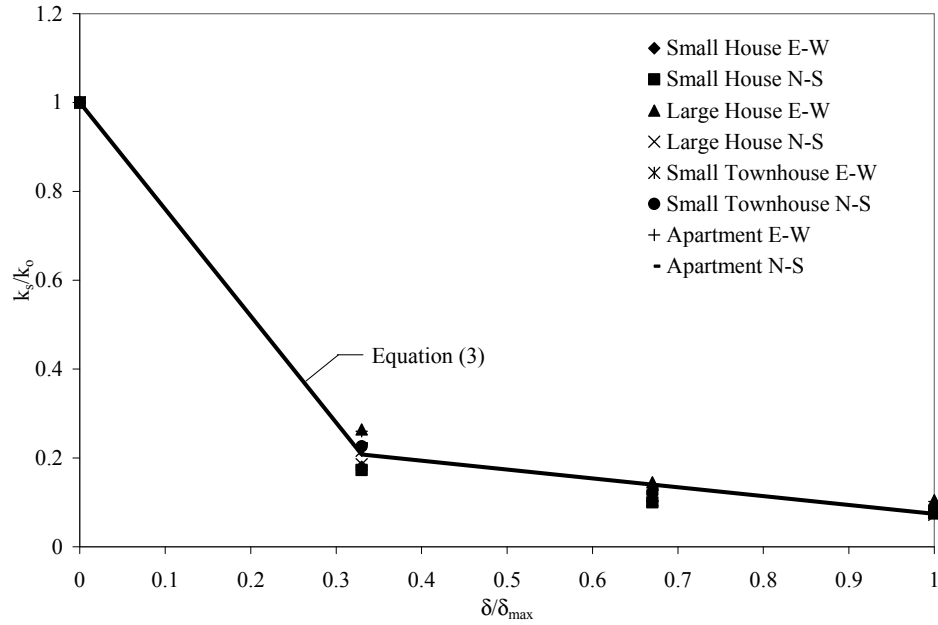


Figure 3-2. Normalized Secant Lateral Stiffness versus Normalized Drift Levels for Woodframe Buildings (from Filiatrault et al., 2004)

In order to capture the energy dissipation characteristics of each building configuration at a given building drift ratio δ , an equivalent viscous damping ratio ζ_{eq} , representative of the hysteretic damping in the structure, was computed from the global hysteretic behavior of each woodframe building configuration:

$$\zeta_{eq} = \frac{E_{D\delta}}{2\pi k_s (\delta h)^2} \quad (4)$$

where $E_{D\delta}$ is the energy dissipated per cycle at the building drift ratio δ , k_s is the overall equivalent (secant) lateral stiffness of the building at the same drift level, and h is height of the building from the ground level to the roof eaves.

Equation (4) was applied twice to compute ζ_{eq} , once over the first hysteretic cycle, and then over the second cycle. The resulting values of ζ_{eq} for all index buildings and drift levels are shown in Fig. 3-3.

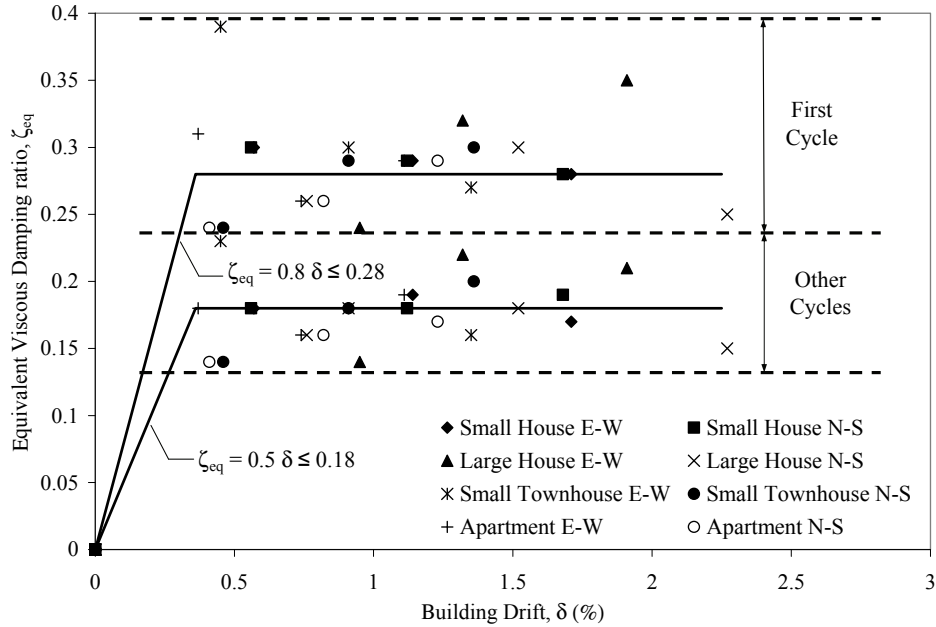


Figure 3-3. Equivalent Viscous Damping Ratios of Woodframe Buildings (from Filiatrault et al., 2004)

The equivalent damping ratios are significantly higher (in the vicinity of 30% of critical) for the first cycle calibration than for the second cycle calibration (in the vicinity of 20% of critical). Over the range of building drifts considered, the equivalent viscous damping ratio remains fairly constant with building drift ratio. Consequently, the variation of equivalent viscous damping ratio ζ_{eq} with building drift ratio δ can be represented reasonably accurately by the following empirical formulas:

$$\zeta_{eq} = \begin{cases} 0.8\delta & \text{for } \delta \leq 0.35 \\ 0.28 & \text{for } \delta > 0.35 \end{cases} \quad (5)$$

for the first hysteretic cycle and:

$$\zeta_{eq} = \begin{cases} 0.5\delta & \text{for } \delta \leq 0.35 \\ 0.18 & \text{for } \delta > 0.35 \end{cases} \quad (6)$$

for all other cycles.

Note that the linear variation of ζ_{eq} , given in Equations (5) and (6), only applies for small values of building drift ratio (less than 0.35%). Numerical data supporting this linear variation in ζ_{eq} was established in a previous study (Filiatrault et al., 2003). This linear relationship is included in the specification of ζ_{eq} since initial cracking of nonstructural wall finishes, such as gypsum wallboards and stucco, can occur at drift level less than 0.35% (Deierlein and Kanvinde, 2003). If cracking of nonstructural wall finishes is not part of the performance matrix, the constant values of ζ_{eq} specified in Equations (5) and (6) can be used.

SECTION 4

RECOMMENDED NUMERICAL CYCLIC LOADING PROTOCOL FOR QUANTIFYING BUILDING PERFORMANCE

4.1 Criteria

From the above review of experimental loading protocols and analytical studies using cyclic pushover analysis, a numerical cyclic loading protocol is recommended based on the following criteria:

- The numerical cyclic loading protocol should be based on similar criteria used to develop experimental cyclic loading protocols since the cyclic analyses to be conducted can be viewed as a “numerical experiments.”
- The numerical cyclic loading protocol should be applicable to all types of building structures and should be independent of the types of structural materials. Therefore, the numerical protocol should be an “average” protocol of the experimental loading protocols reviewed above.
- Since the cyclic analyses will be conducted on models of complete building systems, the proposed numerical cyclic loading protocol should be based on a reference displacement obtained from a preliminary pushover analysis of the building model. The most natural reference displacement to be used is the lateral displacement at the roof of the building model.
- The total number of cycles of the proposed numerical cyclic loading protocol should be close to the mean total number of cycles for the 11 experimental loading protocols reviewed (i.e. 23 cycles as shown in Fig. 2-15).
- The proposed numerical cyclic loading protocol should not include initiation cycles since these initiation cycles will only mobilize the elastic response of the building model, without providing any useful information on its hysteretic response.
- The number of primary cycles of the proposed numerical cyclic loading protocol should be close to the mean number of primary cycles for the 11 experimental protocols reviewed (i.e. 7 primary cycles as shown in Fig. 2-17).
- Although experimental cyclic loading protocol required to generate appropriate mathematical hysteretic models of structural components and systems may require the inclusion of trailing cycles, the proposed numerical cyclic loading protocol itself need not to include trailing cycles since the main objective of the cyclic pushover analyses is to capture the nonlinear response of building models with increasing displacement amplitude.
- The proposed numerical cyclic loading protocol should include repeating cycles. The number of repeating cycles should depend on the type of hysteretic models used. If the hysteretic models exhibit strength and/or stiffness degradation with repeated cycles at the same deformation level, the number of repeating cycles should be equal to two if the hysteresis loops stabilize after the second cycle or three if the loops stabilize after three or more cycles.

- The rate of amplitude increase of primary cycles of the proposed numerical cyclic loading protocol should be similar to that of the CUREE-Caltech loading protocol since this protocol is close to the mean rate of amplitude increase of primary cycles for the 11 loading protocol reviewed, as shown in Fig. 2-19.

4.2 Proposed Numerical Cyclic Protocol

The proposed numerical cyclic loading protocol will first consist of a preliminary monotonic pushover analysis, as shown in Fig. 4-1, in order to establish the expected failure roof displacement (Δ_f) of the building model. The expected failure roof displacement corresponds to a fraction (α) of the maximum base shear (V_{max}) computed. The expected failure displacement should be calibrated based on the results of incremental dynamic analyses, as an interim, a value of $\alpha = 0.80$ is suggested.

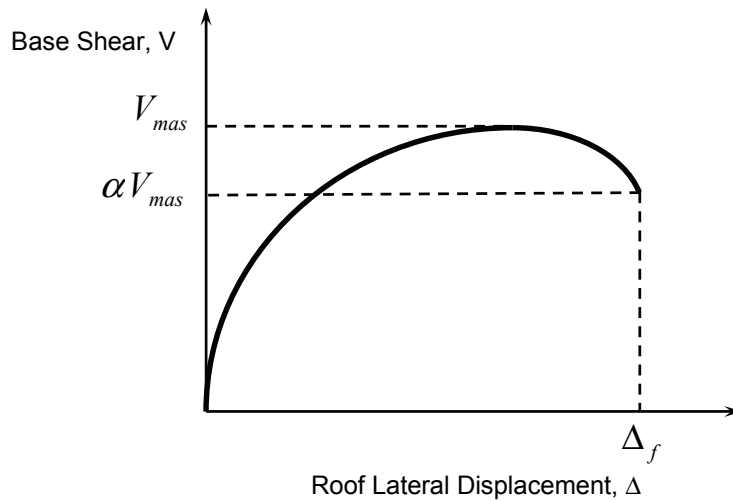


Figure 4-1. Calculation of Δ_f for Proposed Numerical Cyclic Loading Protocol

Once the expected failure roof displacement (Δ_f) is established, the general loading sequence of the proposed numerical loading protocol is established as a fraction of Δ_f , as shown in Fig. 4-2 and Table 4-1.

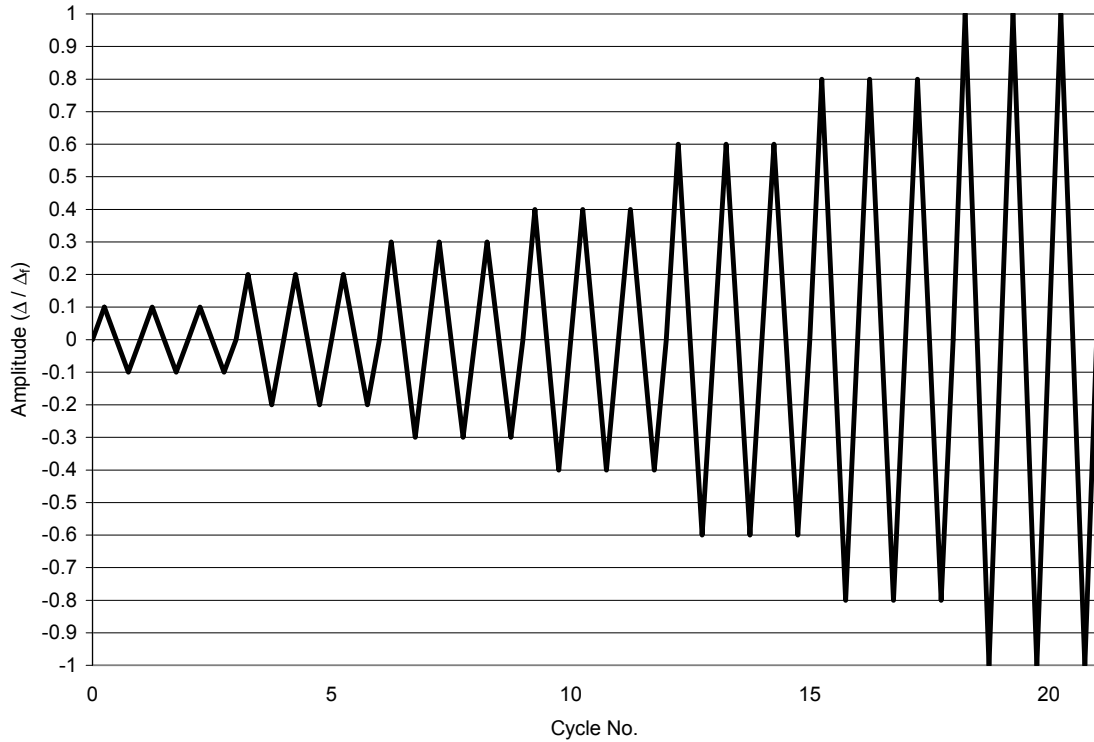


Figure 4-2. Proposed Numerical Cyclic Loading Protocol

Table 4-1. Sequence of Loading of Proposed Numerical Cyclic Loading Protocol

Cycle Group	Number of Cycles	Roof Displacement Amplitude
1	3	$0.10\Delta_f$
2	3	$0.20\Delta_f$
3	3	$0.30\Delta_f$
4	3	$0.40\Delta_f$
5	3	$0.60\Delta_f$
6	3	$0.80\Delta_f$
7	3	$1.0\Delta_f$

The total number of cycles for the proposed numerical cyclic loading protocol is 21, which is close to the mean value of 23 cycles for the 11 loading protocols reviewed.

The proposed numerical cyclic loading protocol contains seven primary cycles, which is equal to the mean number of primary cycles for the 11 experimental loading protocols reviewed.

The proposed numerical cyclic loading protocol contains three repeating cycles for each amplitude of primary cycles. If the strength and/or stiffness degradation of the hysteretic models used stabilize after only two cycles, the number of repeating cycles can be reduced to two. Furthermore, if the hysteretic models used do not exhibit any strength and stiffness degradation, the repeating cycles can be eliminated.

Figure 4-3 compares the rate of amplitude increase of primary cycles of the proposed numerical cyclic loading protocol with that of the CUREE-Caltech loading protocol and the mean rate of increase for the 11 experimental loading protocols reviewed. The three rate of increase curves shown in Fig. 4-3 agree reasonably well.

The proposed numerical cyclic loading protocol, while consistent with experimental cyclic loading protocols, contains a large number of cycles. This may be inappropriate for degrading systems, for which the protocol may generate lower strengths and displacement capacities. Accordingly, alternative protocols consisting of a reduced number of cycles will be investigated in Section 6.

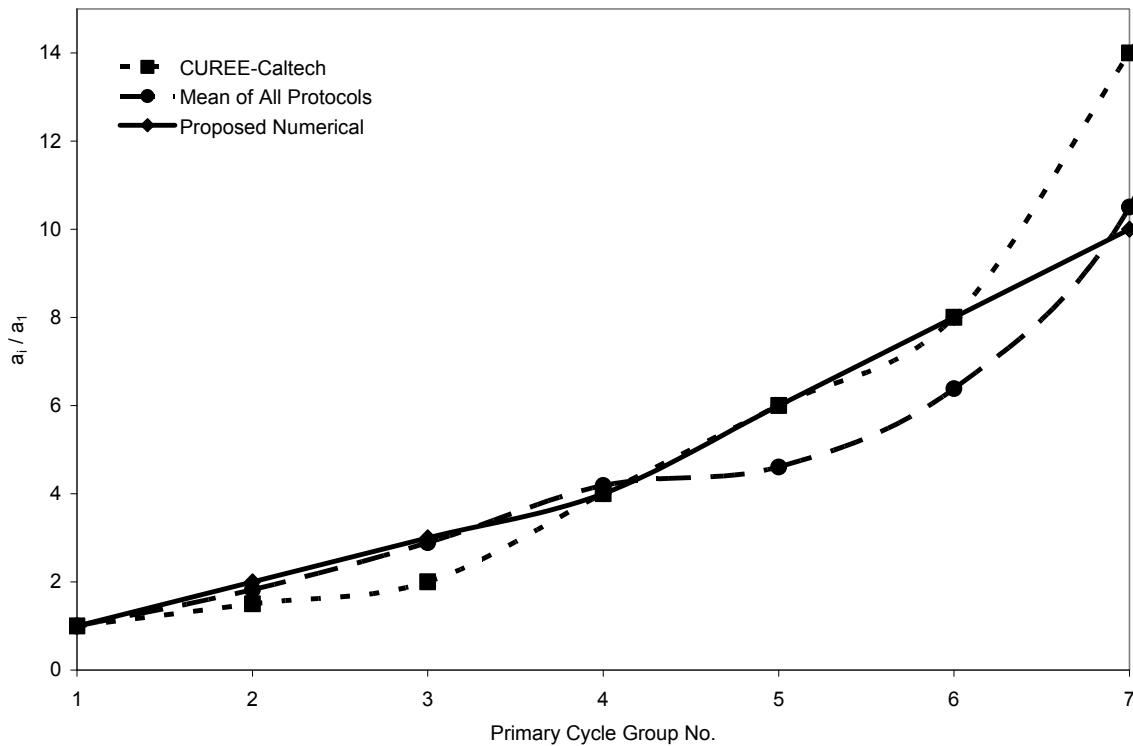


Figure 4-3. Amplitude Increase of Primary Cycles for Proposed Numerical Cyclic Loading Protocols

SECTION 5

LATERAL LOAD DISTRIBUTION FOR CYCLIC PUSHOVER ANALYSIS

The numerical cyclic loading protocol proposed in Section 4 implies that the lateral loading should be implemented using a displacement-based pushover procedure. Note that the recommended numerical cyclic loading protocol is based on experimental cyclic protocols that are typically conducted as displacement-controlled experiments.

The direct application of displacement-based pushover analysis without adaptation in each step could conceal important structural characteristics such as strength irregularities (Antoniou and Pinho, 2004). While it is desirable to implement the numerical cyclic pushover using a displacement-based pushover analysis (and particularly an adaptive displacement-based method), the option is not currently available in most computer programs. Moreover, current pushover analysis methods in various resource documents do not consider displacement-based pushover analysis procedures (e.g., FEMA, 1997, 2005). Accordingly, only force-based pushover analysis procedures were considered.

A review and evaluation of nonlinear static analysis procedures in FEMA 440 (FEMA, 2005; Krawinkler et al., 2005) resulted in the conclusion that the best estimates of displacements were obtained when force-based pushover analysis procedures were used with load vectors being either proportional to the first mode under elastic conditions or having an inverse triangular shape. Moreover, use of adaptive load vectors produced results comparable to those based on the inverse triangular and the first-mode load vectors. This conclusion is similar to the one arrived by Ramirez et al. (2001) in the study of structures with supplemental damping systems.

The cyclic pushover analysis is implemented herein using a force-based procedure with a load vector proportional to the first mode of the analyzed structure under elastic conditions. This approach is consistent with the conclusions of the FEMA 440 study (FEMA, 2005; Krawinkler et al., 2005). The approach is implemented by applying an increasing load vector causing a deformed shape of the structural system equals to its elastic first mode until the roof displacement reaches the value prescribed in the loading protocol. This is then followed by unloading using a decreasing load vector and then the process is repeated in accordance with the proposed numerical cyclic protocol.

Higher mode effects are not considered in this approach. These effects can be incorporated on the basis of the modified modal pushover analysis procedure described in FEMA 440.

SECTION 6

ANALYSIS OF 4-STORY REINFORCED CONCRETE SPECIAL MOMENT FRAME

6.1 Scope

For the purpose of estimating the seismic response of structural systems based on the proposed numerical cyclic loading protocol and alternative protocols, the structure is modeled as a single-degree-of-freedom (SDOF) system with effective (secant) lateral stiffness and viscous damping properties representative of the global behavior of the actual structure at a target roof displacement. In this section, the influence of the number of repeating cycles (referred herein as cyclic dwell) of the proposed numerical cyclic loading protocol on the equivalent (secant) elastic lateral stiffness and viscous damping properties for a 4-story reinforced concrete building model is investigated.

6.2 Four-story Special Moment-Resisting Reinforced Concrete Frame Building

Figure 6-1 presents the geometry of the building model considered in the sensitivity study. This model was used by Haselton et al. (2006) to investigate the collapse mechanisms of building structures using Incremental Dynamic Analysis (IDA). The building consists of 24 in. by 24 in. to 30 in. by 30 in square columns. Beam depth varies from 32 to 42 in. The model represents a 4-story special moment-resisting concrete frame building with member end plasticity incorporating both stiffness and strength degradation. This hysteretic element end model captures four different modes of cyclic deterioration: basic strength deterioration, post-cap strength deterioration, unloading stiffness deterioration, and accelerated reloading stiffness deterioration. Further details of this hysteretic element end model are given by Ibarra (2003).

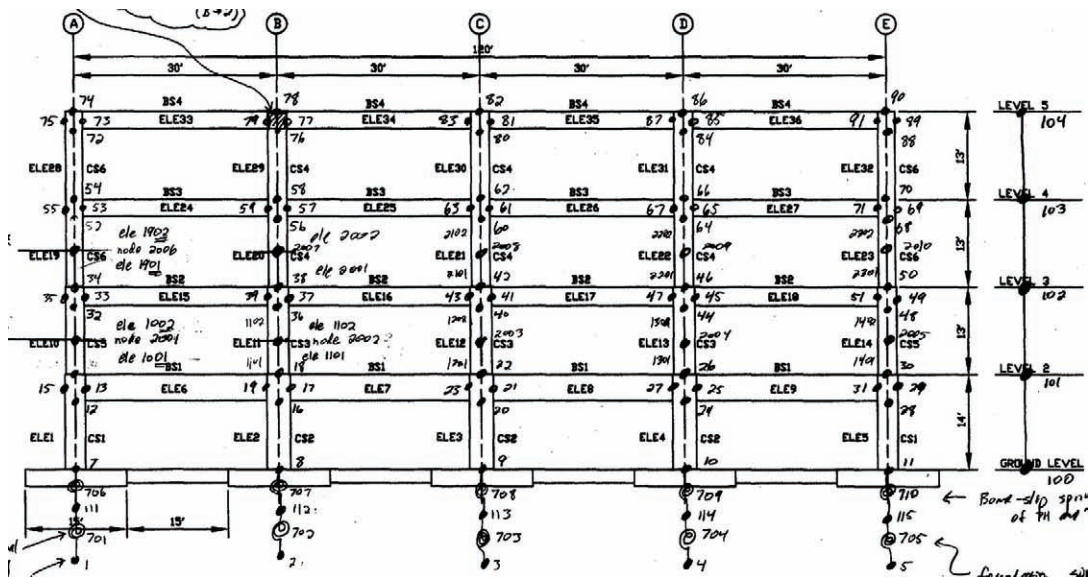


Figure 6-1. Special Moment-Resisting 4-Story Concrete Frame Building Model (Haselton et al., 2006a)

Table 6-1. Lumped Tributary Weights and Modal Properties of Analyzed 4-story Special Moment Frame

Floor	Weight (kips)	Mode 1 (T = 1.35sec)	Mode 2 (T = 0.46sec)	Mode 3 (T = 0.25sec)	Mode 4 (T = 0.17sec)
4 (roof)	1675	1.000	-0.925	-0.676	0.307
3	1717	0.793	0.217	1.000	-0.681
2	1748	0.488	1.000	-0.060	1.000
1	1810	0.204	0.677	-0.940	-0.864

Table 6-1 presents the modal properties of the frame under elastic conditions obtained with the computer program OpenSees. Included in this table are lumped tributary weight per level (or floor), natural periods (T) and modal floor displacements for the first four modes of vibration. Note that the modal floor displacements presented in the table are for horizontal degrees of freedom at the indicated floor.

6.3 Monotonic Pushover Analysis

Before performing the sensitivity study using the proposed numerical cyclic loading protocol and other protocols, a monotonic pushover analysis is performed on the building model. For this purpose a lateral load distribution producing a deformed shape of the building model corresponding to its first elastic mode of vibration is utilized. Figure 6-2 shows the result of the monotonic pushover analysis. For the purpose of this study, it is assumed that the failure roof drift occurs when the lateral force equals 80% of the peak base shear. From Fig. 6-2, a peak base shear of 1729 kips and a roof drift of 5.2% (33.1 in) correspond to this failure point.

6.4 Cyclic Loading Protocols

Three different versions of the proposed numerical cyclic loading protocol are considered in the sensitivity analysis, as illustrated in Fig. 6-3. Each version contains the same sequence of primary cycles but each includes a different number of repeating cycles (referred herein as cyclic dwell). The first version of the loading protocol (cyclic dwell = 1) includes only the sequence of primary cycles without any repeating cycles. The second version of the loading protocol (cyclic dwell = 2) includes one repeating cycle following each primary cycle. Finally, the third version of the loading protocol (cyclic dwell = 3) includes two repeating cycles following each primary cycle. Moreover, for comparison purposes, a fourth “arbitrary” cyclic loading protocol is used that contains a total of ten cycles, without any repeating cycles and with the amplitude increasing by $0.1\Delta_f$ in each cycle. This arbitrary protocol is also illustrated in Fig. 6-3.

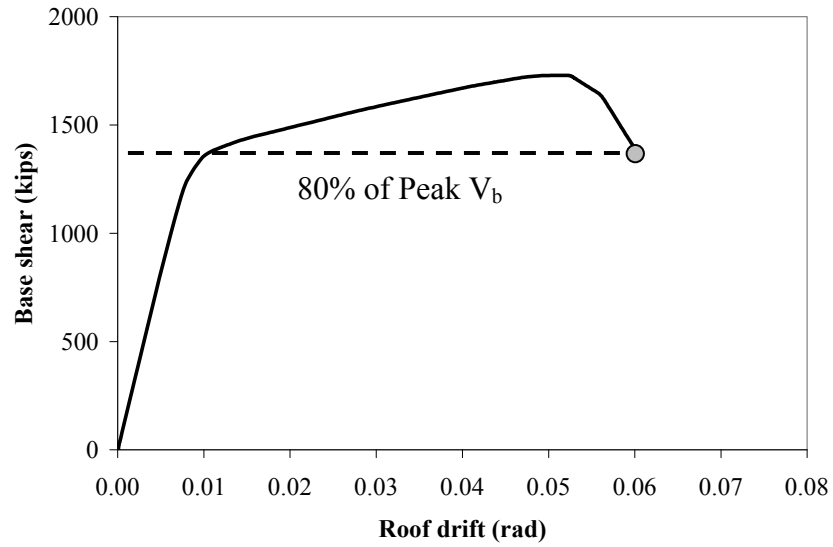


Figure 6-2. Result of Monotonic Pushover Analysis of 4-story SMF

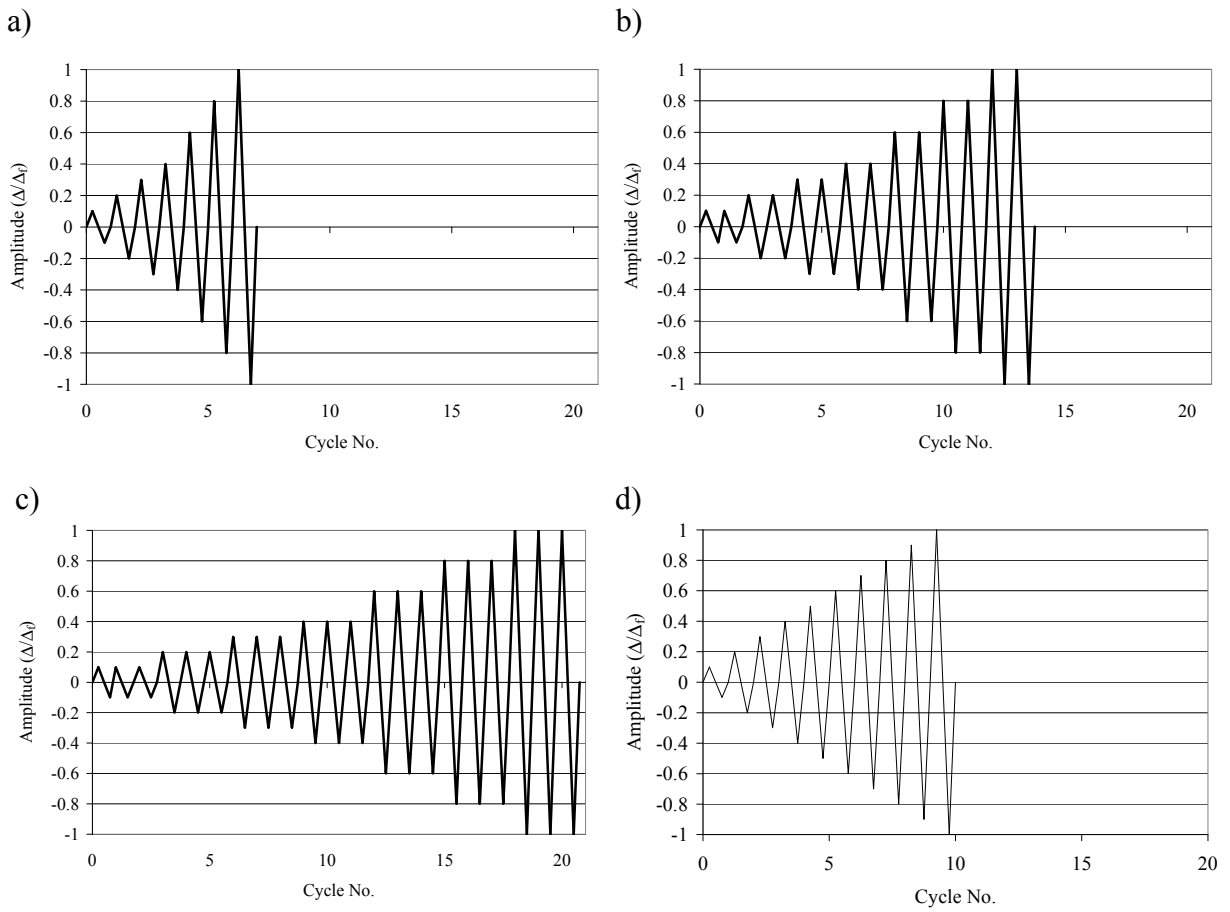


Figure 6-3. Numerical Cyclic Loading Protocols used for 4-story SMF, a) Cyclic Dwell 1, b) Cyclic Dwell 2, c) Cyclic Dwell =3, and d) Arbitrary Protocol

6.5 Cyclic Pushover Analyses

Figure 6-4 presents the results of the cyclic pushover analyses performed on the building model using the three different versions of the proposed numerical loading protocol and the fourth arbitrary protocol. The monotonic pushover curve obtained previously is included on each graph for comparison purposes. The strength and stiffness degradations induced by the cyclic loading protocol are significant. These degradations are more significant as the number of repeating cycles is increased, which is one of the main characteristics of the hysteretic model used for the beams and columns end plasticity (see Section 6.2).

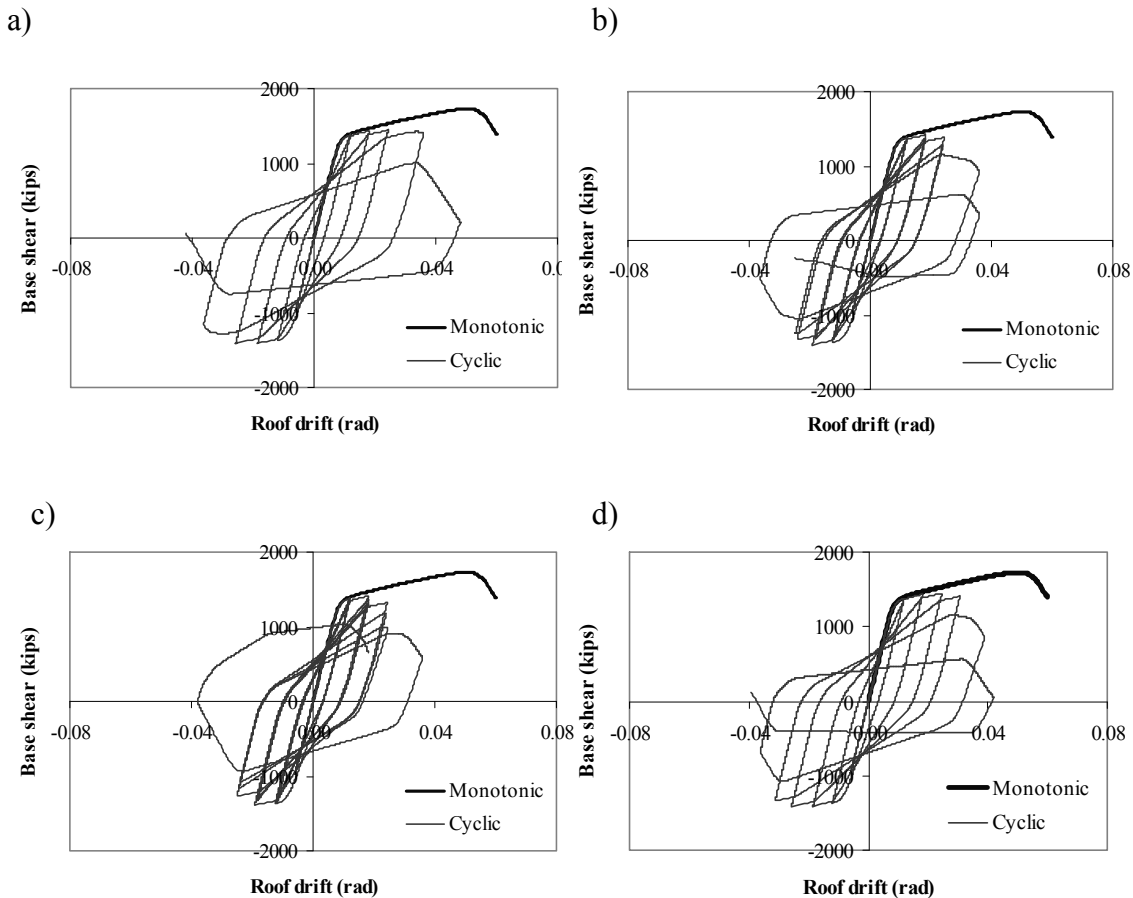


Figure 6-4. Results of Cyclic Pushover Analyses for 4-story SMF, a) Cyclic Dwell 1, b) Cyclic Dwell 2, c) Cyclic Dwell 3, d) Arbitrary Protocol

6.6 Sensitivity of Effective Lateral Stiffness

For each global hysteresis loop obtained for the cyclic pushover analyses shown in Fig. 6-4, the global effective (secant) lateral stiffness of the building, k_{eff} , is obtained through:

$$k_{eff} = \frac{|F^+| + |F^-|}{|U^+| + |U^-|} \quad (7)$$

where F^+ is the force at maximum positive displacement U^+ and F^- is the force at maximum negative displacement U^- . Note that the effective stiffness line is shown in Figure 6-5 not to pass through the origin of the axes, which is the case of hysteresis loops that lack anti-symmetry. Such condition arises in systems in which significant degradation of strength and stiffness occurs over small increments of displacement.

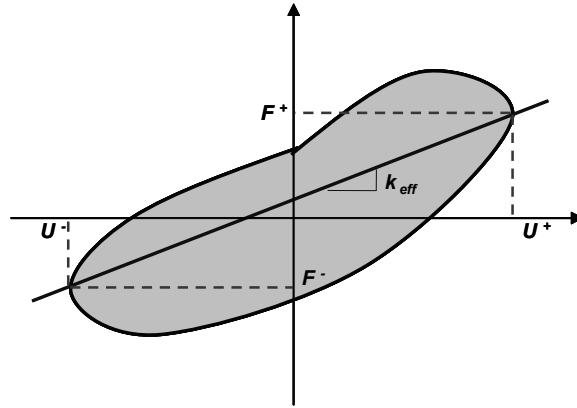


Figure 6-5. Definition of Effective Lateral Stiffness

The variation of effective lateral stiffness with roof displacement could then be plotted. Since the structure is modeled as an equivalent SDOF system, it is useful to plot the variation of effective lateral stiffness with effective spectral displacement. For this purpose, the effective spectral displacement, S_d , can be simply obtained from:

$$S_d = \frac{\Delta_r}{\Gamma_1} \quad (8)$$

where Δ_r is the roof lateral displacement and Γ_1 is the first modal participation factor of the structure

$$\Gamma_1 = \frac{\sum_{i=1}^N w_i \phi_i}{\sum_{i=1}^N w_i \phi_i^2} \quad (9)$$

where w_i is the weight at level i , N is the number of levels ($N = 4$ in the case of the structure of Figure 6-1) and ϕ_i is the first mode modal displacement at level i . Using the data in Table 6-1 for the structure of Fig. 26, $\Gamma_1 = 1.312$.

Figure 6-6 presents the variations of the effective lateral stiffness of the building model with S_d for all the hysteresis loops generated by the three versions of the proposed loading protocol. The stiffness values are normalized to the initial (elastic) lateral

stiffness of the building model, $k_i = 253$ kips/in. The results are presented for each group of primary and repeating cycles of the three versions of the proposed loading protocol as well as for the fourth arbitrary protocol. The number of repeating cycles only has minimal effect on the variation of k_{eff} with S_d . Also shown in Fig. 6-6 are smooth interpolated functions of the form:

$$0 \leq \frac{k_{eff}}{k_i} = -a_1 \ln S_d + a_2 \leq 1 \quad (10)$$

for the proposed numerical cyclic protocol, where the best fit values of a_1 and a_2 are listed in Table 6-2, and:

$$0 \leq \frac{k_{eff}}{k_i} = 1.5091 \cdot e^{-0.1257S_d} \leq 1 \quad (11)$$

for the fourth arbitrary protocol.

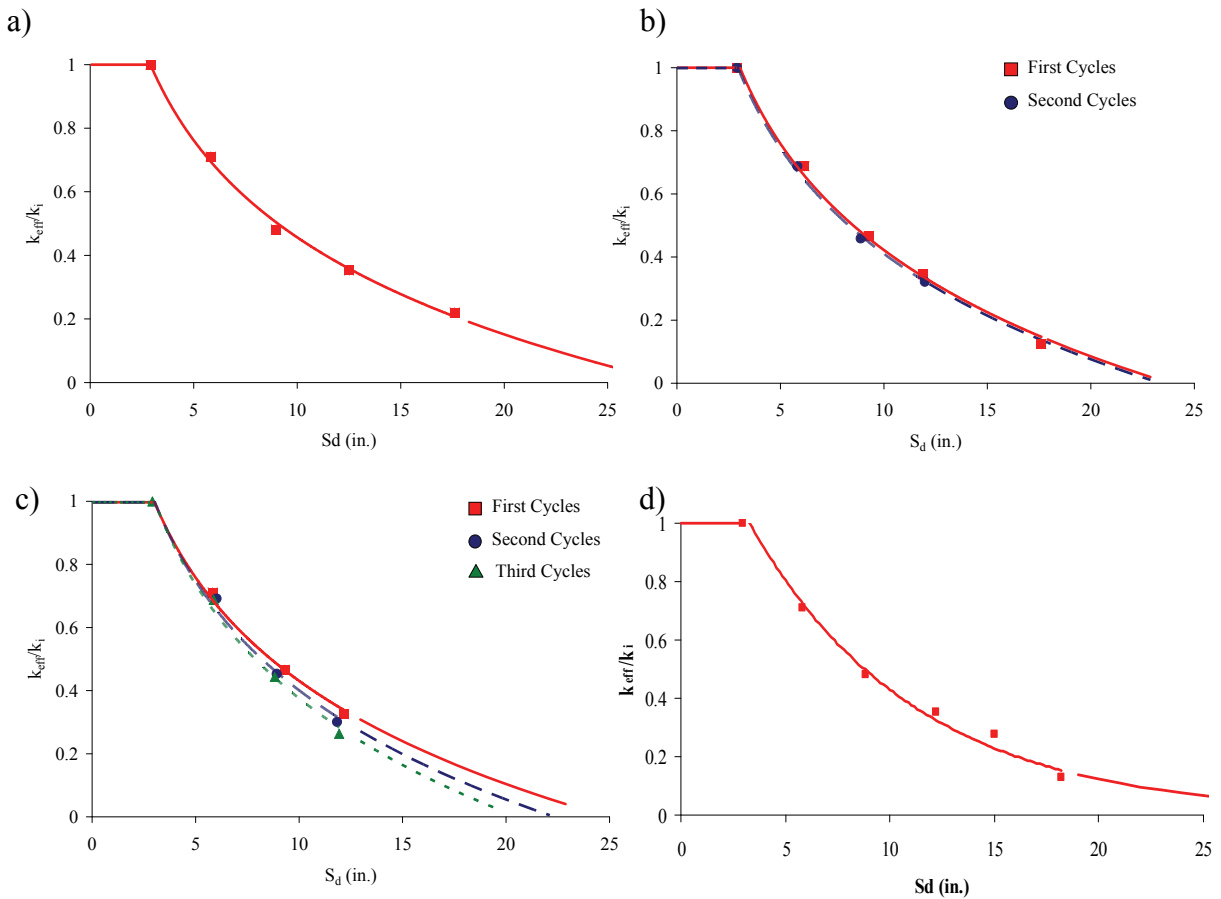


Figure 6-6. Effective Stiffness as Function of Spectral Displacement of 4-story SMF, a) Cyclic Dwell 1, b) Cyclic Dwell 2, c) Cyclic Dwell 3, d) Arbitrary Protocol

While the results of Fig. 6-6 demonstrate that the effective stiffness is accurately interpolated by Equations (10) and (11), the extrapolated stiffness may be slightly

overestimated. This is better observed in the spectral capacity curves presented in Appendix B.

Table 6-2. Best Fit Values of Constants in Equation (10) for 4-story SMF

Protocol	Cycles	a_1	a_2
Cyclic Dwell 1	1	0.44	1.47
Cyclic Dwell 2	1	0.49	1.54
	2	0.48	1.52
Cyclic Dwell 3	1	0.47	1.52
	2	0.50	1.55
	3	0.52	1.57

6.7 Sensitivity of Spectral Capacity Curves

The effective secant stiffness values shown in Fig. 6-6 can be used to construct effective spectral capacity curves for the building model considered. For this purpose, the spectral capacity curve is defined as the envelope (or backbone curve) of the cyclic pushover curves for the building model expressed in terms of effective SDOF spectral acceleration, S_a , and spectral displacement, S_d . The effective spectral displacement, S_d , was already obtained from the roof lateral displacement per Equation (8). The effective spectral acceleration, S_a , can be obtained by:

$$S_a = \frac{k_{\text{eff}} \Gamma_1 S_d}{\bar{W}_1} \quad (12)$$

where \bar{W}_1 is the first modal weight

$$\bar{W}_1 = \Gamma_1 \sum_{i=1}^N w_i \phi_i \quad (13)$$

For the structure of Figure 6-1 and based on the data of Table 11, $\bar{W}_1 = 5587 \text{kip}$.

Figure 6-7 presents the spectral capacity curves for the building model based on the three versions of the proposed numerical cyclic loading protocol and the fourth arbitrary protocol. The effect of repeating cycles on the spectral capacity curve of the building model considered is moderate. The peak spectral acceleration based on first cycles when no repeating cycles are present (Cyclic Dwell = 1) is reduced by 8% when two repeating cycles are introduced (Cyclic Dwell = 3). When one repeating cycle is introduced (Cyclic Dwell = 2), the peak spectral acceleration based on second cycles is 3% less than the peak spectral acceleration based on first cycles. A more pronounced strength degradation is observed when 2 repeating cycles are introduced (Cyclic Dwell = 3), where the peak spectral acceleration based on third cycles is 9% less than the peak spectral acceleration based on first cycles. The spectral capacity curve for the fourth arbitrary protocol is

almost identical to that obtained with the first cycles of the proposed numerical cyclic protocol since the arbitrary protocol does not include repeating cycles.

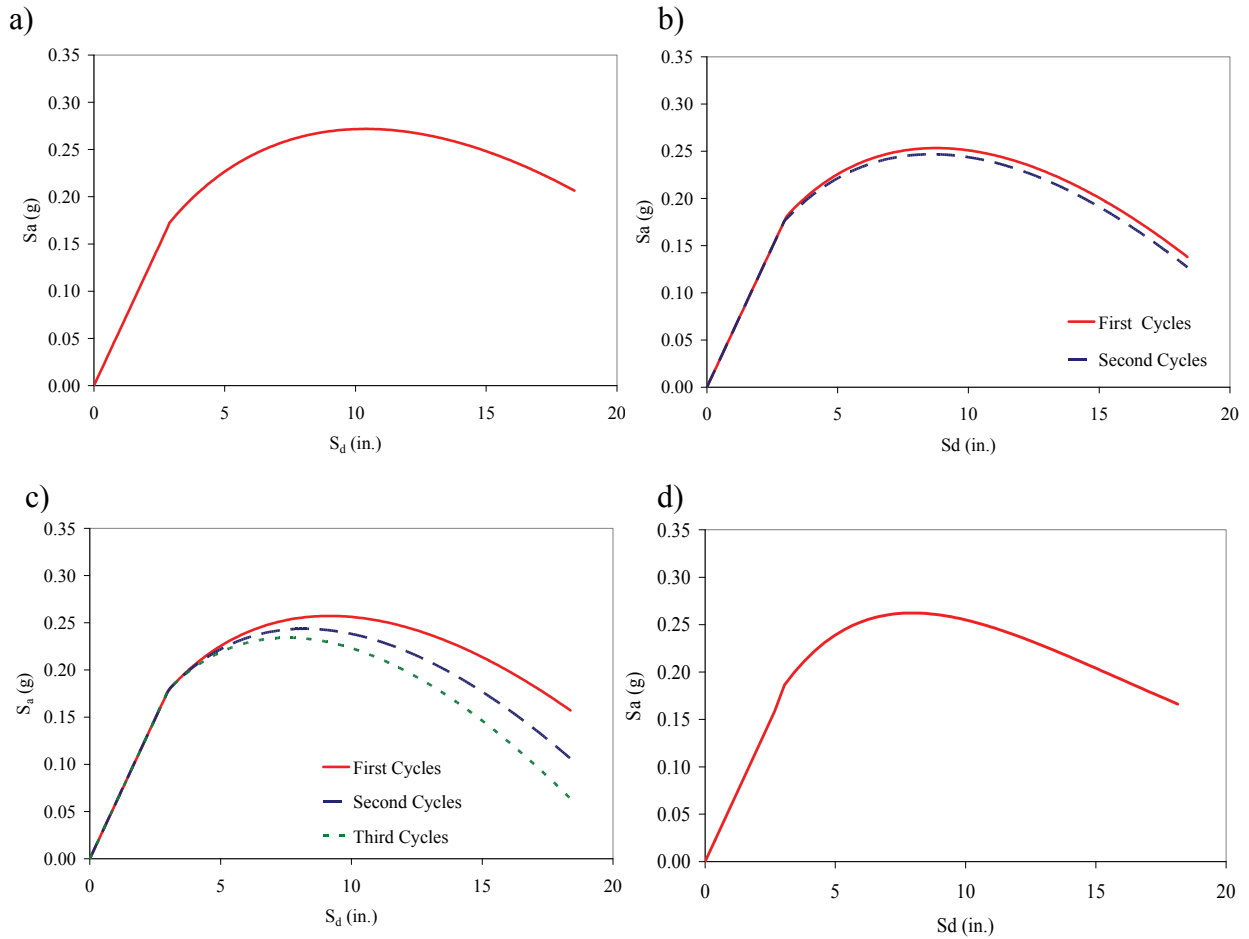


**Figure 6-7. Spectral Capacity Curves of 4-story SMF,
a) Cyclic Dwell 1, b) Cyclic Dwell 2, c) Cyclic Dwell 3, d) Arbitrary Protocol**

6.8 Sensitivity of Hysteretic Energy

The energy dissipated by hysteresis actions during a given cyclic response of the building model loaded by the proposed numerical cyclic loading protocol and by the arbitrary protocol can be obtained by computing the area under the corresponding hysteresis loop, as illustrated by the shaded area in Fig. 6-5. The variation of this hysteretic energy, E_h , with effective spectral displacement, S_d , can then be obtained. Figure 6-8 presents these variations for all the hysteresis loops of the three versions of the proposed loading protocol.

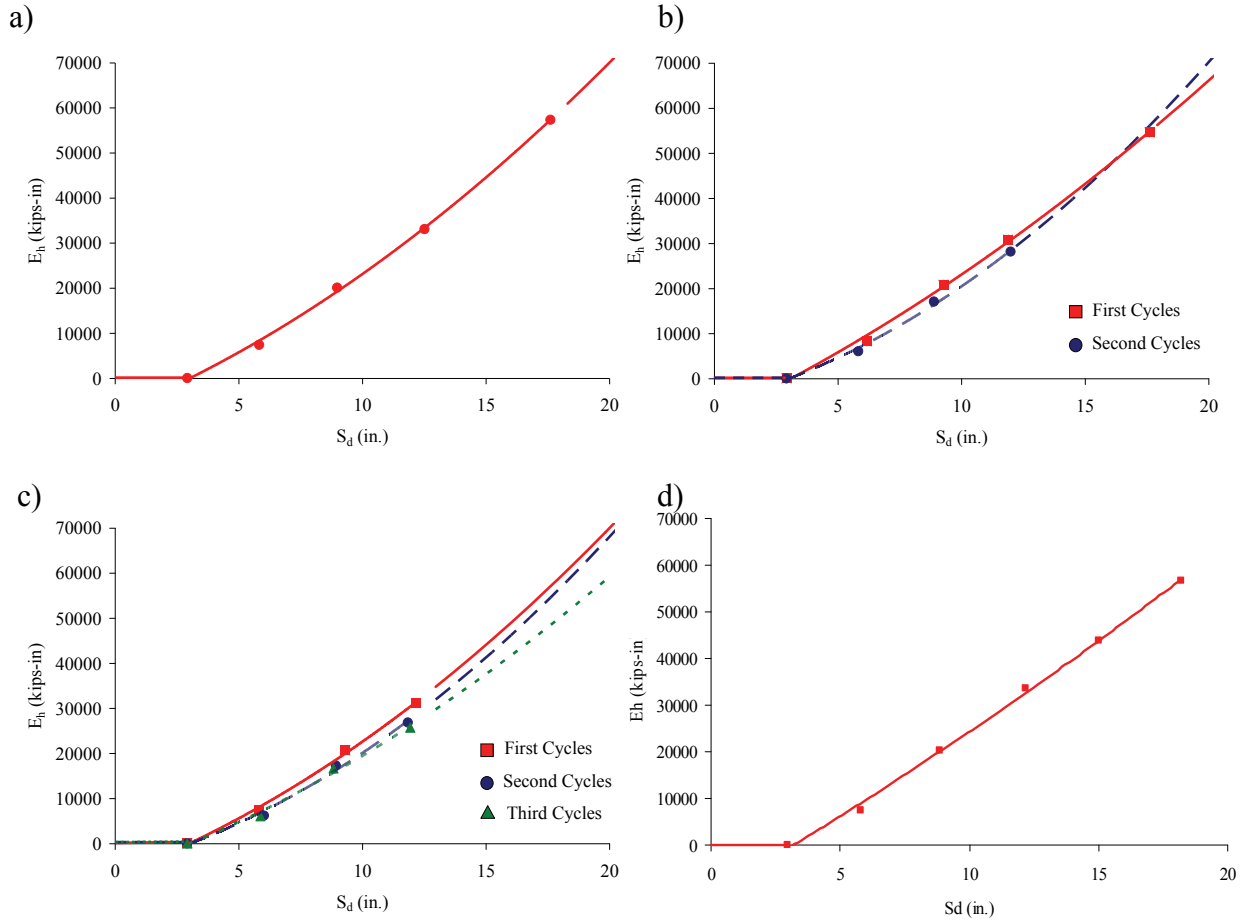


Figure 6-8. Variations of Hysteretic Energy Dissipated by 4-story SMF with Spectral Displacement, a) Cyclic Dwell 1, b) Cyclic Dwell 2, c) Cyclic Dwell 3, d) Arbitrary Protocol

The number of repeating cycles only has a very minor effect on the variation of E_h with S_d . Also shown in Fig. 6-8 are smooth interpolated functions of the form:

$$E_h = b_1 S_d^2 + b_2 S_d - b_3 \geq 0 \quad (14)$$

where the best fit values of b_1 , b_2 and b_3 are listed in Table 6-3.

Table 6-3. Best Fit Values of Constants in Equation (14) for 4-story SMF

Protocol	Cycles	b_1	b_2	b_3
Cyclic Dwell 1	1	81.3	2252.7	7473.6
Cyclic Dwell 2	1	56.8	2600.6	8534.5
	2	120.5	1361.0	5154.4
Cyclic Dwell 3	1	89.0	2067.9	6918.4
	2	112.6	1420.4	5327.0
	3	69.7	1889.1	6362.2
Arbitrary	1	28.9	3179.2	10430.0

6.9 Sensitivity of Equivalent Viscous Damping Ratio

By expressing Equation (4) in terms of effective spectral values and substituting Equation (14), an explicit expression for the equivalent viscous damping ratio, ζ_{eq} , can be obtained:

$$0.05 \leq \zeta_{eq} = \frac{E_h}{2\pi k_{eff}(\Gamma_1 S_d)^2} = \frac{b_1 S_d^2 + b_2 S_d - b_3}{2\pi k_{eff}(\Gamma_1 S_d)^2} \leq \frac{2}{\pi} \quad (15)$$

Figure 6-9 presents the variation of ζ_{eq} , as computed from Equation (15), with effective spectral displacement, S_d , for all the hysteresis loops of the three versions of the proposed loading protocol and for the fourth arbitrary protocol. The equivalent viscous damping ratios is artificially limited by a lower bound equal to 5% of critical corresponding to the energy dissipated by the building model prior to yielding of the main structural elements and by an upper bound of $2/\pi$ (or 64% of critical) corresponding to a perfect rectangular hysteresis loop. Again, the number of repeating cycles has only a minor effect on the variations of ζ_{eq} with S_d .

6.10 Estimation of Seismic Response

The seismic response of the building model is estimated using a simplified capacity spectrum methodology based on the proposed numerical cyclic loading protocol and is compared to the median seismic response of the same building model obtained by Nonlinear Dynamic Analyses (NDA) under an ensemble 60 strong motion records scaled at different intensities (Haselton et al., 2006a). For comparison purposes, the same methodology is used with the fourth arbitrary protocol.

For this purpose the spectral capacity curves (or capacity spectra) of the building model shown in Fig. 6-7 are compared to the median elastic response spectra of the strong motion ensemble at damping ratios corresponding to the relationships given by Equation (15) and shown in Fig. 6-9. For each value of spectral displacement, the corresponding damping ratio is obtained from Equation (15) and the spectral amplitude corresponding to

this damping is retained. The point of intersection between the resulting spectral demand curve connecting the spectral values corresponding to the proper damping ratios and the capacity spectrum represents the estimated median seismic response of the building model, as illustrated in Fig. 6-10.

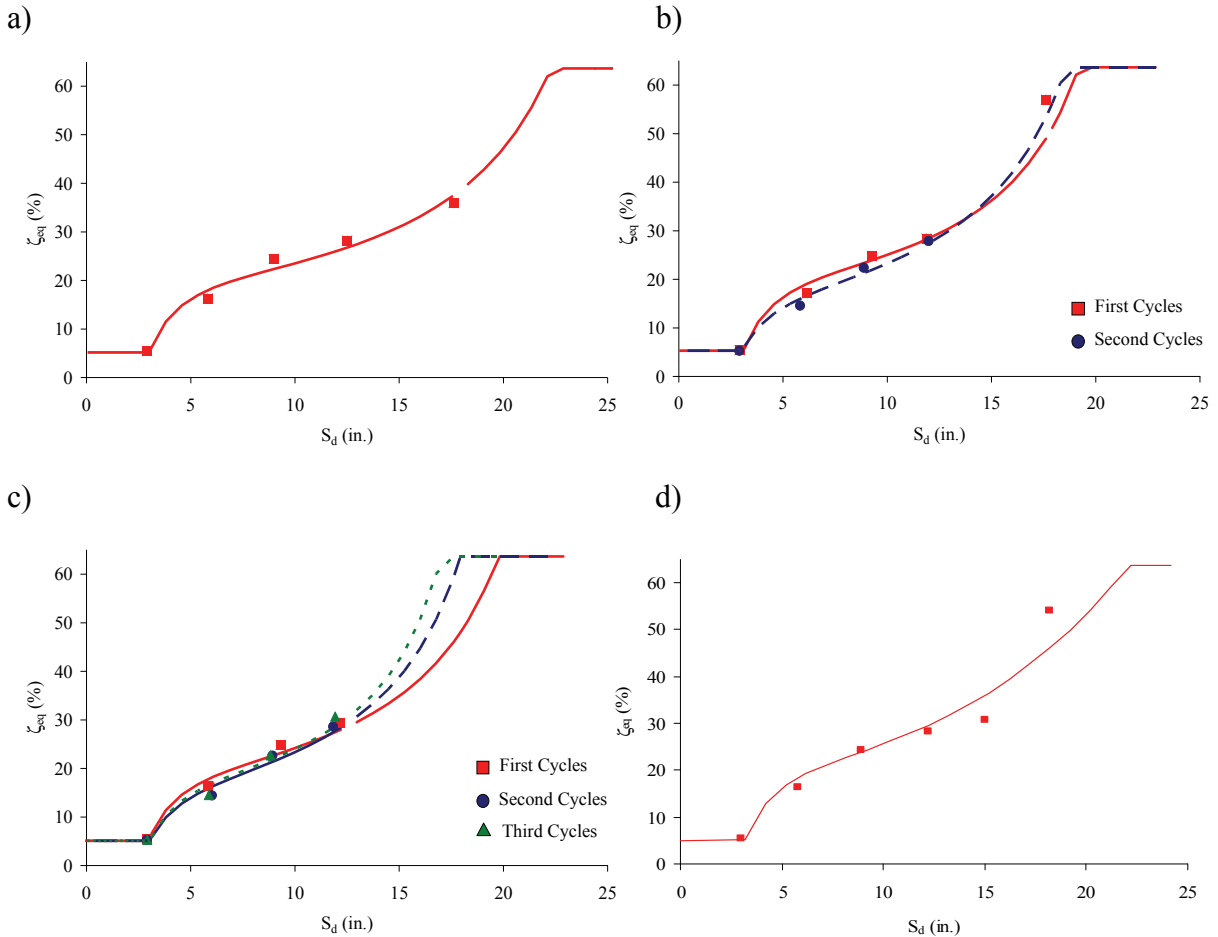


Figure 6-9. Variations of Equivalent Viscous Damping Ratio with Spectral Displacement for 4-story SMF, a) Cyclic Dwell 1, b) Cyclic Dwell 2, c) Cyclic Dwell 3, d) Arbitrary Protocol

Once the estimated median spectral displacement response, S_d , is obtained, the estimated median roof lateral displacement of the building model can be obtained from Equation (8).

6.11 Response Spectra used in Simplified Analysis

The response spectra used in the simplified analysis are the median response spectra of an ensemble of 60 strong motion records that were scaled at different intensities and used in the Incremental Dynamic Analysis of the building of Fig. 6-1 (Haselton et al., 2006a). Four intensities of these motions are used herein for analysis. They are characterized in terms of the spectral acceleration at 1 second: $S_{a1} = 0.11$ g, 0.32 g, 1.12 g and 1.92 g.

Figures 6-11 through 6-14 present the median response spectra of the 60 scaled motions at the four selected intensities. Spectra for damping ratios of 5, 10, 15, 20, 25 and 30-percent are presented. Note that the spectra for higher than 5-percent damping were directly obtained by response history analysis and not by the use of the 5-percent damped spectra and damping coefficients (B factors) for higher damping. Moreover, Figs. 6-15 through 6-18 present the median, maximum and minimum 5-percent damped spectra values for each of the four intensities of ground motion. These spectra reveal the variability in the scaled motions. Values of the median spectra acceleration are presented in Appendix A.

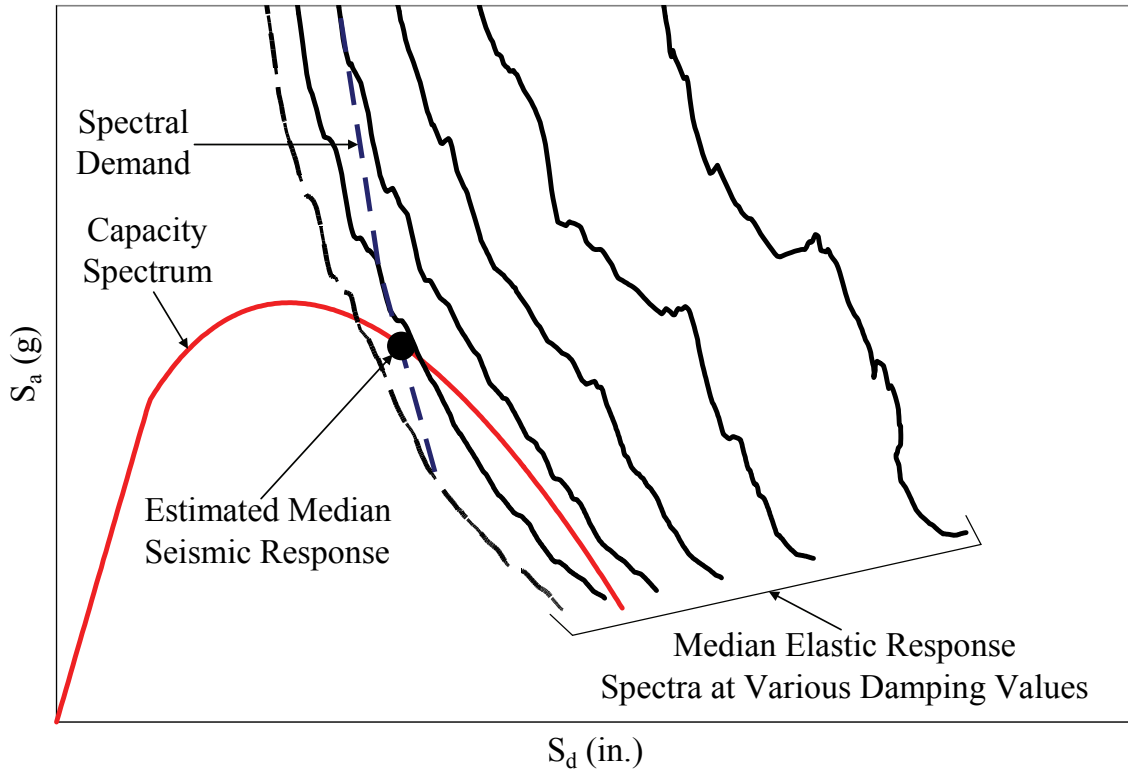


Figure 6-10. Estimation of Seismic Response of Building Model

Median Spectra: Sa (1 sec) = 0.11g

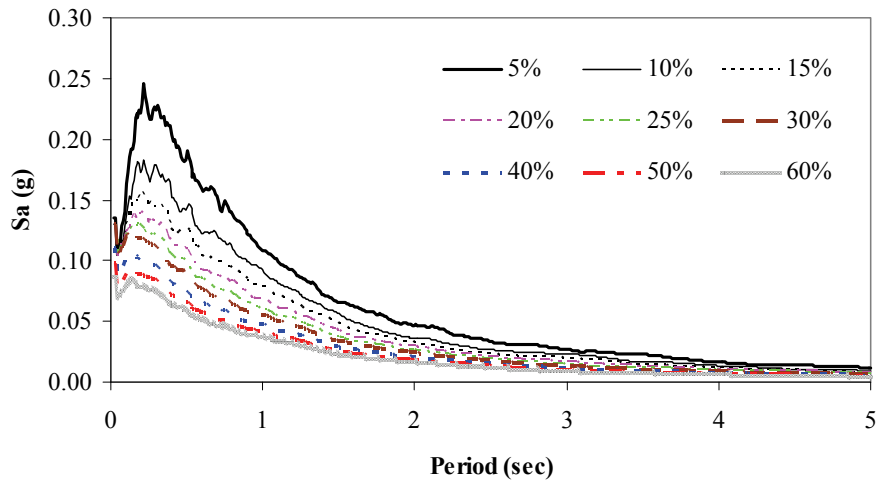


Figure 6-11. Median Response Spectra for 0.11g Intensity Motions

Median Spectra: Sa (1 sec) = 0.32g

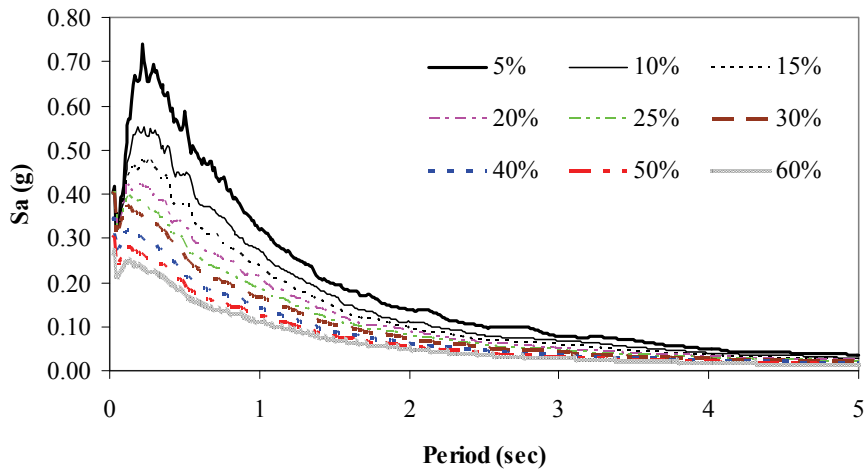


Figure 6-12. Median Response Spectra for 0.32g Intensity Motions

Median Spectra: Sa (1 sec) = 1.12g

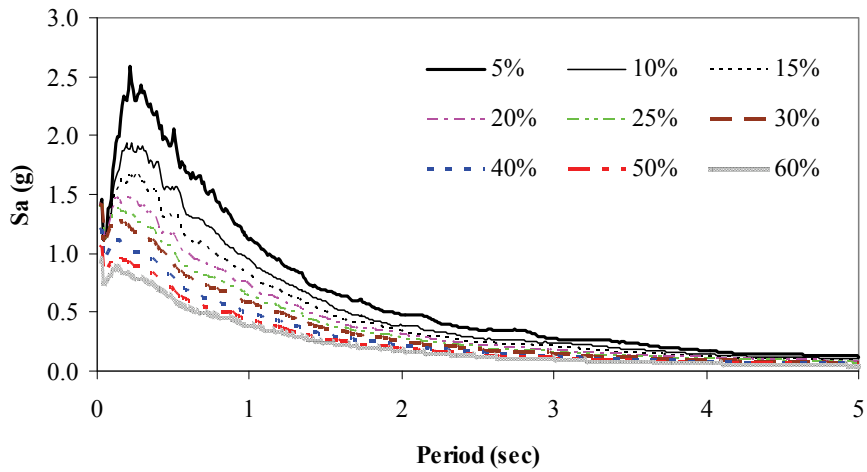


Figure 6-13. Median Response Spectra for 1.12 g Intensity Motions

Median Spectra: Sa (1 sec) = 1.92g

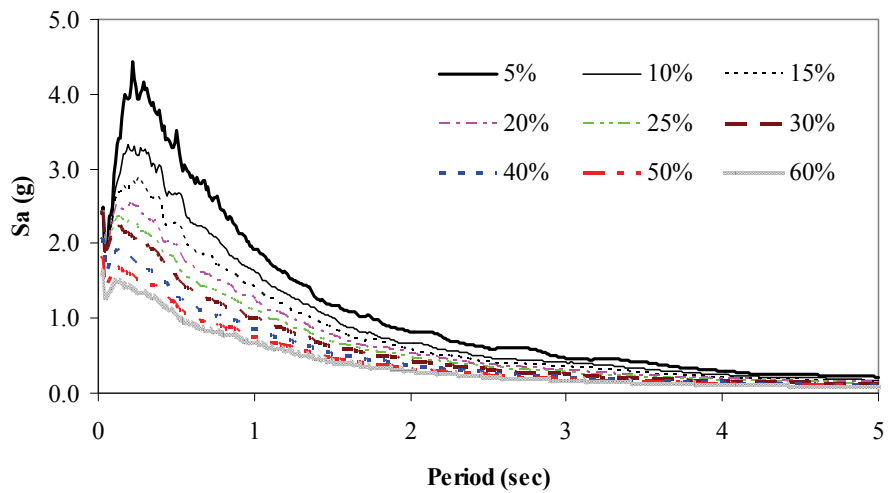


Figure 6-14. Median Response Spectra for 1.92g Intensity Motions

Spectra at 5% damping: $S_a(1 \text{ sec}) = 0.11\text{g}$

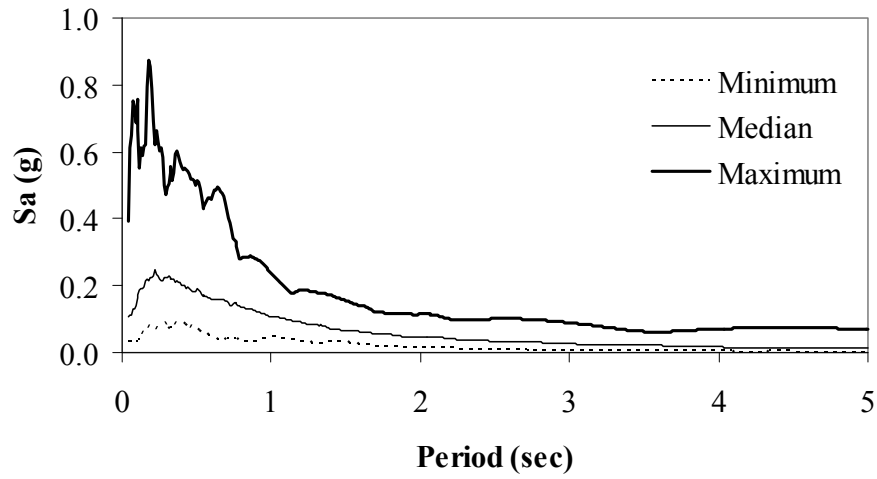


Figure 6-15. Median, Maximum and Minimum Spectral Values for 0.11g Intensity Motions

Spectra at 5% damping: $S_a(1 \text{ sec}) = 0.32\text{g}$

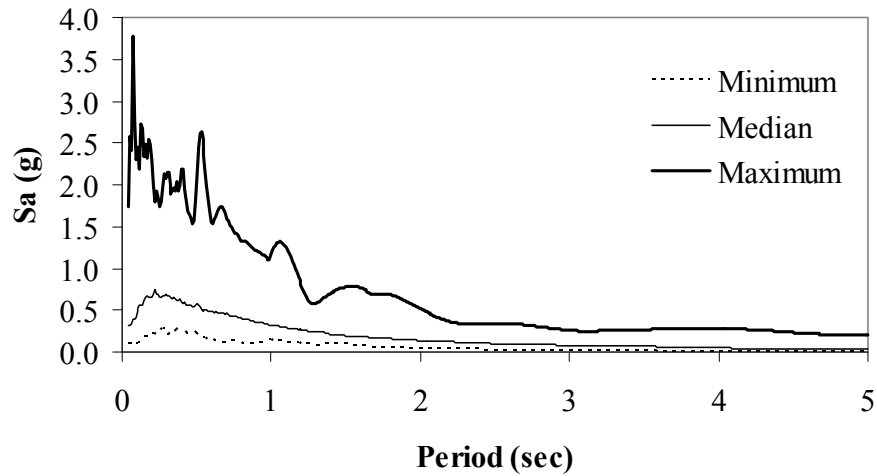


Figure 6-16. Median, Maximum and Minimum Spectral Values for 0.32g Intensity Motions

Spectra at 5% damping: $S_a(1 \text{ sec}) = 1.12\text{g}$

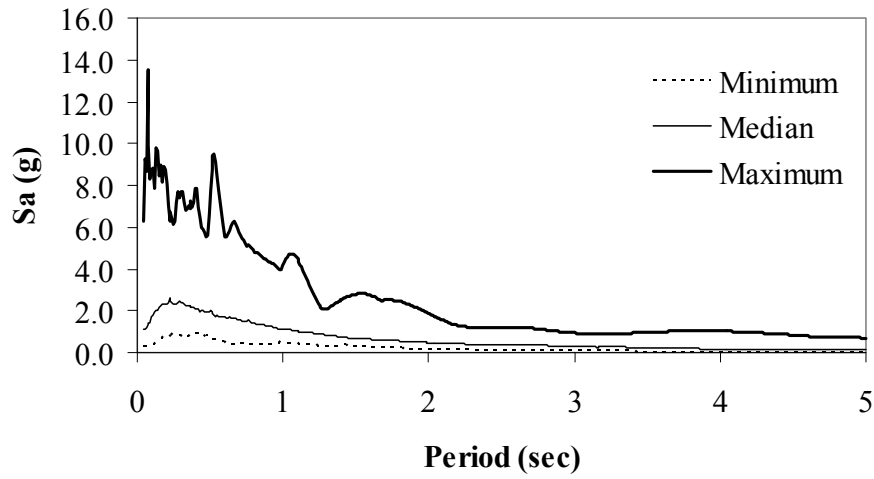


Figure 6-17. Median, Maximum and Minimum Spectral Values for 1.12g Intensity Motions

Spectra at 5% damping: $S_a(1 \text{ sec}) = 1.92\text{g}$

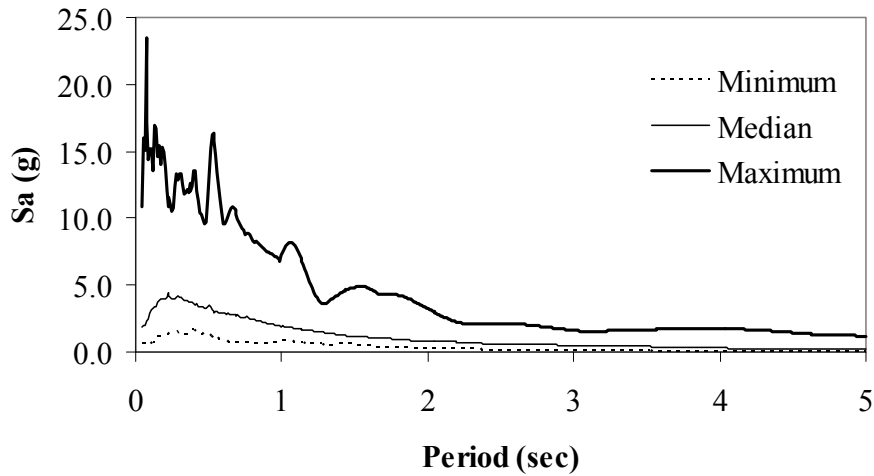


Figure 6-18. Median, Maximum and Minimum Spectral Values for 1.92g Intensity Motions

6.12 Calculation of Response and Comparison to Results of Nonlinear Dynamic Analysis

The response of the structure of Fig. 6-1 was calculated using the simplified procedure described in Section 6.10 and the median spectra of Figs. 6-11 to 6-14. Appendix B presents detailed results for all cases considered in this study.

Tables 6-4 to 6-7 compare the estimated median peak roof displacement for the building model using the procedure outlined above with that obtained from nonlinear dynamic analyses (Haselton et al., 2006a). The median roof displacement was calculated from the results of dynamic analysis using (a) the counted median (Shome and Cornell, 2000) and (b) the surviving median. The former is the median from the middle of the ordered response results, including the cases in which “collapse” (actually numerical instability in the analysis program) occurred. The latter is the median from the ordered response results excluding the “collapse” cases. Each table corresponds to a different intensity of the ground motions expressed in terms of spectral acceleration at 1 second: $S_{a1} = 0.11$ g, 0.32 g, 1.12 g and 1.92 g.

Table 6-4. Estimated Median Roof Displacement of 4-story SMF, $S_{a1} = 0.11$ g

Protocol	Cycles	Median Peak Roof Displacement (in)	
		Proposed Procedure	Nonlinear Dynamic Analysis (Haselton et al. 2006a)
Cyclic Dwell 1	1	1.86	Surviving Median 2.11 Counted Median 2.11 (no collapses)
Cyclic Dwell 2	1	1.86	
	2	1.86	
Cyclic Dwell 3	1	1.86	
	2	1.86	
	3	1.86	
Arbitrary	1	1.86	

Table 6-5. Estimated Median Roof Displacement of 4-story SMF, $S_{a1} = 0.32$ g

Protocol	Cycles	Median Peak Roof Displacement (in)	
		Proposed Procedure	Nonlinear Dynamic Analysis (Haselton et al. 2006a)
Cyclic Dwell 1	1	4.74	Surviving Median 5.63 Counted Median 5.63 (no collapses)
Cyclic Dwell 2	1	4.83	
	2	4.89	
Cyclic Dwell 3	1	4.68	
	2	4.91	
	3	4.91	
Arbitrary	1	4.72	

Table 6-6. Estimated Median Roof Displacement of 4-story SMF, $S_{a1} = 1.12$ g

Protocol	Cycles	Median Peak Roof Displacement (in)	
		Proposed Procedure	Nonlinear Dynamic Analysis (Haselton et al. 2006a)
Cyclic Dwell 1	1	14.65	Surviving Median 17.80 Counted Median 18.31 (4 collapses out of 60 cases)
Cyclic Dwell 2	1	14.76	
	2	15.09	
Cyclic Dwell 3	1	14.88	
	2	15.18	
	3	15.48	
Arbitrary	1	14.41	

Table 6-7. Estimated Median Roof Displacement of 4-story SMF, $S_{a1} = 1.92$ g

Protocol	Cycles	Median Peak Roof Displacement (in)	
		Proposed Procedure	Nonlinear Dynamic Analysis (Haselton et al. 2006a)
Cyclic Dwell 1	1	24.82	Surviving Median 27.56 Counted Median 36.11 (24 collapses out of 60 cases)
Cyclic Dwell 2	1	23.29	
	2	22.82	
Cyclic Dwell 3	1	23.57	
	2	22.82	
	3	21.97	
Arbitrary	1	24.37	

An observation to be made is that the simplified procedure predicts displacements in the case of $S_{a1} = 1.92$ g (Table 6-7) that slightly decrease as cyclic dwell increases. This appears as counter-intuitive because it is expected that the displacement should increase as the stiffness of the structure reduces with increasing number of cycles. However, in this case the increase of effective damping associated with increasing number of cycles (see Figure 6-9c) counteracts the effect of reducing stiffness with a net effect of a slightly reduced rather than increased displacement.

The simplified procedure predicts identical median roof displacements for all versions of the cyclic protocol (including the arbitrary one) at $S_{a1} = 0.11$ g since the building remains in the elastic range at this low excitation level and its cyclic response is independent of the number of repeating cycles. Also, the simplified procedure predicts similar median roof displacements for all versions of the cyclic protocol at all levels of seismic excitation considered. At high excitation intensity ($S_{a1} = 1.92$ g) the protocols with the least number of cycles (arbitrary protocol with 10 cycles and the cyclic dwell 1 protocol with 7 cycles) result in slightly larger displacements that are closer to the results of dynamic response history analysis. This is due to the fact that the calculated effective damping is less for the protocols with less number of cycles. This indicates that the effective damping may be

adjusted (or the procedure may be calibrated) to obtain results that are closer to the results of response history analysis.

The proposed simplified procedure under-predicts the median roof displacement by 12% to 30% across intensity levels and protocol versions when compared to the surviving median of the response history analysis. When compared to the counted median of the response history analysis, the under-prediction across all levels and protocols is 12% to 39%. The largest under-prediction occurs in the case of the strongest seismic input. In the case of the least number of cycles (case of one cyclic dwell with a total of seven cycles) the simplified procedure under-predicts the counted median roof displacement response by 12% to 31% across all intensity levels. Note that in all cases, the median peak roof displacements predicted by the simplified procedures are less than the estimated failure roof displacement of 33.1 in (Fig. 6-2), thereby indicating that no failure (in a median sense) is predicted by the simplified procedure. However, an inspection of the graphs in Appendix B reveals that for the case of the strongest excitation (1.92g) the capacity spectral curve and the spectral demand curve are nearly asymptotic, which indicates that collapse is imminent. Therefore, a small increase in the level of excitation would have resulted in prediction of collapse. Moreover, one may observe in the graphs of Appendix B (particularly those for the proposed 3-cycle dwell with results for the second cycle) that a different extrapolation of the spectral capacity curve (one that better represents the available data at large displacements) would have resulted in prediction of collapse at the excitation level of 1.92g.

6.13 Damage Predicted by Simplified Analysis and by Nonlinear Dynamic Analysis

Haselton et al. (2006a) reported on the damage patterns observed in the nonlinear dynamic analysis. Figure 6-19 presents the collapse modes observed in the dynamic analysis. The percentage figures shown in the graphs are the percentage of the 60 ground motions records that resulted in the shown failure mode. Several different collapse modes are possible for the same structure.

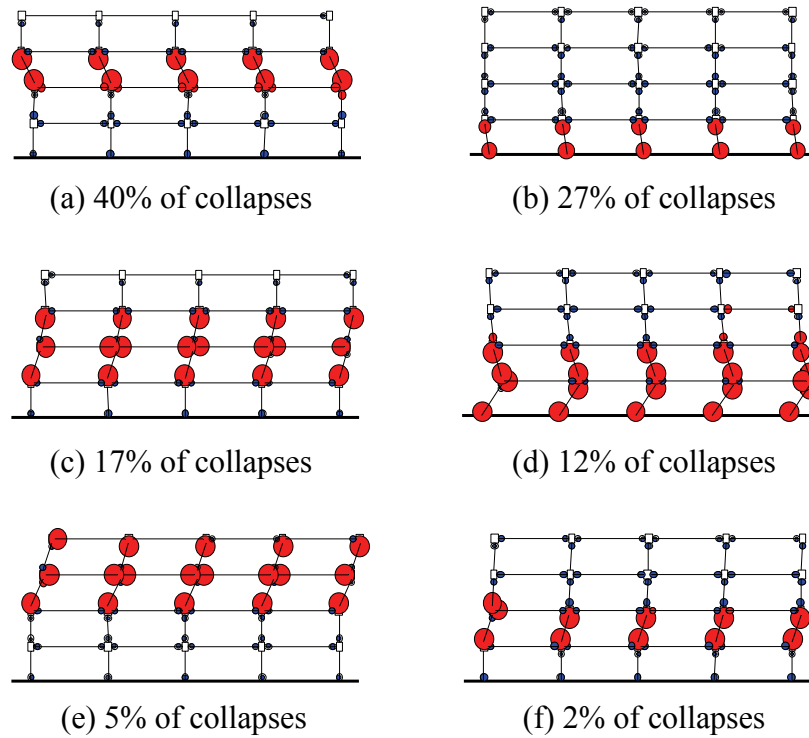


Figure 6-19. Diagrams Showing Collapse Modes of 4-story SMF Observed in Dynamic Analysis (Haselton et al., 2006a)

The simplified analysis is capable of predicting a single failure mode. Figure 6-20 presents the damage pattern observed in the simplified analysis for the case of $S_{a1} = 1.92$ g ground motion intensity. The simplified analysis in this case shows that the structure is near collapse (as evident from the spectral capacity and spectral demand curves being nearly asymptotic). The large circles in the figure denote locations of very large plastic curvature. Evidently, this damage pattern agrees well with failure mode (c) in Fig. 6-19.

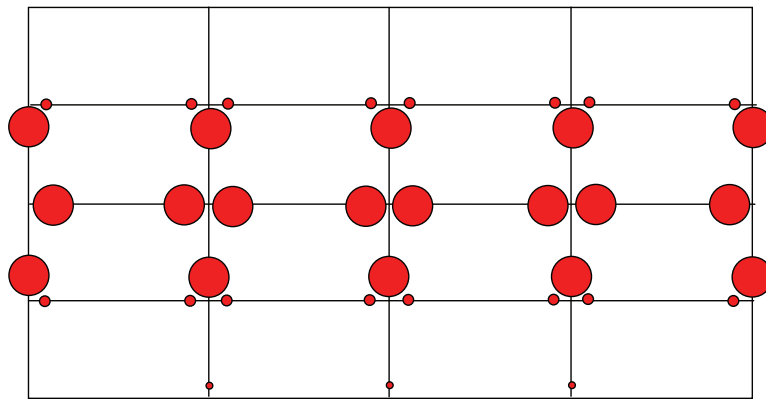


Figure 6-20. Damage Pattern of 4-story SMF Observed in Simplified Analysis at $S_{a1} = 1.92$ g (near collapse)

SECTION 7

ANALYSIS OF 4-STORY REINFORCED CONCRETE INTERMEDIATE MOMENT FRAME

In this section, a 4-story reinforced concrete intermediate moment frame (IMF) described in Liel et al. (2006) was analyzed using the proposed simplified capacity spectrum method and compared with the results of incremental dynamic analyses. The structure has a similar geometry as the 4-story special moment frame shown in Fig. 6-1 but with the columns having dimensions of 20 in. by 22 in. to 28 in. by 28 in. and beams having depth between 10 in. and 26 in. The model used to represent the structure is identical to the one used for the 4-story special moment frame but with plastic rotation capacities limited to 2/3 of those used for the special moment frame.

Table 7-1 presents the modal properties of the analyzed frame under elastic conditions obtained with the computer program OpenSees. Included in this table are lumped tributary weight per level (or floor), natural periods (T) and modal floor displacements for the first four modes of vibration.

Table 7-1. Lumped Tributary Weights and Modal Properties of Analyzed 4-story Intermediate Moment Frame

Floor	Weight (kips)	Mode 1 (T = 3.10 sec)	Mode 2 (T = 1.11 sec)	Mode 3 (T = 0.62 sec)	Mode 4 (T = 0.42 sec)
4 (roof)	1675	1.000	-0.940	-0.587	-0.162
3	1717	0.796	0.302	1.000	0.441
2	1748	0.484	1.000	-0.305	-0.865
1	1810	0.194	0.602	-0.740	1.000

Analyses are performed for two cyclic loading protocols: (a) the full proposed numerical cyclic protocol incorporating 21 total cycles of loading, 3 repeating cycles (otherwise indicated as cyclic dwell 3) and using the results obtained for the second repeating cycle, and (b) a simplified version of the proposed numerical cyclic protocol obtained by considering only the 7 primary cycles of loading; i.e. only one repeating cycle (otherwise indicated as cyclic dwell 1). In both cases the loading was developed in proportion to the first mode shape as calculated using the elastic properties (Table 7-1). The first modal participating factor and the first modal weight were calculated by use of Equations (9) and (13) as $\Gamma_1 = 1.31$ and $\bar{W}_1 = 5545 \text{ kip}$.

Figure 7-1 presents the monotonic pushover curve obtained for the 4-story IMF. The roof displacement at “collapse” was estimated to be $\Delta_f = 22.4$ in. Figure 7-2 presents the results of the cyclic pushover analysis for the two protocols considered. Also, Figs. 7-3 to 7-5 present the effective stiffness and effective damping as functions of the spectral displacement and the spectral capacity curves of the 4-story IMF as calculated for each two loading protocol, respectively.

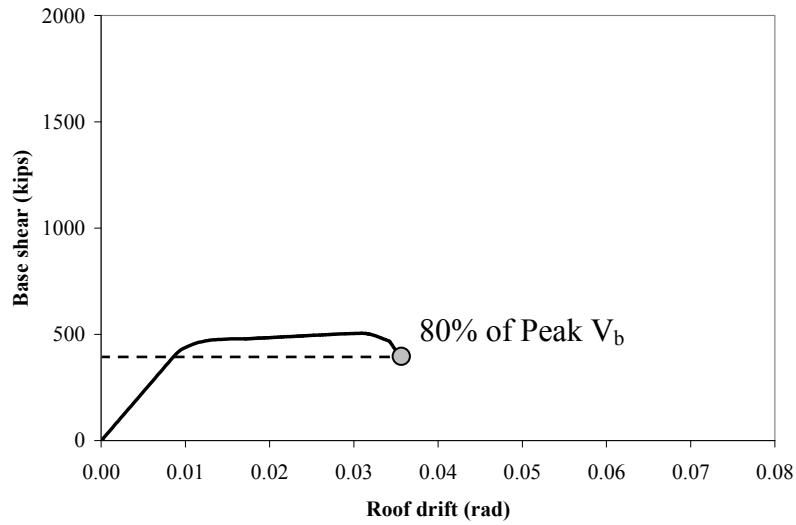


Figure 7-1. Result of Monotonic Pushover Analysis of 4-story IMF

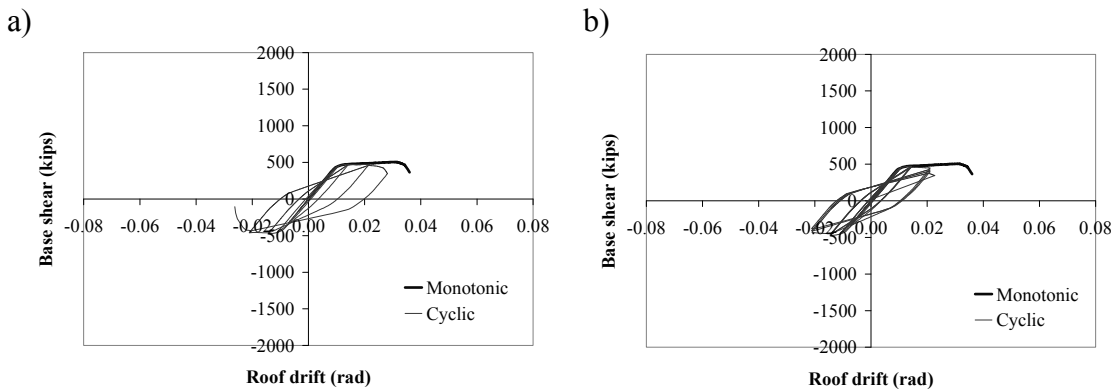


Figure 7-2. Results of Cyclic Pushover Analyses for 4-story IMF, a) Cyclic Dwell 1, b) Cyclic Dwell 3

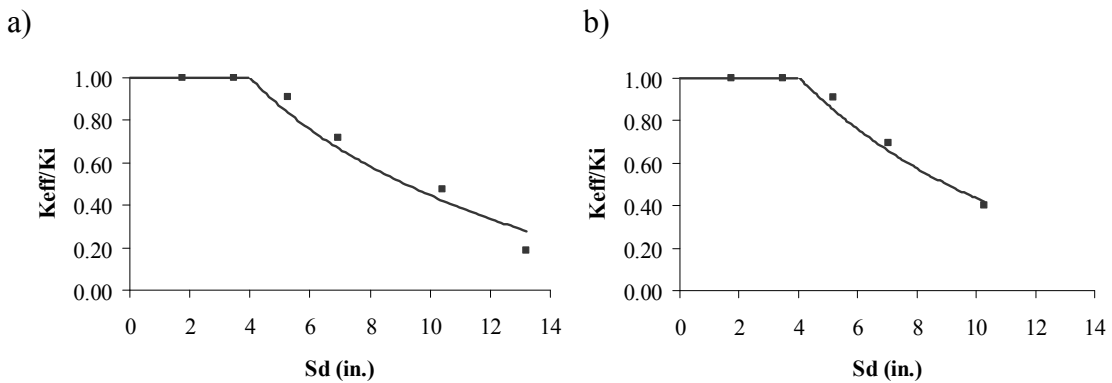


Figure 7-3. Effective Stiffness as Function of Spectral Displacement of 4-story IMF. a) Cyclic Dwell 1, b) Cyclic Dwell 3

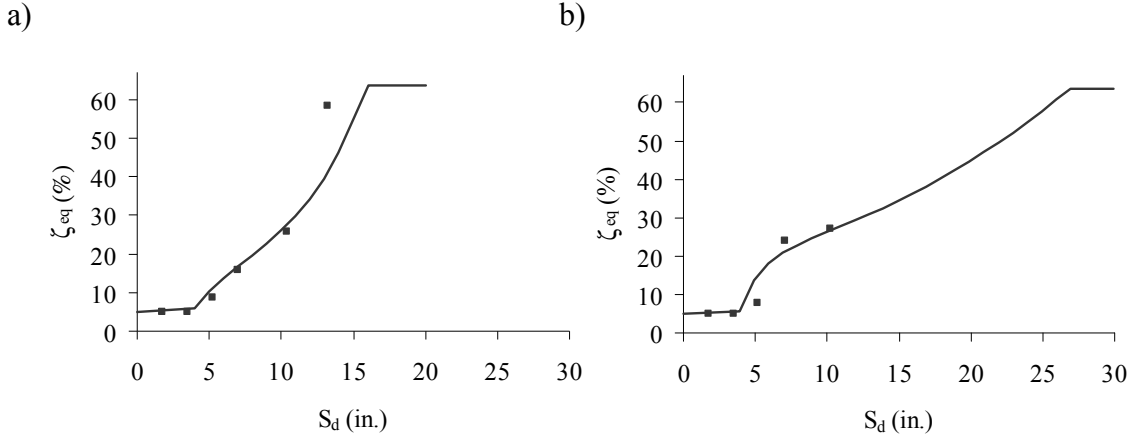


Figure 7-4. Effective Damping as Function of Spectral Displacement of 4-story IMF, a) Cyclic Dwell 1, b) Cyclic Dwell 3

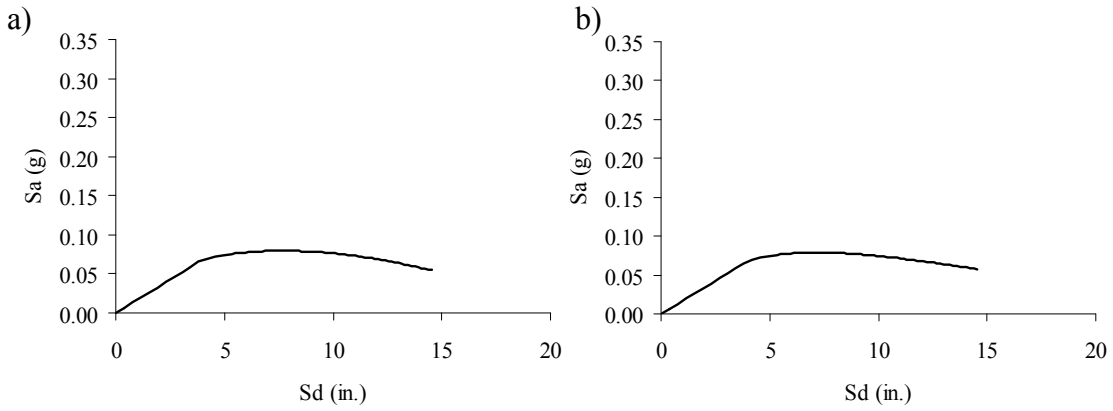


Figure 7-5. Spectral Capacity Curves of 4-story IMF, a) Cyclic Dwell 1, b) Cyclic Dwell 3

Appendix C presents detailed results for each case of the 4-story IMF analyzed. Tables 7-2 to 7-4 tabulate results of simplified and response history analysis obtained from Liel et al. (2006).

Table 7-2. Estimated Median Roof Displacement of 4-story IMF, $S_{a1} = 0.11$ g

Protocol	Cycle	Median Peak Roof Displacement (in)	
		Proposed Procedure	Nonlinear Dynamic Analysis (Liel et al., 2006)
Cyclic Dwell 1	1	2.83	Surviving Median 3.03 Counted Median 3.03 (no collapses)
Cyclic Dwell 3	2	2.83	

Table 7-3. Estimated Median Roof Displacement of 4-story IMF, $S_{a1} = 0.32$ g

Protocol	Cycle	Median Peak Roof Displacement (in)	
		Proposed Procedure	Nonlinear Dynamic Analysis (Liel et al., 2006)
Cyclic Dwell 1	1	7.53	Surviving Median 7.36 Counted Median NA (30 collapses)
Cyclic Dwell 3	2	6.68	

Table 7-4. Estimated Median Roof Displacement of 4-story IMF, $S_{a1} = 1.12$ g

Protocol	Cycle	Median Peak Roof Displacement (in)	
		Proposed Procedure	Nonlinear Dynamic Analyses (Liel et al., 2006)
			Surviving Median 14.74 Counted Median NA (54 collapses)
Cyclic Dwell 1	1	17.48	
Cyclic Dwell 3	2	18.21	

No results are presented for $S_{a1} = 1.92$ g since at this intensity, the seismic demand curve does not intersect with the spectral capacity curve, thereby indicating collapse of the structure. This result obtained from the simplified capacity spectrum method is consistent with the results obtained from incremental dynamic analyses where 59 of 60 cases collapsed. Moreover, inspection of the graphs of Appendix C reveals, as in the case of the 4-story SMF, that an alternative extrapolation of results for the spectral capacity curve (one that better represents the available data at large displacements-particularly for the case of the one cycle dwell) would have likely resulted in prediction of collapse at the excitation level of 1.12g.

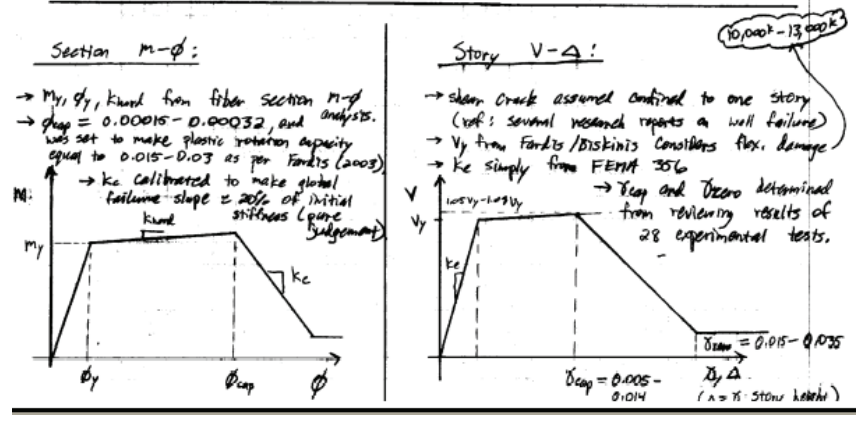
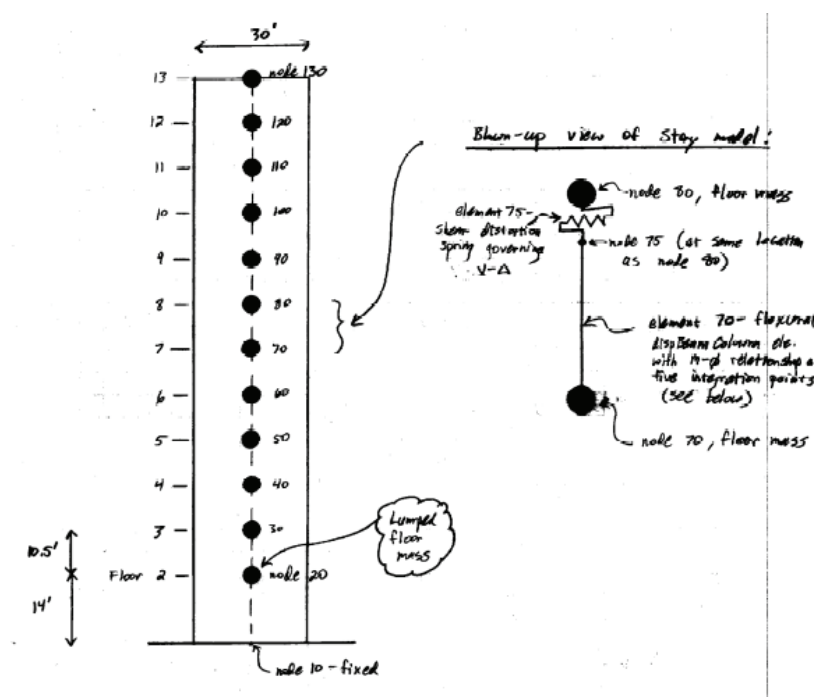


Figure 8-2. 12-story with Special Core Wall Building Model (Haselton et al., 2006b)

The tributary weight per level, modal properties, natural periods (T) and modal floor displacements for the first four modes of the structure are summarized in Table 8-1.

Table 8-1. Lumped Tributary Weights and Modal Properties of Analyzed 12-story Special Wall Building

Floor	Weight (kips)	Mode 1 (T = 1.41 sec)	Mode 2 (T = 0.84 sec)	Mode 3 (T = 0.34 sec)	Mode 4 (T = 0.19 sec)
12 (roof)	2939	1.000	1.000	1.000	-0.866
11	2939	0.891	0.503	0.066	0.405
10	2939	0.769	0.043	-0.638	0.994
9	2939	0.649	-0.340	-0.917	0.644
8	2939	0.535	-0.617	-0.757	-0.214
7	2939	0.427	-0.772	-0.299	-0.872
6	2939	0.328	-0.819	0.252	-0.923
5	2939	0.239	-0.764	0.717	-0.386
4	2939	0.162	-0.632	0.958	0.390
3	2939	0.099	-0.458	0.932	0.932
2	2939	0.051	-0.273	0.690	1.000
1	2939	0.018	-0.115	0.346	0.627

Similar to the case of the 4-story IMF building, analyses were performed for two cyclic loading protocols: (a) the full proposed numerical cyclic protocol incorporating 21 total cycles of loading, 3 repeating cycles (otherwise indicated as cyclic dwell 3) and using the results obtained for the second repeating cycle, and (b) a simplified version of the proposed numerical cyclic protocol obtained by considering only the 7 primary cycles of loading; i.e. only one repeating cycle (otherwise indicated as cyclic dwell 1).

Figure 8-3 shows the monotonic pushover curve obtained for the 12-story special wall building. The collapse roof displacement (Δ_f) was determined to be 77.4 in. Figure 8-4 presents the results of the cyclic pushover analyses with the two protocols considered. Also, Figs. 8-5 to 8-7 present the effective stiffness and effective damping as functions of the spectral displacement and the spectral capacity curves of the 12-story special wall as calculated for each loading protocol, respectively.

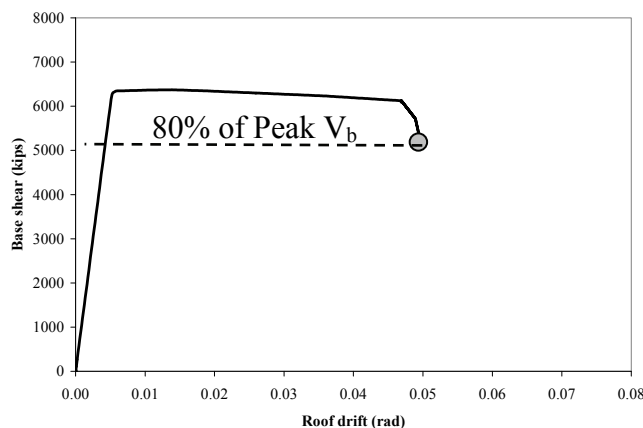


Figure 8-3. Result of Monotonic Pushover Analysis of 12-story Special Wall Building

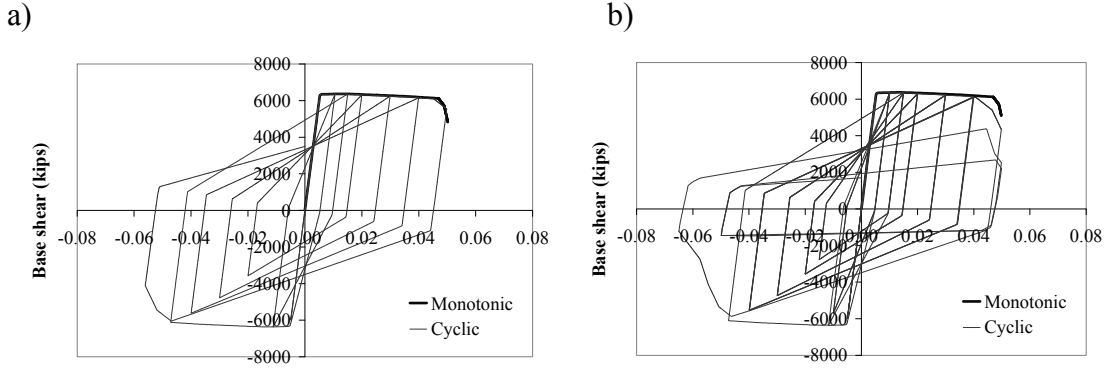


Figure 8-4. Results of Cyclic Pushover Analyses for 12-story Special Wall Building, a) Cyclic Dwell 1, b) Cyclic Dwell 3

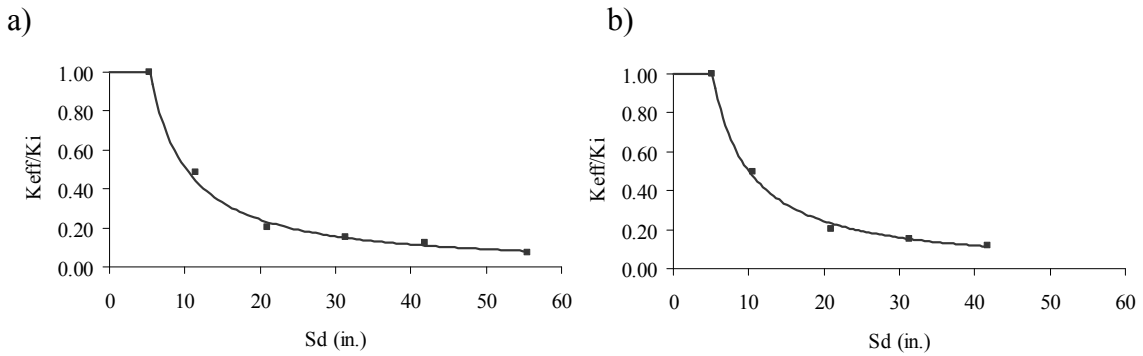


Figure 8-5. Effective Stiffness as Function of Spectral Displacement of 12-story Special Wall Building, a) Cyclic Dwell 1, b) Cyclic Dwell 3

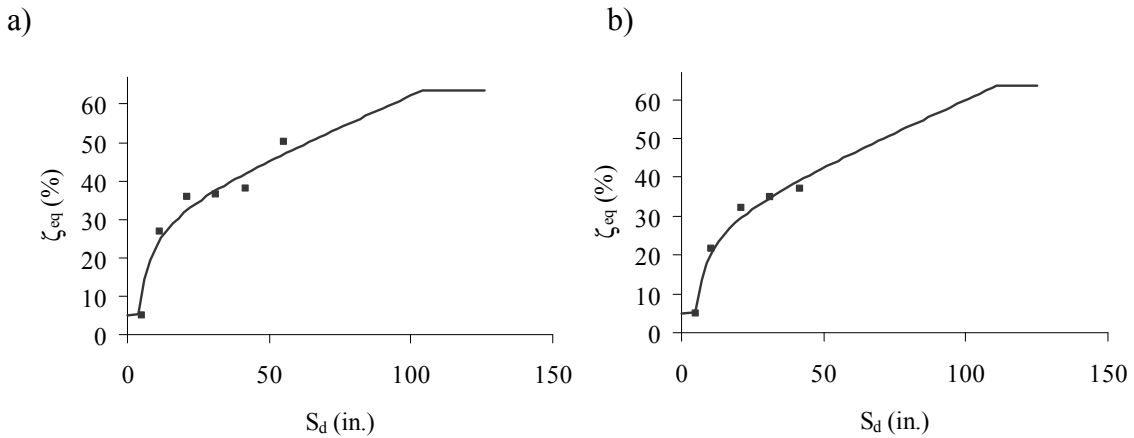
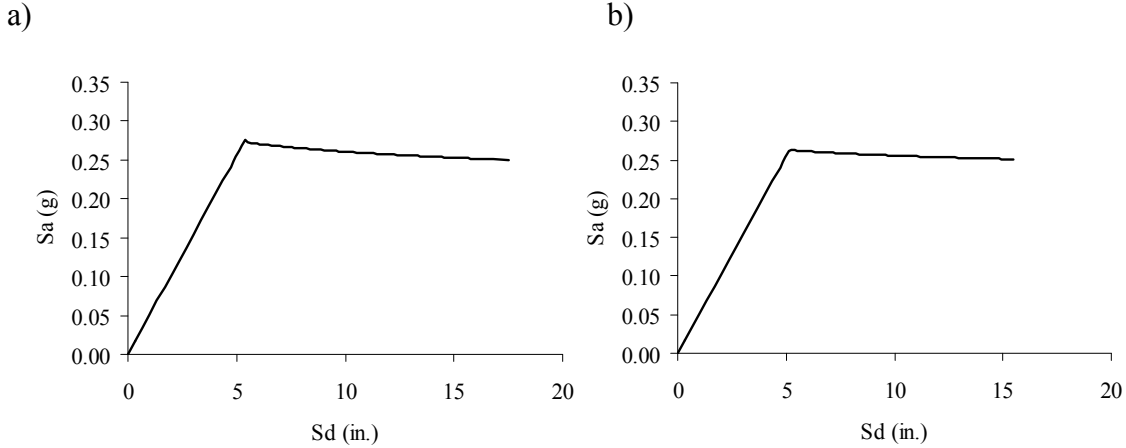


Figure 8-6. Effective Damping as Function of Spectral Displacement of 12-story Special Wall Building, a) Cyclic Dwell 1, b) Cyclic Dwell 3



**Figure 8-7. Spectral Capacity Curves of 12-story Special Wall Building,
a) Cyclic Dwell 1, b) Cyclic Dwell 3**

The hysteresis loops shown in Fig. 54 exhibit an asymmetry with the portion for negative displacement showing “degradation” that is believed to be the result of numerical problems experienced in OpenSees during the cyclic pushover analysis. This problem could not be corrected and it did not appear in the response history analysis of the structure. As a result of this problem, the actual spectral capacity curve of the structure (see Appendix D-discrete data shown in circles) recovers at spectral displacements of over 30in. after a substantial drop at a spectral displacement of about 20in. It appears that the results of the simplified analysis for this building are valid to spectral displacements of about 20in.

The first modal participating factor and the first modal weight were calculated by use of Equations (9) and (13) as $\Gamma_1 = 1.49$ and $\bar{W}_1 = 22565kip$. Detailed results for each case of the 12-story special wall building analyzed are shown in Appendix D. Tables 8-2 to 8-5 tabulate results of simplified and response history analyses obtained from Haselton et al. (2006b). Note that in all cases the median peak roof displacement predicted by the simplified capacity spectrum method is well below the estimated collapse value of 77.4 in, thereby indicating that no failure (in a median sense) is predicted by the simplified procedure.

**Table 8-2. Estimated Median Roof Displacement of 12-story Special Wall Building,
 $S_{a1} = 0.11 g$**

Protocol	Cycle	Median Peak Roof Displacement (in)	
		Proposed Procedure	Nonlinear Dynamic Analysis (Haselton et al., 2006b)
Cyclic Dwell 1	1	2.12	Surviving Median 2.08 Counted Median 2.08 (no collapses)
Cyclic Dwell 3	2	2.12	

Table 8-3. Estimated Median Roof Displacement of 12-story Special Wall Building, $S_{a1} = 0.32$ g

Protocol	Cycle	Median Peak Roof Displacement (in)	
		Proposed Procedure	Nonlinear Dynamic Analysis (Haselton et al., 2006b)
Cyclic Dwell 1	1	6.57	Surviving Median 6.06 Counted Median 6.06 (no collapses)
Cyclic Dwell 3	2	6.57	

Table 8-4. Estimated Median Roof Displacement of 12-story Special Wall Building, $S_{a1} = 1.12$ g

Protocol	Cycle	Median Peak Roof Displacement (in)	
		Proposed Procedure	Nonlinear Dynamic Analysis (Haselton et al., 2006b)
Cyclic Dwell 1	1	17.14	Surviving Median 19.12 Counted Median 19.31 (4 collapses)
Cyclic Dwell 3	2	18.33	

Table 8-5. Estimated Median Roof Displacement of 12-story Special Wall Building, $S_{a1} = 1.92$ g

Protocol	Cycle	Median Peak Roof Displacement (in)	
		Proposed Procedure	Nonlinear Dynamic Analysis (Haselton et al., 2006b)
Cyclic Dwell 1	1	28.46	Surviving Median 28.08 Counted Median NA (37 collapses)
Cyclic Dwell 3	2	33.57	

Note that the results for the case of excitation with $S_{a1} = 1.92$ g the results of the simplified analysis are likely wrong due to the suspected errors in the OpenSees model as described previously.

8.1 Calculation of Damage Predicted by Simplified Analysis and by Nonlinear Dynamic Analysis

Haselton et al. (2006b) reported on the damage patterns of the 12-story special wall building observed in the nonlinear dynamic analyses. Figure 8-8 presents the collapse modes observed in the dynamic analyses. The percentage figures shown in the graphs are

the percentage of the 60 ground motions records that resulted in the shown failure mode. Several different collapse modes are possible for the same structure; however, almost all cases are governed by a shear failure in the first story.

The simplified analysis is capable of predicting a single failure mode. Figure 8-9 presents the damage pattern observed in the simplified analysis using the loading protocol with 3 repeating cycles for the case of $S_{a1} = 1.92$ g ground motion. The circles in the figure denote locations of plastic curvature, while the large rectangle shows location of a large shear deformation. Evidently, the damage pattern obtained from the simplified analysis governs by the shear failure in the first story, which agrees well with the dominant failure mode (a) in Fig. 8-8.

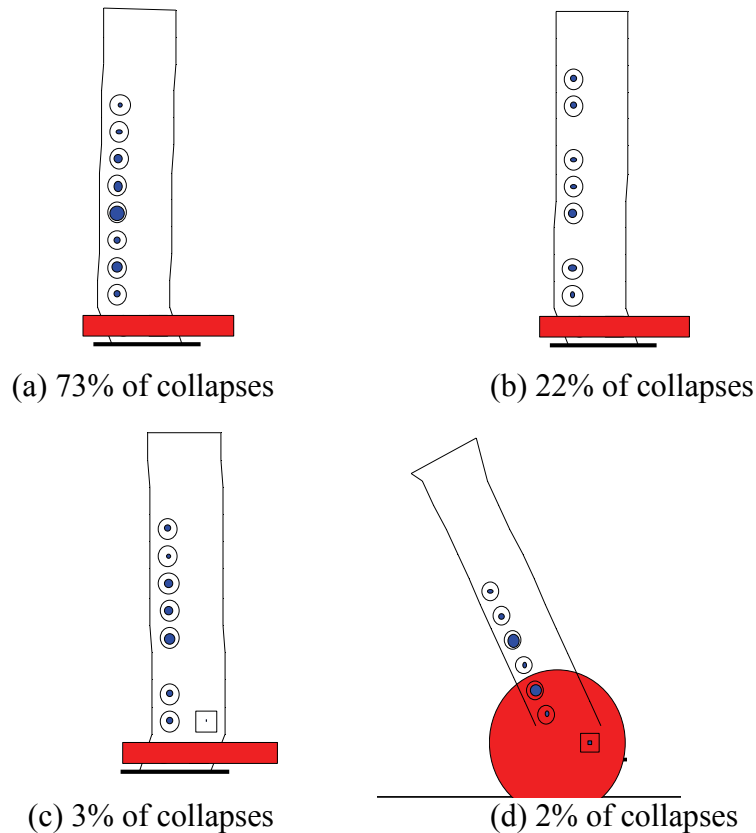


Figure 8-8. Diagrams Showing Collapse Modes of 12-story Special Wall Building Observed in Dynamic Analysis (Haselton et al., 2006b), Rectangles: Inelastic Shears, Circles: Flexural Hinges

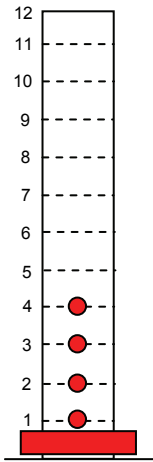


Figure 8-9. Damage Pattern of 12-story Special Wall Building Observed in Simplified Analysis at $S_{a1} = 1.92$ g (near collapse), Rectangles: Inelastic Shears, Circles: Flexural Hinges

SECTION 9

SUMMARY OF PROPOSED NUMERICAL CYCLIC LOADING PROTOCOL AND ESTIMATION OF SEISMIC RESPONSE

The three steps required to construct the proposed numerical cyclic loading protocol are summarized as follows:

1. A preliminary monotonic pushover analysis is first conducted on the building model in order to establish its expected failure roof displacement of the building model (see Fig.4-1).
2. The expected failure roof displacement corresponding to a fraction of the maximum base shear computed is established. This expected failure displacement should be calibrated based on the results of incremental dynamic analyses . A roof displacement value corresponding to 80% of the maximum base shear is suggested in the interim.
3. The general loading sequence of the proposed numerical loading protocol is established as a fraction of the expected failure roof displacement (see Fig. 4-2 and Table 4-1).

The main characteristics of the proposed numerical cyclic loading protocol are summarized as follows:

- The total number of cycles is 21,
- The number of primary cycles is 7.
- The number of repeating cycles following each primary cycle is 2 (that is there is a total of three repeated cycles). The analysis is performed using the effective stiffness and damping of the second cycle of the three repeating cycles).
- If the strength and/or stiffness degradation of the hysteretic models used stabilize after only two cycles, the number of repeating cycles can be reduced to two. If the hysteretic models used do not exhibit any strength and stiffness degradation, the repeating cycles can be eliminated.
- Based on the results obtained on 3 different building structures in this study, the predictions of the proposed simplified capacity spectrum method are not sensitive to the number of repeated cycles. Therefore, the proposed numerical cyclic loading protocol could be simplified by considering only 7 primary cycles (cyclic dwell 1).

The proposed numerical cyclic loading protocol should be implemented using a force-based procedure with a load vector proportional to the first mode of the analyzed structure under elastic conditions. An increasing load vector causing a deformed shape of the structural system equals to its elastic first mode is applied until the roof displacement reaches the value prescribed in the loading protocol. This is then followed by unloading using a decreasing load vector and then the process is repeated in accordance with the proposed numerical cyclic protocol.

The steps required to estimate the seismic response of a nonlinear building system using a capacity spectrum methodology based on the proposed numerical cyclic loading protocol are summarized as follows:

1. Perform a cyclic pushover analysis of the building model using the procedure described above and generate global *base shear – roof displacement* hysteresis loops.
2. Based on the global hysteresis loops obtained in 1, construct a relationship between the secant stiffness and the equivalent spectral displacement using Equation (8). This relationship should be based on each last cycle considered in the loading protocol.
3. Using the *secant stiffness – spectral displacement* relationship obtained in 2, construct a capacity curve for the building system (S_a vs S_d) using Equations (8) and (11).
4. Based on the global hysteresis loops obtained in 1, compute the energy dissipated per cycle and construct a relationship between the equivalent viscous damping and the equivalent spectral displacement using Equation (14). This relationship should be based on each last cycle considered in the loading protocol.
5. Estimate the median elastic response spectra for various damping ratios at the site of the building.
6. Plot on the same S_a vs S_d graph the capacity curve obtained in 3 and the median elastic response spectra estimated in 5.
7. Based on the *equivalent viscous damping – spectral displacement* relationship obtained in 4, trace a seismic demand curve by connecting the appropriate damped spectral ordinates corresponding to each spectral displacement value.
8. The intersection between the seismic demand curve and the spectral capacity curve represents an estimate of the median seismic response of the building model.

SECTION 10 CONCLUSIONS

In this report, a numerical cyclic loading protocol is recommended to be used for quantifying building system performance based on a review of available experimental and numerical studies. The proposed loading protocol first consists of a preliminary monotonic pushover analysis in order to establish the expected failure roof displacement of the building model considered. The expected failure roof displacement needs to be calibrated based on the results of incremental dynamic analyses. A roof displacement value corresponding to 80% of the maximum base shear is suggested in the interim.

Once the expected failure roof displacement of the building model considered is established, the general loading sequence of the proposed numerical cyclic loading protocol is established as a fraction of this expected failure roof displacement. The total number of cycles for the proposed loading protocol is 21, which is close to the mean value of 23 cycles for 11 experimental loading protocols reviewed. The proposed loading protocol contains seven primary cycles, which is equal to the mean number of primary cycles for 11 experimental loading protocols reviewed. The proposed loading protocol contains three repeating cycles for primary cycle. If the strength and/or stiffness degradation of the hysteretic models used stabilize after only two cycles, the number of repeating cycles can be reduced to two. Furthermore, if the hysteretic models used do not exhibit any strength and stiffness degradation, the number of repeating cycles can be eliminated. Finally, rate of amplitude increase of primary cycles of the proposed loading protocol agrees well with the mean rate of increase for the 11 experimental loading protocol reviewed.

A sensitivity analysis on the influence of the number of repeating cycles of the proposed numerical cyclic loading protocol on the equivalent elastic lateral stiffness and viscous damping properties of a 4-story SMF reinforced concrete building model was investigated. The numerical cyclic loading protocol was implemented using a force-based procedure in which the load vector was proportional to the first mode shape of the building under elastic conditions. Higher mode effects were disregarded. It is found that the number of repeating cycles has minor influences on the effective lateral stiffness and energy dissipation characteristics of the building model. Based on these results, the proposed numerical cyclic loading protocol was used in a simplified capacity spectrum methodology to estimate the seismic response of the same building model. It was found that the recommended simplified analysis procedure under-estimated the predictions of nonlinear dynamic analyses by 12% to 39% across intensity levels and protocol versions when compared to the counted median of the response history analysis. (When compared to the surviving median of the response history analysis, the under-prediction across all levels and protocols was lesser). The largest under-prediction occurred in the case of the strongest seismic input. In the case of the least number of cycles (case of one cyclic dwell with a total of seven cycles) the simplified procedure under-predicted the counted median roof displacement response by 12% to 31% across all intensity levels. Inspection of the graphs comparing the spectral capacity and the spectral demand curves for all cases analyzed revealed that for the case of the strongest excitation the two curves were nearly

asymptotic, which indicates that collapse is imminent. Therefore, a small increase in the level of excitation would have resulted in prediction of collapse. Conversely, a different extrapolation of results for the spectral capacity curve (one that better represents the available data at large displacements) would have resulted in prediction of collapse at lower excitation level, that is, in better agreement with the results of response history analysis.

Similar results were obtained through the study of a 4-story reinforced concrete intermediate moment frame and of a 12-story special wall building. However, in the latter case the cyclic pushover analysis are suspected to be erroneous, which likely affected the results of the simplified analysis.

On the basis of the results obtained in the sensitivity study on the influence of the number of repeating cycles, it appears that the proposed numerical cyclic loading protocol could be simplified by considering only 7 primary cycles (cyclic dwell 1).

SECTION 11

REFERENCES

- American Society for Testing and Materials, 1995a. "E 72—Standard Test Methods of Conducting Strength Tests of Panels for Building Construction," West Conshohocken, PA.
- American Society for Testing and Materials, 1995b. "E 564—Static Load Test for Shear Resistance of Framed Walls for Buildings," West Conshohocken, PA.
- Antoniou, S. and Pinho, R., 2004. "Development and Verification of a Displacement-based Adaptive Pushover Procedure," *Journal of Earthquake Engineering*, 8(5), 643-661.
- Applied Technology Council (ATC). 1992. "Guidelines for Cyclic Seismic Testing of Components for Steel Structures," ATC-24 Report, Redwood City, CA.
- CEN, 1995. "Timber Structures—Test Methods—Cyclic Testing of Joints Made with Mechanical Fasteners," Comité Européen de Normalisation, IN TC 124.117, European Committee for Standardization, Brussels, Belgium.
- Cheung, P.C., Pauley, T. and Park, R. 1991. "New Zealand Tests on Full-Scale Reinforced Concrete Beam-Column-Slab Sub-assemblages Designed for Earthquake Resistance," ACI Special Publication SP-123, Design of Beam-Column Joints for Seismic Resistance, American Concrete Institute, Detroit, MI, 1-37.
- Deierlein, G. and Kanvinde, A. 2003. "Seismic Performance of Gypsum Walls - Analytical Investigation," CUREE Report No W-23, Consortium of Universities for Earthquake Engineering, Richmond, CA, 122 p.
- Federal Emergency Management Agency (FEMA), 1997. "NEHRP Guidelines for the Seismic Rehabilitation of Buildings and NEHRP Commentary on the Guidelines for the Seismic Rehabilitation of Buildings," Report Nos. FEMA 273 and 274, Washington, DC.
- Federal Emergency Management Agency (FEMA), 2005. "Improvement of Nonlinear Static Seismic Analysis Procedures," Report No. FEMA 440, Washington, D.C.
- Filiatrault, A., Isoda, H., and Folz, B. 2003. "Hysteretic Damping of Wood Framed Buildings," *Engineering Structures*, Vol. 25, No. 4, 461-471.
- Filiatrault, A., Epperson, M., and Folz, B. 2004. "On the Equivalent Elastic Modeling for the Direct-Displacement Based Seismic Design of Wood Structures," Special Edition of the *ISET Journal of Earthquake Technology on Performance Based Design*, Vol. 41, No. 1, 75-100.

- Gatto, K. and Uang, C-M. 2003. "Effects of Loading Protocol on the Cyclic Response of Woodframe Shearwalls," ASCE Journal of Structural Engineering, 129(10), 1384-1393.
- Hadidi-Tamjed, H. 1987. "Statistical Response of Inelastic SDOF Systems Subjected to Earthquakes," Ph.D. Dissertation, Department of Civil Engineering, Stanford University, Stanford, CA
- Haselton, C., Liel, A. and Deierlein, G. 2006a. "Summary of Results, Four Story SMF (design A, Version 9)," Department of Civil and Environmental Engineering, Stanford University, Stanford, CA.
- Haselton, C., Takagi, J., and Deierlein, G. 2006b. "Summary of Results for Twelve Story Special Wall Including Damage Patterns (Design A, Version 26)," Department of Civil and Environmental Engineering, Stanford University, Stanford, CA.
- He, M., Lam, F. and Prion, G. L. 1998. "Influence of Cyclic Test Protocols on Performance of Wood-Based Shear Walls." Canadian Journal of Civil Engineering, 25(3), 539-550.
- Ibarra, L. 2003. "Global Collapse of Frame Structures under Seismic Excitation," Ph.D. Dissertation, Department of Civil and Environmental Engineering, Stanford University, Stanford, CA.
- International Standards Organization (ISO). 2003. "Timber Structures-Joints Made with Mechanical Fasteners – Quasi-Static Reversed-Cyclic Test Method," International Standards Organization 16670:2003(E). ISO, Switzerland.
- Karacabeyli, E., 1998. "Lateral Resistance of Nailed Shear Walls Subjected to Static and Cyclic Displacements," Research Report, FPS 49th Annual Meeting, Portland, OR.
- Krawinkler, H., Bonowitz, D., Goodno, B., Kuan, S., Maffei, J., Memari, A., Restrepo, J. and Uang, C-M. 2005. "Racking Testing of Drift Sensitive Nonstructural Components," in Interim Protocols for Seismic Performance Testing of Architectural, Mechanical and Electrical Components – Third Draft, ATC-58 Project, Applied Technology Council, Redwood City, CA.
- Krawinkler, Parisi, F., Ibarra, L., Ayoub, A., and Medina, R. 2000. "Development of a Testing Protocol for Wood Frame Structures," CUREE Publication No. W-02, Consortium of Universities for Research in Earthquake Engineering, Richmond, CA.
- Liel, A., Haselton, C. and Deierlein, G. 2006. "4 Story IMF (Design C, Version 9)," Department of Civil and Environmental Engineering, Stanford University, Stanford, CA.
- Nassar, A.A. and Krawinkler, H. 1991. "Seismic Demands for SDOF and MDOF Systems," John A. Blume Earthquake Engineering Research Report No. 95, Department of Civil Engineering, Stanford University, Stanford, CA.

- Nathan, S.V., Dameron, R.A. and Danielians, A. 1995. "Seismic Retrofit of Historical Cesar E Chavez Ave Bridge Using Linear and 3D Nonlinear Pushover Analysis," National Seismic Conference on Bridges and Highways: Progress in Research and Practice; San Diego, CA.
- Porter, M.L., 1987. "Sequential Phased Displacement (SPD) Procedure for TCCMAR Testing," Proceedings, 3rd Meeting of the Joint Technical Coordinating Committee on Masonry Research, US-Japan Coordinated Research Program.
- Ramirez, O.M., Constantinou, M.C., Kircher, C.A., Whittaker, A.S., Johnson, M.W., Gomez, J.D., and C.Z. Chrysostomou, 2001. "Development and Evaluation of Simplified Procedures For Analysis and Design of Buildings with Passive Energy Dissipation Systems," Report No. MCEER-00-0010, Revision 1, Multidisciplinary Center for Earthquake Engineering Research, Buffalo, NY.
- SAC Joint Venture. 1997. "Protocol for Fabrication, Inspection, Testing and Documentation of Beam-Column Connection and Other Experimental Specimens," Report No. SAC/BD-97/02, Sacramento, CA.
- Shome, N. and Cornell, C.A. 2000. "Structural Seismic Demand Analysis: Consideration of Collapse," 8th ASCE Specialty Conference on Probabilistic Mechanics and Structural Reliability, Paper PMC2000-119.
- Yasumura, M. 1999. "Testing and Evaluation of Seismic Performance of Woodframe Structures in Japan: State-of-the-Art and Research Needs." Invitational Workshop on Seismic Testing, Analysis, and Design of Woodframe Construction; Los Angeles, CA, Seible, F. et al., eds. Consortium of Universities for Research in Earthquake Engineering, Richmond, CA, 93-97.

APPENDIX A

MEDIAN SPECTRAL ACCELERATION VALUES FOR 60 GROUND MOTIONS USED IN ANALYSES

Table A-1. Median Response Spectra for 0.11g Intensity Motions

Median Sa (g) at various damping level									
T (sec)	5%	10%	15%	20%	25%	30%	40%	50%	60%
0.1	0.163	0.138	0.130	0.123	0.122	0.120	0.103	0.090	0.080
0.5	0.190	0.144	0.126	0.109	0.096	0.086	0.074	0.065	0.058
1.0	0.108	0.092	0.079	0.068	0.060	0.055	0.047	0.042	0.037
1.5	0.066	0.056	0.048	0.042	0.037	0.034	0.029	0.025	0.023
2.0	0.047	0.036	0.033	0.029	0.026	0.024	0.021	0.018	0.016
2.5	0.033	0.027	0.023	0.021	0.019	0.018	0.015	0.013	0.012
3.0	0.027	0.023	0.020	0.017	0.015	0.013	0.011	0.010	0.009
3.5	0.023	0.017	0.015	0.013	0.012	0.011	0.009	0.008	0.007
4.0	0.017	0.013	0.011	0.010	0.010	0.009	0.008	0.007	0.006
4.5	0.014	0.010	0.010	0.009	0.008	0.008	0.007	0.006	0.005
5.0	0.012	0.009	0.008	0.007	0.007	0.006	0.005	0.005	0.004

Table A-2. Median Response Spectra for 0.32g Intensity Motions

Median Sa (g) at various damping level									
T (sec)	5%	10%	15%	20%	25%	30%	40%	50%	60%
0.1	0.488	0.437	0.404	0.391	0.381	0.368	0.314	0.276	0.245
0.5	0.587	0.441	0.381	0.329	0.286	0.258	0.220	0.194	0.172
1.0	0.320	0.273	0.236	0.208	0.183	0.167	0.143	0.126	0.111
1.5	0.196	0.169	0.143	0.128	0.112	0.103	0.088	0.077	0.069
2.0	0.138	0.111	0.096	0.087	0.079	0.072	0.061	0.054	0.048
2.5	0.100	0.080	0.069	0.063	0.057	0.053	0.045	0.040	0.035
3.0	0.078	0.068	0.059	0.050	0.046	0.043	0.037	0.032	0.029
3.5	0.069	0.054	0.045	0.039	0.036	0.033	0.028	0.025	0.022
4.0	0.049	0.041	0.035	0.032	0.029	0.027	0.023	0.020	0.018
4.5	0.041	0.035	0.030	0.026	0.025	0.023	0.020	0.018	0.016
5.0	0.036	0.029	0.025	0.023	0.021	0.019	0.017	0.015	0.013

Table A-3. Median Response Spectra for 1.12g Intensity Motions

T (sec)	Median Sa (g) at various damping level								
	5%	10%	15%	20%	25%	30%	40%	50%	60%
0.1	1.707	1.528	1.414	1.369	1.334	1.287	1.100	0.968	0.858
0.5	2.053	1.544	1.333	1.152	1.001	0.902	0.771	0.679	0.602
1.0	1.120	0.955	0.825	0.727	0.639	0.585	0.500	0.440	0.390
1.5	0.686	0.591	0.500	0.448	0.392	0.360	0.308	0.271	0.240
2.0	0.481	0.389	0.336	0.305	0.277	0.252	0.215	0.189	0.168
2.5	0.349	0.279	0.242	0.219	0.201	0.185	0.158	0.139	0.123
3.0	0.273	0.239	0.205	0.176	0.162	0.150	0.128	0.113	0.100
3.5	0.242	0.190	0.156	0.137	0.125	0.115	0.099	0.087	0.077
4.0	0.173	0.142	0.123	0.111	0.102	0.094	0.080	0.070	0.062
4.5	0.144	0.122	0.104	0.091	0.087	0.082	0.070	0.061	0.054
5.0	0.126	0.101	0.089	0.080	0.072	0.068	0.058	0.051	0.045

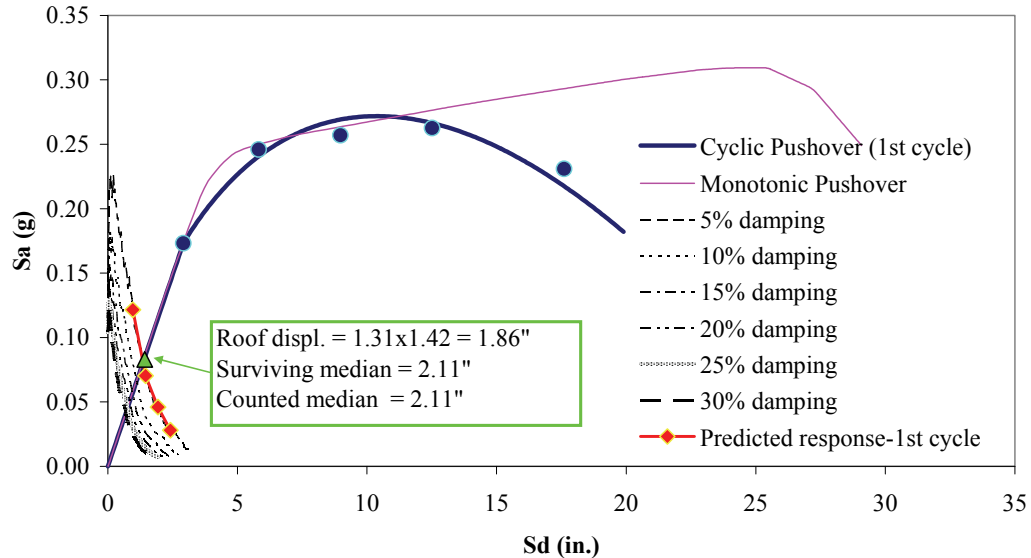
Table A-4. Median Response Spectra for 1.92g Intensity Motions

T (sec)	Median Sa (g) at various damping level								
	5%	10%	15%	20%	25%	30%	40%	50%	60%
0.1	2.926	2.620	2.424	2.347	2.286	2.206	1.885	1.659	1.471
0.5	3.519	2.647	2.286	1.975	1.717	1.547	1.322	1.163	1.031
1.0	1.920	1.638	1.414	1.246	1.095	1.003	0.857	0.754	0.668
1.5	1.176	1.014	0.857	0.768	0.673	0.617	0.527	0.464	0.411
2.0	0.825	0.667	0.575	0.523	0.474	0.432	0.369	0.325	0.288
2.5	0.599	0.479	0.415	0.376	0.345	0.317	0.271	0.239	0.212
3.0	0.468	0.409	0.352	0.302	0.278	0.257	0.220	0.193	0.171
3.5	0.415	0.325	0.267	0.234	0.214	0.198	0.169	0.149	0.132
4.0	0.296	0.243	0.211	0.190	0.175	0.160	0.137	0.121	0.107
4.5	0.247	0.208	0.178	0.156	0.149	0.140	0.120	0.105	0.093
5.0	0.216	0.172	0.152	0.137	0.123	0.116	0.099	0.087	0.077

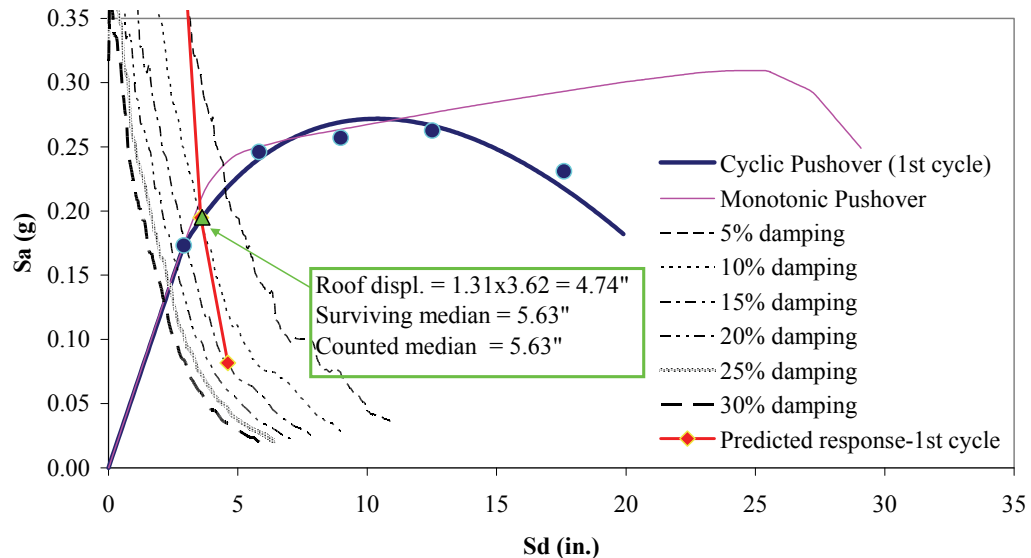
APPENDIX B

PREDICTIONS OF MEDIAN ROOF DISPLACEMENT OF 4-STORY SMF USING SIMPLIFIED CAPACITY SPECTRUM METHOD

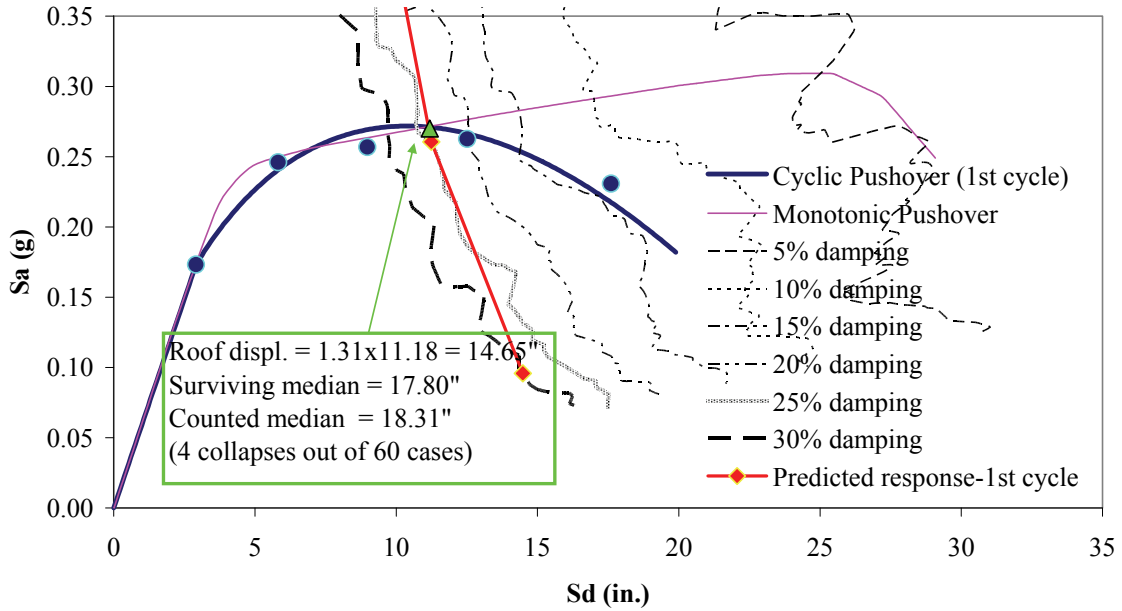
Spectral Capacity Curve: 4-Story SMF (DesA v.6)
Proposed Protocol, 1 Cyclic Dwell
"Median" of Actual Spectra, Sa (1 sec) = 0.11g



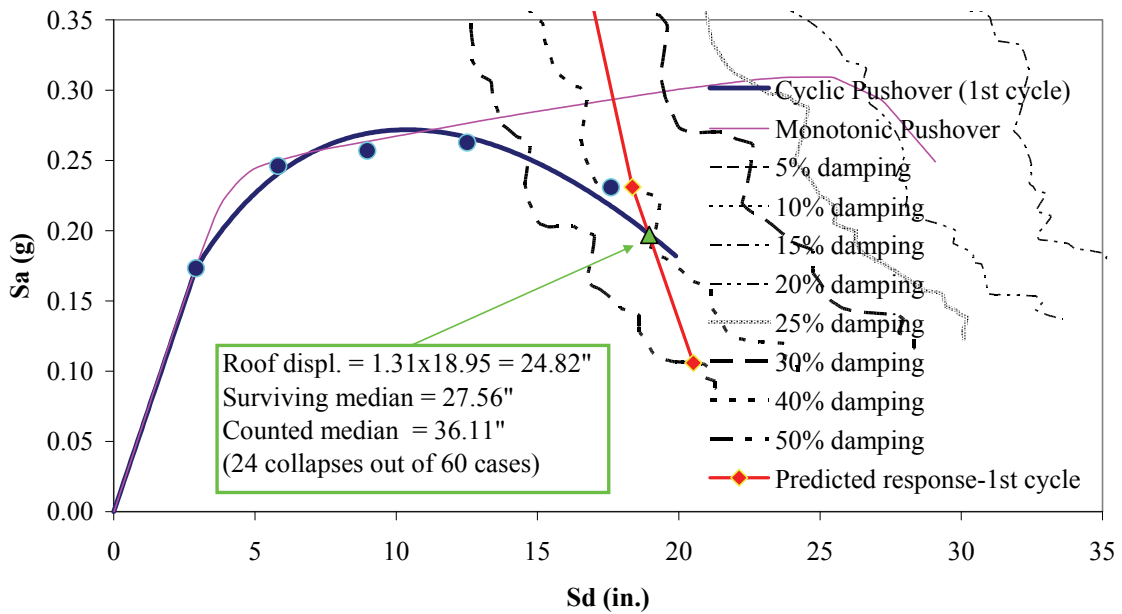
Spectral Capacity Curve: 4-Story SMF (DesA v.6)
Proposed Protocol, 1 Cyclic Dwell
"Median" of Actual Spectra, Sa (1 sec) = 0.32g



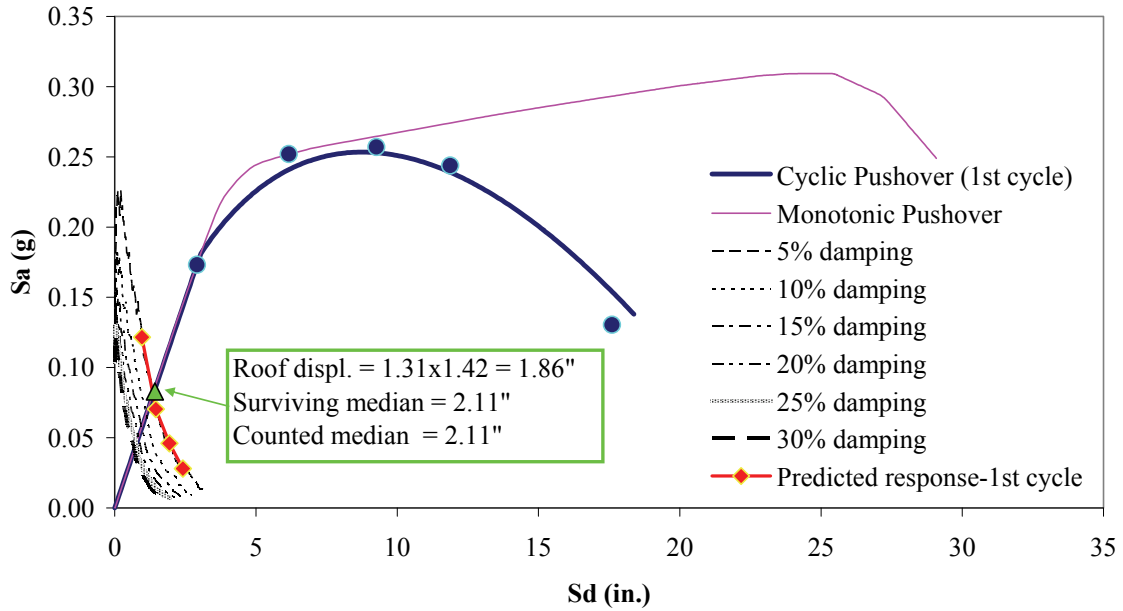
Spectral Capacity Curve: 4-Story SMF (DesA v.6)
Proposed Protocol, 1 Cyclic Dwell
"Median" of Actual Spectra, Sa (1 sec) = 1.12g



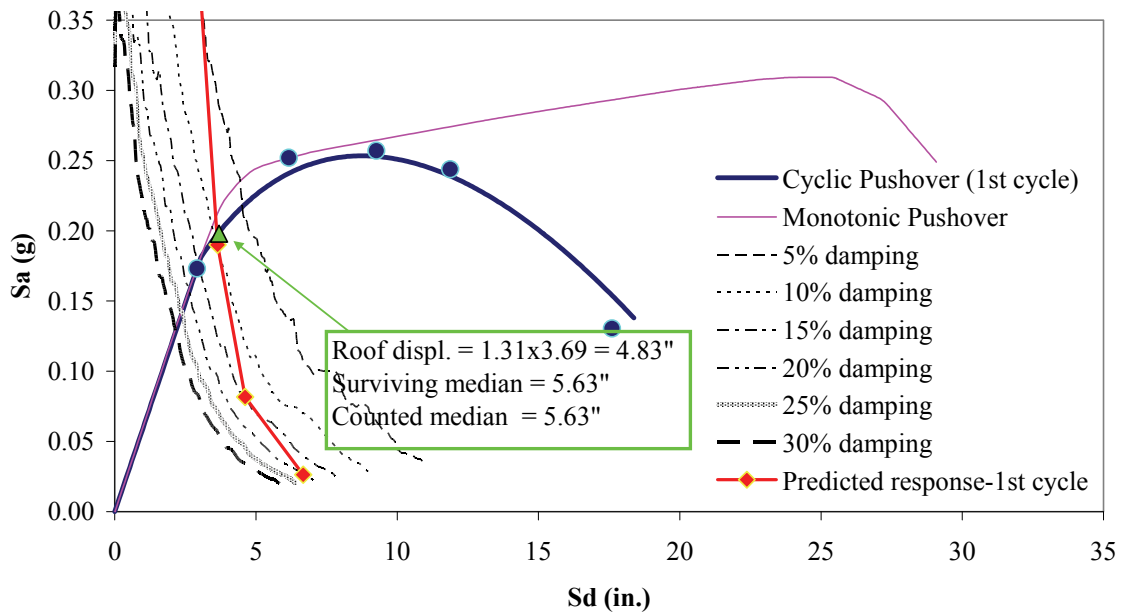
Spectral Capacity Curve: 4-Story SMF (DesA v.6)
Proposed Protocol, 1 Cyclic Dwell
"Median" of Actual Spectra, Sa (1 sec) = 1.92g



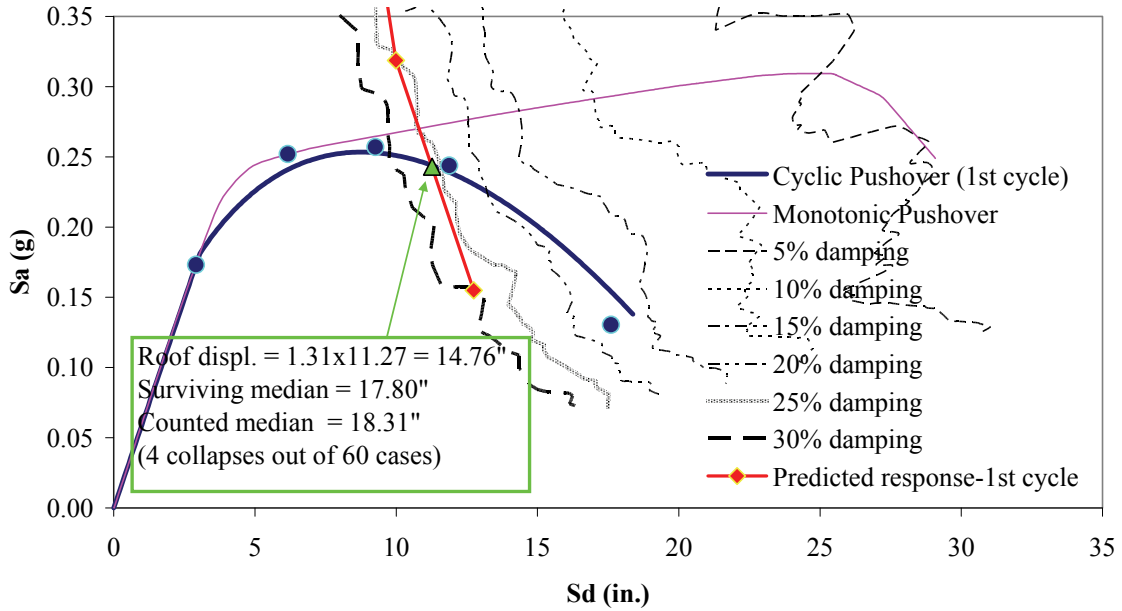
Spectral Capacity Curve: 4-Story SMF (DesA v.6)
Proposed Protocol, 2 Cyclic Dwell, 1st Cycle
"Median" of Actual Spectra, Sa (1 sec) = 0.11g



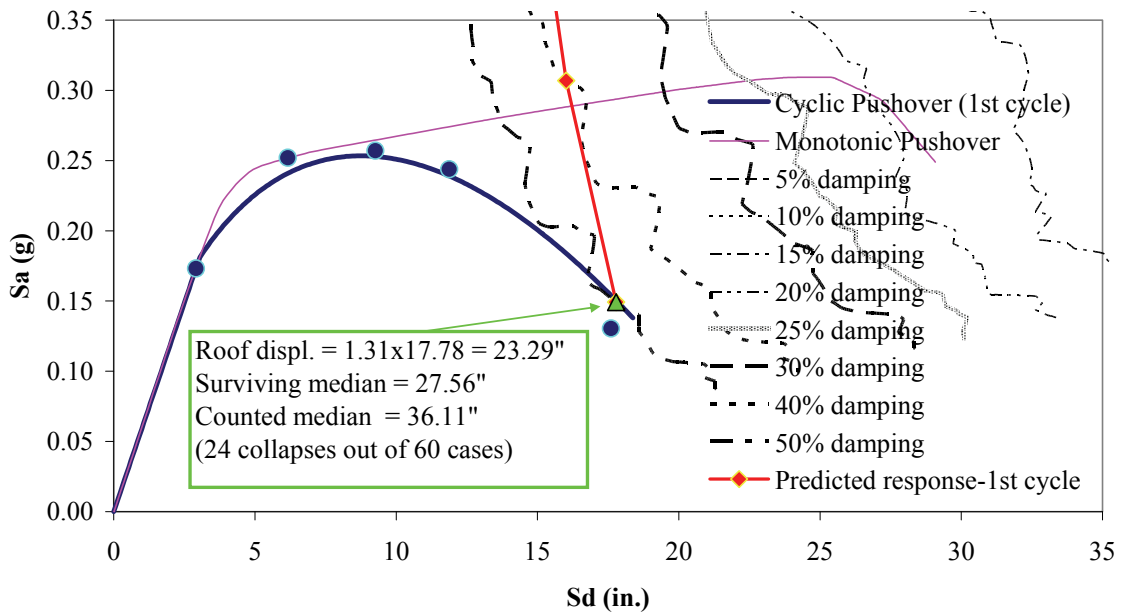
Spectral Capacity Curve: 4-Story SMF (DesA v.6)
Proposed Protocol, 2 Cyclic Dwell, 1st Cycle
"Median" of Actual Spectra, Sa (1 sec) = 0.32g



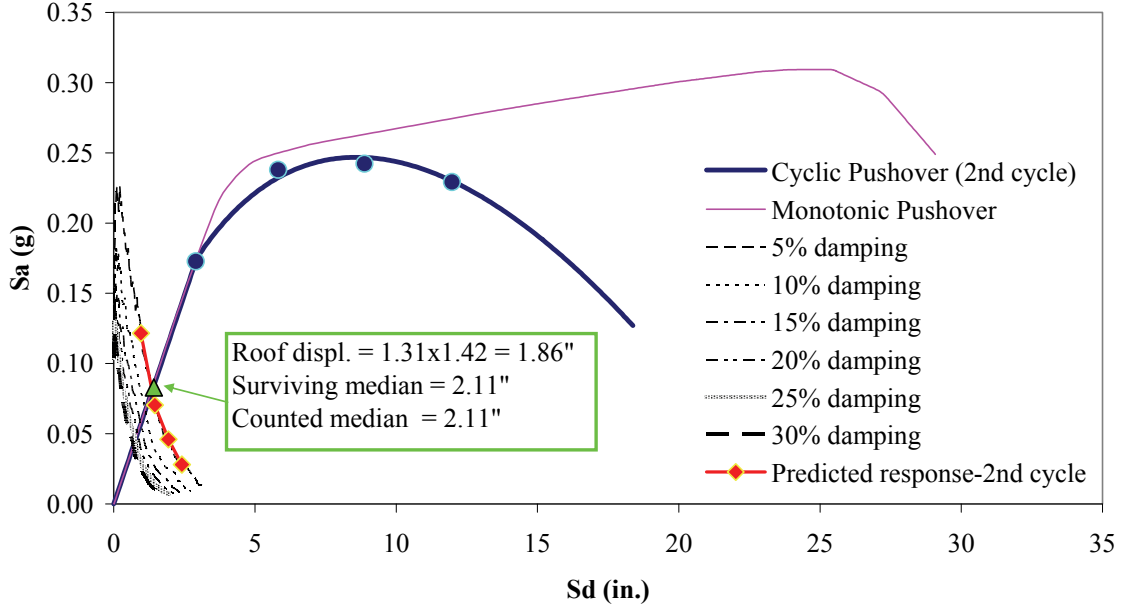
Spectral Capacity Curve: 4-Story SMF (DesA v.6)
Proposed Protocol, 2 Cyclic Dwell, 1st Cycle
"Median" of Actual Spectra, Sa (1 sec) = 1.12g



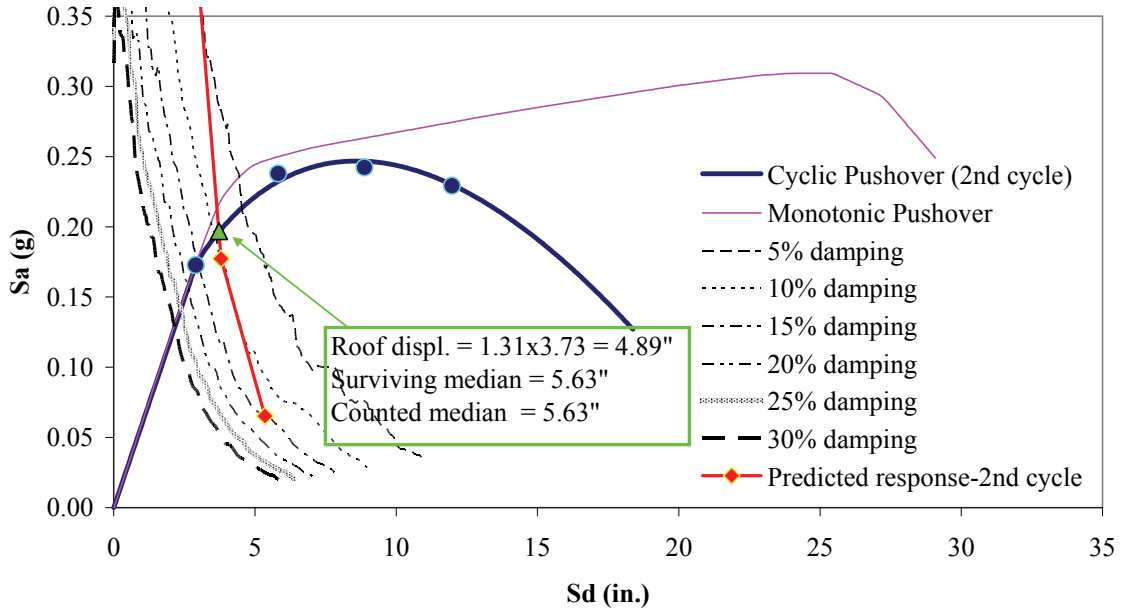
Spectral Capacity Curve: 4-Story SMF (DesA v.6)
Proposed Protocol, 2 Cyclic Dwell, 1st Cycle
"Median" of Actual Spectra, Sa (1 sec) = 1.92g



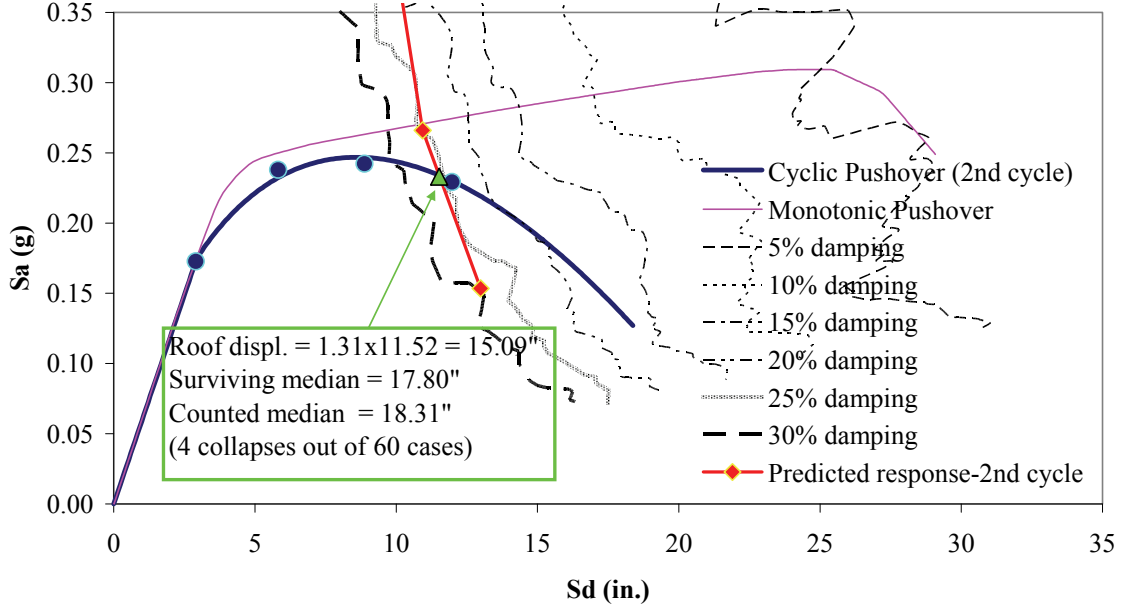
Spectral Capacity Curve: 4-Story SMF (DesA v.6)
Proposed Protocol, 2 Cyclic Dwell, 2nd Cycle
"Median" of Actual Spectra, Sa (1 sec) = 0.11g



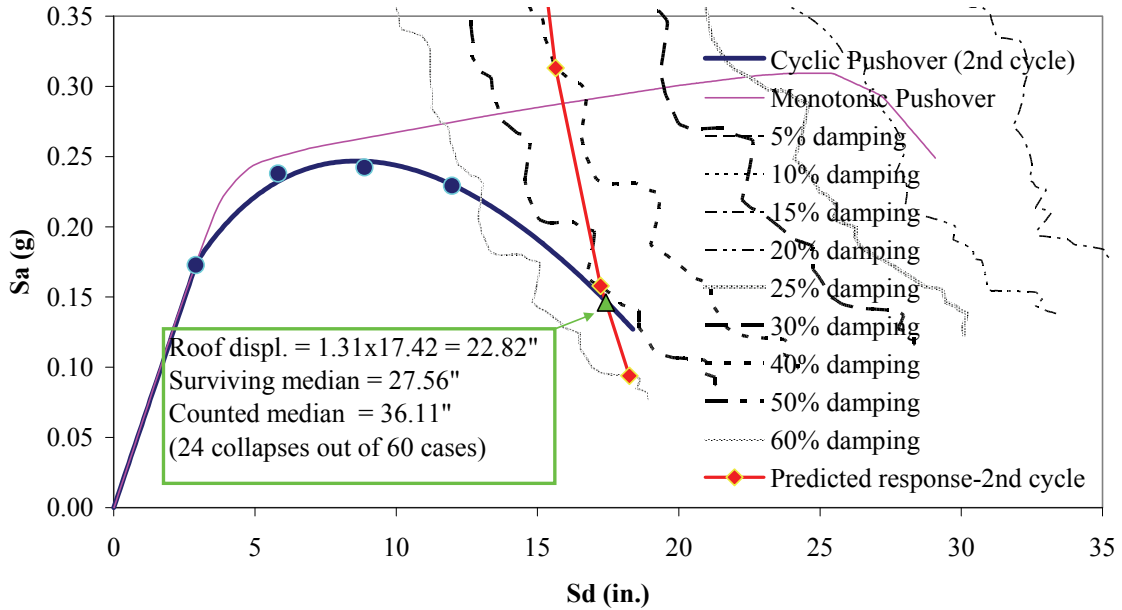
Spectral Capacity Curve: 4-Story SMF (DesA v.6)
Proposed Protocol, 2 Cyclic Dwell, 2nd Cycle
"Median" of Actual Spectra, Sa (1 sec) = 0.32g



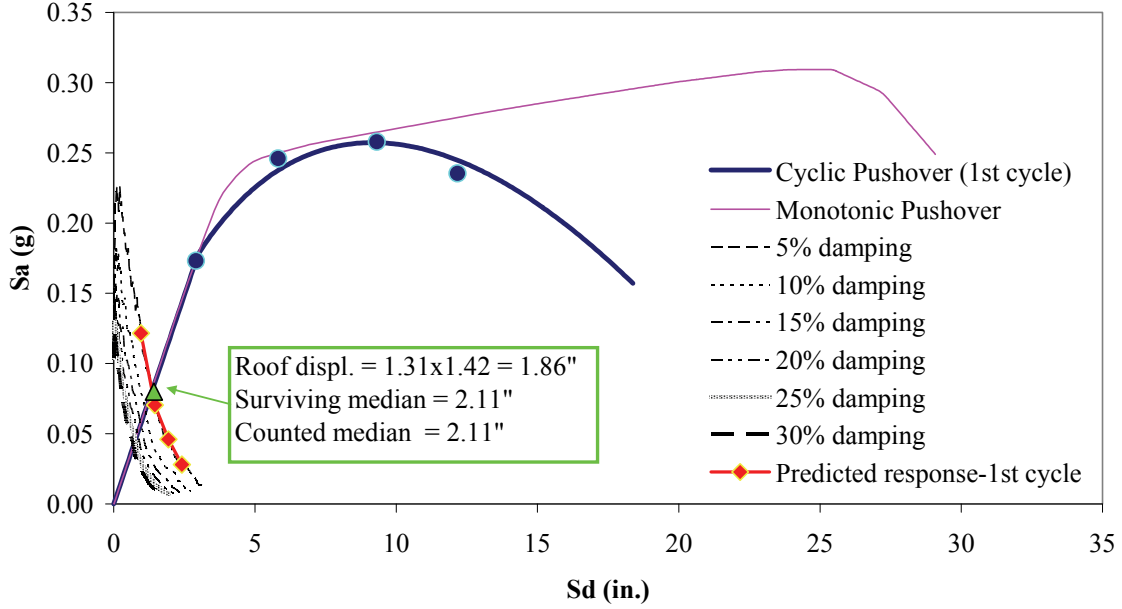
Spectral Capacity Curve: 4-Story SMF (DesA v.6)
Proposed Protocol, 2 Cyclic Dwell, 2nd Cycle
"Median" of Actual Spectra, Sa (1 sec) = 1.12g



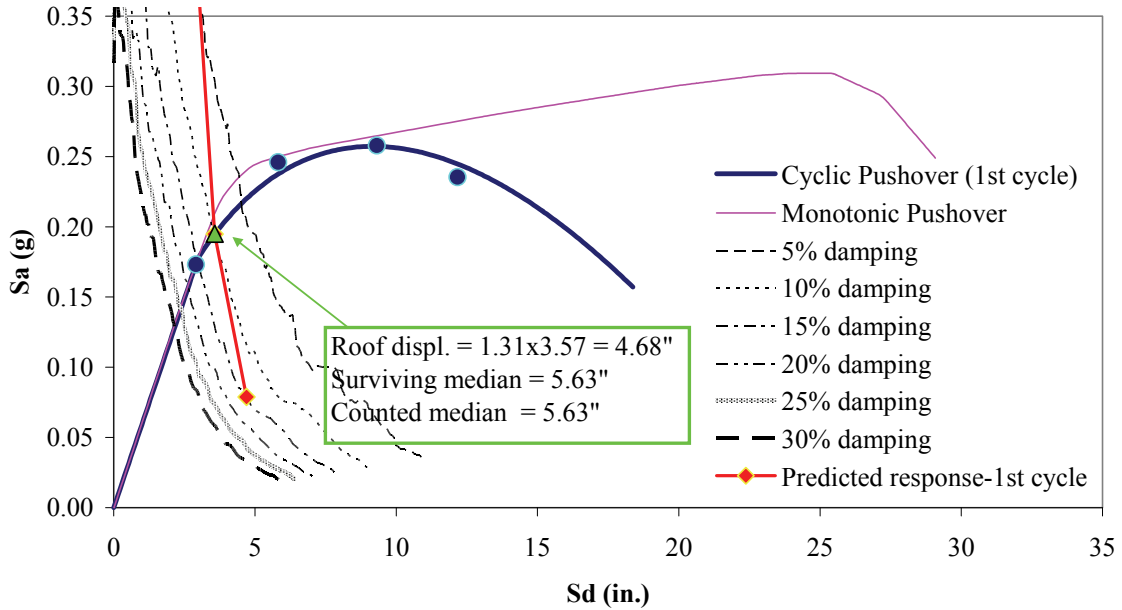
Spectral Capacity Curve: 4-Story SMF (DesA v.6)
Proposed Protocol, 2 Cyclic Dwell, 2nd Cycle
"Median" of Actual Spectra, Sa (1 sec) = 1.92g



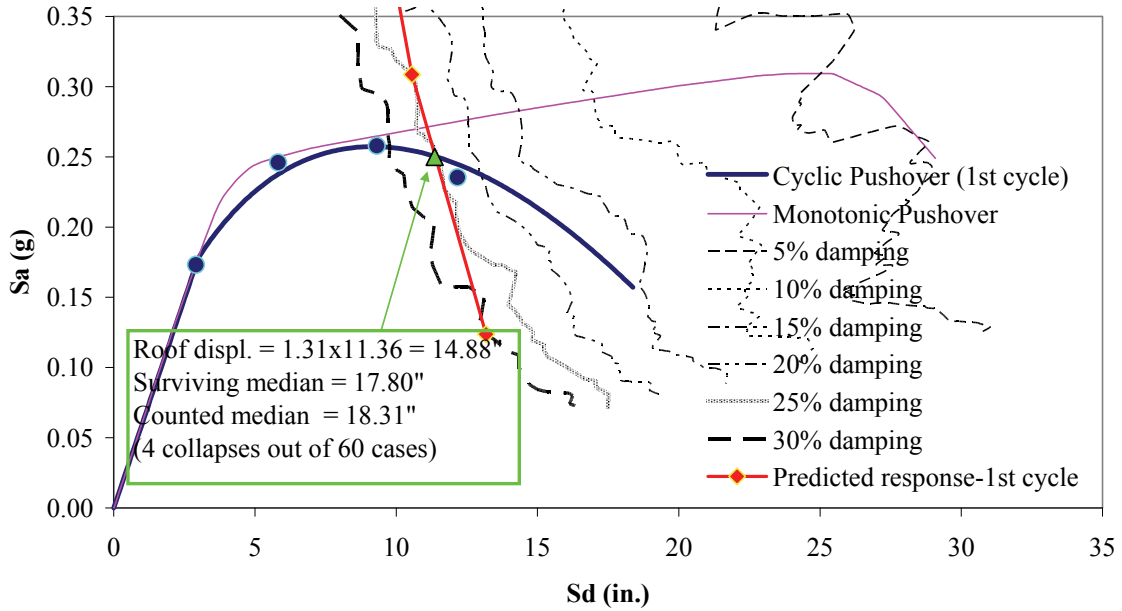
Spectral Capacity Curve: 4-Story SMF (DesA v.6)
Proposed Protocol, 3 Cyclic Dwell, 1st Cycle
"Median" of Actual Spectra, Sa (1 sec) = 0.11g



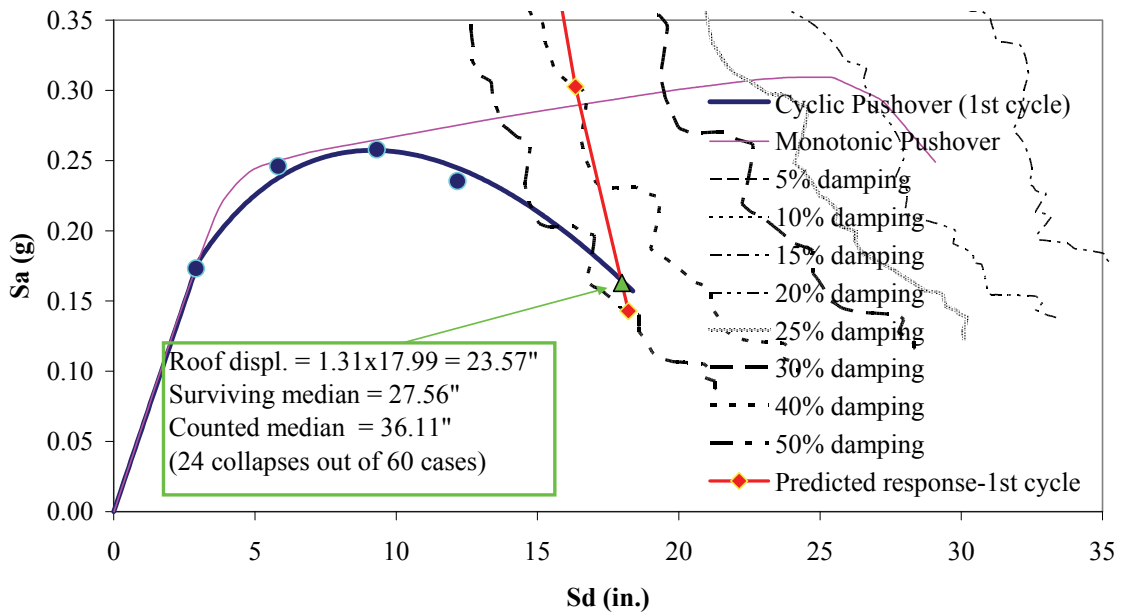
Spectral Capacity Curve: 4-Story SMF (DesA v.6)
Proposed Protocol, 3 Cyclic Dwell, 1st Cycle
"Median" of Actual Spectra, Sa (1 sec) = 0.32g



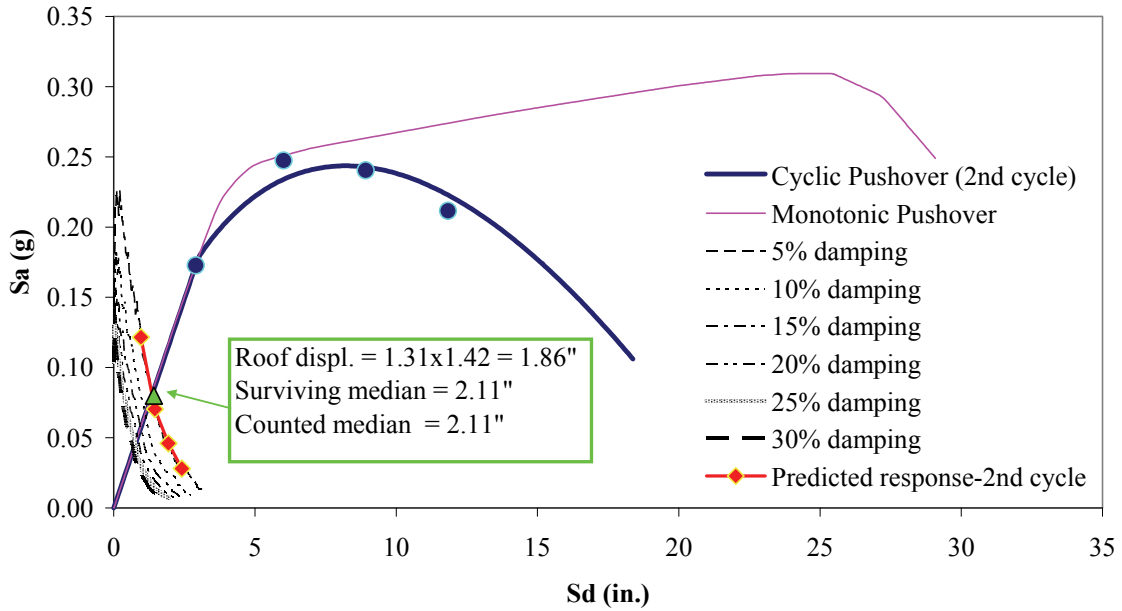
Spectral Capacity Curve: 4-Story SMF (DesA v.6)
Proposed Protocol, 3 Cyclic Dwell, 1st Cycle
"Median" of Actual Spectra, Sa (1 sec) = 1.12g



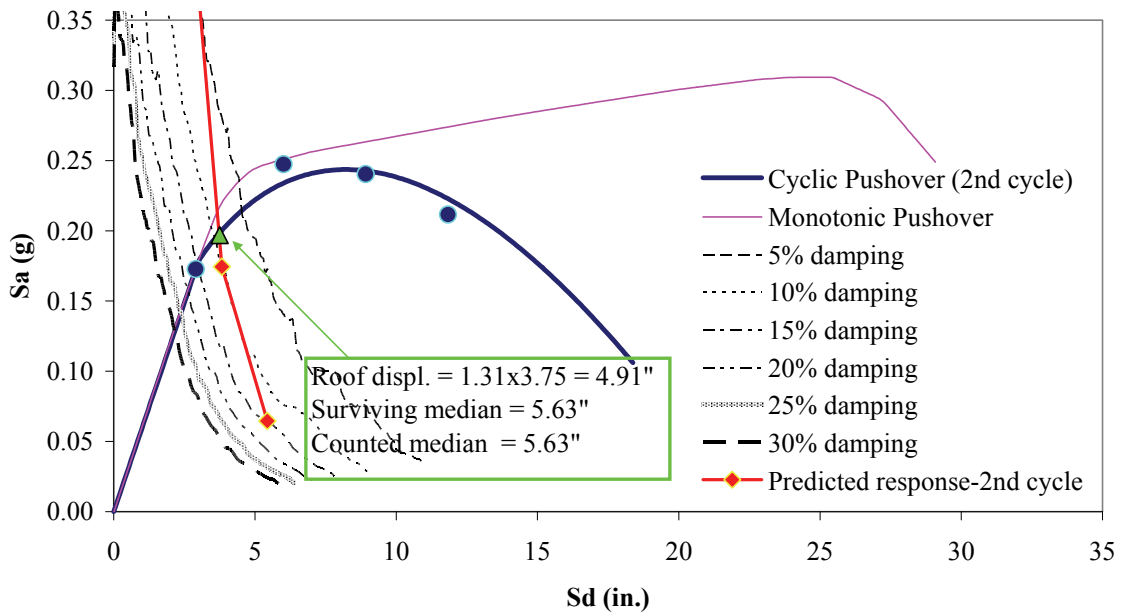
Spectral Capacity Curve: 4-Story SMF (DesA v.6)
Proposed Protocol, 3 Cyclic Dwell, 1st Cycle
"Median" of Actual Spectra, Sa (1 sec) = 1.92g



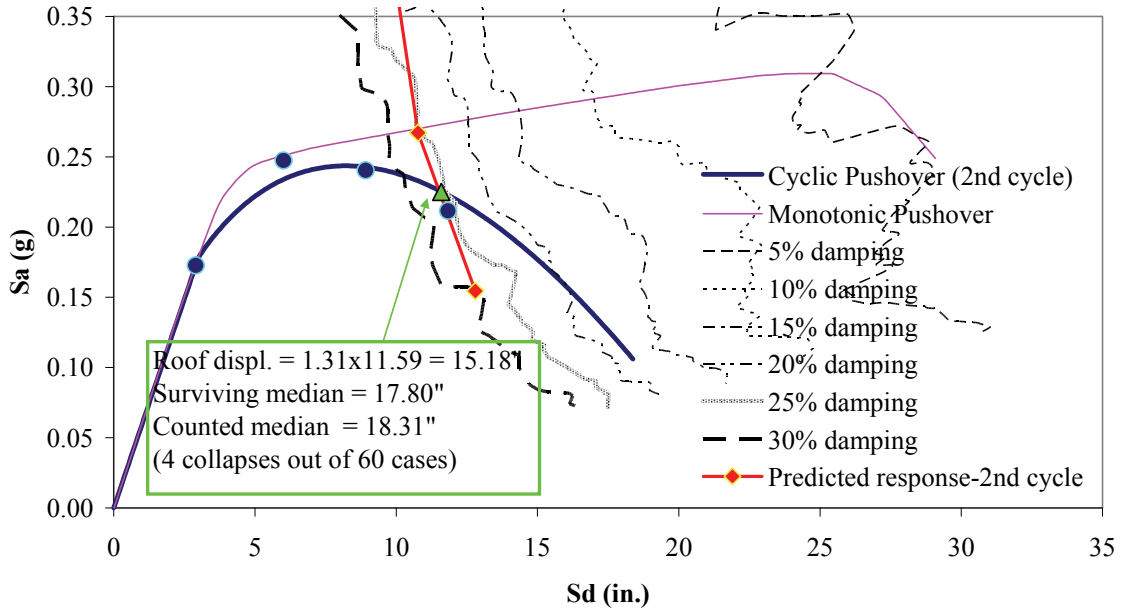
Spectral Capacity Curve: 4-Story SMF (DesA v.6)
Proposed Protocol, 3 Cyclic Dwell, 2nd Cycle
"Median" of Actual Spectra, Sa (1 sec) = 0.11g



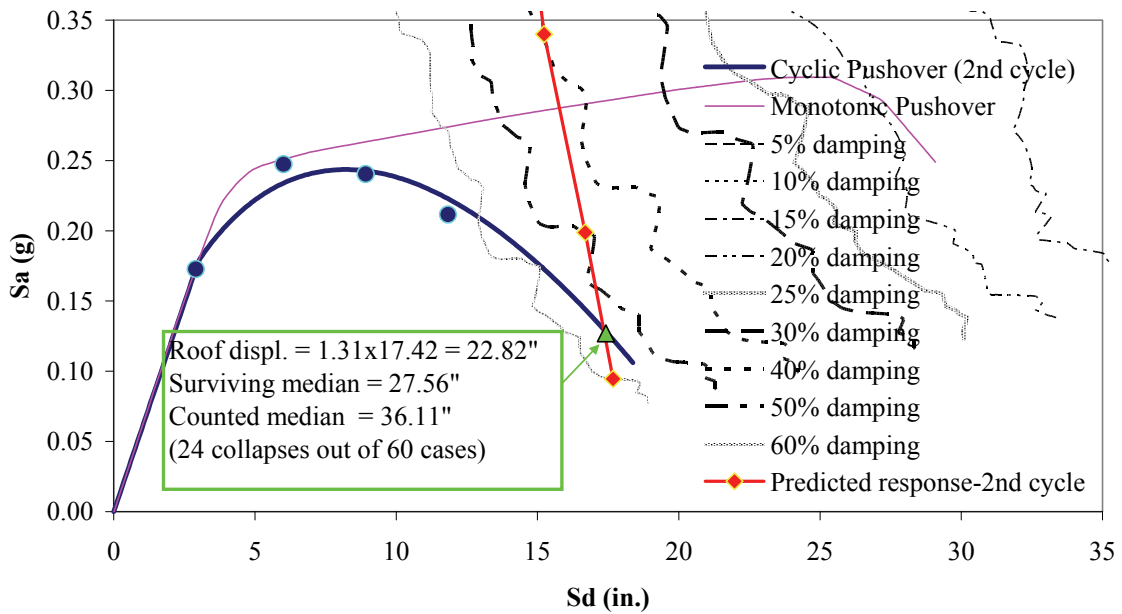
Spectral Capacity Curve: 4-Story SMF (DesA v.6)
Proposed Protocol, 3 Cyclic Dwell, 2nd Cycle
"Median" of Actual Spectra, Sa (1 sec) = 0.32g



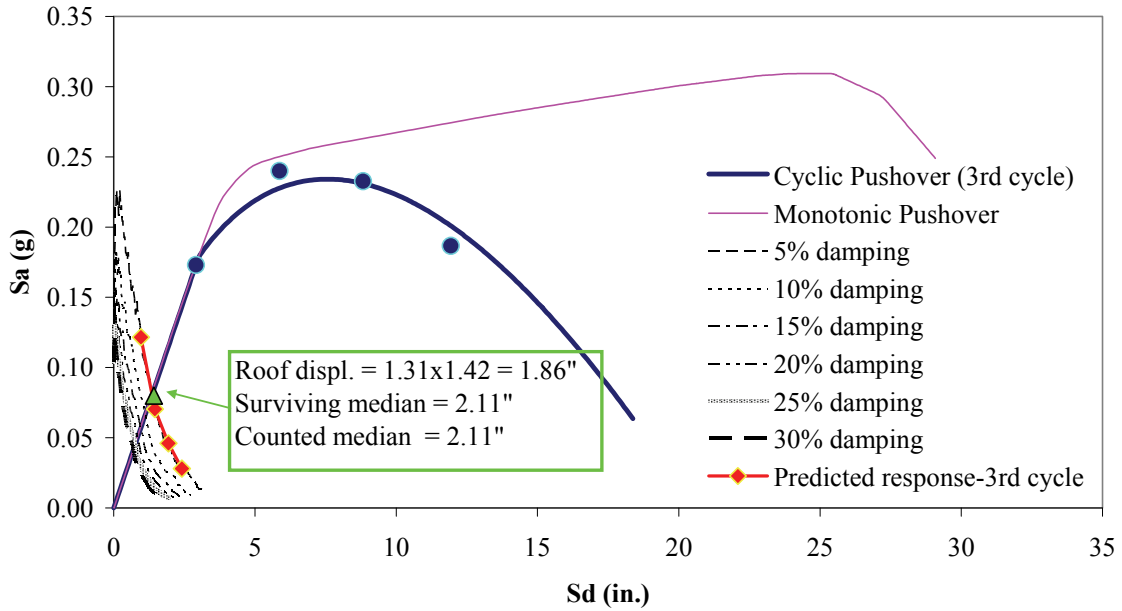
Spectral Capacity Curve: 4-Story SMF (DesA v.6)
Proposed Protocol, 3 Cyclic Dwell, 2nd Cycle
"Median" of Actual Spectra, Sa (1 sec) = 1.12g



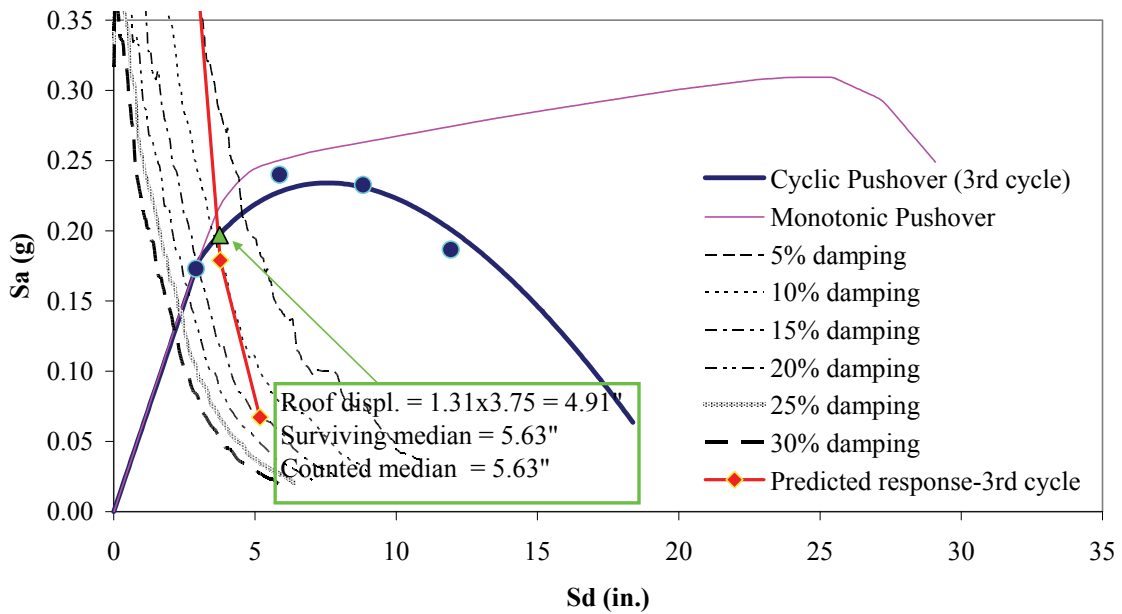
Spectral Capacity Curve: 4-Story SMF (DesA v.6)
Proposed Protocol, 3 Cyclic Dwell, 2nd Cycle
"Median" of Actual Spectra, Sa (1 sec) = 1.92g



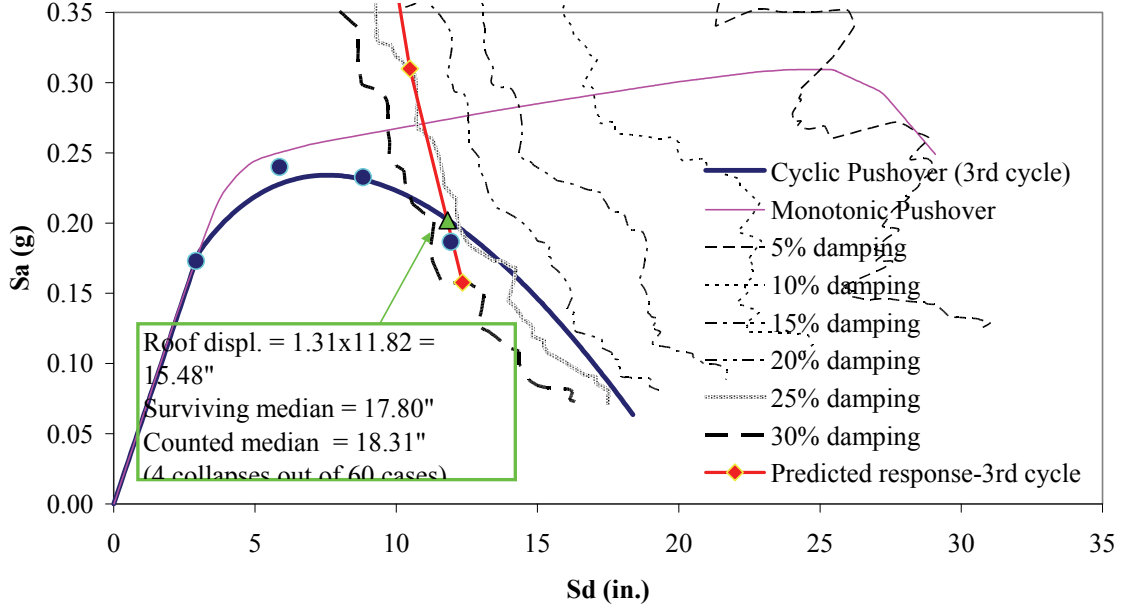
Spectral Capacity Curve: 4-Story SMF (DesA v.6)
Proposed Protocol, 3 Cyclic Dwell, 3rd Cycle
"Median" of Actual Spectra, Sa (1 sec) = 0.11g



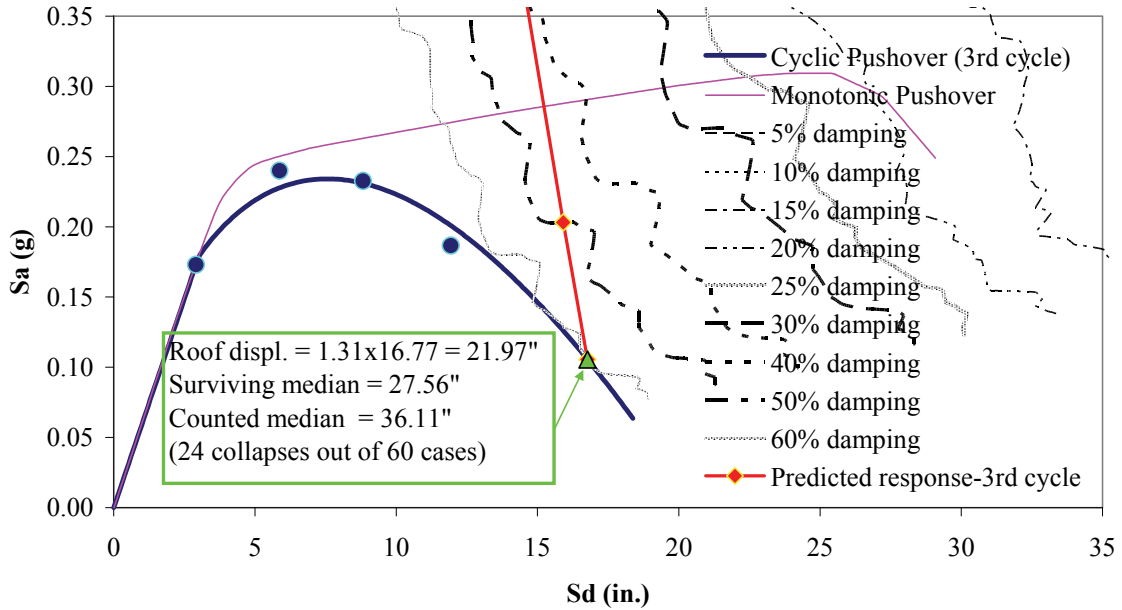
Spectral Capacity Curve: 4-Story SMF (DesA v.6)
Proposed Protocol, 3 Cyclic Dwell, 3rd Cycle
"Median" of Actual Spectra, Sa (1 sec) = 0.32g



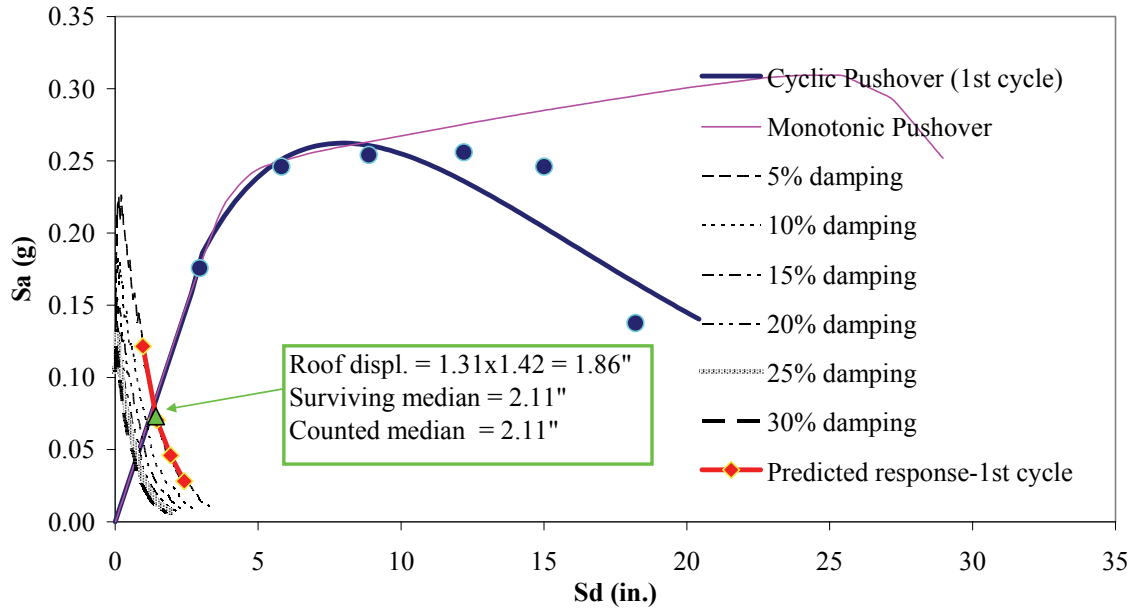
Spectral Capacity Curve: 4-Story SMF (DesA v.6)
Proposed Protocol, 3 Cyclic Dwell, 3rd Cycle
"Median" of Actual Spectra, Sa (1 sec) = 1.12g



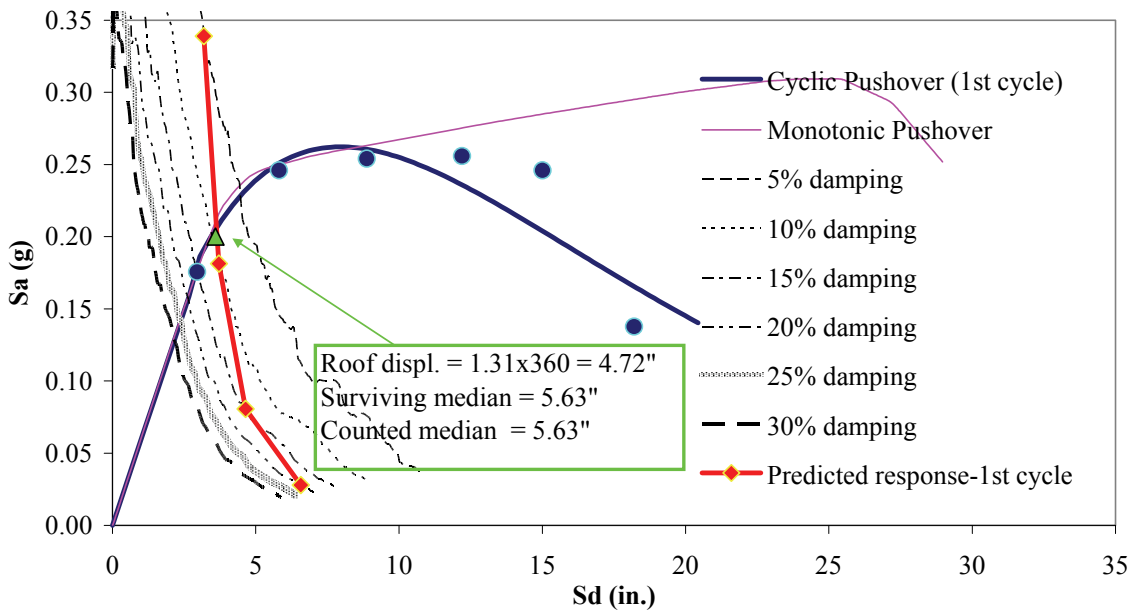
Spectral Capacity Curve: 4-Story SMF (DesA v.6)
Proposed Protocol, 3 Cyclic Dwell, 3rd Cycle
"Median" of Actual Spectra, Sa (1 sec) = 1.92g



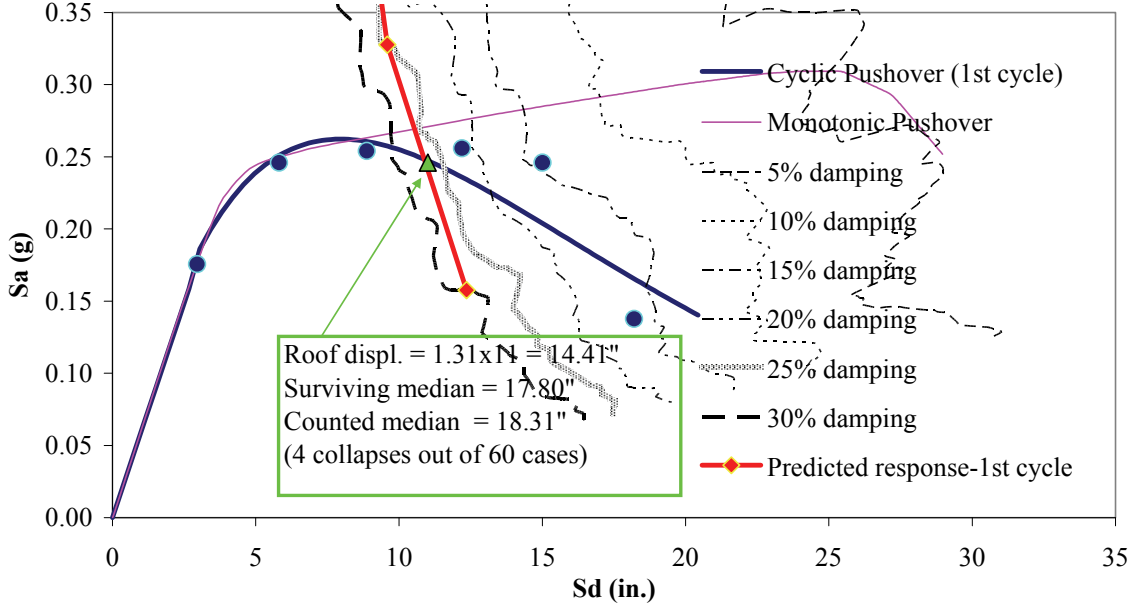
Spectral Capacity Curve: 4-Story SMF (DesA v.6)
Arbitrary Protocol, 1 Cyclic Dwell
"Median" of Actual Spectra, Sa (1 sec) = 0.11g



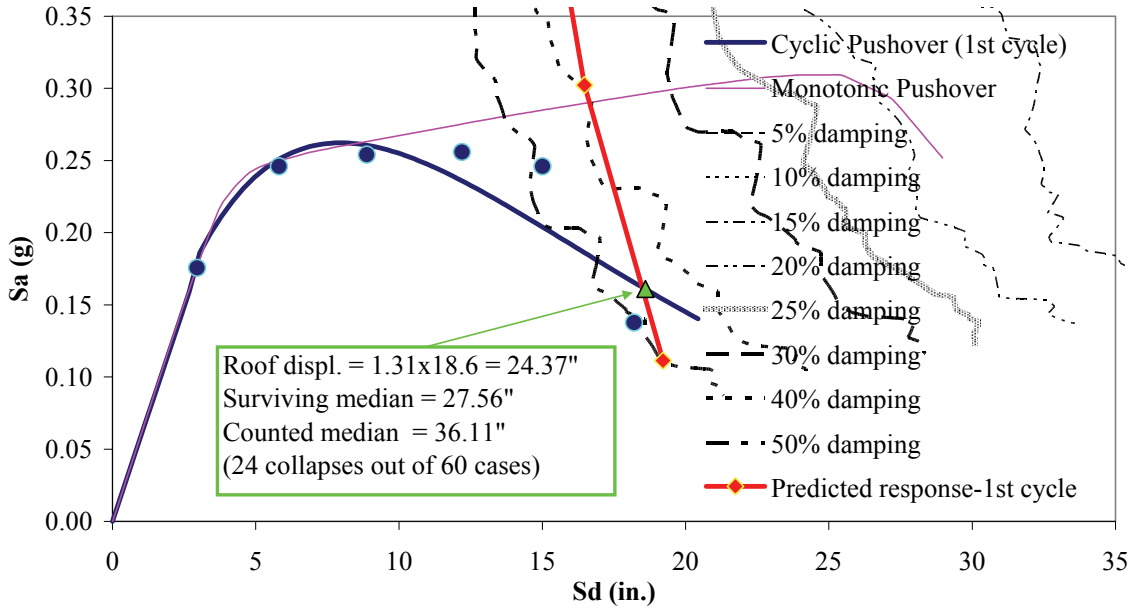
Spectral Capacity Curve: 4-Story SMF (DesA v.6)
Arbitrary Protocol, 1 Cyclic Dwell
"Median" of Actual Spectra, Sa (1 sec) = 0.32g



Spectral Capacity Curve: 4-Story SMF (DesA v.6)
Arbitrary Protocol, 1 Cyclic Dwell
"Median" of Actual Spectra, Sa (1 sec) = 1.12g



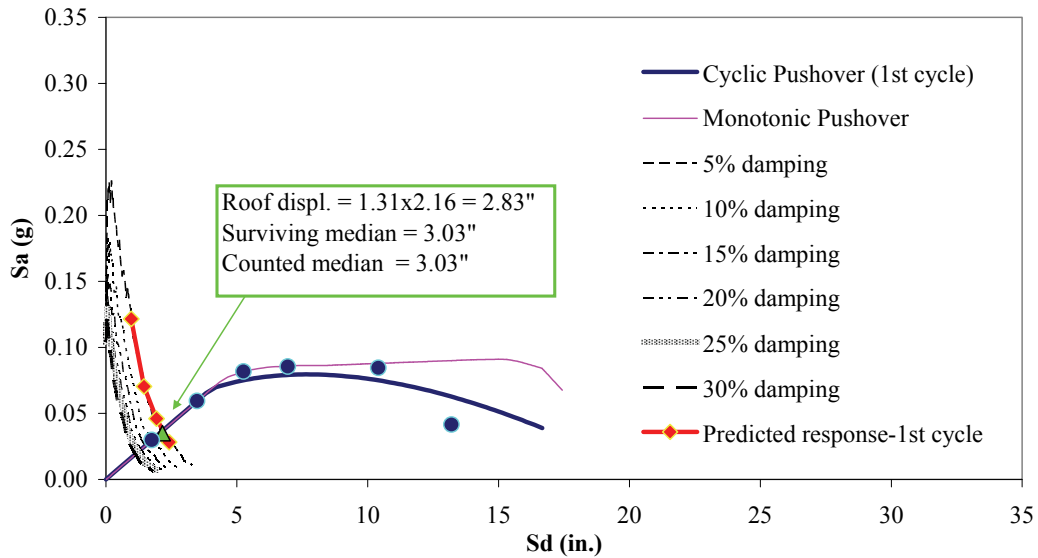
Spectral Capacity Curve: 4-Story SMF (DesA v.6)
Arbitrary Protocol, 1 Cyclic Dwell
"Median" of Actual Spectra, Sa (1 sec) = 1.92g



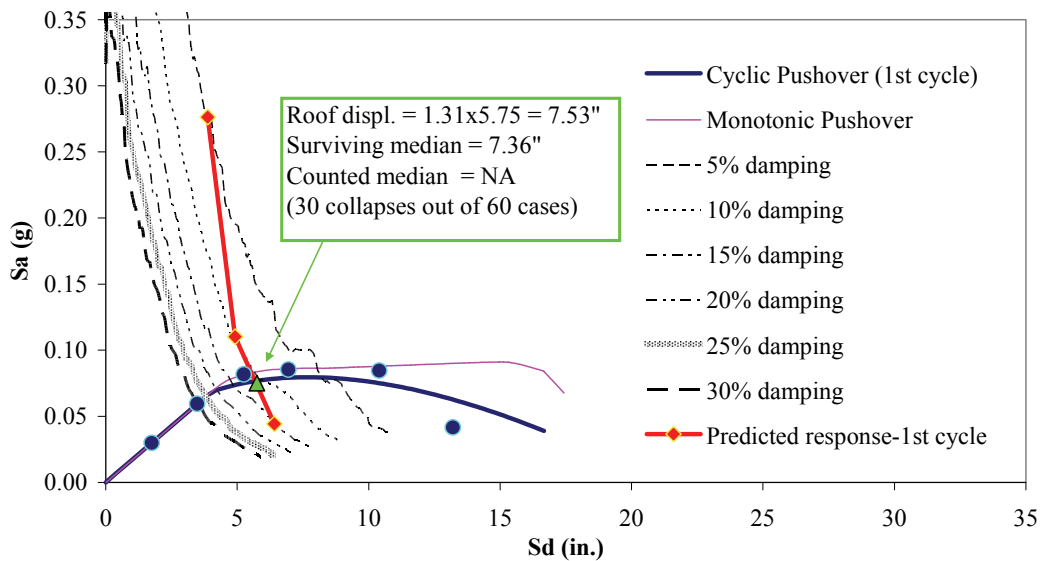
APPENDIX C

PREDICTIONS OF MEDIAN ROOF DISPLACEMENT OF 4-STORY IMF USING SIMPLIFIED CAPACITY SPECTRUM METHOD

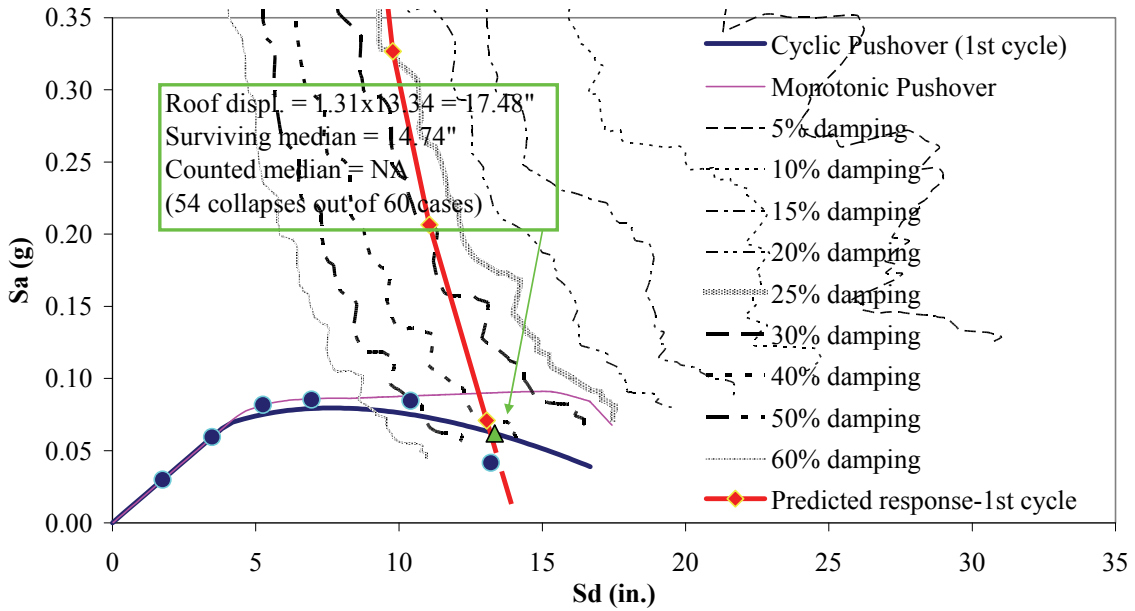
Spectral Capacity Curve: 4-Story IMF (DesC v.9)
Proposed Protocol, 1 Cyclic Dwell
"Median" of Actual Spectra, S_a (1 sec) = 0.11g



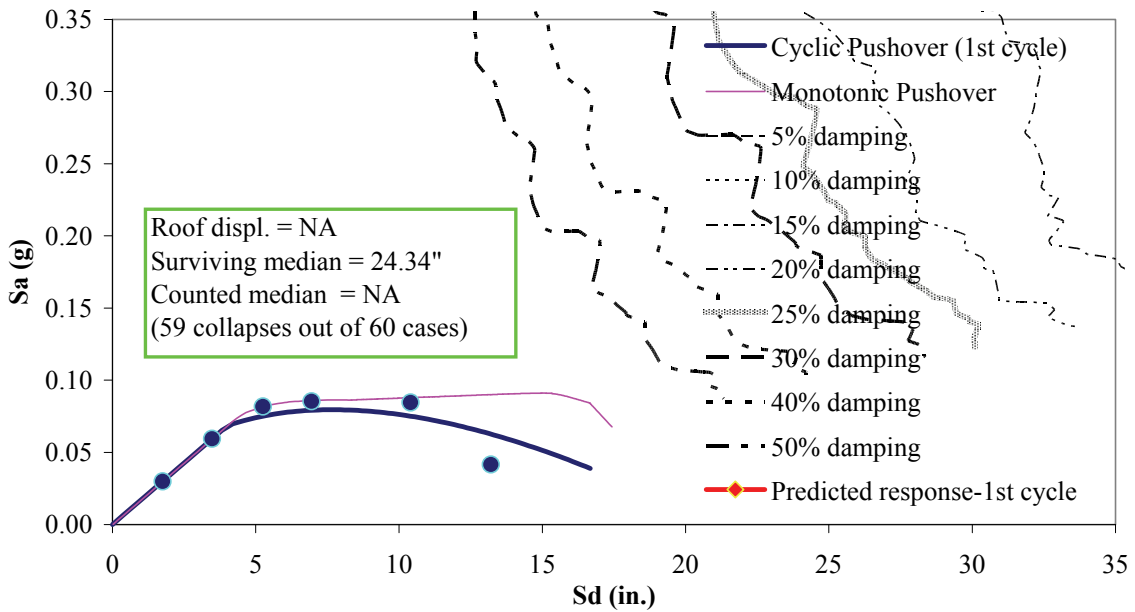
Spectral Capacity Curve: 4-Story IMF (DesC v.9)
Proposed Protocol, 1 Cyclic Dwell
"Median" of Actual Spectra, S_a (1 sec) = 0.32g



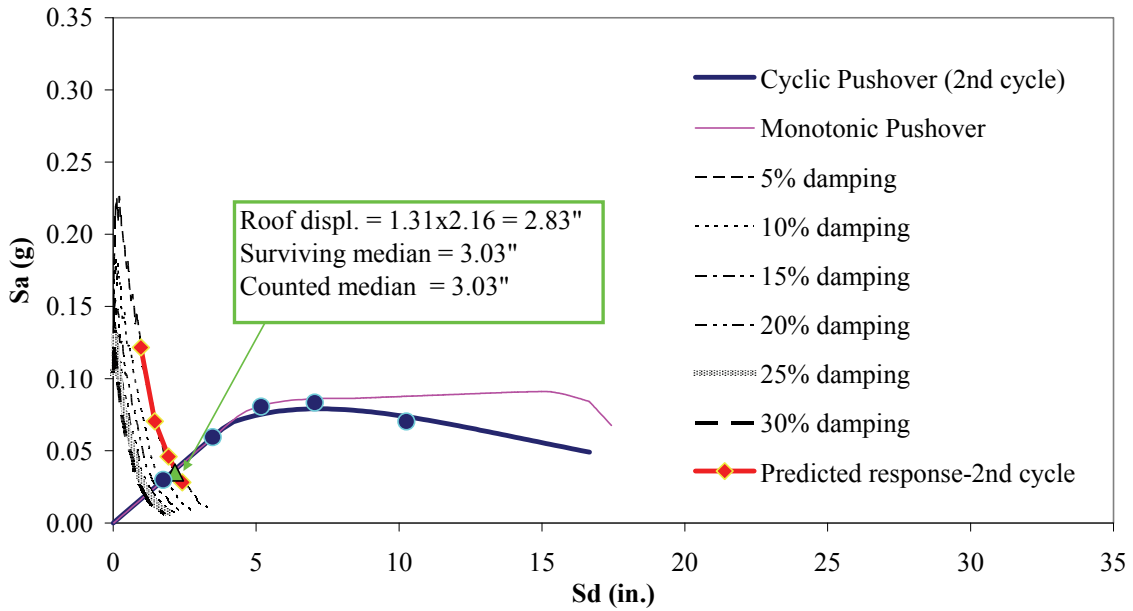
Spectral Capacity Curve: 4-Story IMF (DesC v.9)
Proposed Protocol, 1 Cyclic Dwell
"Median" of Actual Spectra, Sa (1 sec) = 1.12g



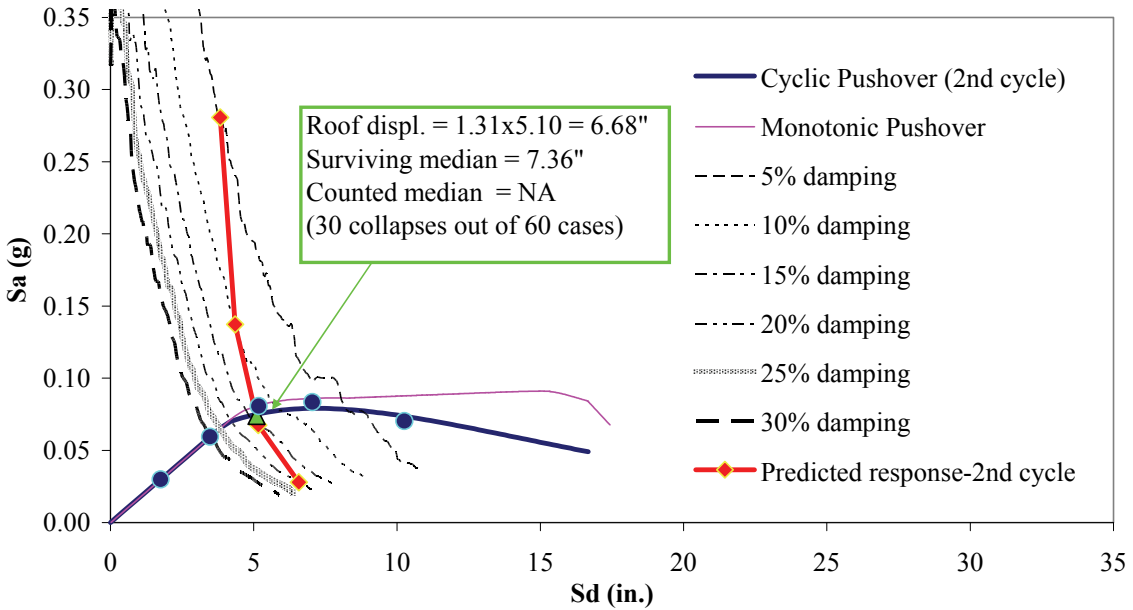
Spectral Capacity Curve: 4-Story IMF (DesC v.9)
Proposed Protocol, 1 Cyclic Dwell
"Median" of Actual Spectra, Sa (1 sec) = 1.92g



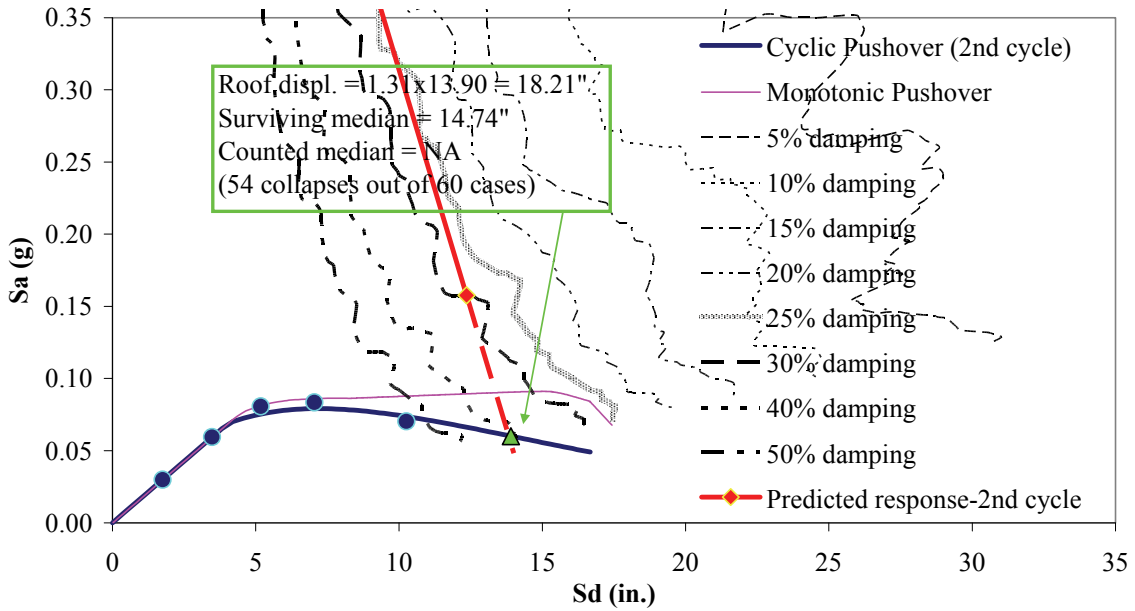
Spectral Capacity Curve: 4-Story IMF (DesC v.9)
Proposed Protocol, 3 Cyclic Dwell, 2nd Cycle
"Median" of Actual Spectra, Sa (1 sec) = 0.11g



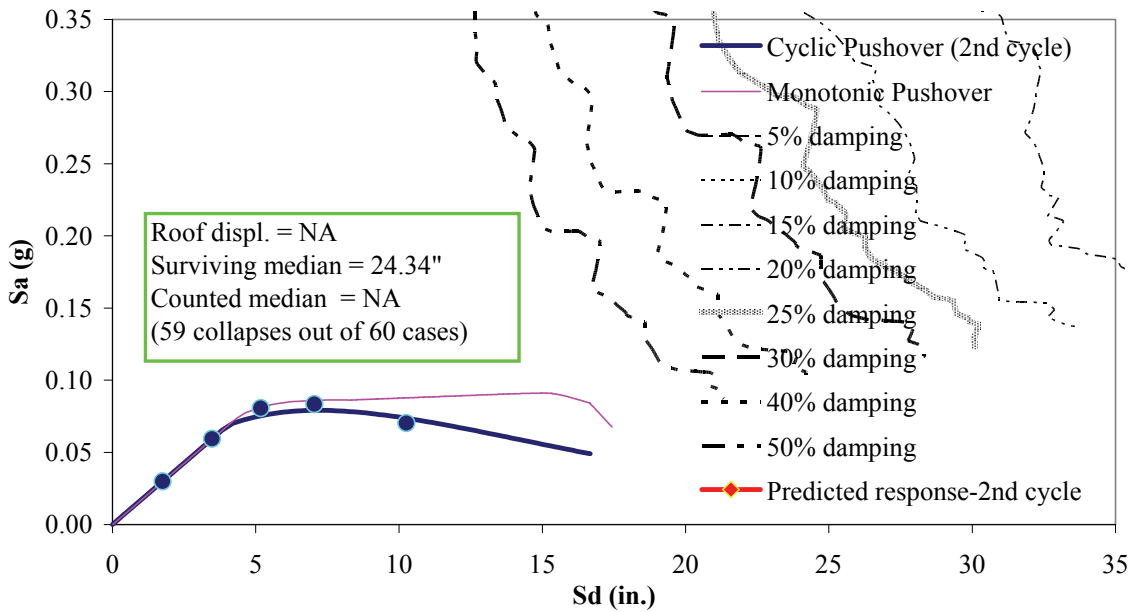
Spectral Capacity Curve: 4-Story IMF (DesC v.9)
Proposed Protocol, 3 Cyclic Dwell, 2nd Cycle
"Median" of Actual Spectra, Sa (1 sec) = 0.32g



Spectral Capacity Curve: 4-Story IMF (DesC v.9)
Proposed Protocol, 3 Cyclic Dwell, 2nd Cycle
"Median" of Actual Spectra, Sa (1 sec) = 1.12g



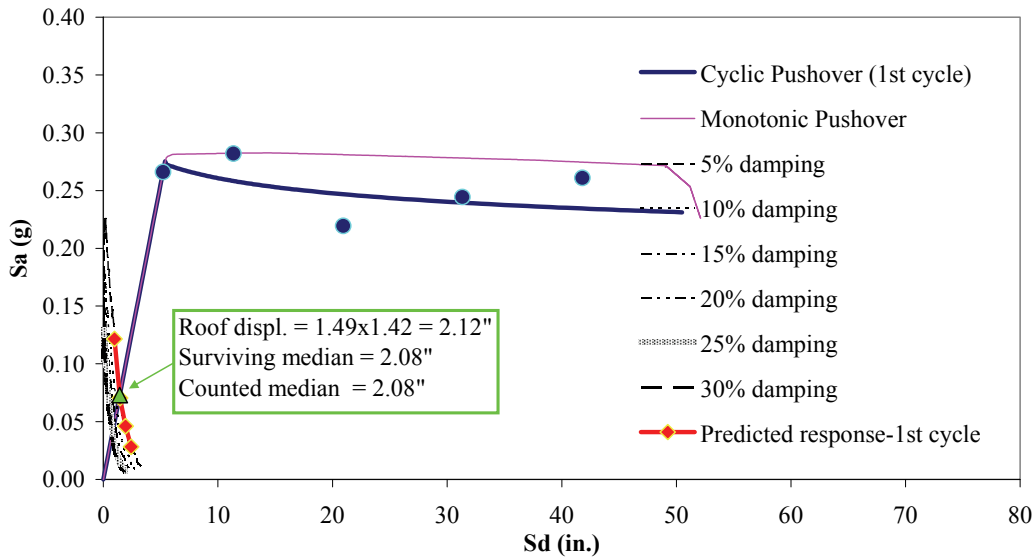
Spectral Capacity Curve: 4-Story IMF (DesC v.9)
Proposed Protocol, 3 Cyclic Dwell, 2nd Cycle
"Median" of Actual Spectra, Sa (1 sec) = 1.92g



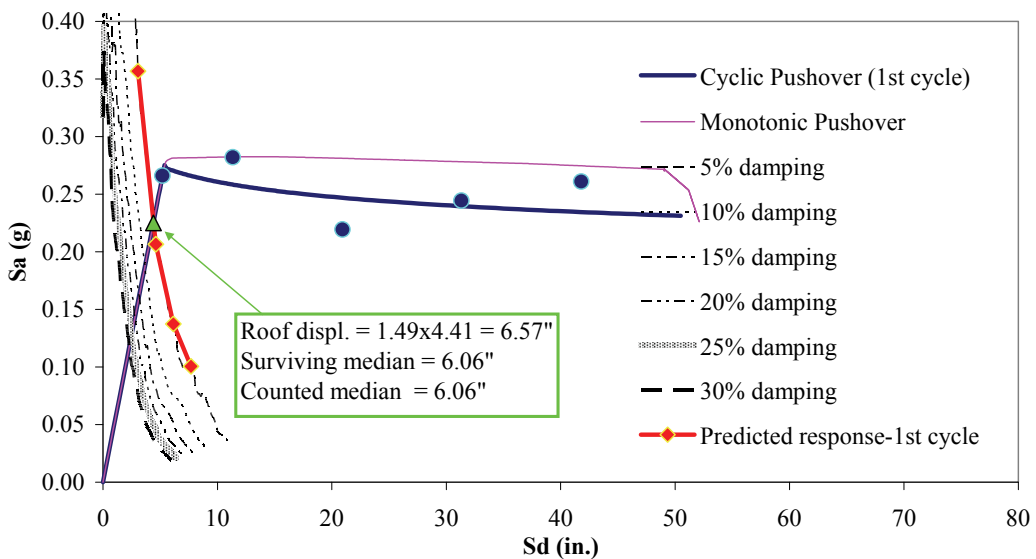
APPENDIX D

PREDICTIONS OF MEDIAN ROOF DISPLACEMENT OF 12-STORY SPECIAL WALL BUILDING USING SIMPLIFIED CAPACITY SPECTRUM METHOD

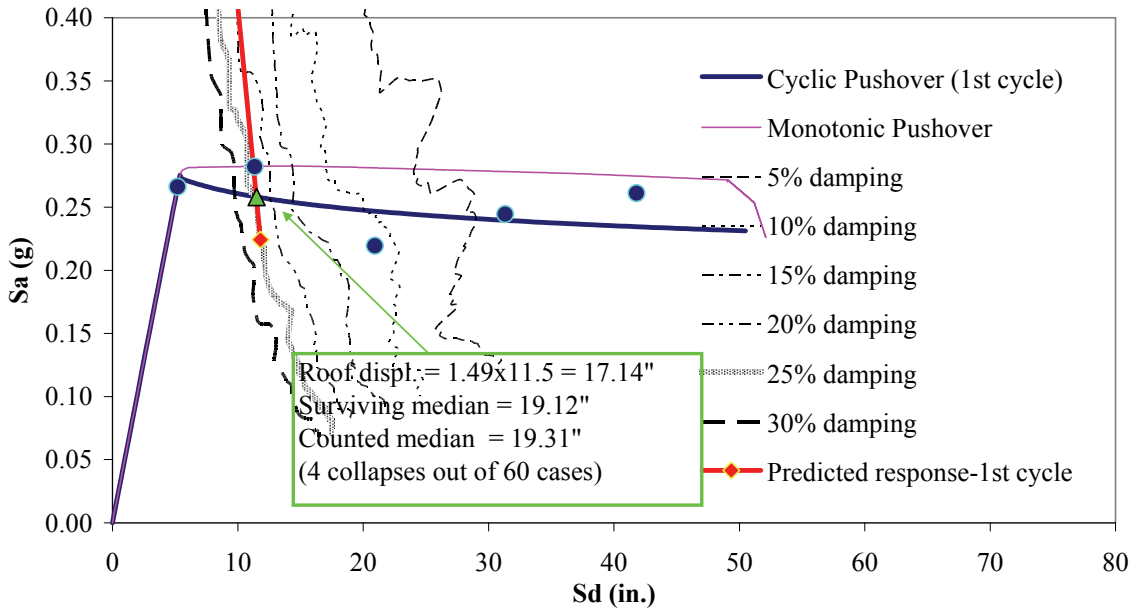
Spectral Capacity Curve: 12-Story Special Wall (DesWA v.26)
Proposed Protocol, 1 Cyclic Dwell
"Median" of Actual Spectra, S_a (1 sec) = 0.11g



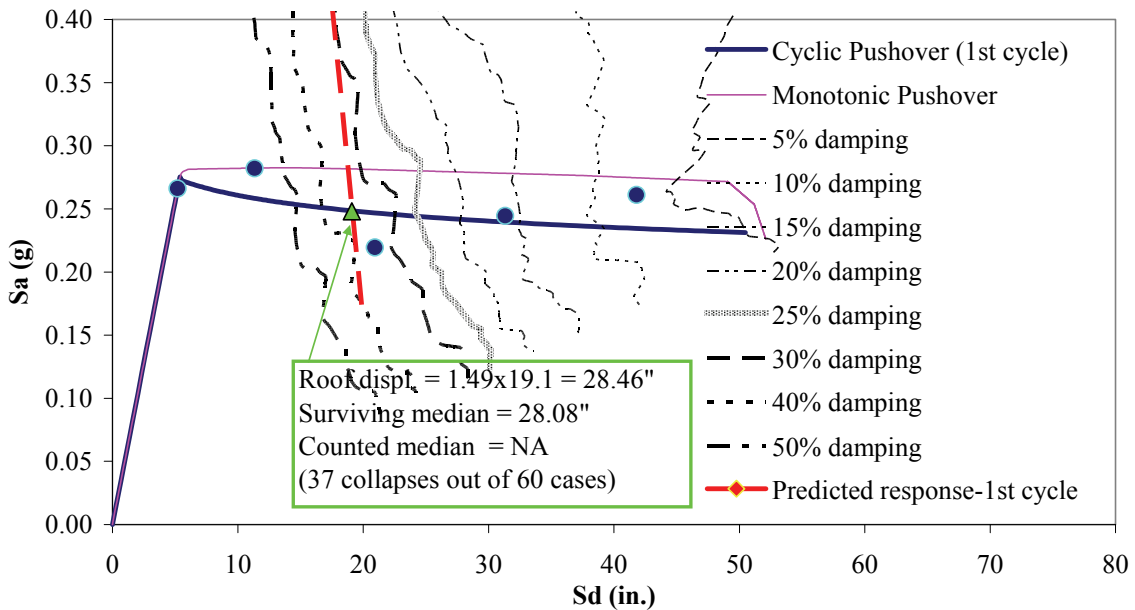
Spectral Capacity Curve: 12-Story Special Wall (DesWA v.26)
Proposed Protocol, 1 Cyclic Dwell
"Median" of Actual Spectra, S_a (1 sec) = 0.32g



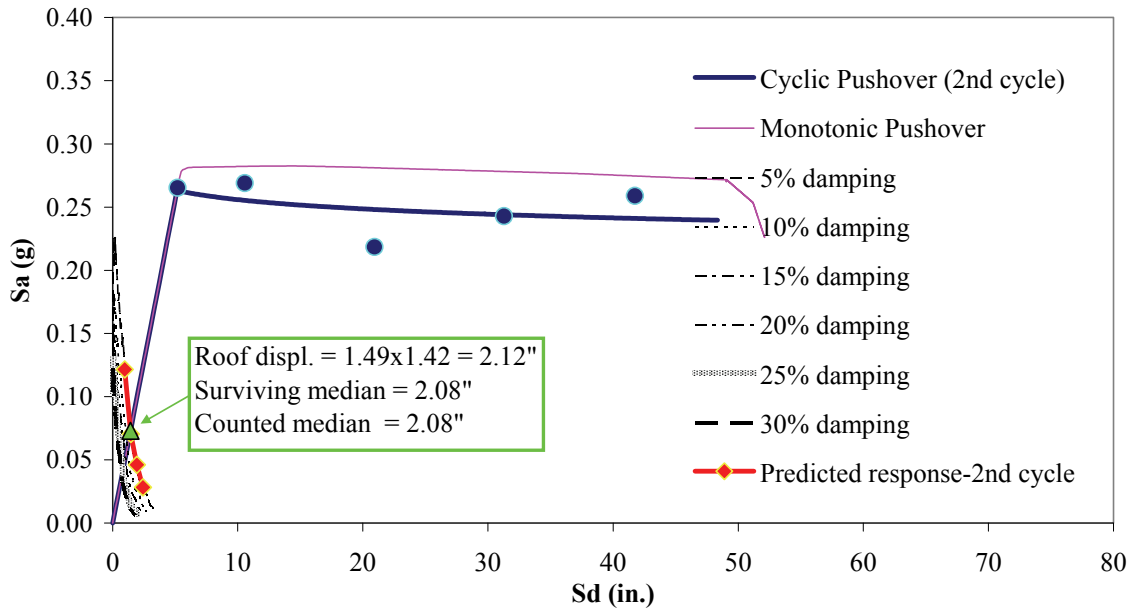
Spectral Capacity Curve: 12-Story Special Wall (DesWA v.26)
Proposed Protocol, 1 Cyclic Dwell
"Median" of Actual Spectra, Sa (1 sec) = 1.12g



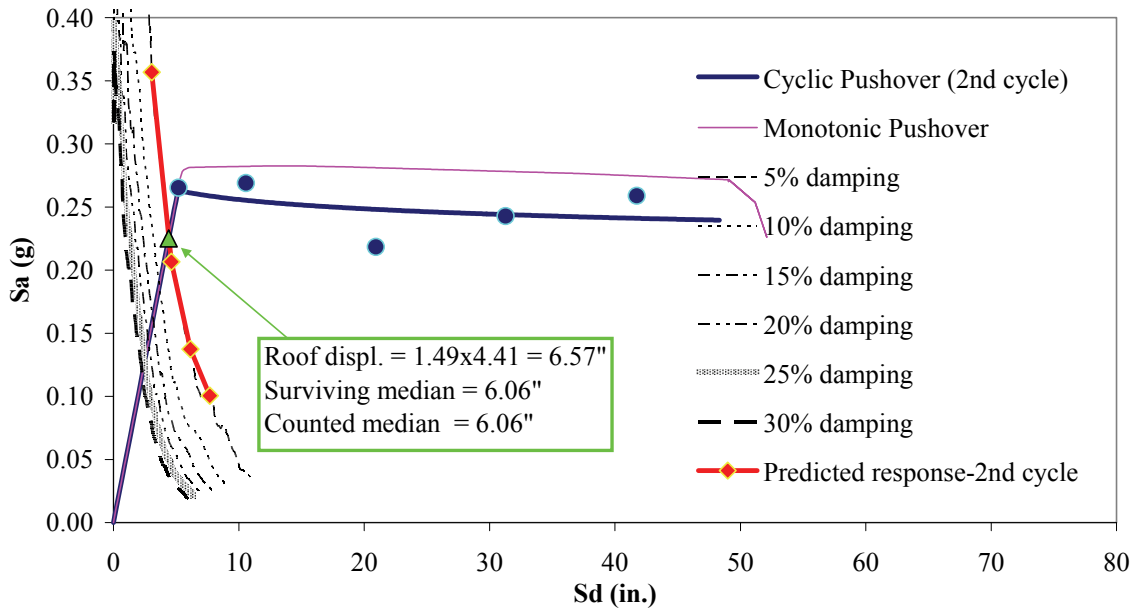
Spectral Capacity Curve: 12-Story Special Wall (DesWA v.26)
Proposed Protocol, 1 Cyclic Dwell
"Median" of Actual Spectra, Sa (1 sec) = 1.92g



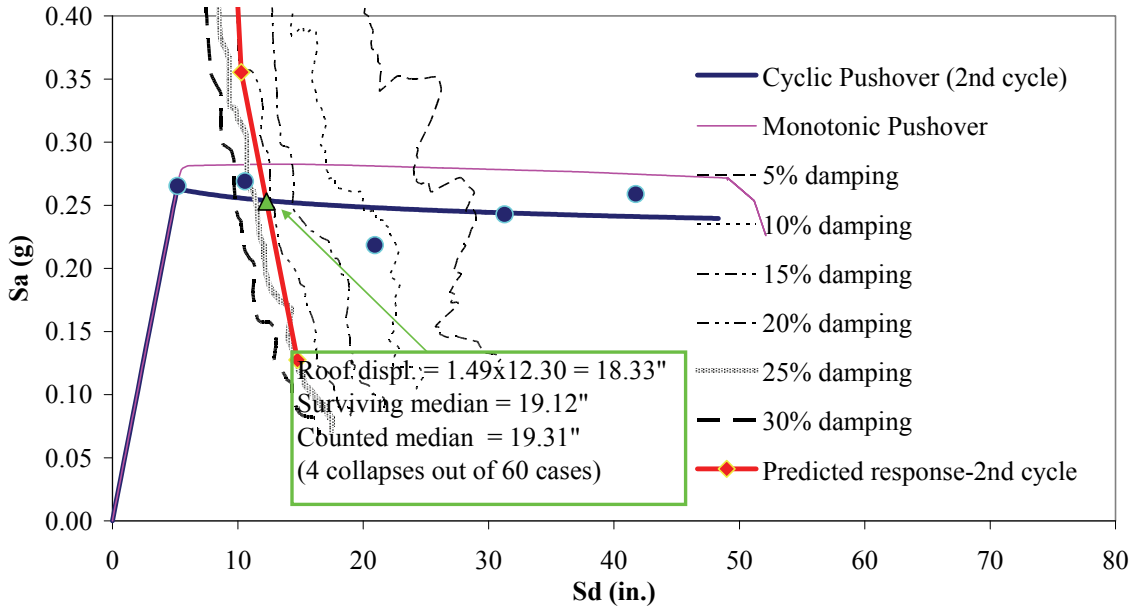
Spectral Capacity Curve: 12-Story Special Wall (DesWA v.26)
Proposed Protocol, 3 Cyclic Dwell, 2nd Cycle
"Median" of Actual Spectra, Sa (1 sec) = 0.11g



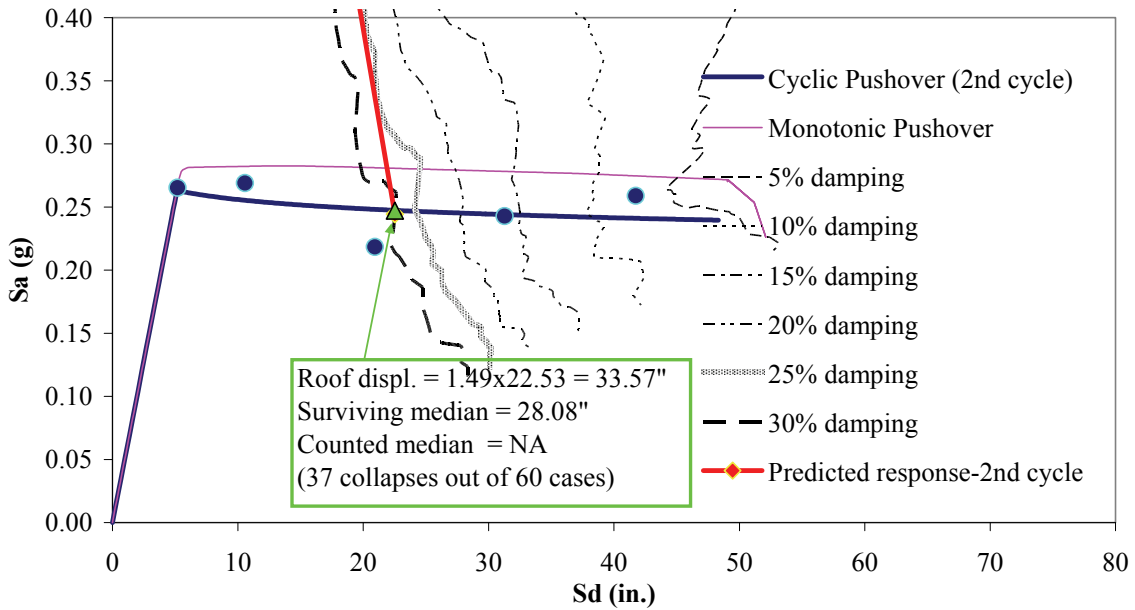
Spectral Capacity Curve: 12-Story Special Wall (DesWA v.26)
Proposed Protocol, 3 Cyclic Dwell, 2nd Cycle
"Median" of Actual Spectra, Sa (1 sec) = 0.32g



Spectral Capacity Curve: 12-Story Special Wall (DesWA v.26)
Proposed Protocol, 3 Cyclic Dwell, 2nd Cycle
"Median" of Actual Spectra, Sa (1 sec) = 1.12g



Spectral Capacity Curve: 12-Story Special Wall (DesWA v.26)
Proposed Protocol, 3 Cyclic Dwell, 2nd Cycle
"Median" of Actual Spectra, Sa (1 sec) = 1.92g



MCEER Technical Reports

MCEER publishes technical reports on a variety of subjects written by authors funded through MCEER. These reports are available from both MCEER Publications and the National Technical Information Service (NTIS). Requests for reports should be directed to MCEER Publications, MCEER, University at Buffalo, State University of New York, Red Jacket Quadrangle, Buffalo, New York 14261. Reports can also be requested through NTIS, 5285 Port Royal Road, Springfield, Virginia 22161. NTIS accession numbers are shown in parenthesis, if available.

- NCEER-87-0001 "First-Year Program in Research, Education and Technology Transfer," 3/5/87, (PB88-134275, A04, MF-A01).
- NCEER-87-0002 "Experimental Evaluation of Instantaneous Optimal Algorithms for Structural Control," by R.C. Lin, T.T. Soong and A.M. Reinhorn, 4/20/87, (PB88-134341, A04, MF-A01).
- NCEER-87-0003 "Experimentation Using the Earthquake Simulation Facilities at University at Buffalo," by A.M. Reinhorn and R.L. Ketter, to be published.
- NCEER-87-0004 "The System Characteristics and Performance of a Shaking Table," by J.S. Hwang, K.C. Chang and G.C. Lee, 6/1/87, (PB88-134259, A03, MF-A01). This report is available only through NTIS (see address given above).
- NCEER-87-0005 "A Finite Element Formulation for Nonlinear Viscoplastic Material Using a Q Model," by O. Gyebe and G. Dasgupta, 11/2/87, (PB88-213764, A08, MF-A01).
- NCEER-87-0006 "Symbolic Manipulation Program (SMP) - Algebraic Codes for Two and Three Dimensional Finite Element Formulations," by X. Lee and G. Dasgupta, 11/9/87, (PB88-218522, A05, MF-A01).
- NCEER-87-0007 "Instantaneous Optimal Control Laws for Tall Buildings Under Seismic Excitations," by J.N. Yang, A. Akbarpour and P. Ghaemmaghami, 6/10/87, (PB88-134333, A06, MF-A01). This report is only available through NTIS (see address given above).
- NCEER-87-0008 "IDARC: Inelastic Damage Analysis of Reinforced Concrete Frame - Shear-Wall Structures," by Y.J. Park, A.M. Reinhorn and S.K. Kunnath, 7/20/87, (PB88-134325, A09, MF-A01). This report is only available through NTIS (see address given above).
- NCEER-87-0009 "Liquefaction Potential for New York State: A Preliminary Report on Sites in Manhattan and Buffalo," by M. Budhu, V. Vijayakumar, R.F. Giese and L. Baumgras, 8/31/87, (PB88-163704, A03, MF-A01). This report is available only through NTIS (see address given above).
- NCEER-87-0010 "Vertical and Torsional Vibration of Foundations in Inhomogeneous Media," by A.S. Veletsos and K.W. Dotson, 6/1/87, (PB88-134291, A03, MF-A01). This report is only available through NTIS (see address given above).
- NCEER-87-0011 "Seismic Probabilistic Risk Assessment and Seismic Margins Studies for Nuclear Power Plants," by Howard H.M. Hwang, 6/15/87, (PB88-134267, A03, MF-A01). This report is only available through NTIS (see address given above).
- NCEER-87-0012 "Parametric Studies of Frequency Response of Secondary Systems Under Ground-Acceleration Excitations," by Y. Yong and Y.K. Lin, 6/10/87, (PB88-134309, A03, MF-A01). This report is only available through NTIS (see address given above).
- NCEER-87-0013 "Frequency Response of Secondary Systems Under Seismic Excitation," by J.A. HoLung, J. Cai and Y.K. Lin, 7/31/87, (PB88-134317, A05, MF-A01). This report is only available through NTIS (see address given above).
- NCEER-87-0014 "Modelling Earthquake Ground Motions in Seismically Active Regions Using Parametric Time Series Methods," by G.W. Ellis and A.S. Cakmak, 8/25/87, (PB88-134283, A08, MF-A01). This report is only available through NTIS (see address given above).
- NCEER-87-0015 "Detection and Assessment of Seismic Structural Damage," by E. DiPasquale and A.S. Cakmak, 8/25/87, (PB88-163712, A05, MF-A01). This report is only available through NTIS (see address given above).

- NCEER-87-0016 "Pipeline Experiment at Parkfield, California," by J. Isenberg and E. Richardson, 9/15/87, (PB88-163720, A03, MF-A01). This report is available only through NTIS (see address given above).
- NCEER-87-0017 "Digital Simulation of Seismic Ground Motion," by M. Shinozuka, G. Deodatis and T. Harada, 8/31/87, (PB88-155197, A04, MF-A01). This report is available only through NTIS (see address given above).
- NCEER-87-0018 "Practical Considerations for Structural Control: System Uncertainty, System Time Delay and Truncation of Small Control Forces," J.N. Yang and A. Akbarpour, 8/10/87, (PB88-163738, A08, MF-A01). This report is only available through NTIS (see address given above).
- NCEER-87-0019 "Modal Analysis of Nonclassically Damped Structural Systems Using Canonical Transformation," by J.N. Yang, S. Sarkani and F.X. Long, 9/27/87, (PB88-187851, A04, MF-A01).
- NCEER-87-0020 "A Nonstationary Solution in Random Vibration Theory," by J.R. Red-Horse and P.D. Spanos, 11/3/87, (PB88-163746, A03, MF-A01).
- NCEER-87-0021 "Horizontal Impedances for Radially Inhomogeneous Viscoelastic Soil Layers," by A.S. Veletsos and K.W. Dotson, 10/15/87, (PB88-150859, A04, MF-A01).
- NCEER-87-0022 "Seismic Damage Assessment of Reinforced Concrete Members," by Y.S. Chung, C. Meyer and M. Shinozuka, 10/9/87, (PB88-150867, A05, MF-A01). This report is available only through NTIS (see address given above).
- NCEER-87-0023 "Active Structural Control in Civil Engineering," by T.T. Soong, 11/11/87, (PB88-187778, A03, MF-A01).
- NCEER-87-0024 "Vertical and Torsional Impedances for Radially Inhomogeneous Viscoelastic Soil Layers," by K.W. Dotson and A.S. Veletsos, 12/87, (PB88-187786, A03, MF-A01).
- NCEER-87-0025 "Proceedings from the Symposium on Seismic Hazards, Ground Motions, Soil-Liquefaction and Engineering Practice in Eastern North America," October 20-22, 1987, edited by K.H. Jacob, 12/87, (PB88-188115, A23, MF-A01). This report is available only through NTIS (see address given above).
- NCEER-87-0026 "Report on the Whittier-Narrows, California, Earthquake of October 1, 1987," by J. Pantelic and A. Reinhorn, 11/87, (PB88-187752, A03, MF-A01). This report is available only through NTIS (see address given above).
- NCEER-87-0027 "Design of a Modular Program for Transient Nonlinear Analysis of Large 3-D Building Structures," by S. Srivastav and J.F. Abel, 12/30/87, (PB88-187950, A05, MF-A01). This report is only available through NTIS (see address given above).
- NCEER-87-0028 "Second-Year Program in Research, Education and Technology Transfer," 3/8/88, (PB88-219480, A04, MF-A01).
- NCEER-88-0001 "Workshop on Seismic Computer Analysis and Design of Buildings With Interactive Graphics," by W. McGuire, J.F. Abel and C.H. Conley, 1/18/88, (PB88-187760, A03, MF-A01). This report is only available through NTIS (see address given above).
- NCEER-88-0002 "Optimal Control of Nonlinear Flexible Structures," by J.N. Yang, F.X. Long and D. Wong, 1/22/88, (PB88-213772, A06, MF-A01).
- NCEER-88-0003 "Substructuring Techniques in the Time Domain for Primary-Secondary Structural Systems," by G.D. Manolis and G. Juhn, 2/10/88, (PB88-213780, A04, MF-A01).
- NCEER-88-0004 "Iterative Seismic Analysis of Primary-Secondary Systems," by A. Singhal, L.D. Lutes and P.D. Spanos, 2/23/88, (PB88-213798, A04, MF-A01).
- NCEER-88-0005 "Stochastic Finite Element Expansion for Random Media," by P.D. Spanos and R. Ghanem, 3/14/88, (PB88-213806, A03, MF-A01).

- NCEER-88-0006 "Combining Structural Optimization and Structural Control," by F.Y. Cheng and C.P. Pantelides, 1/10/88, (PB88-213814, A05, MF-A01).
- NCEER-88-0007 "Seismic Performance Assessment of Code-Designed Structures," by H.H-M. Hwang, J-W. Jaw and H-J. Shau, 3/20/88, (PB88-219423, A04, MF-A01). This report is only available through NTIS (see address given above).
- NCEER-88-0008 "Reliability Analysis of Code-Designed Structures Under Natural Hazards," by H.H-M. Hwang, H. Ushiba and M. Shinozuka, 2/29/88, (PB88-229471, A07, MF-A01). This report is only available through NTIS (see address given above).
- NCEER-88-0009 "Seismic Fragility Analysis of Shear Wall Structures," by J-W Jaw and H.H-M. Hwang, 4/30/88, (PB89-102867, A04, MF-A01).
- NCEER-88-0010 "Base Isolation of a Multi-Story Building Under a Harmonic Ground Motion - A Comparison of Performances of Various Systems," by F-G Fan, G. Ahmadi and I.G. Tadjbakhsh, 5/18/88, (PB89-122238, A06, MF-A01). This report is only available through NTIS (see address given above).
- NCEER-88-0011 "Seismic Floor Response Spectra for a Combined System by Green's Functions," by F.M. Lavelle, L.A. Bergman and P.D. Spanos, 5/1/88, (PB89-102875, A03, MF-A01).
- NCEER-88-0012 "A New Solution Technique for Randomly Excited Hysteretic Structures," by G.Q. Cai and Y.K. Lin, 5/16/88, (PB89-102883, A03, MF-A01).
- NCEER-88-0013 "A Study of Radiation Damping and Soil-Structure Interaction Effects in the Centrifuge," by K. Weissman, supervised by J.H. Prevost, 5/24/88, (PB89-144703, A06, MF-A01).
- NCEER-88-0014 "Parameter Identification and Implementation of a Kinematic Plasticity Model for Frictional Soils," by J.H. Prevost and D.V. Griffiths, to be published.
- NCEER-88-0015 "Two- and Three- Dimensional Dynamic Finite Element Analyses of the Long Valley Dam," by D.V. Griffiths and J.H. Prevost, 6/17/88, (PB89-144711, A04, MF-A01).
- NCEER-88-0016 "Damage Assessment of Reinforced Concrete Structures in Eastern United States," by A.M. Reinhorn, M.J. Seidel, S.K. Kunnath and Y.J. Park, 6/15/88, (PB89-122220, A04, MF-A01). This report is only available through NTIS (see address given above).
- NCEER-88-0017 "Dynamic Compliance of Vertically Loaded Strip Foundations in Multilayered Viscoelastic Soils," by S. Ahmad and A.S.M. Israil, 6/17/88, (PB89-102891, A04, MF-A01).
- NCEER-88-0018 "An Experimental Study of Seismic Structural Response With Added Viscoelastic Dampers," by R.C. Lin, Z. Liang, T.T. Soong and R.H. Zhang, 6/30/88, (PB89-122212, A05, MF-A01). This report is available only through NTIS (see address given above).
- NCEER-88-0019 "Experimental Investigation of Primary - Secondary System Interaction," by G.D. Manolis, G. Juhn and A.M. Reinhorn, 5/27/88, (PB89-122204, A04, MF-A01).
- NCEER-88-0020 "A Response Spectrum Approach For Analysis of Nonclassically Damped Structures," by J.N. Yang, S. Sarkani and F.X. Long, 4/22/88, (PB89-102909, A04, MF-A01).
- NCEER-88-0021 "Seismic Interaction of Structures and Soils: Stochastic Approach," by A.S. Veletsos and A.M. Prasad, 7/21/88, (PB89-122196, A04, MF-A01). This report is only available through NTIS (see address given above).
- NCEER-88-0022 "Identification of the Serviceability Limit State and Detection of Seismic Structural Damage," by E. DiPasquale and A.S. Cakmak, 6/15/88, (PB89-122188, A05, MF-A01). This report is available only through NTIS (see address given above).
- NCEER-88-0023 "Multi-Hazard Risk Analysis: Case of a Simple Offshore Structure," by B.K. Bhartia and E.H. Vanmarcke, 7/21/88, (PB89-145213, A05, MF-A01).

- NCEER-88-0024 "Automated Seismic Design of Reinforced Concrete Buildings," by Y.S. Chung, C. Meyer and M. Shinozuka, 7/5/88, (PB89-122170, A06, MF-A01). This report is available only through NTIS (see address given above).
- NCEER-88-0025 "Experimental Study of Active Control of MDOF Structures Under Seismic Excitations," by L.L. Chung, R.C. Lin, T.T. Soong and A.M. Reinhorn, 7/10/88, (PB89-122600, A04, MF-A01).
- NCEER-88-0026 "Earthquake Simulation Tests of a Low-Rise Metal Structure," by J.S. Hwang, K.C. Chang, G.C. Lee and R.L. Ketter, 8/1/88, (PB89-102917, A04, MF-A01).
- NCEER-88-0027 "Systems Study of Urban Response and Reconstruction Due to Catastrophic Earthquakes," by F. Kozin and H.K. Zhou, 9/22/88, (PB90-162348, A04, MF-A01).
- NCEER-88-0028 "Seismic Fragility Analysis of Plane Frame Structures," by H.H-M. Hwang and Y.K. Low, 7/31/88, (PB89-131445, A06, MF-A01).
- NCEER-88-0029 "Response Analysis of Stochastic Structures," by A. Kardara, C. Bucher and M. Shinozuka, 9/22/88, (PB89-174429, A04, MF-A01).
- NCEER-88-0030 "Nonnormal Accelerations Due to Yielding in a Primary Structure," by D.C.K. Chen and L.D. Lutes, 9/19/88, (PB89-131437, A04, MF-A01).
- NCEER-88-0031 "Design Approaches for Soil-Structure Interaction," by A.S. Veletsos, A.M. Prasad and Y. Tang, 12/30/88, (PB89-174437, A03, MF-A01). This report is available only through NTIS (see address given above).
- NCEER-88-0032 "A Re-evaluation of Design Spectra for Seismic Damage Control," by C.J. Turkstra and A.G. Tallin, 11/7/88, (PB89-145221, A05, MF-A01).
- NCEER-88-0033 "The Behavior and Design of Noncontact Lap Splices Subjected to Repeated Inelastic Tensile Loading," by V.E. Sagan, P. Gergely and R.N. White, 12/8/88, (PB89-163737, A08, MF-A01).
- NCEER-88-0034 "Seismic Response of Pile Foundations," by S.M. Mamoon, P.K. Banerjee and S. Ahmad, 11/1/88, (PB89-145239, A04, MF-A01).
- NCEER-88-0035 "Modeling of R/C Building Structures With Flexible Floor Diaphragms (IDARC2)," by A.M. Reinhorn, S.K. Kunnath and N. Panahshahi, 9/7/88, (PB89-207153, A07, MF-A01).
- NCEER-88-0036 "Solution of the Dam-Reservoir Interaction Problem Using a Combination of FEM, BEM with Particular Integrals, Modal Analysis, and Substructuring," by C-S. Tsai, G.C. Lee and R.L. Ketter, 12/31/88, (PB89-207146, A04, MF-A01).
- NCEER-88-0037 "Optimal Placement of Actuators for Structural Control," by F.Y. Cheng and C.P. Pantelides, 8/15/88, (PB89-162846, A05, MF-A01).
- NCEER-88-0038 "Teflon Bearings in Aseismic Base Isolation: Experimental Studies and Mathematical Modeling," by A. Mokha, M.C. Constantinou and A.M. Reinhorn, 12/5/88, (PB89-218457, A10, MF-A01). This report is available only through NTIS (see address given above).
- NCEER-88-0039 "Seismic Behavior of Flat Slab High-Rise Buildings in the New York City Area," by P. Weidlinger and M. Ettouney, 10/15/88, (PB90-145681, A04, MF-A01).
- NCEER-88-0040 "Evaluation of the Earthquake Resistance of Existing Buildings in New York City," by P. Weidlinger and M. Ettouney, 10/15/88, to be published.
- NCEER-88-0041 "Small-Scale Modeling Techniques for Reinforced Concrete Structures Subjected to Seismic Loads," by W. Kim, A. El-Attar and R.N. White, 11/22/88, (PB89-189625, A05, MF-A01).
- NCEER-88-0042 "Modeling Strong Ground Motion from Multiple Event Earthquakes," by G.W. Ellis and A.S. Cakmak, 10/15/88, (PB89-174445, A03, MF-A01).

- NCEER-88-0043 "Nonstationary Models of Seismic Ground Acceleration," by M. Grigoriu, S.E. Ruiz and E. Rosenblueth, 7/15/88, (PB89-189617, A04, MF-A01).
- NCEER-88-0044 "SARCF User's Guide: Seismic Analysis of Reinforced Concrete Frames," by Y.S. Chung, C. Meyer and M. Shinozuka, 11/9/88, (PB89-174452, A08, MF-A01).
- NCEER-88-0045 "First Expert Panel Meeting on Disaster Research and Planning," edited by J. Pantelic and J. Stoyke, 9/15/88, (PB89-174460, A05, MF-A01).
- NCEER-88-0046 "Preliminary Studies of the Effect of Degrading Infill Walls on the Nonlinear Seismic Response of Steel Frames," by C.Z. Chrysostomou, P. Gergely and J.F. Abel, 12/19/88, (PB89-208383, A05, MF-A01).
- NCEER-88-0047 "Reinforced Concrete Frame Component Testing Facility - Design, Construction, Instrumentation and Operation," by S.P. Pessiki, C. Conley, T. Bond, P. Gergely and R.N. White, 12/16/88, (PB89-174478, A04, MF-A01).
- NCEER-89-0001 "Effects of Protective Cushion and Soil Compliancy on the Response of Equipment Within a Seismically Excited Building," by J.A. HoLung, 2/16/89, (PB89-207179, A04, MF-A01).
- NCEER-89-0002 "Statistical Evaluation of Response Modification Factors for Reinforced Concrete Structures," by H.H-M. Hwang and J-W. Jaw, 2/17/89, (PB89-207187, A05, MF-A01).
- NCEER-89-0003 "Hysteretic Columns Under Random Excitation," by G-Q. Cai and Y.K. Lin, 1/9/89, (PB89-196513, A03, MF-A01).
- NCEER-89-0004 "Experimental Study of 'Elephant Foot Bulge' Instability of Thin-Walled Metal Tanks," by Z-H. Jia and R.L. Ketter, 2/22/89, (PB89-207195, A03, MF-A01).
- NCEER-89-0005 "Experiment on Performance of Buried Pipelines Across San Andreas Fault," by J. Isenberg, E. Richardson and T.D. O'Rourke, 3/10/89, (PB89-218440, A04, MF-A01). This report is available only through NTIS (see address given above).
- NCEER-89-0006 "A Knowledge-Based Approach to Structural Design of Earthquake-Resistant Buildings," by M. Subramani, P. Gergely, C.H. Conley, J.F. Abel and A.H. Zaghaw, 1/15/89, (PB89-218465, A06, MF-A01).
- NCEER-89-0007 "Liquefaction Hazards and Their Effects on Buried Pipelines," by T.D. O'Rourke and P.A. Lane, 2/1/89, (PB89-218481, A09, MF-A01).
- NCEER-89-0008 "Fundamentals of System Identification in Structural Dynamics," by H. Imai, C-B. Yun, O. Maruyama and M. Shinozuka, 1/26/89, (PB89-207211, A04, MF-A01).
- NCEER-89-0009 "Effects of the 1985 Michoacan Earthquake on Water Systems and Other Buried Lifelines in Mexico," by A.G. Ayala and M.J. O'Rourke, 3/8/89, (PB89-207229, A06, MF-A01).
- NCEER-89-R010 "NCEER Bibliography of Earthquake Education Materials," by K.E.K. Ross, Second Revision, 9/1/89, (PB90-125352, A05, MF-A01). This report is replaced by NCEER-92-0018.
- NCEER-89-0011 "Inelastic Three-Dimensional Response Analysis of Reinforced Concrete Building Structures (IDARC-3D), Part I - Modeling," by S.K. Kunnath and A.M. Reinhorn, 4/17/89, (PB90-114612, A07, MF-A01). This report is available only through NTIS (see address given above).
- NCEER-89-0012 "Recommended Modifications to ATC-14," by C.D. Poland and J.O. Malley, 4/12/89, (PB90-108648, A15, MF-A01).
- NCEER-89-0013 "Repair and Strengthening of Beam-to-Column Connections Subjected to Earthquake Loading," by M. Corazao and A.J. Durrani, 2/28/89, (PB90-109885, A06, MF-A01).
- NCEER-89-0014 "Program EXKAL2 for Identification of Structural Dynamic Systems," by O. Maruyama, C-B. Yun, M. Hoshiya and M. Shinozuka, 5/19/89, (PB90-109877, A09, MF-A01).

- NCEER-89-0015 "Response of Frames With Bolted Semi-Rigid Connections, Part I - Experimental Study and Analytical Predictions," by P.J. DiCorso, A.M. Reinhorn, J.R. Dickerson, J.B. Radzinski and W.L. Harper, 6/1/89, to be published.
- NCEER-89-0016 "ARMA Monte Carlo Simulation in Probabilistic Structural Analysis," by P.D. Spanos and M.P. Mignolet, 7/10/89, (PB90-109893, A03, MF-A01).
- NCEER-89-P017 "Preliminary Proceedings from the Conference on Disaster Preparedness - The Place of Earthquake Education in Our Schools," Edited by K.E.K. Ross, 6/23/89, (PB90-108606, A03, MF-A01).
- NCEER-89-0017 "Proceedings from the Conference on Disaster Preparedness - The Place of Earthquake Education in Our Schools," Edited by K.E.K. Ross, 12/31/89, (PB90-207895, A012, MF-A02). This report is available only through NTIS (see address given above).
- NCEER-89-0018 "Multidimensional Models of Hysteretic Material Behavior for Vibration Analysis of Shape Memory Energy Absorbing Devices, by E.J. Graesser and F.A. Cozzarelli, 6/7/89, (PB90-164146, A04, MF-A01).
- NCEER-89-0019 "Nonlinear Dynamic Analysis of Three-Dimensional Base Isolated Structures (3D-BASIS)," by S. Nagarajaiah, A.M. Reinhorn and M.C. Constantinou, 8/3/89, (PB90-161936, A06, MF-A01). This report has been replaced by NCEER-93-0011.
- NCEER-89-0020 "Structural Control Considering Time-Rate of Control Forces and Control Rate Constraints," by F.Y. Cheng and C.P. Pantelides, 8/3/89, (PB90-120445, A04, MF-A01).
- NCEER-89-0021 "Subsurface Conditions of Memphis and Shelby County," by K.W. Ng, T-S. Chang and H-H.M. Hwang, 7/26/89, (PB90-120437, A03, MF-A01).
- NCEER-89-0022 "Seismic Wave Propagation Effects on Straight Jointed Buried Pipelines," by K. Elhadi and M.J. O'Rourke, 8/24/89, (PB90-162322, A10, MF-A02).
- NCEER-89-0023 "Workshop on Serviceability Analysis of Water Delivery Systems," edited by M. Grigoriu, 3/6/89, (PB90-127424, A03, MF-A01).
- NCEER-89-0024 "Shaking Table Study of a 1/5 Scale Steel Frame Composed of Tapered Members," by K.C. Chang, J.S. Hwang and G.C. Lee, 9/18/89, (PB90-160169, A04, MF-A01).
- NCEER-89-0025 "DYNA1D: A Computer Program for Nonlinear Seismic Site Response Analysis - Technical Documentation," by Jean H. Prevost, 9/14/89, (PB90-161944, A07, MF-A01). This report is available only through NTIS (see address given above).
- NCEER-89-0026 "1:4 Scale Model Studies of Active Tendon Systems and Active Mass Dampers for Aseismic Protection," by A.M. Reinhorn, T.T. Soong, R.C. Lin, Y.P. Yang, Y. Fukao, H. Abe and M. Nakai, 9/15/89, (PB90-173246, A10, MF-A02). This report is available only through NTIS (see address given above).
- NCEER-89-0027 "Scattering of Waves by Inclusions in a Nonhomogeneous Elastic Half Space Solved by Boundary Element Methods," by P.K. Hadley, A. Askar and A.S. Cakmak, 6/15/89, (PB90-145699, A07, MF-A01).
- NCEER-89-0028 "Statistical Evaluation of Deflection Amplification Factors for Reinforced Concrete Structures," by H.H.M. Hwang, J-W. Jaw and A.L. Ch'ng, 8/31/89, (PB90-164633, A05, MF-A01).
- NCEER-89-0029 "Bedrock Accelerations in Memphis Area Due to Large New Madrid Earthquakes," by H.H.M. Hwang, C.H.S. Chen and G. Yu, 11/7/89, (PB90-162330, A04, MF-A01).
- NCEER-89-0030 "Seismic Behavior and Response Sensitivity of Secondary Structural Systems," by Y.Q. Chen and T.T. Soong, 10/23/89, (PB90-164658, A08, MF-A01).
- NCEER-89-0031 "Random Vibration and Reliability Analysis of Primary-Secondary Structural Systems," by Y. Ibrahim, M. Grigoriu and T.T. Soong, 11/10/89, (PB90-161951, A04, MF-A01).

- NCEER-89-0032 "Proceedings from the Second U.S. - Japan Workshop on Liquefaction, Large Ground Deformation and Their Effects on Lifelines, September 26-29, 1989," Edited by T.D. O'Rourke and M. Hamada, 12/1/89, (PB90-209388, A22, MF-A03).
- NCEER-89-0033 "Deterministic Model for Seismic Damage Evaluation of Reinforced Concrete Structures," by J.M. Bracci, A.M. Reinhorn, J.B. Mander and S.K. Kunnath, 9/27/89, (PB91-108803, A06, MF-A01).
- NCEER-89-0034 "On the Relation Between Local and Global Damage Indices," by E. DiPasquale and A.S. Cakmak, 8/15/89, (PB90-173865, A05, MF-A01).
- NCEER-89-0035 "Cyclic Undrained Behavior of Nonplastic and Low Plasticity Silts," by A.J. Walker and H.E. Stewart, 7/26/89, (PB90-183518, A10, MF-A01).
- NCEER-89-0036 "Liquefaction Potential of Surficial Deposits in the City of Buffalo, New York," by M. Budhu, R. Giese and L. Baumgrass, 1/17/89, (PB90-208455, A04, MF-A01).
- NCEER-89-0037 "A Deterministic Assessment of Effects of Ground Motion Incoherence," by A.S. Veletsos and Y. Tang, 7/15/89, (PB90-164294, A03, MF-A01).
- NCEER-89-0038 "Workshop on Ground Motion Parameters for Seismic Hazard Mapping," July 17-18, 1989, edited by R.V. Whitman, 12/1/89, (PB90-173923, A04, MF-A01).
- NCEER-89-0039 "Seismic Effects on Elevated Transit Lines of the New York City Transit Authority," by C.J. Costantino, C.A. Miller and E. Heymsfield, 12/26/89, (PB90-207887, A06, MF-A01).
- NCEER-89-0040 "Centrifugal Modeling of Dynamic Soil-Structure Interaction," by K. Weissman, Supervised by J.H. Prevost, 5/10/89, (PB90-207879, A07, MF-A01).
- NCEER-89-0041 "Linearized Identification of Buildings With Cores for Seismic Vulnerability Assessment," by I-K. Ho and A.E. Aktan, 11/1/89, (PB90-251943, A07, MF-A01).
- NCEER-90-0001 "Geotechnical and Lifeline Aspects of the October 17, 1989 Loma Prieta Earthquake in San Francisco," by T.D. O'Rourke, H.E. Stewart, F.T. Blackburn and T.S. Dickerman, 1/90, (PB90-208596, A05, MF-A01).
- NCEER-90-0002 "Nonnormal Secondary Response Due to Yielding in a Primary Structure," by D.C.K. Chen and L.D. Lutes, 2/28/90, (PB90-251976, A07, MF-A01).
- NCEER-90-0003 "Earthquake Education Materials for Grades K-12," by K.E.K. Ross, 4/16/90, (PB91-251984, A05, MF-A05). This report has been replaced by NCEER-92-0018.
- NCEER-90-0004 "Catalog of Strong Motion Stations in Eastern North America," by R.W. Busby, 4/3/90, (PB90-251984, A05, MF-A01).
- NCEER-90-0005 "NCEER Strong-Motion Data Base: A User Manual for the GeoBase Release (Version 1.0 for the Sun3)," by P. Friberg and K. Jacob, 3/31/90 (PB90-258062, A04, MF-A01).
- NCEER-90-0006 "Seismic Hazard Along a Crude Oil Pipeline in the Event of an 1811-1812 Type New Madrid Earthquake," by H.H.M. Hwang and C-H.S. Chen, 4/16/90, (PB90-258054, A04, MF-A01).
- NCEER-90-0007 "Site-Specific Response Spectra for Memphis Sheahan Pumping Station," by H.H.M. Hwang and C.S. Lee, 5/15/90, (PB91-108811, A05, MF-A01).
- NCEER-90-0008 "Pilot Study on Seismic Vulnerability of Crude Oil Transmission Systems," by T. Ariman, R. Dobry, M. Grigoriu, F. Kozin, M. O'Rourke, T. O'Rourke and M. Shinozuka, 5/25/90, (PB91-108837, A06, MF-A01).
- NCEER-90-0009 "A Program to Generate Site Dependent Time Histories: EQGEN," by G.W. Ellis, M. Srinivasan and A.S. Cakmak, 1/30/90, (PB91-108829, A04, MF-A01).
- NCEER-90-0010 "Active Isolation for Seismic Protection of Operating Rooms," by M.E. Talbott, Supervised by M. Shinozuka, 6/8/9, (PB91-110205, A05, MF-A01).

- NCEER-90-0011 "Program LINEARID for Identification of Linear Structural Dynamic Systems," by C-B. Yun and M. Shinozuka, 6/25/90, (PB91-110312, A08, MF-A01).
- NCEER-90-0012 "Two-Dimensional Two-Phase Elasto-Plastic Seismic Response of Earth Dams," by A.N. Yiagos, Supervised by J.H. Prevost, 6/20/90, (PB91-110197, A13, MF-A02).
- NCEER-90-0013 "Secondary Systems in Base-Isolated Structures: Experimental Investigation, Stochastic Response and Stochastic Sensitivity," by G.D. Manolis, G. Juhn, M.C. Constantinou and A.M. Reinhorn, 7/1/90, (PB91-110320, A08, MF-A01).
- NCEER-90-0014 "Seismic Behavior of Lightly-Reinforced Concrete Column and Beam-Column Joint Details," by S.P. Pessiki, C.H. Conley, P. Gergely and R.N. White, 8/22/90, (PB91-108795, A11, MF-A02).
- NCEER-90-0015 "Two Hybrid Control Systems for Building Structures Under Strong Earthquakes," by J.N. Yang and A. Daniellians, 6/29/90, (PB91-125393, A04, MF-A01).
- NCEER-90-0016 "Instantaneous Optimal Control with Acceleration and Velocity Feedback," by J.N. Yang and Z. Li, 6/29/90, (PB91-125401, A03, MF-A01).
- NCEER-90-0017 "Reconnaissance Report on the Northern Iran Earthquake of June 21, 1990," by M. Mehrain, 10/4/90, (PB91-125377, A03, MF-A01).
- NCEER-90-0018 "Evaluation of Liquefaction Potential in Memphis and Shelby County," by T.S. Chang, P.S. Tang, C.S. Lee and H. Hwang, 8/10/90, (PB91-125427, A09, MF-A01).
- NCEER-90-0019 "Experimental and Analytical Study of a Combined Sliding Disc Bearing and Helical Steel Spring Isolation System," by M.C. Constantinou, A.S. Mokha and A.M. Reinhorn, 10/4/90, (PB91-125385, A06, MF-A01). This report is available only through NTIS (see address given above).
- NCEER-90-0020 "Experimental Study and Analytical Prediction of Earthquake Response of a Sliding Isolation System with a Spherical Surface," by A.S. Mokha, M.C. Constantinou and A.M. Reinhorn, 10/11/90, (PB91-125419, A05, MF-A01).
- NCEER-90-0021 "Dynamic Interaction Factors for Floating Pile Groups," by G. Gazetas, K. Fan, A. Kaynia and E. Kausel, 9/10/90, (PB91-170381, A05, MF-A01).
- NCEER-90-0022 "Evaluation of Seismic Damage Indices for Reinforced Concrete Structures," by S. Rodriguez-Gomez and A.S. Cakmak, 9/30/90, PB91-171322, A06, MF-A01).
- NCEER-90-0023 "Study of Site Response at a Selected Memphis Site," by H. Desai, S. Ahmad, E.S. Gazetas and M.R. Oh, 10/11/90, (PB91-196857, A03, MF-A01).
- NCEER-90-0024 "A User's Guide to Strongmo: Version 1.0 of NCEER's Strong-Motion Data Access Tool for PCs and Terminals," by P.A. Friberg and C.A.T. Susch, 11/15/90, (PB91-171272, A03, MF-A01).
- NCEER-90-0025 "A Three-Dimensional Analytical Study of Spatial Variability of Seismic Ground Motions," by L-L. Hong and A.H.-S. Ang, 10/30/90, (PB91-170399, A09, MF-A01).
- NCEER-90-0026 "MUMOID User's Guide - A Program for the Identification of Modal Parameters," by S. Rodriguez-Gomez and E. DiPasquale, 9/30/90, (PB91-171298, A04, MF-A01).
- NCEER-90-0027 "SARCF-II User's Guide - Seismic Analysis of Reinforced Concrete Frames," by S. Rodriguez-Gomez, Y.S. Chung and C. Meyer, 9/30/90, (PB91-171280, A05, MF-A01).
- NCEER-90-0028 "Viscous Dampers: Testing, Modeling and Application in Vibration and Seismic Isolation," by N. Makris and M.C. Constantinou, 12/20/90 (PB91-190561, A06, MF-A01).
- NCEER-90-0029 "Soil Effects on Earthquake Ground Motions in the Memphis Area," by H. Hwang, C.S. Lee, K.W. Ng and T.S. Chang, 8/2/90, (PB91-190751, A05, MF-A01).

- NCEER-91-0001 "Proceedings from the Third Japan-U.S. Workshop on Earthquake Resistant Design of Lifeline Facilities and Countermeasures for Soil Liquefaction, December 17-19, 1990," edited by T.D. O'Rourke and M. Hamada, 2/1/91, (PB91-179259, A99, MF-A04).
- NCEER-91-0002 "Physical Space Solutions of Non-Proportionally Damped Systems," by M. Tong, Z. Liang and G.C. Lee, 1/15/91, (PB91-179242, A04, MF-A01).
- NCEER-91-0003 "Seismic Response of Single Piles and Pile Groups," by K. Fan and G. Gazetas, 1/10/91, (PB92-174994, A04, MF-A01).
- NCEER-91-0004 "Damping of Structures: Part 1 - Theory of Complex Damping," by Z. Liang and G. Lee, 10/10/91, (PB92-197235, A12, MF-A03).
- NCEER-91-0005 "3D-BASIS - Nonlinear Dynamic Analysis of Three Dimensional Base Isolated Structures: Part II," by S. Nagarajaiah, A.M. Reinhorn and M.C. Constantinou, 2/28/91, (PB91-190553, A07, MF-A01). This report has been replaced by NCEER-93-0011.
- NCEER-91-0006 "A Multidimensional Hysteretic Model for Plasticity Deforming Metals in Energy Absorbing Devices," by E.J. Graesser and F.A. Cozzarelli, 4/9/91, (PB92-108364, A04, MF-A01).
- NCEER-91-0007 "A Framework for Customizable Knowledge-Based Expert Systems with an Application to a KBES for Evaluating the Seismic Resistance of Existing Buildings," by E.G. Ibarra-Anaya and S.J. Fennes, 4/9/91, (PB91-210930, A08, MF-A01).
- NCEER-91-0008 "Nonlinear Analysis of Steel Frames with Semi-Rigid Connections Using the Capacity Spectrum Method," by G.G. Deierlein, S-H. Hsieh, Y-J. Shen and J.F. Abel, 7/2/91, (PB92-113828, A05, MF-A01).
- NCEER-91-0009 "Earthquake Education Materials for Grades K-12," by K.E.K. Ross, 4/30/91, (PB91-212142, A06, MF-A01). This report has been replaced by NCEER-92-0018.
- NCEER-91-0010 "Phase Wave Velocities and Displacement Phase Differences in a Harmonically Oscillating Pile," by N. Makris and G. Gazetas, 7/8/91, (PB92-108356, A04, MF-A01).
- NCEER-91-0011 "Dynamic Characteristics of a Full-Size Five-Story Steel Structure and a 2/5 Scale Model," by K.C. Chang, G.C. Yao, G.C. Lee, D.S. Hao and Y.C. Yeh," 7/2/91, (PB93-116648, A06, MF-A02).
- NCEER-91-0012 "Seismic Response of a 2/5 Scale Steel Structure with Added Viscoelastic Dampers," by K.C. Chang, T.T. Soong, S-T. Oh and M.L. Lai, 5/17/91, (PB92-110816, A05, MF-A01).
- NCEER-91-0013 "Earthquake Response of Retaining Walls; Full-Scale Testing and Computational Modeling," by S. Alampalli and A-W.M. Elgamal, 6/20/91, to be published.
- NCEER-91-0014 "3D-BASIS-M: Nonlinear Dynamic Analysis of Multiple Building Base Isolated Structures," by P.C. Tsopelas, S. Nagarajaiah, M.C. Constantinou and A.M. Reinhorn, 5/28/91, (PB92-113885, A09, MF-A02).
- NCEER-91-0015 "Evaluation of SEAOC Design Requirements for Sliding Isolated Structures," by D. Theodossiou and M.C. Constantinou, 6/10/91, (PB92-114602, A11, MF-A03).
- NCEER-91-0016 "Closed-Loop Modal Testing of a 27-Story Reinforced Concrete Flat Plate-Core Building," by H.R. Somaprasad, T. Toksoy, H. Yoshiyuki and A.E. Aktan, 7/15/91, (PB92-129980, A07, MF-A02).
- NCEER-91-0017 "Shake Table Test of a 1/6 Scale Two-Story Lightly Reinforced Concrete Building," by A.G. El-Attar, R.N. White and P. Gergely, 2/28/91, (PB92-222447, A06, MF-A02).
- NCEER-91-0018 "Shake Table Test of a 1/8 Scale Three-Story Lightly Reinforced Concrete Building," by A.G. El-Attar, R.N. White and P. Gergely, 2/28/91, (PB93-116630, A08, MF-A02).
- NCEER-91-0019 "Transfer Functions for Rigid Rectangular Foundations," by A.S. Veletsos, A.M. Prasad and W.H. Wu, 7/31/91, to be published.

- NCEER-91-0020 "Hybrid Control of Seismic-Excited Nonlinear and Inelastic Structural Systems," by J.N. Yang, Z. Li and A. Daniellians, 8/1/91, (PB92-143171, A06, MF-A02).
- NCEER-91-0021 "The NCEER-91 Earthquake Catalog: Improved Intensity-Based Magnitudes and Recurrence Relations for U.S. Earthquakes East of New Madrid," by L. Seeber and J.G. Armbruster, 8/28/91, (PB92-176742, A06, MF-A02).
- NCEER-91-0022 "Proceedings from the Implementation of Earthquake Planning and Education in Schools: The Need for Change - The Roles of the Changemakers," by K.E.K. Ross and F. Winslow, 7/23/91, (PB92-129998, A12, MF-A03).
- NCEER-91-0023 "A Study of Reliability-Based Criteria for Seismic Design of Reinforced Concrete Frame Buildings," by H.H.M. Hwang and H-M. Hsu, 8/10/91, (PB92-140235, A09, MF-A02).
- NCEER-91-0024 "Experimental Verification of a Number of Structural System Identification Algorithms," by R.G. Ghanem, H. Gavin and M. Shinozuka, 9/18/91, (PB92-176577, A18, MF-A04).
- NCEER-91-0025 "Probabilistic Evaluation of Liquefaction Potential," by H.H.M. Hwang and C.S. Lee, 11/25/91, (PB92-143429, A05, MF-A01).
- NCEER-91-0026 "Instantaneous Optimal Control for Linear, Nonlinear and Hysteretic Structures - Stable Controllers," by J.N. Yang and Z. Li, 11/15/91, (PB92-163807, A04, MF-A01).
- NCEER-91-0027 "Experimental and Theoretical Study of a Sliding Isolation System for Bridges," by M.C. Constantinou, A. Kartoum, A.M. Reinhorn and P. Bradford, 11/15/91, (PB92-176973, A10, MF-A03).
- NCEER-92-0001 "Case Studies of Liquefaction and Lifeline Performance During Past Earthquakes, Volume 1: Japanese Case Studies," Edited by M. Hamada and T. O'Rourke, 2/17/92, (PB92-197243, A18, MF-A04).
- NCEER-92-0002 "Case Studies of Liquefaction and Lifeline Performance During Past Earthquakes, Volume 2: United States Case Studies," Edited by T. O'Rourke and M. Hamada, 2/17/92, (PB92-197250, A20, MF-A04).
- NCEER-92-0003 "Issues in Earthquake Education," Edited by K. Ross, 2/3/92, (PB92-222389, A07, MF-A02).
- NCEER-92-0004 "Proceedings from the First U.S. - Japan Workshop on Earthquake Protective Systems for Bridges," Edited by I.G. Buckle, 2/4/92, (PB94-142239, A99, MF-A06).
- NCEER-92-0005 "Seismic Ground Motion from a Haskell-Type Source in a Multiple-Layered Half-Space," A.P. Theoharis, G. Deodatis and M. Shinozuka, 1/2/92, to be published.
- NCEER-92-0006 "Proceedings from the Site Effects Workshop," Edited by R. Whitman, 2/29/92, (PB92-197201, A04, MF-A01).
- NCEER-92-0007 "Engineering Evaluation of Permanent Ground Deformations Due to Seismically-Induced Liquefaction," by M.H. Baziar, R. Dobry and A-W.M. Elgamal, 3/24/92, (PB92-222421, A13, MF-A03).
- NCEER-92-0008 "A Procedure for the Seismic Evaluation of Buildings in the Central and Eastern United States," by C.D. Poland and J.O. Malley, 4/2/92, (PB92-222439, A20, MF-A04).
- NCEER-92-0009 "Experimental and Analytical Study of a Hybrid Isolation System Using Friction Controllable Sliding Bearings," by M.Q. Feng, S. Fujii and M. Shinozuka, 5/15/92, (PB93-150282, A06, MF-A02).
- NCEER-92-0010 "Seismic Resistance of Slab-Column Connections in Existing Non-Ductile Flat-Plate Buildings," by A.J. Durrani and Y. Du, 5/18/92, (PB93-116812, A06, MF-A02).
- NCEER-92-0011 "The Hysteretic and Dynamic Behavior of Brick Masonry Walls Upgraded by Ferrocement Coatings Under Cyclic Loading and Strong Simulated Ground Motion," by H. Lee and S.P. Prawl, 5/11/92, to be published.
- NCEER-92-0012 "Study of Wire Rope Systems for Seismic Protection of Equipment in Buildings," by G.F. Demetriades, M.C. Constantinou and A.M. Reinhorn, 5/20/92, (PB93-116655, A08, MF-A02).

- NCEER-92-0013 "Shape Memory Structural Dampers: Material Properties, Design and Seismic Testing," by P.R. Witting and F.A. Cozzarelli, 5/26/92, (PB93-116663, A05, MF-A01).
- NCEER-92-0014 "Longitudinal Permanent Ground Deformation Effects on Buried Continuous Pipelines," by M.J. O'Rourke, and C. Nordberg, 6/15/92, (PB93-116671, A08, MF-A02).
- NCEER-92-0015 "A Simulation Method for Stationary Gaussian Random Functions Based on the Sampling Theorem," by M. Grigoriu and S. Balopoulou, 6/11/92, (PB93-127496, A05, MF-A01).
- NCEER-92-0016 "Gravity-Load-Designed Reinforced Concrete Buildings: Seismic Evaluation of Existing Construction and Detailing Strategies for Improved Seismic Resistance," by G.W. Hoffmann, S.K. Kunnath, A.M. Reinhorn and J.B. Mander, 7/15/92, (PB94-142007, A08, MF-A02).
- NCEER-92-0017 "Observations on Water System and Pipeline Performance in the Limón Area of Costa Rica Due to the April 22, 1991 Earthquake," by M. O'Rourke and D. Ballantyne, 6/30/92, (PB93-126811, A06, MF-A02).
- NCEER-92-0018 "Fourth Edition of Earthquake Education Materials for Grades K-12," Edited by K.E.K. Ross, 8/10/92, (PB93-114023, A07, MF-A02).
- NCEER-92-0019 "Proceedings from the Fourth Japan-U.S. Workshop on Earthquake Resistant Design of Lifeline Facilities and Countermeasures for Soil Liquefaction," Edited by M. Hamada and T.D. O'Rourke, 8/12/92, (PB93-163939, A99, MF-E11).
- NCEER-92-0020 "Active Bracing System: A Full Scale Implementation of Active Control," by A.M. Reinhorn, T.T. Soong, R.C. Lin, M.A. Riley, Y.P. Wang, S. Aizawa and M. Higashino, 8/14/92, (PB93-127512, A06, MF-A02).
- NCEER-92-0021 "Empirical Analysis of Horizontal Ground Displacement Generated by Liquefaction-Induced Lateral Spreads," by S.F. Bartlett and T.L. Youd, 8/17/92, (PB93-188241, A06, MF-A02).
- NCEER-92-0022 "IDARC Version 3.0: Inelastic Damage Analysis of Reinforced Concrete Structures," by S.K. Kunnath, A.M. Reinhorn and R.F. Lobo, 8/31/92, (PB93-227502, A07, MF-A02).
- NCEER-92-0023 "A Semi-Empirical Analysis of Strong-Motion Peaks in Terms of Seismic Source, Propagation Path and Local Site Conditions, by M. Kamiyama, M.J. O'Rourke and R. Flores-Berrones, 9/9/92, (PB93-150266, A08, MF-A02).
- NCEER-92-0024 "Seismic Behavior of Reinforced Concrete Frame Structures with Nonductile Details, Part I: Summary of Experimental Findings of Full Scale Beam-Column Joint Tests," by A. Beres, R.N. White and P. Gergely, 9/30/92, (PB93-227783, A05, MF-A01).
- NCEER-92-0025 "Experimental Results of Repaired and Retrofitted Beam-Column Joint Tests in Lightly Reinforced Concrete Frame Buildings," by A. Beres, S. El-Borgi, R.N. White and P. Gergely, 10/29/92, (PB93-227791, A05, MF-A01).
- NCEER-92-0026 "A Generalization of Optimal Control Theory: Linear and Nonlinear Structures," by J.N. Yang, Z. Li and S. Vongchavalitkul, 11/2/92, (PB93-188621, A05, MF-A01).
- NCEER-92-0027 "Seismic Resistance of Reinforced Concrete Frame Structures Designed Only for Gravity Loads: Part I - Design and Properties of a One-Third Scale Model Structure," by J.M. Bracci, A.M. Reinhorn and J.B. Mander, 12/1/92, (PB94-104502, A08, MF-A02).
- NCEER-92-0028 "Seismic Resistance of Reinforced Concrete Frame Structures Designed Only for Gravity Loads: Part II - Experimental Performance of Subassemblages," by L.E. Aycaardi, J.B. Mander and A.M. Reinhorn, 12/1/92, (PB94-104510, A08, MF-A02).
- NCEER-92-0029 "Seismic Resistance of Reinforced Concrete Frame Structures Designed Only for Gravity Loads: Part III - Experimental Performance and Analytical Study of a Structural Model," by J.M. Bracci, A.M. Reinhorn and J.B. Mander, 12/1/92, (PB93-227528, A09, MF-A01).

- NCEER-92-0030 "Evaluation of Seismic Retrofit of Reinforced Concrete Frame Structures: Part I - Experimental Performance of Retrofitted Subassemblages," by D. Choudhuri, J.B. Mander and A.M. Reinhorn, 12/8/92, (PB93-198307, A07, MF-A02).
- NCEER-92-0031 "Evaluation of Seismic Retrofit of Reinforced Concrete Frame Structures: Part II - Experimental Performance and Analytical Study of a Retrofitted Structural Model," by J.M. Bracci, A.M. Reinhorn and J.B. Mander, 12/8/92, (PB93-198315, A09, MF-A03).
- NCEER-92-0032 "Experimental and Analytical Investigation of Seismic Response of Structures with Supplemental Fluid Viscous Dampers," by M.C. Constantinou and M.D. Symans, 12/21/92, (PB93-191435, A10, MF-A03). This report is available only through NTIS (see address given above).
- NCEER-92-0033 "Reconnaissance Report on the Cairo, Egypt Earthquake of October 12, 1992," by M. Khater, 12/23/92, (PB93-188621, A03, MF-A01).
- NCEER-92-0034 "Low-Level Dynamic Characteristics of Four Tall Flat-Plate Buildings in New York City," by H. Gavin, S. Yuan, J. Grossman, E. Pekelis and K. Jacob, 12/28/92, (PB93-188217, A07, MF-A02).
- NCEER-93-0001 "An Experimental Study on the Seismic Performance of Brick-Infilled Steel Frames With and Without Retrofit," by J.B. Mander, B. Nair, K. Wojtkowski and J. Ma, 1/29/93, (PB93-227510, A07, MF-A02).
- NCEER-93-0002 "Social Accounting for Disaster Preparedness and Recovery Planning," by S. Cole, E. Pantoja and V. Razak, 2/22/93, (PB94-142114, A12, MF-A03).
- NCEER-93-0003 "Assessment of 1991 NEHRP Provisions for Nonstructural Components and Recommended Revisions," by T.T. Soong, G. Chen, Z. Wu, R-H. Zhang and M. Grigoriu, 3/1/93, (PB93-188639, A06, MF-A02).
- NCEER-93-0004 "Evaluation of Static and Response Spectrum Analysis Procedures of SEAOC/UBC for Seismic Isolated Structures," by C.W. Winters and M.C. Constantinou, 3/23/93, (PB93-198299, A10, MF-A03).
- NCEER-93-0005 "Earthquakes in the Northeast - Are We Ignoring the Hazard? A Workshop on Earthquake Science and Safety for Educators," edited by K.E.K. Ross, 4/2/93, (PB94-103066, A09, MF-A02).
- NCEER-93-0006 "Inelastic Response of Reinforced Concrete Structures with Viscoelastic Braces," by R.F. Lobo, J.M. Bracci, K.L. Shen, A.M. Reinhorn and T.T. Soong, 4/5/93, (PB93-227486, A05, MF-A02).
- NCEER-93-0007 "Seismic Testing of Installation Methods for Computers and Data Processing Equipment," by K. Kosar, T.T. Soong, K.L. Shen, J.A. HoLung and Y.K. Lin, 4/12/93, (PB93-198299, A07, MF-A02).
- NCEER-93-0008 "Retrofit of Reinforced Concrete Frames Using Added Dampers," by A. Reinhorn, M. Constantinou and C. Li, to be published.
- NCEER-93-0009 "Seismic Behavior and Design Guidelines for Steel Frame Structures with Added Viscoelastic Dampers," by K.C. Chang, M.L. Lai, T.T. Soong, D.S. Hao and Y.C. Yeh, 5/1/93, (PB94-141959, A07, MF-A02).
- NCEER-93-0010 "Seismic Performance of Shear-Critical Reinforced Concrete Bridge Piers," by J.B. Mander, S.M. Waheed, M.T.A. Chaudhary and S.S. Chen, 5/12/93, (PB93-227494, A08, MF-A02).
- NCEER-93-0011 "3D-BASIS-TABS: Computer Program for Nonlinear Dynamic Analysis of Three Dimensional Base Isolated Structures," by S. Nagarajaiah, C. Li, A.M. Reinhorn and M.C. Constantinou, 8/2/93, (PB94-141819, A09, MF-A02).
- NCEER-93-0012 "Effects of Hydrocarbon Spills from an Oil Pipeline Break on Ground Water," by O.J. Helweg and H.H.M. Hwang, 8/3/93, (PB94-141942, A06, MF-A02).
- NCEER-93-0013 "Simplified Procedures for Seismic Design of Nonstructural Components and Assessment of Current Code Provisions," by M.P. Singh, L.E. Suarez, E.E. Matheu and G.O. Maldonado, 8/4/93, (PB94-141827, A09, MF-A02).
- NCEER-93-0014 "An Energy Approach to Seismic Analysis and Design of Secondary Systems," by G. Chen and T.T. Soong, 8/6/93, (PB94-142767, A11, MF-A03).

- NCEER-93-0015 "Proceedings from School Sites: Becoming Prepared for Earthquakes - Commemorating the Third Anniversary of the Loma Prieta Earthquake," Edited by F.E. Winslow and K.E.K. Ross, 8/16/93, (PB94-154275, A16, MF-A02).
- NCEER-93-0016 "Reconnaissance Report of Damage to Historic Monuments in Cairo, Egypt Following the October 12, 1992 Dahshur Earthquake," by D. Sykora, D. Look, G. Croci, E. Karaesmen and E. Karaesmen, 8/19/93, (PB94-142221, A08, MF-A02).
- NCEER-93-0017 "The Island of Guam Earthquake of August 8, 1993," by S.W. Swan and S.K. Harris, 9/30/93, (PB94-141843, A04, MF-A01).
- NCEER-93-0018 "Engineering Aspects of the October 12, 1992 Egyptian Earthquake," by A.W. Elgamal, M. Amer, K. Adalier and A. Abul-Fadl, 10/7/93, (PB94-141983, A05, MF-A01).
- NCEER-93-0019 "Development of an Earthquake Motion Simulator and its Application in Dynamic Centrifuge Testing," by I. Krstelj, Supervised by J.H. Prevost, 10/23/93, (PB94-181773, A-10, MF-A03).
- NCEER-93-0020 "NCEER-Taisei Corporation Research Program on Sliding Seismic Isolation Systems for Bridges: Experimental and Analytical Study of a Friction Pendulum System (FPS)," by M.C. Constantinou, P. Tsopelas, Y-S. Kim and S. Okamoto, 11/1/93, (PB94-142775, A08, MF-A02).
- NCEER-93-0021 "Finite Element Modeling of Elastomeric Seismic Isolation Bearings," by L.J. Billings, Supervised by R. Shepherd, 11/8/93, to be published.
- NCEER-93-0022 "Seismic Vulnerability of Equipment in Critical Facilities: Life-Safety and Operational Consequences," by K. Porter, G.S. Johnson, M.M. Zadeh, C. Scawthorn and S. Eder, 11/24/93, (PB94-181765, A16, MF-A03).
- NCEER-93-0023 "Hokkaido Nansei-oki, Japan Earthquake of July 12, 1993, by P.I. Yanev and C.R. Scawthorn, 12/23/93, (PB94-181500, A07, MF-A01).
- NCEER-94-0001 "An Evaluation of Seismic Serviceability of Water Supply Networks with Application to the San Francisco Auxiliary Water Supply System," by I. Markov, Supervised by M. Grigoriu and T. O'Rourke, 1/21/94, (PB94-204013, A07, MF-A02).
- NCEER-94-0002 "NCEER-Taisei Corporation Research Program on Sliding Seismic Isolation Systems for Bridges: Experimental and Analytical Study of Systems Consisting of Sliding Bearings, Rubber Restoring Force Devices and Fluid Dampers," Volumes I and II, by P. Tsopelas, S. Okamoto, M.C. Constantinou, D. Ozaki and S. Fujii, 2/4/94, (PB94-181740, A09, MF-A02 and PB94-181757, A12, MF-A03).
- NCEER-94-0003 "A Markov Model for Local and Global Damage Indices in Seismic Analysis," by S. Rahman and M. Grigoriu, 2/18/94, (PB94-206000, A12, MF-A03).
- NCEER-94-0004 "Proceedings from the NCEER Workshop on Seismic Response of Masonry Infills," edited by D.P. Abrams, 3/1/94, (PB94-180783, A07, MF-A02).
- NCEER-94-0005 "The Northridge, California Earthquake of January 17, 1994: General Reconnaissance Report," edited by J.D. Goltz, 3/11/94, (PB94-193943, A10, MF-A03).
- NCEER-94-0006 "Seismic Energy Based Fatigue Damage Analysis of Bridge Columns: Part I - Evaluation of Seismic Capacity," by G.A. Chang and J.B. Mander, 3/14/94, (PB94-219185, A11, MF-A03).
- NCEER-94-0007 "Seismic Isolation of Multi-Story Frame Structures Using Spherical Sliding Isolation Systems," by T.M. Al-Hussaini, V.A. Zayas and M.C. Constantinou, 3/17/94, (PB94-193745, A09, MF-A02).
- NCEER-94-0008 "The Northridge, California Earthquake of January 17, 1994: Performance of Highway Bridges," edited by I.G. Buckle, 3/24/94, (PB94-193851, A06, MF-A02).
- NCEER-94-0009 "Proceedings of the Third U.S.-Japan Workshop on Earthquake Protective Systems for Bridges," edited by I.G. Buckle and I. Friedland, 3/31/94, (PB94-195815, A99, MF-A06).

- NCEER-94-0010 "3D-BASIS-ME: Computer Program for Nonlinear Dynamic Analysis of Seismically Isolated Single and Multiple Structures and Liquid Storage Tanks," by P.C. Tsopelas, M.C. Constantinou and A.M. Reinhorn, 4/12/94, (PB94-204922, A09, MF-A02).
- NCEER-94-0011 "The Northridge, California Earthquake of January 17, 1994: Performance of Gas Transmission Pipelines," by T.D. O'Rourke and M.C. Palmer, 5/16/94, (PB94-204989, A05, MF-A01).
- NCEER-94-0012 "Feasibility Study of Replacement Procedures and Earthquake Performance Related to Gas Transmission Pipelines," by T.D. O'Rourke and M.C. Palmer, 5/25/94, (PB94-206638, A09, MF-A02).
- NCEER-94-0013 "Seismic Energy Based Fatigue Damage Analysis of Bridge Columns: Part II - Evaluation of Seismic Demand," by G.A. Chang and J.B. Mander, 6/1/94, (PB95-18106, A08, MF-A02).
- NCEER-94-0014 "NCEER-Taisei Corporation Research Program on Sliding Seismic Isolation Systems for Bridges: Experimental and Analytical Study of a System Consisting of Sliding Bearings and Fluid Restoring Force/Damping Devices," by P. Tsopelas and M.C. Constantinou, 6/13/94, (PB94-219144, A10, MF-A03).
- NCEER-94-0015 "Generation of Hazard-Consistent Fragility Curves for Seismic Loss Estimation Studies," by H. Hwang and J-R. Huo, 6/14/94, (PB95-181996, A09, MF-A02).
- NCEER-94-0016 "Seismic Study of Building Frames with Added Energy-Absorbing Devices," by W.S. Pong, C.S. Tsai and G.C. Lee, 6/20/94, (PB94-219136, A10, A03).
- NCEER-94-0017 "Sliding Mode Control for Seismic-Excited Linear and Nonlinear Civil Engineering Structures," by J. Yang, J. Wu, A. Agrawal and Z. Li, 6/21/94, (PB95-138483, A06, MF-A02).
- NCEER-94-0018 "3D-BASIS-TABS Version 2.0: Computer Program for Nonlinear Dynamic Analysis of Three Dimensional Base Isolated Structures," by A.M. Reinhorn, S. Nagarajaiah, M.C. Constantinou, P. Tsopelas and R. Li, 6/22/94, (PB95-182176, A08, MF-A02).
- NCEER-94-0019 "Proceedings of the International Workshop on Civil Infrastructure Systems: Application of Intelligent Systems and Advanced Materials on Bridge Systems," Edited by G.C. Lee and K.C. Chang, 7/18/94, (PB95-252474, A20, MF-A04).
- NCEER-94-0020 "Study of Seismic Isolation Systems for Computer Floors," by V. Lambrou and M.C. Constantinou, 7/19/94, (PB95-138533, A10, MF-A03).
- NCEER-94-0021 "Proceedings of the U.S.-Italian Workshop on Guidelines for Seismic Evaluation and Rehabilitation of Unreinforced Masonry Buildings," Edited by D.P. Abrams and G.M. Calvi, 7/20/94, (PB95-138749, A13, MF-A03).
- NCEER-94-0022 "NCEER-Taisei Corporation Research Program on Sliding Seismic Isolation Systems for Bridges: Experimental and Analytical Study of a System Consisting of Lubricated PTFE Sliding Bearings and Mild Steel Dampers," by P. Tsopelas and M.C. Constantinou, 7/22/94, (PB95-182184, A08, MF-A02).
- NCEER-94-0023 "Development of Reliability-Based Design Criteria for Buildings Under Seismic Load," by Y.K. Wen, H. Hwang and M. Shinozuka, 8/1/94, (PB95-211934, A08, MF-A02).
- NCEER-94-0024 "Experimental Verification of Acceleration Feedback Control Strategies for an Active Tendon System," by S.J. Dyke, B.F. Spencer, Jr., P. Quast, M.K. Sain, D.C. Kaspari, Jr. and T.T. Soong, 8/29/94, (PB95-212320, A05, MF-A01).
- NCEER-94-0025 "Seismic Retrofitting Manual for Highway Bridges," Edited by I.G. Buckle and I.F. Friedland, published by the Federal Highway Administration (PB95-212676, A15, MF-A03).
- NCEER-94-0026 "Proceedings from the Fifth U.S.-Japan Workshop on Earthquake Resistant Design of Lifeline Facilities and Countermeasures Against Soil Liquefaction," Edited by T.D. O'Rourke and M. Hamada, 11/7/94, (PB95-220802, A99, MF-E08).

- NCEER-95-0001 “Experimental and Analytical Investigation of Seismic Retrofit of Structures with Supplemental Damping: Part 1 - Fluid Viscous Damping Devices,” by A.M. Reinhorn, C. Li and M.C. Constantinou, 1/3/95, (PB95-266599, A09, MF-A02).
- NCEER-95-0002 “Experimental and Analytical Study of Low-Cycle Fatigue Behavior of Semi-Rigid Top-And-Seat Angle Connections,” by G. Pekcan, J.B. Mander and S.S. Chen, 1/5/95, (PB95-220042, A07, MF-A02).
- NCEER-95-0003 “NCEER-ATC Joint Study on Fragility of Buildings,” by T. Anagnos, C. Rojahn and A.S. Kiremidjian, 1/20/95, (PB95-220026, A06, MF-A02).
- NCEER-95-0004 “Nonlinear Control Algorithms for Peak Response Reduction,” by Z. Wu, T.T. Soong, V. Gattulli and R.C. Lin, 2/16/95, (PB95-220349, A05, MF-A01).
- NCEER-95-0005 “Pipeline Replacement Feasibility Study: A Methodology for Minimizing Seismic and Corrosion Risks to Underground Natural Gas Pipelines,” by R.T. Eguchi, H.A. Seligson and D.G. Honegger, 3/2/95, (PB95-252326, A06, MF-A02).
- NCEER-95-0006 “Evaluation of Seismic Performance of an 11-Story Frame Building During the 1994 Northridge Earthquake,” by F. Naeim, R. DiSulio, K. Benuska, A. Reinhorn and C. Li, to be published.
- NCEER-95-0007 “Prioritization of Bridges for Seismic Retrofitting,” by N. Basöz and A.S. Kiremidjian, 4/24/95, (PB95-252300, A08, MF-A02).
- NCEER-95-0008 “Method for Developing Motion Damage Relationships for Reinforced Concrete Frames,” by A. Singhal and A.S. Kiremidjian, 5/11/95, (PB95-266607, A06, MF-A02).
- NCEER-95-0009 “Experimental and Analytical Investigation of Seismic Retrofit of Structures with Supplemental Damping: Part II - Friction Devices,” by C. Li and A.M. Reinhorn, 7/6/95, (PB96-128087, A11, MF-A03).
- NCEER-95-0010 “Experimental Performance and Analytical Study of a Non-Ductile Reinforced Concrete Frame Structure Retrofitted with Elastomeric Spring Dampers,” by G. Pekcan, J.B. Mander and S.S. Chen, 7/14/95, (PB96-137161, A08, MF-A02).
- NCEER-95-0011 “Development and Experimental Study of Semi-Active Fluid Damping Devices for Seismic Protection of Structures,” by M.D. Symans and M.C. Constantinou, 8/3/95, (PB96-136940, A23, MF-A04).
- NCEER-95-0012 “Real-Time Structural Parameter Modification (RSPM): Development of Innervated Structures,” by Z. Liang, M. Tong and G.C. Lee, 4/11/95, (PB96-137153, A06, MF-A01).
- NCEER-95-0013 “Experimental and Analytical Investigation of Seismic Retrofit of Structures with Supplemental Damping: Part III - Viscous Damping Walls,” by A.M. Reinhorn and C. Li, 10/1/95, (PB96-176409, A11, MF-A03).
- NCEER-95-0014 “Seismic Fragility Analysis of Equipment and Structures in a Memphis Electric Substation,” by J-R. Huo and H.H.M. Hwang, 8/10/95, (PB96-128087, A09, MF-A02).
- NCEER-95-0015 “The Hanshin-Awaji Earthquake of January 17, 1995: Performance of Lifelines,” Edited by M. Shinozuka, 11/3/95, (PB96-176383, A15, MF-A03).
- NCEER-95-0016 “Highway Culvert Performance During Earthquakes,” by T.L. Youd and C.J. Beckman, available as NCEER-96-0015.
- NCEER-95-0017 “The Hanshin-Awaji Earthquake of January 17, 1995: Performance of Highway Bridges,” Edited by I.G. Buckle, 12/1/95, to be published.
- NCEER-95-0018 “Modeling of Masonry Infill Panels for Structural Analysis,” by A.M. Reinhorn, A. Madan, R.E. Valles, Y. Reichmann and J.B. Mander, 12/8/95, (PB97-110886, MF-A01, A06).
- NCEER-95-0019 “Optimal Polynomial Control for Linear and Nonlinear Structures,” by A.K. Agrawal and J.N. Yang, 12/11/95, (PB96-168737, A07, MF-A02).

- NCEER-95-0020 "Retrofit of Non-Ductile Reinforced Concrete Frames Using Friction Dampers," by R.S. Rao, P. Gergely and R.N. White, 12/22/95, (PB97-133508, A10, MF-A02).
- NCEER-95-0021 "Parametric Results for Seismic Response of Pile-Supported Bridge Bents," by G. Mylonakis, A. Nikolaou and G. Gazetas, 12/22/95, (PB97-100242, A12, MF-A03).
- NCEER-95-0022 "Kinematic Bending Moments in Seismically Stressed Piles," by A. Nikolaou, G. Mylonakis and G. Gazetas, 12/23/95, (PB97-113914, MF-A03, A13).
- NCEER-96-0001 "Dynamic Response of Unreinforced Masonry Buildings with Flexible Diaphragms," by A.C. Costley and D.P. Abrams, 10/10/96, (PB97-133573, MF-A03, A15).
- NCEER-96-0002 "State of the Art Review: Foundations and Retaining Structures," by I. Po Lam, to be published.
- NCEER-96-0003 "Ductility of Rectangular Reinforced Concrete Bridge Columns with Moderate Confinement," by N. Wehbe, M. Saiidi, D. Sanders and B. Douglas, 11/7/96, (PB97-133557, A06, MF-A02).
- NCEER-96-0004 "Proceedings of the Long-Span Bridge Seismic Research Workshop," edited by I.G. Buckle and I.M. Friedland, to be published.
- NCEER-96-0005 "Establish Representative Pier Types for Comprehensive Study: Eastern United States," by J. Kulicki and Z. Prucz, 5/28/96, (PB98-119217, A07, MF-A02).
- NCEER-96-0006 "Establish Representative Pier Types for Comprehensive Study: Western United States," by R. Imbsen, R.A. Schamber and T.A. Osterkamp, 5/28/96, (PB98-118607, A07, MF-A02).
- NCEER-96-0007 "Nonlinear Control Techniques for Dynamical Systems with Uncertain Parameters," by R.G. Ghanem and M.I. Bujakov, 5/27/96, (PB97-100259, A17, MF-A03).
- NCEER-96-0008 "Seismic Evaluation of a 30-Year Old Non-Ductile Highway Bridge Pier and Its Retrofit," by J.B. Mander, B. Mahmoodzadegan, S. Bhadra and S.S. Chen, 5/31/96, (PB97-110902, MF-A03, A10).
- NCEER-96-0009 "Seismic Performance of a Model Reinforced Concrete Bridge Pier Before and After Retrofit," by J.B. Mander, J.H. Kim and C.A. Ligozio, 5/31/96, (PB97-110910, MF-A02, A10).
- NCEER-96-0010 "IDARC2D Version 4.0: A Computer Program for the Inelastic Damage Analysis of Buildings," by R.E. Valles, A.M. Reinhorn, S.K. Kunnath, C. Li and A. Madan, 6/3/96, (PB97-100234, A17, MF-A03).
- NCEER-96-0011 "Estimation of the Economic Impact of Multiple Lifeline Disruption: Memphis Light, Gas and Water Division Case Study," by S.E. Chang, H.A. Seligson and R.T. Eguchi, 8/16/96, (PB97-133490, A11, MF-A03).
- NCEER-96-0012 "Proceedings from the Sixth Japan-U.S. Workshop on Earthquake Resistant Design of Lifeline Facilities and Countermeasures Against Soil Liquefaction, Edited by M. Hamada and T. O'Rourke, 9/11/96, (PB97-133581, A99, MF-A06).
- NCEER-96-0013 "Chemical Hazards, Mitigation and Preparedness in Areas of High Seismic Risk: A Methodology for Estimating the Risk of Post-Earthquake Hazardous Materials Release," by H.A. Seligson, R.T. Eguchi, K.J. Tierney and K. Richmond, 11/7/96, (PB97-133565, MF-A02, A08).
- NCEER-96-0014 "Response of Steel Bridge Bearings to Reversed Cyclic Loading," by J.B. Mander, D-K. Kim, S.S. Chen and G.J. Premus, 11/13/96, (PB97-140735, A12, MF-A03).
- NCEER-96-0015 "Highway Culvert Performance During Past Earthquakes," by T.L. Youd and C.J. Beckman, 11/25/96, (PB97-133532, A06, MF-A01).
- NCEER-97-0001 "Evaluation, Prevention and Mitigation of Pounding Effects in Building Structures," by R.E. Valles and A.M. Reinhorn, 2/20/97, (PB97-159552, A14, MF-A03).
- NCEER-97-0002 "Seismic Design Criteria for Bridges and Other Highway Structures," by C. Rojahn, R. Mayes, D.G. Anderson, J. Clark, J.H. Hom, R.V. Nutt and M.J. O'Rourke, 4/30/97, (PB97-194658, A06, MF-A03).

- NCEER-97-0003 "Proceedings of the U.S.-Italian Workshop on Seismic Evaluation and Retrofit," Edited by D.P. Abrams and G.M. Calvi, 3/19/97, (PB97-194666, A13, MF-A03).
- NCEER-97-0004 "Investigation of Seismic Response of Buildings with Linear and Nonlinear Fluid Viscous Dampers," by A.A. Seleemah and M.C. Constantinou, 5/21/97, (PB98-109002, A15, MF-A03).
- NCEER-97-0005 "Proceedings of the Workshop on Earthquake Engineering Frontiers in Transportation Facilities," edited by G.C. Lee and I.M. Friedland, 8/29/97, (PB98-128911, A25, MR-A04).
- NCEER-97-0006 "Cumulative Seismic Damage of Reinforced Concrete Bridge Piers," by S.K. Kunnath, A. El-Bahy, A. Taylor and W. Stone, 9/2/97, (PB98-108814, A11, MF-A03).
- NCEER-97-0007 "Structural Details to Accommodate Seismic Movements of Highway Bridges and Retaining Walls," by R.A. Imbsen, R.A. Schamber, E. Thorkildsen, A. Kartoum, B.T. Martin, T.N. Rosser and J.M. Kulicki, 9/3/97, (PB98-108996, A09, MF-A02).
- NCEER-97-0008 "A Method for Earthquake Motion-Damage Relationships with Application to Reinforced Concrete Frames," by A. Singhal and A.S. Kiremidjian, 9/10/97, (PB98-108988, A13, MF-A03).
- NCEER-97-0009 "Seismic Analysis and Design of Bridge Abutments Considering Sliding and Rotation," by K. Fishman and R. Richards, Jr., 9/15/97, (PB98-108897, A06, MF-A02).
- NCEER-97-0010 "Proceedings of the FHWA/NCEER Workshop on the National Representation of Seismic Ground Motion for New and Existing Highway Facilities," edited by I.M. Friedland, M.S. Power and R.L. Mayes, 9/22/97, (PB98-128903, A21, MF-A04).
- NCEER-97-0011 "Seismic Analysis for Design or Retrofit of Gravity Bridge Abutments," by K.L. Fishman, R. Richards, Jr. and R.C. Divito, 10/2/97, (PB98-128937, A08, MF-A02).
- NCEER-97-0012 "Evaluation of Simplified Methods of Analysis for Yielding Structures," by P. Tsopelas, M.C. Constantinou, C.A. Kircher and A.S. Whittaker, 10/31/97, (PB98-128929, A10, MF-A03).
- NCEER-97-0013 "Seismic Design of Bridge Columns Based on Control and Repairability of Damage," by C-T. Cheng and J.B. Mander, 12/8/97, (PB98-144249, A11, MF-A03).
- NCEER-97-0014 "Seismic Resistance of Bridge Piers Based on Damage Avoidance Design," by J.B. Mander and C-T. Cheng, 12/10/97, (PB98-144223, A09, MF-A02).
- NCEER-97-0015 "Seismic Response of Nominally Symmetric Systems with Strength Uncertainty," by S. Balopoulou and M. Grigoriu, 12/23/97, (PB98-153422, A11, MF-A03).
- NCEER-97-0016 "Evaluation of Seismic Retrofit Methods for Reinforced Concrete Bridge Columns," by T.J. Wipf, F.W. Klaiber and F.M. Russo, 12/28/97, (PB98-144215, A12, MF-A03).
- NCEER-97-0017 "Seismic Fragility of Existing Conventional Reinforced Concrete Highway Bridges," by C.L. Mullen and A.S. Cakmak, 12/30/97, (PB98-153406, A08, MF-A02).
- NCEER-97-0018 "Loss Assessment of Memphis Buildings," edited by D.P. Abrams and M. Shinozuka, 12/31/97, (PB98-144231, A13, MF-A03).
- NCEER-97-0019 "Seismic Evaluation of Frames with Infill Walls Using Quasi-static Experiments," by K.M. Mosalam, R.N. White and P. Gergely, 12/31/97, (PB98-153455, A07, MF-A02).
- NCEER-97-0020 "Seismic Evaluation of Frames with Infill Walls Using Pseudo-dynamic Experiments," by K.M. Mosalam, R.N. White and P. Gergely, 12/31/97, (PB98-153430, A07, MF-A02).
- NCEER-97-0021 "Computational Strategies for Frames with Infill Walls: Discrete and Smeared Crack Analyses and Seismic Fragility," by K.M. Mosalam, R.N. White and P. Gergely, 12/31/97, (PB98-153414, A10, MF-A02).

- NCEER-97-0022 "Proceedings of the NCEER Workshop on Evaluation of Liquefaction Resistance of Soils," edited by T.L. Youd and I.M. Idriss, 12/31/97, (PB98-155617, A15, MF-A03).
- MCEER-98-0001 "Extraction of Nonlinear Hysteretic Properties of Seismically Isolated Bridges from Quick-Release Field Tests," by Q. Chen, B.M. Douglas, E.M. Maragakis and I.G. Buckle, 5/26/98, (PB99-118838, A06, MF-A01).
- MCEER-98-0002 "Methodologies for Evaluating the Importance of Highway Bridges," by A. Thomas, S. Eshenaur and J. Kulicki, 5/29/98, (PB99-118846, A10, MF-A02).
- MCEER-98-0003 "Capacity Design of Bridge Piers and the Analysis of Overstrength," by J.B. Mander, A. Dutta and P. Goel, 6/1/98, (PB99-118853, A09, MF-A02).
- MCEER-98-0004 "Evaluation of Bridge Damage Data from the Loma Prieta and Northridge, California Earthquakes," by N. Basoz and A. Kiremidjian, 6/2/98, (PB99-118861, A15, MF-A03).
- MCEER-98-0005 "Screening Guide for Rapid Assessment of Liquefaction Hazard at Highway Bridge Sites," by T. L. Youd, 6/16/98, (PB99-118879, A06, not available on microfiche).
- MCEER-98-0006 "Structural Steel and Steel/Concrete Interface Details for Bridges," by P. Ritchie, N. Kauh and J. Kulicki, 7/13/98, (PB99-118945, A06, MF-A01).
- MCEER-98-0007 "Capacity Design and Fatigue Analysis of Confined Concrete Columns," by A. Dutta and J.B. Mander, 7/14/98, (PB99-118960, A14, MF-A03).
- MCEER-98-0008 "Proceedings of the Workshop on Performance Criteria for Telecommunication Services Under Earthquake Conditions," edited by A.J. Schiff, 7/15/98, (PB99-118952, A08, MF-A02).
- MCEER-98-0009 "Fatigue Analysis of Unconfined Concrete Columns," by J.B. Mander, A. Dutta and J.H. Kim, 9/12/98, (PB99-123655, A10, MF-A02).
- MCEER-98-0010 "Centrifuge Modeling of Cyclic Lateral Response of Pile-Cap Systems and Seat-Type Abutments in Dry Sands," by A.D. Gadre and R. Dobry, 10/2/98, (PB99-123606, A13, MF-A03).
- MCEER-98-0011 "IDARC-BRIDGE: A Computational Platform for Seismic Damage Assessment of Bridge Structures," by A.M. Reinhorn, V. Simeonov, G. Mylonakis and Y. Reichman, 10/2/98, (PB99-162919, A15, MF-A03).
- MCEER-98-0012 "Experimental Investigation of the Dynamic Response of Two Bridges Before and After Retrofitting with Elastomeric Bearings," by D.A. Wendichansky, S.S. Chen and J.B. Mander, 10/2/98, (PB99-162927, A15, MF-A03).
- MCEER-98-0013 "Design Procedures for Hinge Restrainers and Hinge Sear Width for Multiple-Frame Bridges," by R. Des Roches and G.L. Fenves, 11/3/98, (PB99-140477, A13, MF-A03).
- MCEER-98-0014 "Response Modification Factors for Seismically Isolated Bridges," by M.C. Constantinou and J.K. Quarshie, 11/3/98, (PB99-140485, A14, MF-A03).
- MCEER-98-0015 "Proceedings of the U.S.-Italy Workshop on Seismic Protective Systems for Bridges," edited by I.M. Friedland and M.C. Constantinou, 11/3/98, (PB2000-101711, A22, MF-A04).
- MCEER-98-0016 "Appropriate Seismic Reliability for Critical Equipment Systems: Recommendations Based on Regional Analysis of Financial and Life Loss," by K. Porter, C. Scawthorn, C. Taylor and N. Blais, 11/10/98, (PB99-157265, A08, MF-A02).
- MCEER-98-0017 "Proceedings of the U.S. Japan Joint Seminar on Civil Infrastructure Systems Research," edited by M. Shinozuka and A. Rose, 11/12/98, (PB99-156713, A16, MF-A03).
- MCEER-98-0018 "Modeling of Pile Footings and Drilled Shafts for Seismic Design," by I. PoLam, M. Kapuskar and D. Chaudhuri, 12/21/98, (PB99-157257, A09, MF-A02).

- MCEER-99-0001 "Seismic Evaluation of a Masonry Infilled Reinforced Concrete Frame by Pseudodynamic Testing," by S.G. Buonopane and R.N. White, 2/16/99, (PB99-162851, A09, MF-A02).
- MCEER-99-0002 "Response History Analysis of Structures with Seismic Isolation and Energy Dissipation Systems: Verification Examples for Program SAP2000," by J. Scheller and M.C. Constantinou, 2/22/99, (PB99-162869, A08, MF-A02).
- MCEER-99-0003 "Experimental Study on the Seismic Design and Retrofit of Bridge Columns Including Axial Load Effects," by A. Dutta, T. Kokorina and J.B. Mander, 2/22/99, (PB99-162877, A09, MF-A02).
- MCEER-99-0004 "Experimental Study of Bridge Elastomeric and Other Isolation and Energy Dissipation Systems with Emphasis on Uplift Prevention and High Velocity Near-source Seismic Excitation," by A. Kasalanati and M. C. Constantinou, 2/26/99, (PB99-162885, A12, MF-A03).
- MCEER-99-0005 "Truss Modeling of Reinforced Concrete Shear-flexure Behavior," by J.H. Kim and J.B. Mander, 3/8/99, (PB99-163693, A12, MF-A03).
- MCEER-99-0006 "Experimental Investigation and Computational Modeling of Seismic Response of a 1:4 Scale Model Steel Structure with a Load Balancing Supplemental Damping System," by G. Pekcan, J.B. Mander and S.S. Chen, 4/2/99, (PB99-162893, A11, MF-A03).
- MCEER-99-0007 "Effect of Vertical Ground Motions on the Structural Response of Highway Bridges," by M.R. Button, C.J. Cronin and R.L. Mayes, 4/10/99, (PB2000-101411, A10, MF-A03).
- MCEER-99-0008 "Seismic Reliability Assessment of Critical Facilities: A Handbook, Supporting Documentation, and Model Code Provisions," by G.S. Johnson, R.E. Sheppard, M.D. Quilici, S.J. Eder and C.R. Scawthorn, 4/12/99, (PB2000-101701, A18, MF-A04).
- MCEER-99-0009 "Impact Assessment of Selected MCEER Highway Project Research on the Seismic Design of Highway Structures," by C. Rojahn, R. Mayes, D.G. Anderson, J.H. Clark, D'Appolonia Engineering, S. Gloyd and R.V. Nutt, 4/14/99, (PB99-162901, A10, MF-A02).
- MCEER-99-0010 "Site Factors and Site Categories in Seismic Codes," by R. Dobry, R. Ramos and M.S. Power, 7/19/99, (PB2000-101705, A08, MF-A02).
- MCEER-99-0011 "Restrainer Design Procedures for Multi-Span Simply-Supported Bridges," by M.J. Randall, M. Saiidi, E. Maragakis and T. Isakovic, 7/20/99, (PB2000-101702, A10, MF-A02).
- MCEER-99-0012 "Property Modification Factors for Seismic Isolation Bearings," by M.C. Constantinou, P. Tsopelas, A. Kasalanati and E. Wolff, 7/20/99, (PB2000-103387, A11, MF-A03).
- MCEER-99-0013 "Critical Seismic Issues for Existing Steel Bridges," by P. Ritchie, N. Kauh and J. Kulicki, 7/20/99, (PB2000-101697, A09, MF-A02).
- MCEER-99-0014 "Nonstructural Damage Database," by A. Kao, T.T. Soong and A. Vender, 7/24/99, (PB2000-101407, A06, MF-A01).
- MCEER-99-0015 "Guide to Remedial Measures for Liquefaction Mitigation at Existing Highway Bridge Sites," by H.G. Cooke and J. K. Mitchell, 7/26/99, (PB2000-101703, A11, MF-A03).
- MCEER-99-0016 "Proceedings of the MCEER Workshop on Ground Motion Methodologies for the Eastern United States," edited by N. Abrahamson and A. Becker, 8/11/99, (PB2000-103385, A07, MF-A02).
- MCEER-99-0017 "Quindío, Colombia Earthquake of January 25, 1999: Reconnaissance Report," by A.P. Asfura and P.J. Flores, 10/4/99, (PB2000-106893, A06, MF-A01).
- MCEER-99-0018 "Hysteretic Models for Cyclic Behavior of Deteriorating Inelastic Structures," by M.V. Sivaselvan and A.M. Reinhorn, 11/5/99, (PB2000-103386, A08, MF-A02).

- MCEER-99-0019 "Proceedings of the 7th U.S.- Japan Workshop on Earthquake Resistant Design of Lifeline Facilities and Countermeasures Against Soil Liquefaction," edited by T.D. O'Rourke, J.P. Bardet and M. Hamada, 11/19/99, (PB2000-103354, A99, MF-A06).
- MCEER-99-0020 "Development of Measurement Capability for Micro-Vibration Evaluations with Application to Chip Fabrication Facilities," by G.C. Lee, Z. Liang, J.W. Song, J.D. Shen and W.C. Liu, 12/1/99, (PB2000-105993, A08, MF-A02).
- MCEER-99-0021 "Design and Retrofit Methodology for Building Structures with Supplemental Energy Dissipating Systems," by G. Pekcan, J.B. Mander and S.S. Chen, 12/31/99, (PB2000-105994, A11, MF-A03).
- MCEER-00-0001 "The Marmara, Turkey Earthquake of August 17, 1999: Reconnaissance Report," edited by C. Scawthorn; with major contributions by M. Bruneau, R. Eguchi, T. Holzer, G. Johnson, J. Mander, J. Mitchell, W. Mitchell, A. Papageorgiou, C. Scaethorn, and G. Webb, 3/23/00, (PB2000-106200, A11, MF-A03).
- MCEER-00-0002 "Proceedings of the MCEER Workshop for Seismic Hazard Mitigation of Health Care Facilities," edited by G.C. Lee, M. Ettouney, M. Grigoriu, J. Hauer and J. Nigg, 3/29/00, (PB2000-106892, A08, MF-A02).
- MCEER-00-0003 "The Chi-Chi, Taiwan Earthquake of September 21, 1999: Reconnaissance Report," edited by G.C. Lee and C.H. Loh, with major contributions by G.C. Lee, M. Bruneau, I.G. Buckle, S.E. Chang, P.J. Flores, T.D. O'Rourke, M. Shinozuka, T.T. Soong, C-H. Loh, K-C. Chang, Z-J. Chen, J-S. Hwang, M-L. Lin, G-Y. Liu, K-C. Tsai, G.C. Yao and C-L. Yen, 4/30/00, (PB2001-100980, A10, MF-A02).
- MCEER-00-0004 "Seismic Retrofit of End-Sway Frames of Steel Deck-Truss Bridges with a Supplemental Tendon System: Experimental and Analytical Investigation," by G. Pekcan, J.B. Mander and S.S. Chen, 7/1/00, (PB2001-100982, A10, MF-A02).
- MCEER-00-0005 "Sliding Fragility of Unrestrained Equipment in Critical Facilities," by W.H. Chong and T.T. Soong, 7/5/00, (PB2001-100983, A08, MF-A02).
- MCEER-00-0006 "Seismic Response of Reinforced Concrete Bridge Pier Walls in the Weak Direction," by N. Abo-Shadi, M. Saiidi and D. Sanders, 7/17/00, (PB2001-100981, A17, MF-A03).
- MCEER-00-0007 "Low-Cycle Fatigue Behavior of Longitudinal Reinforcement in Reinforced Concrete Bridge Columns," by J. Brown and S.K. Kunnath, 7/23/00, (PB2001-104392, A08, MF-A02).
- MCEER-00-0008 "Soil Structure Interaction of Bridges for Seismic Analysis," I. PoLam and H. Law, 9/25/00, (PB2001-105397, A08, MF-A02).
- MCEER-00-0009 "Proceedings of the First MCEER Workshop on Mitigation of Earthquake Disaster by Advanced Technologies (MEDAT-1), edited by M. Shinozuka, D.J. Inman and T.D. O'Rourke, 11/10/00, (PB2001-105399, A14, MF-A03).
- MCEER-00-0010 "Development and Evaluation of Simplified Procedures for Analysis and Design of Buildings with Passive Energy Dissipation Systems, Revision 01," by O.M. Ramirez, M.C. Constantinou, C.A. Kircher, A.S. Whittaker, M.W. Johnson, J.D. Gomez and C. Chrysostomou, 11/16/01, (PB2001-105523, A23, MF-A04).
- MCEER-00-0011 "Dynamic Soil-Foundation-Structure Interaction Analyses of Large Caissons," by C-Y. Chang, C-M. Mok, Z-L. Wang, R. Settgast, F. Waggoner, M.A. Ketchum, H.M. Gonnermann and C-C. Chin, 12/30/00, (PB2001-104373, A07, MF-A02).
- MCEER-00-0012 "Experimental Evaluation of Seismic Performance of Bridge Restrainers," by A.G. Vlassis, E.M. Maragakis and M. Saiid Saiidi, 12/30/00, (PB2001-104354, A09, MF-A02).
- MCEER-00-0013 "Effect of Spatial Variation of Ground Motion on Highway Structures," by M. Shinozuka, V. Saxena and G. Deodatis, 12/31/00, (PB2001-108755, A13, MF-A03).
- MCEER-00-0014 "A Risk-Based Methodology for Assessing the Seismic Performance of Highway Systems," by S.D. Werner, C.E. Taylor, J.E. Moore, II, J.S. Walton and S. Cho, 12/31/00, (PB2001-108756, A14, MF-A03).


- MCEER-01-0001 “Experimental Investigation of P-Delta Effects to Collapse During Earthquakes,” by D. Vian and M. Bruneau, 6/25/01, (PB2002-100534, A17, MF-A03).
- MCEER-01-0002 “Proceedings of the Second MCEER Workshop on Mitigation of Earthquake Disaster by Advanced Technologies (MEDAT-2),” edited by M. Bruneau and D.J. Inman, 7/23/01, (PB2002-100434, A16, MF-A03).
- MCEER-01-0003 “Sensitivity Analysis of Dynamic Systems Subjected to Seismic Loads,” by C. Roth and M. Grigoriu, 9/18/01, (PB2003-100884, A12, MF-A03).
- MCEER-01-0004 “Overcoming Obstacles to Implementing Earthquake Hazard Mitigation Policies: Stage 1 Report,” by D.J. Alesch and W.J. Petak, 12/17/01, (PB2002-107949, A07, MF-A02).
- MCEER-01-0005 “Updating Real-Time Earthquake Loss Estimates: Methods, Problems and Insights,” by C.E. Taylor, S.E. Chang and R.T. Eguchi, 12/17/01, (PB2002-107948, A05, MF-A01).
- MCEER-01-0006 “Experimental Investigation and Retrofit of Steel Pile Foundations and Pile Bents Under Cyclic Lateral Loadings,” by A. Shama, J. Mander, B. Blabac and S. Chen, 12/31/01, (PB2002-107950, A13, MF-A03).
- MCEER-02-0001 “Assessment of Performance of Bolu Viaduct in the 1999 Duzce Earthquake in Turkey” by P.C. Roussis, M.C. Constantinou, M. Erdik, E. Durukal and M. Dicleli, 5/8/02, (PB2003-100883, A08, MF-A02).
- MCEER-02-0002 “Seismic Behavior of Rail Counterweight Systems of Elevators in Buildings,” by M.P. Singh, Rildova and L.E. Suarez, 5/27/02. (PB2003-100882, A11, MF-A03).
- MCEER-02-0003 “Development of Analysis and Design Procedures for Spread Footings,” by G. Mylonakis, G. Gazetas, S. Nikolaou and A. Chauncey, 10/02/02, (PB2004-101636, A13, MF-A03, CD-A13).
- MCEER-02-0004 “Bare-Earth Algorithms for Use with SAR and LIDAR Digital Elevation Models,” by C.K. Huyck, R.T. Eguchi and B. Houshmand, 10/16/02, (PB2004-101637, A07, CD-A07).
- MCEER-02-0005 “Review of Energy Dissipation of Compression Members in Concentrically Braced Frames,” by K.Lee and M. Bruneau, 10/18/02, (PB2004-101638, A10, CD-A10).
- MCEER-03-0001 “Experimental Investigation of Light-Gauge Steel Plate Shear Walls for the Seismic Retrofit of Buildings” by J. Berman and M. Bruneau, 5/2/03, (PB2004-101622, A10, MF-A03, CD-A10).
- MCEER-03-0002 “Statistical Analysis of Fragility Curves,” by M. Shinozuka, M.Q. Feng, H. Kim, T. Uzawa and T. Ueda, 6/16/03, (PB2004-101849, A09, CD-A09).
- MCEER-03-0003 “Proceedings of the Eighth U.S.-Japan Workshop on Earthquake Resistant Design of Lifeline Facilities and Countermeasures Against Liquefaction,” edited by M. Hamada, J.P. Bardet and T.D. O’Rourke, 6/30/03, (PB2004-104386, A99, CD-A99).
- MCEER-03-0004 “Proceedings of the PRC-US Workshop on Seismic Analysis and Design of Special Bridges,” edited by L.C. Fan and G.C. Lee, 7/15/03, (PB2004-104387, A14, CD-A14).
- MCEER-03-0005 “Urban Disaster Recovery: A Framework and Simulation Model,” by S.B. Miles and S.E. Chang, 7/25/03, (PB2004-104388, A07, CD-A07).
- MCEER-03-0006 “Behavior of Underground Piping Joints Due to Static and Dynamic Loading,” by R.D. Meis, M. Maragakis and R. Siddharthan, 11/17/03, (PB2005-102194, A13, MF-A03, CD-A00).
- MCEER-04-0001 “Experimental Study of Seismic Isolation Systems with Emphasis on Secondary System Response and Verification of Accuracy of Dynamic Response History Analysis Methods,” by E. Wolff and M. Constantinou, 1/16/04 (PB2005-102195, A99, MF-E08, CD-A00).
- MCEER-04-0002 “Tension, Compression and Cyclic Testing of Engineered Cementitious Composite Materials,” by K. Kesner and S.L. Billington, 3/1/04, (PB2005-102196, A08, CD-A08).

- MCEER-04-0003 “Cyclic Testing of Braces Laterally Restrained by Steel Studs to Enhance Performance During Earthquakes,” by O.C. Celik, J.W. Berman and M. Bruneau, 3/16/04, (PB2005-102197, A13, MF-A03, CD-A00).
- MCEER-04-0004 “Methodologies for Post Earthquake Building Damage Detection Using SAR and Optical Remote Sensing: Application to the August 17, 1999 Marmara, Turkey Earthquake,” by C.K. Huyck, B.J. Adams, S. Cho, R.T. Eguchi, B. Mansouri and B. Houshmand, 6/15/04, (PB2005-104888, A10, CD-A00).
- MCEER-04-0005 “Nonlinear Structural Analysis Towards Collapse Simulation: A Dynamical Systems Approach,” by M.V. Sivaselvan and A.M. Reinhorn, 6/16/04, (PB2005-104889, A11, MF-A03, CD-A00).
- MCEER-04-0006 “Proceedings of the Second PRC-US Workshop on Seismic Analysis and Design of Special Bridges,” edited by G.C. Lee and L.C. Fan, 6/25/04, (PB2005-104890, A16, CD-A00).
- MCEER-04-0007 “Seismic Vulnerability Evaluation of Axially Loaded Steel Built-up Laced Members,” by K. Lee and M. Bruneau, 6/30/04, (PB2005-104891, A16, CD-A00).
- MCEER-04-0008 “Evaluation of Accuracy of Simplified Methods of Analysis and Design of Buildings with Damping Systems for Near-Fault and for Soft-Soil Seismic Motions,” by E.A. Pavlou and M.C. Constantinou, 8/16/04, (PB2005-104892, A08, MF-A02, CD-A00).
- MCEER-04-0009 “Assessment of Geotechnical Issues in Acute Care Facilities in California,” by M. Lew, T.D. O’Rourke, R. Dobry and M. Koch, 9/15/04, (PB2005-104893, A08, CD-A00).
- MCEER-04-0010 “Scissor-Jack-Damper Energy Dissipation System,” by A.N. Sigaher-Boyle and M.C. Constantinou, 12/1/04 (PB2005-108221).
- MCEER-04-0011 “Seismic Retrofit of Bridge Steel Truss Piers Using a Controlled Rocking Approach,” by M. Pollino and M. Bruneau, 12/20/04 (PB2006-105795).
- MCEER-05-0001 “Experimental and Analytical Studies of Structures Seismically Isolated with an Uplift-Restraint Isolation System,” by P.C. Roussis and M.C. Constantinou, 1/10/05 (PB2005-108222).
- MCEER-05-0002 “A Versatile Experimentation Model for Study of Structures Near Collapse Applied to Seismic Evaluation of Irregular Structures,” by D. Kusumastuti, A.M. Reinhorn and A. Rutenberg, 3/31/05 (PB2006-101523).
- MCEER-05-0003 “Proceedings of the Third PRC-US Workshop on Seismic Analysis and Design of Special Bridges,” edited by L.C. Fan and G.C. Lee, 4/20/05, (PB2006-105796).
- MCEER-05-0004 “Approaches for the Seismic Retrofit of Braced Steel Bridge Piers and Proof-of-Concept Testing of an Eccentrically Braced Frame with Tubular Link,” by J.W. Berman and M. Bruneau, 4/21/05 (PB2006-101524).
- MCEER-05-0005 “Simulation of Strong Ground Motions for Seismic Fragility Evaluation of Nonstructural Components in Hospitals,” by A. Wanitkorkul and A. Filiatrault, 5/26/05 (PB2006-500027).
- MCEER-05-0006 “Seismic Safety in California Hospitals: Assessing an Attempt to Accelerate the Replacement or Seismic Retrofit of Older Hospital Facilities,” by D.J. Alesch, L.A. Arendt and W.J. Petak, 6/6/05 (PB2006-105794).
- MCEER-05-0007 “Development of Seismic Strengthening and Retrofit Strategies for Critical Facilities Using Engineered Cementitious Composite Materials,” by K. Kesner and S.L. Billington, 8/29/05 (PB2006-111701).
- MCEER-05-0008 “Experimental and Analytical Studies of Base Isolation Systems for Seismic Protection of Power Transformers,” by N. Murota, M.Q. Feng and G-Y. Liu, 9/30/05 (PB2006-111702).
- MCEER-05-0009 “3D-BASIS-ME-MB: Computer Program for Nonlinear Dynamic Analysis of Seismically Isolated Structures,” by P.C. Tsopelas, P.C. Roussis, M.C. Constantinou, R. Buchanan and A.M. Reinhorn, 10/3/05 (PB2006-111703).
- MCEER-05-0010 “Steel Plate Shear Walls for Seismic Design and Retrofit of Building Structures,” by D. Vian and M. Bruneau, 12/15/05 (PB2006-111704).

- MCEER-05-0011 "The Performance-Based Design Paradigm," by M.J. Astrella and A. Whittaker, 12/15/05 (PB2006-111705).
- MCEER-06-0001 "Seismic Fragility of Suspended Ceiling Systems," H. Badillo-Almaraz, A.S. Whittaker, A.M. Reinhorn and G.P. Cimellaro, 2/4/06 (PB2006-111706).
- MCEER-06-0002 "Multi-Dimensional Fragility of Structures," by G.P. Cimellaro, A.M. Reinhorn and M. Bruneau, 3/1/06 (PB2007-106974, A09, MF-A02, CD A00).
- MCEER-06-0003 "Built-Up Shear Links as Energy Dissipators for Seismic Protection of Bridges," by P. Dusicka, A.M. Itani and I.G. Buckle, 3/15/06 (PB2006-111708).
- MCEER-06-0004 "Analytical Investigation of the Structural Fuse Concept," by R.E. Vargas and M. Bruneau, 3/16/06 (PB2006-111709).
- MCEER-06-0005 "Experimental Investigation of the Structural Fuse Concept," by R.E. Vargas and M. Bruneau, 3/17/06 (PB2006-111710).
- MCEER-06-0006 "Further Development of Tubular Eccentrically Braced Frame Links for the Seismic Retrofit of Braced Steel Truss Bridge Piers," by J.W. Berman and M. Bruneau, 3/27/06 (PB2007-105147).
- MCEER-06-0007 "REDARS Validation Report," by S. Cho, C.K. Huyck, S. Ghosh and R.T. Eguchi, 8/8/06 (PB2007-106983).
- MCEER-06-0008 "Review of Current NDE Technologies for Post-Earthquake Assessment of Retrofitted Bridge Columns," by J.W. Song, Z. Liang and G.C. Lee, 8/21/06 (PB2007-106984).
- MCEER-06-0009 "Liquefaction Remediation in Silty Soils Using Dynamic Compaction and Stone Columns," by S. Thevanayagam, G.R. Martin, R. Nashed, T. Shenthan, T. Kanagalingam and N. Ecemis, 8/28/06 (PB2007-106985).
- MCEER-06-0010 "Conceptual Design and Experimental Investigation of Polymer Matrix Composite Infill Panels for Seismic Retrofitting," by W. Jung, M. Chiewanichakorn and A.J. Aref, 9/21/06 (PB2007-106986).
- MCEER-06-0011 "A Study of the Coupled Horizontal-Vertical Behavior of Elastomeric and Lead-Rubber Seismic Isolation Bearings," by G.P. Warn and A.S. Whittaker, 9/22/06 (PB2007-108679).
- MCEER-06-0012 "Proceedings of the Fourth PRC-US Workshop on Seismic Analysis and Design of Special Bridges: Advancing Bridge Technologies in Research, Design, Construction and Preservation," Edited by L.C. Fan, G.C. Lee and L. Ziang, 10/12/06 (PB2007-109042).
- MCEER-06-0013 "Cyclic Response and Low Cycle Fatigue Characteristics of Plate Steels," by P. Dusicka, A.M. Itani and I.G. Buckle, 11/1/06 06 (PB2007-106987).
- MCEER-06-0014 "Proceedings of the Second US-Taiwan Bridge Engineering Workshop," edited by W.P. Yen, J. Shen, J-Y. Chen and M. Wang, 11/15/06 (PB2008-500041).
- MCEER-06-0015 "User Manual and Technical Documentation for the REDARSTM Import Wizard," by S. Cho, S. Ghosh, C.K. Huyck and S.D. Werner, 11/30/06 (PB2007-114766).
- MCEER-06-0016 "Hazard Mitigation Strategy and Monitoring Technologies for Urban and Infrastructure Public Buildings: Proceedings of the China-US Workshops," edited by X.Y. Zhou, A.L. Zhang, G.C. Lee and M. Tong, 12/12/06 (PB2008-500018).
- MCEER-07-0001 "Static and Kinetic Coefficients of Friction for Rigid Blocks," by C. Kafali, S. Fathali, M. Grigoriu and A.S. Whittaker, 3/20/07 (PB2007-114767).
- MCEER-07-0002 "Hazard Mitigation Investment Decision Making: Organizational Response to Legislative Mandate," by L.A. Arendt, D.J. Alesch and W.J. Petak, 4/9/07 (PB2007-114768).
- MCEER-07-0003 "Seismic Behavior of Bidirectional-Resistant Ductile End Diaphragms with Unbonded Braces in Straight or Skewed Steel Bridges," by O. Celik and M. Bruneau, 4/11/07 (PB2008-105141).


- MCEER-07-0004 "Modeling Pile Behavior in Large Pile Groups Under Lateral Loading," by A.M. Dodds and G.R. Martin, 4/16/07(PB2008-105142).
- MCEER-07-0005 "Experimental Investigation of Blast Performance of Seismically Resistant Concrete-Filled Steel Tube Bridge Piers," by S. Fujikura, M. Bruneau and D. Lopez-Garcia, 4/20/07 (PB2008-105143).
- MCEER-07-0006 "Seismic Analysis of Conventional and Isolated Liquefied Natural Gas Tanks Using Mechanical Analogs," by I.P. Christovasilis and A.S. Whittaker, 5/1/07.
- MCEER-07-0007 "Experimental Seismic Performance Evaluation of Isolation/Restraint Systems for Mechanical Equipment – Part 1: Heavy Equipment Study," by S. Fathali and A. Filiatrault, 6/6/07 (PB2008-105144).
- MCEER-07-0008 "Seismic Vulnerability of Timber Bridges and Timber Substructures," by A.A. Sharma, J.B. Mander, I.M. Friedland and D.R. Allicock, 6/7/07 (PB2008-105145).
- MCEER-07-0009 "Experimental and Analytical Study of the XY-Friction Pendulum (XY-FP) Bearing for Bridge Applications," by C.C. Marin-Artieda, A.S. Whittaker and M.C. Constantinou, 6/7/07 (PB2008-105191).
- MCEER-07-0010 "Proceedings of the PRC-US Earthquake Engineering Forum for Young Researchers," Edited by G.C. Lee and X.Z. Qi, 6/8/07.
- MCEER-07-0011 "Design Recommendations for Perforated Steel Plate Shear Walls," by R. Purba and M. Bruneau, 6/18/07, (PB2008-105192).
- MCEER-07-0012 "Performance of Seismic Isolation Hardware Under Service and Seismic Loading," by M.C. Constantinou, A.S. Whittaker, Y. Kalpakidis, D.M. Fenz and G.P. Warn, 8/27/07, (PB2008-105193).
- MCEER-07-0013 "Experimental Evaluation of the Seismic Performance of Hospital Piping Subassemblies," by E.R. Goodwin, E. Maragakis and A.M. Itani, 9/4/07, (PB2008-105194).
- MCEER-07-0014 "A Simulation Model of Urban Disaster Recovery and Resilience: Implementation for the 1994 Northridge Earthquake," by S. Miles and S.E. Chang, 9/7/07, (PB2008-106426).
- MCEER-07-0015 "Statistical and Mechanistic Fragility Analysis of Concrete Bridges," by M. Shinozuka, S. Banerjee and S-H. Kim, 9/10/07, (PB2008-106427).
- MCEER-07-0016 "Three-Dimensional Modeling of Inelastic Buckling in Frame Structures," by M. Schachter and AM. Reinhorn, 9/13/07, (PB2008-108125).
- MCEER-07-0017 "Modeling of Seismic Wave Scattering on Pile Groups and Caissons," by I. Po Lam, H. Law and C.T. Yang, 9/17/07 (PB2008-108150).
- MCEER-07-0018 "Bridge Foundations: Modeling Large Pile Groups and Caissons for Seismic Design," by I. Po Lam, H. Law and G.R. Martin (Coordinating Author), 12/1/07 (PB2008-111190).
- MCEER-07-0019 "Principles and Performance of Roller Seismic Isolation Bearings for Highway Bridges," by G.C. Lee, Y.C. Ou, Z. Liang, T.C. Niu and J. Song, 12/10/07.
- MCEER-07-0020 "Centrifuge Modeling of Permeability and Pinning Reinforcement Effects on Pile Response to Lateral Spreading," by L.L. Gonzalez-Lagos, T. Abdoun and R. Dobry, 12/10/07 (PB2008-111191).
- MCEER-07-0021 "Damage to the Highway System from the Pisco, Perú Earthquake of August 15, 2007," by J.S. O'Connor, L. Mesa and M. Nykamp, 12/10/07, (PB2008-108126).
- MCEER-07-0022 "Experimental Seismic Performance Evaluation of Isolation/Restraint Systems for Mechanical Equipment – Part 2: Light Equipment Study," by S. Fathali and A. Filiatrault, 12/13/07 (PB2008-111192).
- MCEER-07-0023 "Fragility Considerations in Highway Bridge Design," by M. Shinozuka, S. Banerjee and S.H. Kim, 12/14/07 (PB2008-111193).

- MCEER-07-0024 “Performance Estimates for Seismically Isolated Bridges,” by G.P. Warn and A.S. Whittaker, 12/30/07 (PB2008-112230).
- MCEER-08-0001 “Seismic Performance of Steel Girder Bridge Superstructures with Conventional Cross Frames,” by L.P. Carden, A.M. Itani and I.G. Buckle, 1/7/08, (PB2008-112231).
- MCEER-08-0002 “Seismic Performance of Steel Girder Bridge Superstructures with Ductile End Cross Frames with Seismic Isolators,” by L.P. Carden, A.M. Itani and I.G. Buckle, 1/7/08 (PB2008-112232).
- MCEER-08-0003 “Analytical and Experimental Investigation of a Controlled Rocking Approach for Seismic Protection of Bridge Steel Truss Piers,” by M. Pollino and M. Bruneau, 1/21/08 (PB2008-112233).
- MCEER-08-0004 “Linking Lifeline Infrastructure Performance and Community Disaster Resilience: Models and Multi-Stakeholder Processes,” by S.E. Chang, C. Pasion, K. Tatebe and R. Ahmad, 3/3/08 (PB2008-112234).
- MCEER-08-0005 “Modal Analysis of Generally Damped Linear Structures Subjected to Seismic Excitations,” by J. Song, Y-L. Chu, Z. Liang and G.C. Lee, 3/4/08.
- MCEER-08-0006 “System Performance Under Multi-Hazard Environments,” by C. Kafali and M. Grigoriu, 3/4/08 (PB2008-112235).
- MCEER-08-0007 “Mechanical Behavior of Multi-Spherical Sliding Bearings,” by D.M. Fenz and M.C. Constantinou, 3/6/08 (PB2008-112236).
- MCEER-08-0008 “Post-Earthquake Restoration of the Los Angeles Water Supply System,” by T.H.P. Tabucchi and R.A. Davidson, 3/7/08 (PB2008-112237).
- MCEER-08-0009 “Fragility Analysis of Water Supply Systems,” by A. Jacobson and M. Grigoriu, 3/10/08.
- MCEER-08-0010 “Experimental Investigation of Full-Scale Two-Story Steel Plate Shear Walls with Reduced Beam Section Connections,” by B. Qu, M. Bruneau, C-H. Lin and K-C. Tsai, 3/17/08.
- MCEER-08-0011 “Seismic Evaluation and Rehabilitation of Critical Components of Electrical Power Systems,” S. Ersoy, B. Feizi, A. Ashrafi and M. Ala Saadeghvaziri, 3/17/08.
- MCEER-08-0012 “Seismic Behavior and Design of Boundary Frame Members of Steel Plate Shear Walls,” by B. Qu and M. Bruneau, 4/26/08.
- MCEER-08-0013 “Development and Appraisal of a Numerical Cyclic Loading Protocol for Quantifying Building System Performance,” by A. Filiatrault, A. Wanitkorkul and M. Constantinou, 4/27/08.
- MCEER-08-0014 “Structural and Nonstructural Earthquake Design: The Challenge of Integrating Specialty Areas in Designing Complex, Critical Facilities,” by W.J. Petak and D.J. Alesch, 4/30/08.



EARTHQUAKE ENGINEERING TO EXTREME EVENTS

University at Buffalo, The State University of New York
Red Jacket Quadrangle ■ Buffalo, New York 14261
Phone: (716) 645-3391 ■ Fax: (716) 645-3399
E-mail: mceer@buffalo.edu ■ WWW Site <http://mceer.buffalo.edu>



University at Buffalo *The State University of New York*

ISSN 1520-295X